To the Graduate Council:

I am submitting herewith a dissertation written by Charles W. Lafon entitled "Patterns and Consequences of Ice Storms in Forested Appalachian Landscapes." I have examined the final copy of this dissertation for form and content and recommend that it be accepted in partial fulfillment of the requirements for the degree of Doctor of Philosophy, with a major in Geography.

Sally P. Horn

Sally P. Horn, Major Professor

We have read this dissertation
and recommend its acceptance:

Accepted for the Council:

Associate Vice Chancellor and
Dean of the Graduate School

PATTERNS AND CONSEQUENCES OF ICE STORMS IN FORESTED APPALACHIAN LANDSCAPES

A Dissertation
Presented for the
Doctor of Philosophy
Degree
The University of Tennessee, Knoxville

Charles W. Lafon
August 2000

Dedication

To Rachel and Annie

Acknowledgements

I wish to thank my major professor, Dr. Sally Horn, and the other members of my dissertation committee, Drs. Michael Huston, Carol Harden, and Ken Orvis, for their guidance during my graduate program. It has been an outstanding privilege to learn from these four dedicated scientists, from whom I have gained insights into plant ecology and all the major fields of physical geography.

My dissertation research was supported primarily by Environmental Protection Agency STAR grant EPA R825157-01-1, on which Michael Huston was principal investigator. Although not my committee chair, Dr. Huston deserves special recognition for his major role in directing my thoughts and research.

Small parts of the research were supported by research grants I received from the Biogeography Specialty Group of the Association of American Geographers (AAG), the Otis Paul Starkey Fund of the AAG, and the Stewart K. McCroskey Memorial Fund of the University of Tennessee Department of Geography. The Dendroclimatology Laboratory housed in the Department of Geography helped support the tree-ring analyses reported in this dissertation.

I wrote two of the chapters in this dissertation with the help of co-authors for submission to academic journals. I wish to acknowledge the role of these co-authors – Dan Graybeal, Ken Orvis, and Jim Speer – in the development of this dissertation. I have learned much about climatology, dendrochronology, and plant geography from these people.

Several people provided field assistance. Roger Brown and Evan Hart accompanied me to northern New York to sample forests disturbed by a major ice storm. Roger Brown, Nelson Lafon (my brother), and Roger Tankersley accompanied me on my first trip to New York and helped me find sites to sample on my return trip. Dan Graybeal and my father, Wade Lafon, assisted me in sampling ice storm disturbance in Southwest Virginia. Katherine Becksvoort, Evan Hart, Sally Horn, and Ken Orvis assisted Jim Speer and me in the collection of tree cores

and cross-sections for tree-ring analysis. They also assisted in the mounting and sanding of these samples. My parents, Wade and Pearl Lafon, provided a place for me to stay while conducting my field research in Virginia. I thank Dr. Bruce Ralston and Bob Muenchen for their assistance with statistical analyses.

I also wish to thank all those individuals, in addition to my committee, who have taken the time to discuss my research with me and help me improve its quality. These include Roger Brown, Rachel Clement, Dan Graybeal, Henri Grissino-Mayer, Evan Hart, Lisa Kennedy, Nelson Lafon, Kim Raia, Jim Speer, and Roger Tankersley. I thank Ed Leonard, Mike Antalosky, Mike Mabe, Steve Croy, and Jesse Overcash of the Jefferson National Forest for access to aerial photographs, for discussions of ice storm damage patterns, and for permission to sample forest disturbance. I also thank Peter Fischer of the Jefferson National Forest for helping me understand the disturbance pattern resulting from a recent windstorm in Southwest Virginia. John Gibbs of the New York State Department of Environmental Conservation (DEC) provided much information about the ice storm of January 1998 and furnished access to DEC lands. Bambi Teague granted permission to conduct research on lands owned by the Blue Ridge Parkway. Shawn Green and Rolf Gubler of Shenandoah National Park provided information on a February 1998 ice storm that affected the Virginia Blue Ridge. I gained valuable information on ice storm disturbances in the southern Appalachians from conversations with Henry McNab and Erik Berg of the Bent Creek Experimental Forest, North Carolina. Dr. Bob Davis and Dustin Hux of the University of Virginia Department of Environmental Sciences provided information and publications on meteorology of Appalachian ice storms. My undergraduate advisor, Dr. John Morgan, from Emory & Henry College, Virginia, has maintained a strong interest in my dissertation research and my professional development.

Finally, I wish to thank my wonderful family – my parents, my brother Nelson, my wife Rachel, my daughter Annie, and other relatives – for their love, support, and patience during my entire life and during these graduate school years.

Abstract

Major ice storms deposit heavy loads of freezing rain on trees, causing intense disturbances in eastern North American forests. Two ice storms that affected southwestern Virginia in 1994 caused heaviest damage on windward mountain slopes (those facing southeast or east). Several processes may have contributed to aspect-related variations in ice accretion, including orographic effects on rainfall and influences of wind on twig-surface and raindrop thermodynamics. These topographic patterns in ice storm disturbance appear to be typical in the Appalachians. Another characteristic pattern is the confinement of damage to specific elevation zones. Elevational zonation was evident in forests of Virginia and New York that were affected by ice storms during 1998.

Several factors, including tree size, wood strength, and canopy architecture, influence tree damage characteristics within stands. Small trees typically suffer bent or broken stems, and large trees usually sustain canopy damage. Toppling is most common in medium-size trees. Canopy damage is common in species with weak wood and straight boles, whereas toppling is more frequent among trees with stronger wood. Site factors, such as slope and soil depth, also affect damage patterns. Steep slopes and thin soils contribute to higher rates of toppling.

Frequency of ice storm disturbance influences how significant these events are for vegetation dynamics. In the southern Appalachians, ice storms occur most frequently in eastern parts of the region, where subfreezing surface air becomes trapped against the mountains and creates conditions favorable for freezing rain. A dendrochronological analysis indicates that ice storms produce tree-ring signatures that may be useful for detecting fine-scale spatial variations in ice storm frequency.

Forest modeling results suggest that periodic ice storms have significant long-term consequences for Appalachian forest dynamics. These disturbances may reduce species richness on xeric ridgetops and enhance richness on mesic sites, predictions consistent with theoretical

expectations. They are also predicted to reduce the degree of compositional zonation along a topographic gradient of soil moisture and to promote increased *Quercus* importance over much of the landscape. Ice storms may be especially significant for promoting the maintenance of shade-intolerant species, such as *Robinia pseudoacacia* and *Liriodendron tulipifera*, on Appalachian landscapes.

Table of Contents

Chapter **Page**

I. Introduction 1

Purpose 1
Theoretical Context 1
Disturbance Regimes in Appalachian Forests 4
Overview 4
Agents of Forest Disturbance 6
Dissertation Organization 21

II. Patterns of Ice Accumulation and Forest Disturbance During Two Ice Storms in Southwestern Virginia 23

Introduction 23
Study Area 26
Methods 29
Results and Discussion 30
Synoptic-Scale Meteorological Conditions 30
Topographic Patterns of Disturbance 38
Stand Damage 41
Patterns of Forest Disturbance from Other Ice Storms 45
Summary and Conclusions 47

III. Forest Disturbance from Four Recent Ice Storms in Virginia and New York 49

Introduction 49
Study Areas 51
Methods 54
Sampling Locations 54
Sampling Methods 56
Data Analysis 58
Results 60
Discussion 84
Forest Damage Patterns 84
Implications of the Ice Storms for Long-Term Forest Dynamics 91
Conclusions 96

IV. Spatial Patterns of Ice Storm Occurrence in the New River Valley of North Carolina, Virginia, and West Virginia 99

Introduction 99
Study Area 100
Methods 100
Results 103
Discussion 107
Conclusions 109

V. Using Dendrochronology to Identify Ice Storm Events in Oak Forests of Southwestern Virginia 110

Introduction 110
Study Area 115
Methods 117
Results 123
Discussion 130
Climate-Response Models 130
The Ice Storm Signal 130
Directions for Future Research 137
Summary 138

VI. Modeling Influences of Ice Storm Disturbance on Forest Dynamics in an Appalachian Landscape 140

Introduction 140
Description of the Model 142
Subroutine TEMPE 143
Subroutine MOIST 143
Subroutine GMULT 144
Subroutine ICEDIST 145
Subroutine BIRTH 152
Subroutine GROW 157
Subroutine KILL 163
Applying FORICE 165
Results 172
Simulated Temporal Dynamics Along the Topographic Moisture Gradient 172
Special Simulations for Specific Sites 183
Spatial Patterns of Abundance and Diversity 190
FIA Plots 192
Discussion 195
General Patterns of Succession and Zonation – Without-Ice Simulations 195
Predicted Influences of Ice Storm Disturbance 197
Implications of Ice Storms for Landscape-Scale Forest Patterns 199
Conclusions 200

VII. Conclusions 202

References 208

Appendix 225

Vita 229

List of Tables

Table		Page
2.1	Vertical Profiles of Temperature over Roanoke, VA, for Each Ice Event	34
2.2	Thicknesses of Key Diagnostic Layers of the Atmosphere for Each Ice Storm	35
2.3	Three-Hourly Surface Meteorological Conditions at Roanoke, VA, 10 – 11 February and 1 – 2 March 1994	36
2.4	Percent Cover Data for Each Site	43
2.5	Basal Area Changes Resulting from Ice Damage	44
3.1	Damage Categories and Predictor Variables used in Multinomial Logistic Regression (MLR)	59
3.2	Susceptibility Ratings for Each of the Common Species used in the Multinomial Logistic Regression Analysis	61
3.3	Percent Cover Data for Each Forest Type	62
3.4	Pre-Storm and Post-Storm Basal Area (m^2/ha) by Species in Each Forest Type	64
3.5	Seedling and Sapling Frequencies in Each Forest Type	67
3.6	Interspecific Differences in Tree Damage	71
3.7	DBH and Slope Classes used in Scatterplots	77
3.8	Damage Characteristics at Site I, the Table Mountain Pine Stand on a West-Facing Slope	85
5.1	Results of Regression Analysis	121
5.2	Record of Ice Storms Occurring During the Period Spanned by Tree-Ring Chronologies (1901-1998)	128
6.1	Simulated Site and Soil Parameters along the Great Smoky Mountains Moisture Gradient	161
6.2	Input Data for the Site Types for which Simulations Were Conducted	168
6.3	Selected Parameters for Species Used in the Model	169
A.1	Seasonal Temperature and Precipitation Variables Included in the Original Climate Response Models	227

A.2 Results of Regression Analysis Using Seasonal Precipitation and Temperature as Independent Variables 228

List of Figures

Figure		Page
2.1	Study Area	28
2.2	Meteorological Conditions for (Left) 11 February 1994 and (Right) 2 March 1994	31
2.3	Surface Meteorology and Ice Deposition for (Left) 11 February 1994 and (Right) 2 March 1994	32
2.4	Overstory Damage Pattern at Site G	42
3.1	Study Area – Virginia	52
3.2	Study Area – New York	53
3.3	Patterns of Overstory Cover in Three Sampled Stands	63
3.4	Patterns of Species Composition among the Four Forest Types Sampled in the Valley and Ridge Province of Virginia	66
3.5	Percent of Trees in Each Damage Class that were Dead at the Time of Sampling in Stands Disturbed by the Recent Ice Storms	70
3.6	Relationship of Mortality to Percent of Individuals Severely Damaged for Eleven Species in the Virginia Sites	72
3.7	Percent of Individuals of Common Species Exhibiting Canopy Damage and Stem Damage	73
3.8	Percent of Trees with Each Modulus of Rupture that was Toppled	75
3.9	Percent of Trees in Each DBH Class with Each of the Following Damage Types	76
3.10	Percent of Trees on Slopes of Each Class with Each of the Following Damage Types	78
3.11	Percent of Trees in Each Damage Class on Walker Mountain and Little Walker Mountain	79
3.12	Proportion of Total Transect Length at Each Site Occupied by Heavily Damaged Segments, as a Function of Mean Slope of the Site	83
4.1	Counties in the Study Area	101
4.2	Number of Freezing Rain Events Per County, January 1986 – March 1998: (A) Minor Ice Storms, (B) Moderate Ice Storms, and (C) Major Ice Storms	104

4.3 Number of Freezing Rain Events Per County, January 1986 – March 1998: (A) Moderate and Major Ice Storms and (B) All Ice Storms 105

4.4 Number of Freezing Rain Events Per County, December 1993 – March 1998 106

5.1 Location of the Gap Mountain and Walker Mountain Study Sites in Southwestern Virginia 116

5.2 National Climatic Data Center Climate Divisions for Virginia 120

5.3 Climate-Free Chronologies for Chestnut Oak (Top) and Black Oak (Bottom) at the Gap Mountain Site 124

5.4 Climate-Free Chronologies for Chestnut Oak (Top) and Black Oak (Bottom) at the Walker Mountain Site 125

5.5 Percent of Trees Exhibiting Significant Growth Decrease or Increase Each Year for (A) Gap Mountain and (B) Walker Mountain 127

5.6 Between-Tree Variance of Climate-Free Ring-Width Index (Heavy Line) and Sample Size (Thin Line) for (Left) Gap Mountain and (Right) Walker Mountain Series 129

5.7 Percent of Trees Exhibiting Significant Growth Decrease or Increase Each Year for (A) Gap Mountain and (B) Walker Mountain Chronologies Based on Tree-Ring Series without the Climate Signal Subtracted 131

5.8 Percent of Trees at (A) Gap Mountain and (B) Walker Mountain Whose Growth Exceeded Thresholds for Decrease or Increase in Climate-Free Ring Width Index Relative to the Five Years Prior to the Identified Ice Storms, which are Labeled 133

6.1 Function Used to Calculate Growing Degree Day Growth Multiplier (DEGDGF), Based on the Minimum Annual Growing Degree Days Tolerated by the Species 146

6.2 Functions to Calculate the Effect of Each Tree on Relative Stocking 147

6.3 Function Used to Calculate Crowding Growth Multiplier (CROWDGF) Based on Relative Stocking of the Stand 148

6.4 Recovery of Relative Diameter Increment for a Black Oak (*Quercus velutina*) Damaged by an Ice Storm in 1979 154

6.5 Relationship between Canopy Damage and Relative Diameter Increment, Based on Results of Tree-Ring Analysis 155

6.6 Same Relationship as Shown in Figure 6.5, with Axes Switched to Make Intact Canopy Proportion a Function of Relative Diameter Increment 156

6.7 Functions Used to Calculate Available Light Growth Multiplier (ALGF) for Each Tree, According to its Shade-Tolerance Rating 158

6.8 Proportion of Growing Season with Unfavorable Moisture Conditions, as a Function of Distance along the Moisture Gradient Graphed by Whittaker (1956) 162

6.9 Valley and Ridge Landscape of Southwestern Virginia for which Forest Dynamics were Simulated 166

6.10 Landscape on which Forest Modeling was Focused 167

6.11 Virginia Counties for which Forest Inventory and Analysis (FIA) Data were Obtained and Analyzed 173

6.12 Simulated Temporal Dynamics of Forests on Ridgetops 174

6.13 Simulated Temporal Dynamics of Forests on South-Facing Upper Slopes 175

6.14 Simulated Temporal Dynamics of Forests on North-Facing Upper Slopes 177

6.15 Simulated Temporal Dynamics of Forests on South-Facing Middle Slopes 178

6.16 Simulated Temporal Dynamics of Forests on North-Facing Middle Slopes 179

6.17 Simulated Temporal Dynamics of Forests on South-Facing Lower Slopes 180

6.18 Simulated Temporal Dynamics of Forests on North-Facing Lower Slopes 181

6.19 Simulated Temporal Dynamics of Forests in Valleys 182

6.20 Simulated Temporal Dynamics of Species Composition (Left) and Species Richness (Right) for Forests on Xeric Sites Disturbed by Ice Storms but Sheltered from Heavy Ice Accumulation 184

6.21 Simulated Temporal Dynamics of Forests on South-Facing Upper Slopes without Fire 185

6.22 Simulated Temporal Dynamics of Forests on South-Facing Middle Slopes without Fire 186

6.23 Simulated Temporal Dynamics of Forests on Unlogged South-Facing Middle Slopes without Fire 187

6.24 Simulated Temporal Dynamics of Forests on Mesic East-Facing Ravine Slopes 188

6.25 Simulated Temporal Dynamics of Forests in Valleys Subjected to Ice Storms at a Mean Frequency of 100 Years 189

6.26 Simulated Patterns of Species Composition and Richness along the Topographic Moisture Gradient for 100-Year Old Forests (Left) and 400-Year Old Forests (Right) 191

6.27 Spatial Distribution of Modeled Forest Characteristics 193

6.28 Patterns of Species Composition and Richness for Forest Inventory and Analysis (FIA) Plots Arranged along a Gradient of Site Index 194

Chapter 1

Introduction

Purpose

This dissertation seeks to characterize the role of major ice storms as agents of forest disturbance in the southern Appalachian Mountains. Disturbances exert important influences on species composition and diversity (Loucks 1970; Huston 1979). Ice storm disturbance occurs when a heavy coat of freezing rain accumulates on tree surfaces. Tree damage resulting from the weight of ice varies from minor limb breakage to snapping or toppling of stems. Major ice storms typically damage broad areas of forest and create large, interconnected canopy openings. This disturbance pattern differs from the formation of small gaps by single-tree mortality, the disturbance mode thought to dominate natural disturbance regimes over most of the eastern hardwood region of North America (Runkle 1990). The role of larger disturbances, such as ice storms and hurricanes, in these forests is poorly understood.

Theoretical context

An increased awareness of the influence of disturbances on vegetation characteristics has developed over the last two to three decades. In particular, it is now recognized that disturbances can promote the coexistence of species in late-successional communities that would otherwise be occupied solely by the best competitors. Throughout much of the twentieth century, the competitive equilibrium viewpoint dominated understanding of how species coexist on landscapes. A community is in equilibrium if it does not experience compositional or structural change as a result of competition (Pickett 1980). Niche differentiation was considered the primary means by which species could coexist in an equilibrium community without the extinction of inferior competitors (i.e., competitive exclusion). Since the 1970s, however, thinking has shifted to emphasize the role of such events as disturbances, diseases, climate change, and human activities that disrupt the approach to competitive equilibrium and alter

competitive relationships (Huston 1979; White 1979; Rolston 1989; Sprugel 1991). By reducing the biomass of the best competitors, disturbances free resources (e.g., light, water, and nutrients) and permit the survival of opportunists that cannot tolerate the low resource levels of later-successional communities.

Disturbances vary in frequency and magnitude. A level of disturbance exists at which maximum species diversity is maintained, and this has been described as the "intermediate" rate of disturbance (Loucks 1970; Connell 1978; Fox 1979; Huston 1979). Huston (1979) pointed out that the level of disturbance at which the most species can coexist is related to how rapidly a community is approaching competitive equilibrium. According to the dynamic equilibrium model of Huston (1979), diversity is a function of both productivity and disturbance level. Productive vegetation communities require relatively high disturbance levels to prevent exclusion and maintain diversity. Competition should be less pronounced in low-productivity stands, and, in the absence of frequent or severe disturbances, such stands can exhibit relatively high diversity. Heavy disturbance in low-productivity communities is predicted to reduce the number of species, because populations of some species do not recover between disturbances.

Smith and Huston (1989) elaborated the dynamic equilibrium model to predict spatial and temporal dynamics of vegetation along moisture gradients. Smith and Huston hypothesized that successional changes and spatial patterns in species composition are consequences of physiological constraints on resource use by plants. They focused specifically on the use of light and water. They argued that species capable of rapid growth under high resource levels possess attributes that prevent tolerance of low levels. Conversely, species able to grow in sites with low resource levels exhibit low maximum growth rates even where resources are abundant. In addition, tolerance to low levels of light and water are interdependent. Characteristics that confer shade-tolerance preclude drought-tolerance, and attributes that permit survival in dry sites prevent tolerance of shade.

In early succession, competition for light is not severe, and species richness should be highest on mesic sites, where the physiological optima (highest growth in the absence of competition) of most species occur (Smith and Huston 1989; Huston 1994). Rapid growth rates on mesic sites soon lead to canopy closure and increased competition for light, displacing the less competitive species toward the dry end of the gradient. Smith and Huston predict that ultimately, in the absence of disturbance, each species becomes confined to a narrow zone along the gradient as a result of superior competition at high resource levels. Species richness declines as succession proceeds, particularly in mesic sites where slow-growing, shade-tolerant species become dominant. By reducing canopy biomass, disturbance reduces competition for light and permits the maintenance of shade-intolerant species that would otherwise be excluded. Thus disturbance enhances species richness and diminishes the degree of species zonation along a moisture gradient (Huston 1979; Smith and Huston 1989; Huston 1994).

This dissertation applies the dynamic equilibrium model to elucidate consequences of ice storm disturbance on forested Appalachian landscapes. Appalachian forests vary widely in productivity. In valleys and lower slopes, where runoff accumulates and soils are typically deep, sufficient moisture and nutrient levels are available for rapid growth. Thin soils on adjacent ridges may be too droughty and infertile to support the luxuriant growth of the valley sites. The role of ice storms in generating intermediate levels of disturbance will vary according to the productivity of the vegetation at a site. Another important factor is the character of the storms themselves. Little is known about the frequency of major ice storms in the Appalachians (or elsewhere) or about spatial variations in ice storm frequency or magnitude. Appalachian topography creates circumstances that favor pronounced spatial variation in ice storm frequency and magnitude over different spatial scales.

Disturbance regimes in Appalachian forests

Overview

Fine-scale gap dynamics involving frequent creation of small canopy gaps are thought to dominate natural disturbance regimes over interior parts of the temperate forest region of eastern North America, including the Appalachians (Runkle 1990). Runkle (1990) reviewed published articles on natural disturbances in eastern North America and concluded that catastrophic disturbances, such as hurricanes, fires, and tornadoes, are mostly restricted to the margins of the region.

Most work on the role of disturbance in interior eastern forests has focused on mesophytic forests, particularly northern hardwood and cove hardwood forests. Research on old-growth northern hardwoods indicates that catastrophic fires or blowdowns typically recur on the order of about 1,000 years (Lorimer 1989; Lorimer and Frelich 1994). Small gaps, on the other hand, form frequently and cover an average of 0.4% – 2.0% of the land area annually, yielding an average canopy turnover time less than 250 years and contributing to uneven age distributions. Southern Appalachian cove forests may be affected almost entirely by small-scale disturbances (Runkle 1985). Runkle (1982, 1985) found that gaps in several old-growth mesophytic forests in the southern Blue Ridge and the Allegheny Plateau formed primarily as a result of single-tree mortality. However, about 1% of the total land area was in gaps exceeding 400 m^2 in area, the approximate minimum size required for regeneration of shade-intolerant yellow-poplar (*Liriodendron tulipifera*), and most of these larger gaps resulted from the fall of multiple trees. Gap sizes were as large as about 1500 m^2.

Gap creation rates in old-growth mesic forests of the central and southern Appalachians are similar to those in northern hardwood forests, northern coniferous forests, and tropical rainforests (Runkle 1982, 1985). A given average disturbance rate can be achieved by the occurrence of infrequent major disturbances or frequent minor events. Sites in the southern

Appalachians monitored for fifteen years exhibited relatively minor yearly fluctuations in gap formation rates (Runkle 1985), suggesting that the disturbance regime is dominated by frequent disturbances of low intensity. It is important to note, however, that short-term studies may underestimate the role of larger, less frequent events.

In stands characterized by fine-scale gap dynamics, lateral spread of dominant-tree canopies is partly responsible for gap closure, but upward growth of saplings appears to be the primary mode of closure (Runkle 1982). Seedlings are unlikely to reach the canopy except in larger gaps whose radii exceed 5 m (Runkle 1985). Because gaps are small and therefore close rapidly, multiple gap-creation episodes are typically required for understory trees to reach the canopy (Runkle 1985). Given observed average gap creation rates, a high probability exists that new gaps will be created adjacent to an old gap within a relatively short time (Runkle 1990). A study of disturbance history in an old-growth cove forest of western North Carolina revealed that eight disturbances occurred during the last 250 years, most of which removed less than 10% of the canopy trees (Lorimer 1980). This level of disturbance creates large enough gaps for the maintenance of both shade-tolerant and intolerant species in all age classes.

Despite lower frequencies of occurrence, larger disturbances do exert significant influences on forests of the central hardwood region. Even in hemlock (*Tsuga*)-hardwood forests where catastrophic fires recur at 1400-year intervals, more than 20% of the landscape is typically covered with stands that originated following fires (Lorimer and Frelich 1994). Outside mesophytic forests, less information exists for characterizing disturbance regimes (Lorimer and Frelich 1994). Large events may be more important in other forest types. For example, white pine (*Pinus strobus*) forests occurred on presettlement landscapes of the Allegheny Plateau where fires and windstorms opened the canopy and exposed mineral soil (Runkle 1985). These pine forests occupied sandy river bottoms and lower south-facing slopes, whereas mesophytic forests characterized by fine-scale gap creation dominated north-facing slopes. Recent examples of such

disturbances include severe winds that leveled large patches of forest during tornadoes or downbursts on the Allegheny Plateau of Pennsylvania (Peterson and Pickett 1995) and the Valley and Ridge of Tennessee and Virginia (Wilkinson 1993; Peter Fischer personal communication).

Characterizing canopy disturbances either as frequent small-intensity events that create single-tree gaps or as infrequent high-magnitude events that kill all trees in a broad swath oversimplifies disturbance dynamics in the Appalachians and surrounding regions. Greenberg and McNab (1998) argued that intermediate-scale disturbances caused by episodic, high-intensity (but not catastrophic) wind are common in the southern Appalachians and have important consequences for forest dynamics. Their study of hurricane damage in western North Carolina oak forests characterized gaps of 0.2 – 1.1. ha in area. Greenberg and McNab pointed out that such disturbances do not always create "neat" gaps with treeless interiors surrounded by discrete, undamaged forest edges. Rather, standing trees remained within all the gaps they sampled.

Ice storms may be best characterized as intermediate-scale disturbances. Studies of ice storm disturbance does not typically describe gaps at all but imply instead that broad areas of forests are thinned without removal of all canopy trees (Downs 1938; Whitney and Johnson 1984; Bruederle and Stearns 1985; Seischab *et al.* 1993). This level of canopy disturbance may have different consequences for tree species composition and diversity than either fine-scale dynamics associated with single-tree mortality or the infrequent occurrence of large, catastrophic events.

Agents of forest disturbance

In addition to ice storms, several other natural disturbance agents affect Appalachian forests, causing disturbances ranging from mild to catastrophic in their effects. These disturbances can be classed into four main categories: storm disturbance, geomorphic disturbance, fire, and biotic disturbance. I do not provide a literature review on ice storm disturbance in this introductory chapter, because such information is included in the following chapters. The purpose of this section is to describe other types of disturbance that affect

Appalachian forests, thus furnishing a context for my research on ice storms. The concluding chapter of the dissertation compares ice storms to these other disturbance agents.

Storm disturbance – Storm disturbances result from various types of wind events, including thunderstorms and tornadoes, hurricanes, and midlatitude cyclones, as well as ice storms and snow storms. The most catastrophic wind disturbance occurs during tornadoes or downbursts, which may remove virtually all canopy trees in large patches (Peterson and Pickett 1995). A class F4 tornado leveled 400 ha of old-growth forest on the Allegheny Plateau of Pennsylvania in May 1985 (Peterson and Pickett 1995), and downbursts associated with severe squall-line thunderstorms caused similar damage over about 25,000 ha in Minnesota and Wisconsin in July 1977 (Canham and Loucks 1984). In the southern Appalachians, a February 1993 tornado devastated about 100 ha of forest in the University of Tennessee Forestry Experiment Station at Oak Ridge, Tennessee (Wilkinson 1993). Downbursts or a tornado flattened 200 ha of forest on the Clinch Ranger District of the George Washington and Jefferson National Forest of southwestern Virginia in June 1998 (Peter Fischer personal communication). Not all tornado and downburst winds produce such devastating results. The storms described above also caused less severe forest disturbance over broader areas (Canham and Loucks 1984; Wilkinson 1993; Peter Fischer personal communication), and some tornadoes/downbursts do not produce any large patches of complete canopy removal (Glitzenstein and Harcombe 1988; Held *et al.* 1998). Catastrophic winds cause several forms of tree damage, but toppling and stem breakage appear most common (Held and Winstead 1976; Glitzenstein and Harcombe 1988; Peter Fischer personal communication).

Catastrophic windstorm disturbance occurs infrequently in most of the eastern forest region. Canham and Loucks (1984) estimated an average return interval of 1210 years for such events in northeastern Wisconsin, and Glitzenstein and Harcombe (1988) suggested that return intervals in southeastern Texas are on the order of 1,000 – 10,000 years. Given the low frequency

of tornadoes in the Appalachians (Brinkman *et al.* 1975a; Kelly *et al.* 1978; Eagleman 1983; Leathers 1993), it is doubtful that tornadoes are a major component of disturbance regimes in most parts of the region. Downburst winds may be more important.

Spatial patterns of disturbances associated with tornadoes and downbursts undoubtedly exist across the Appalachian region, but there has been little study of these phenomena at fine scales. Based on published maps of tornado frequency (Brinkman *et al.* 1975a; Eagleman 1983), it appears that tornadoes are most common in the extreme southern edge of the Appalachians (the Valley and Ridge section of northwestern Georgia and northeastern Alabama). Bratton and Meier (1998) reported that tornadoes are common in the Chattooga River basin of Georgia, in the southern end of the Blue Ridge. Tornadoes occur there once or twice per decade, on average. However, they rarely move into the higher terrain in the North Carolina section of the basin.

Total annual thunderstorm frequency also decreases from south to north (Brinkman *et al.* 1975a; Eagleman 1983), and it is likely that the frequency of windthrow from thunderstorm winds follows a similar latitudinal gradient. Disturbance resulting from a single catastrophic windstorm may not be predictable at the finer scale of individual topographic features. Downburst and tornado damage in southwestern Virginia and northern Michigan was not related to slope or exposure (Lorimer and Frelich 1994; Peter Fischer personal communication).

Despite their low frequencies, catastrophic winds have important influences on forest characteristics. For example, they may promote increased abundance of shade-intolerant species (Peterson and Pickett 1995), and they create large patches of even-aged forest that are subsequently modified by small disturbances, ultimately producing uneven-aged stands (Dunn *et al.* 1983). The piles of debris provide fuel for fire (Bratton and Meier 1998), and the presence of damaged trees increase the likelihood of insect or disease outbreaks (Schowalter *et al.* 1981; Lovelady *et al.* 1991). Peterson and Pickett (1995) also predicted that piles of storm debris would enhance hemlock regeneration by protecting the seedlings from deer browsing.

Hurricanes may be more significant disturbance agents than tornadoes and downbursts in the Appalachians and regions to their east. In fact, Foster (1988) suggested that hurricanes are the major natural disturbance agent in central New England. Although hurricane winds lose strength as the storms move inland, they nonetheless cause heavy forest damage as far inland as the Appalachians. Hurricane Opal, a moderate-intensity hurricane that affected the southern Blue Ridge in 1995, created at least 21 discrete, multiple-tree gaps of 0.1 – 4.0 ha in the Bent Creek watershed of western North Carolina (Greenberg and McNab 1998). These gaps, which contained variable numbers of standing trees, probably resulted from downburst winds associated with the hurricane. The storm also created numerous single-tree gaps less than 200 m^2 in area. Uprooting was the dominant form of tree damage, which was also the case in New England forests disturbed by a 1938 hurricane (Foster 1988; Greenberg and McNab 1998). Uprooting may result in part because soils become saturated during the heavy rains that accompany hurricanes (Foster 1988).

Broad-scale spatial patterns exist in the frequency and intensity of hurricane disturbance. Forests in coastal zones are obviously affected more than inland forests (Runkle 1990). Further, some segments of the Atlantic and Gulf coasts endure more frequent hurricane occurrence than others (Brinkman *et al.* 1975b). Within the Appalachians, the eastern edge of the mountains (i.e., the Blue Ridge) probably sustains more intense and more frequent hurricane winds than other parts of the region (Brinkman 1975b). The greater proximity of the northern and central Appalachians to the Atlantic coast exposes those parts of the Appalachians to stronger hurricane winds than the southern end of the region typically sustains (Brinkman 1975b). Finer-scale patterns also emerge. In north temperate regions, severe hurricane damage occurs primarily to the right of the storm track, where counterclockwise flow around the cyclone is aligned with the direction of storm movement (Foster and Boose 1995). Further, in hurricanes affecting the southern Appalachians, the right side of the storm is the sector containing onshore winds, which

are the least dissipated winds. The result is that slopes facing east to southwest are exposed to hurricane damage (Foster 1988), whereas forests on other sites may sustain little damage (Foster and Boose 1995). Other topographic influences on wind speed also occur. Wind is accelerated over summits and channeled up valleys (Foster and Boose 1995; Finnigan and Brunet 1995). Greenberg and McNab (1998) reported that nearly all windthrows in Bent Creek watershed occurred on upper and middle slopes. These reported patterns agree with my observations of Hurricane Hugo damage in the Valley and Ridge province of southwestern Virginia, where heavy damage occurred primarily on upper slopes facing southeast.

Hurricanes probably have important consequences for forest patterns in the Appalachians and nearby regions. Basal area losses of 30 – 50% occurred in gaps created by Hurricane Opal at Bent Creek, probably resulting in long-term influences on tree species dominance and diversity (Greenberg and McNab 1998). The 1938 New England storm eliminated white pine from many stands, converting them from white pine-hardwood to hardwood stands and enhancing the growth of hemlock (Foster 1988). The frequency of hurricane damage is high enough to affect substantial portions of the landscape over the lifespan of a tree. Greenberg and McNab (1998) estimated that hurricane-related windstorms create gaps over 6.8% of the southern Appalachian landscape during a 200-year period.

Most windstorms, outside these major events, are too weak to produce heavy forest damage. Winds associated with midlatitude cyclones typically cause small-gap disturbances (Canham and Loucks 1984). Also, according to the *Storm Data* reports of the National Climatic Data Center (NCDC), several forest-damaging thunderstorm episodes occur annually in each state. The most likely consequence of these moderate-intensity winds is the creation of single-tree gaps. Hence, these frequent storms are an important driver of fine-scale gap dynamics in eastern forests.

Some generalizations emerge from examination of literature on windstorm damage. Besides the most catastrophic windstorms, which level virtually all the canopy trees in their paths, windstorms primarily damage the largest trees (Cremeans and Kalisz 1988; Glitzenstein and Harcombe 1988; Walker 1991; Greenberg and McNab 1998). Toppling appears to be the primary form of damage (Cremeans and Kalisz 1988; Foster 1988; Greenberg and McNab 1998; Peter Fischer personal communication), especially among large trees (Walker 1991). Toppling is particularly likely on sites with thin soils (Croker 1958). Cremeans and Kalisz (1988) found that on the Cumberland Plateau of Kentucky uprooting was most common in coves and north-facing slopes, probably reflecting low soil strength in moist sites. This pattern differs from the finding of Greenberg and McNab (1998) that most canopy gaps were created on middle and upper slopes. However, heavy precipitation during the hurricane probably saturated soils over the entire landscape.

Species vary in their susceptibility to wind damage. Early-successional species, especially pines (*Pinus*), appear most vulnerable to wind damage (Foster 1988; Glitzenstein and Harcombe 1988; Brokaw and Walker 1991), especially in stands where these are the largest, most abundant species. Cremeans and Kalisz (1988) and Greenberg and McNab (1998) found that scarlet oak (*Quercus coccinea*) was particularly vulnerable in the southern Appalachian region. Wind has various implications for tree species composition and diversity. By opening stands and reducing abundance of canopy dominants, windstorms probably favor increased species diversity (Doyle 1981). However, wind may also reduce diversity where the dominant species are more resistant than others to wind damage (Brokaw and Walker 1991; Putz and Sharitz 1991).

Snowstorms also disturb forests. Heavy, wet snow can break or topple trees in a similar manner as ice storms, although the damage may be less severe. Virtually no research has been conducted on the effects of heavy snow as an agent of forest disturbance. An early-spring snowstorm in 1958 damaged a seven-year-old paper birch-yellow birch (*Betula papyrifera-B.*

alleghaniensis) stand in New Hampshire (Blum 1966). Approximately 50 – 75% of the stems were injured, primarily by bending or twisting. High mortality occurred in subsequent years, but the stand was well stocked when assessed in 1962. Snow damage causes breakage in conifers of the Pacific northwestern United States (Oliver and Larson 1990). In the Appalachians, heavy snow probably damages southern pines more than hardwoods, although a late snowfall occurring after leaf-out could cause major damage to deciduous trees. Presumably, the frequency of snow damage increases with elevation and latitude. However, when heavy snow loads do occur at low latitudes or elevations, severe damage may result, because tree canopies have not been pruned by other recent winter storms.

Geomorphic disturbances – Floods and debris slides are the primary geomorphic events that cause forest disturbance in the Appalachians. Both types of events can strip off all forest cover and erode much of the substrate. Geomorphic disturbances are restricted to specific parts of the landscape, but they are important disturbance agents in those sites. The best known and most comprehensive work on flooding and debris slides in the Appalachians is that of Hack and Goodlett (1960), who studied effects of an intense convective rainstorm that occurred during June 1949 in the Little River basin of the Ridge and Valley province of western Virginia. Over 100 debris slides occurred on the forested slopes of the watershed, creating scars 6 – 300 m wide. First- and second-order stream channels were scoured, widened, and deepened. The larger valleys, such as that of the Little River itself, were severely eroded. In some sections the entire floodplain (up to about 100 m in width) was denuded of forest vegetation. Debris fans also formed where debris flows ran onto valley floors. Such catastrophic geomorphic events create high-light conditions that permit opportunistic pioneer species to colonize (Flaccus 1959). They also alter soil conditions by eroding or depositing sediment. Flaccus (1959) studied revegetation of debris slide scars in the White Mountain of New Hampshire and found that early-successional forest vegetation on the scars was dominated by the same pioneer species that follow burning,

timber harvest, or windthrow. In the Little River basin of Virginia, mature floodplain forests of white pine and hemlock were converted to young stands of sycamore (*Platanus occidentalis*) and black locust (*Robinia pseudoacacia*) by the time the basin was surveyed in 1955 (Hack and Goodlett 1960). Osterkamp *et al.* (1995) resurveyed geomorphic features and vegetation 35 years later and found that sycamore continued to dominate stands on damaged floodplains, whereas hemlock and white pine dominated on undamaged floodplains. Locust had declined on the disturbed sites, and sugar maple (*Acer saccharum*) and yellow-poplar had increased.

Catastrophic geomorphic events result during heavy rainfall, although snowmelt may be involved in some cases (Jacobson *et al.* 1989). Clark (1987) compiled an inventory of documented historical debris slides in the unglaciated Appalachians and found that most episodes occurred during heavy summer thunderstorms. However, the most widespread damage occurred during hurricanes and midlatitude cyclones, with hurricanes inflicting the most severe damage and property loss. In some cases, such as the central Appalachian flooding of November 1985, heavy rains result when tropical storms interact with extratropical lows (Jacobson *et al.* 1989).

Hack and Goodlett (1960) estimated that the return interval of high-magnitude geomorphic events is probably 100 years or more in the Little River basin. Based on a literature review of debris slides in the Appalachians, Eschner and Patric (1982) concluded that a one-day rainfall of about 12.5 cm is necessary for slides to occur. Return intervals for rainfall of this intensity generally do not exceed 100 years in the Appalachians, although the occurrence of such a rainstorm does not guarantee slope failures. Kochel (1987) estimated a return interval of 3,000 – 4,000 years, based on debris fan stratigraphy in the Blue Ridge of central Virginia. However, this is an "at-a-site" estimate, and Kochel noted that such events occur much more frequently at a regional scale. The occurrence of debris slides in neighboring hillslope hollows or watersheds during different storms could help maintain tree species diversity on the landscape, even if the disturbances are infrequent at a specific site. One factor that determines minimum return interval

of debris slides is the rate of colluvial recharge in a slide chute (Jacobson *et al.* 1989). Where a recent debris slide has flushed all the colluvium from a hollow, another slide will not occur until a sufficient depth of material accumulates.

Geomorphic disturbances undoubtedly exhibit considerable spatial variation in frequency and in the proportion of landscape area affected. At the broadest scale, the entire Appalachian region, with its steep slopes, thin soils, narrow valleys, and orographically enhanced precipitation, is prone to such events (Eschner and Patric 1982). An inventory of historic debris slides in the unglaciated Appalachians (Clark 1987) reveals a pronounced concentration of events in the southern Blue Ridge of North Carolina and Tennessee, with a secondary cluster in the Valley and Ridge and Plateaus of southwestern Virginia. However, major catastrophic events have occurred throughout the Appalachians (Eschner and Patric 1982; Jacobson *et al.* 1989). In their study of catastrophic geomorphic events in the central Appalachians, Jacobson *et al.* (1989) concluded that severe floodplain damage and hillslope failures are predominant in the Ridge and Valley and the Blue Ridge and less important in the Piedmont and the Allegheny Plateau. This spatial pattern reflects differences in both the climatology of heavy rainfall and the physical characteristics of watersheds among the physiographic provinces. Values for extreme, short duration rainfall events (e.g., the 100-year maximum daily rainfall) decline from east to west, reflecting primarily the greater influence of tropical storms to the east (Jacobson *et al.* 1989). Despite frequent heavy rain in the Piedmont, the thick, highly permeable saprolite permits infiltration and drainage. Thus, the high soil moisture levels required for slope failure are not likely (Jacobson *et al.* 1989). Fluvial regimes in the low-power Piedmont streams are dominated by moderate events that probably have only minor consequences for vegetation disturbance. In contrast, the thin soils, high stream power, coarse sediment, steep slopes, and high relief of the Blue Ridge and Ridge and Valley contribute to occurrence of catastrophic flood damage and slope failures (Jacobson *et*

al. 1989). Allegheny Plateau hillslopes are mostly affected by frequent, minor slips during wet periods in the springtime (Jacobson *et al.* 1989).

At finer scales, catastrophic flooding and debris sliding that produce significant forest disturbance primarily occur in low-order drainage basins, a pattern that reflects the small mesoscale organization of extreme rainfall (Jacobson *et al.* 1989) and the steep hydrologic slopes of low-order basins. Within a landscape or watershed, lithologic and topographic differences contribute to spatial patterns in slope failure and flood damage. For example, debris slides are particularly common in the pyritiferous Anakeesta Formation of the Great Smoky Mountains (Clark *et al.* 1987). Hillslope hollows are typically the initiation sites for debris slides (Kochel 1987), and high antecedent moisture in hollows facing northwest, north, northeast, or east may contribute to higher incidences of slope failure on those aspects during rainfall events of marginal intensity (Clark 1987). In fluvial systems, constrictions formed by water gaps funnel water into jets that erode downstream floodplain reaches (Jacobson *et al.* 1989).

Fire – Fire is thought to have been a major influence on Appalachian forest vegetation prior to the advent of effective fire suppression. The prevalence of oak and southern pine forests over much of the region apparently results in part from frequent, widespread burning in the past (Abrams 1992; Bratton and Meier 1998; Harrod *et al.* 1998; Williams 1998). Both oaks and southern pines, especially table mountain pine (*Pinus pungens*) and pitch pine (*P. rigida*), possess characteristics (e.g., thick bark or serotinous cones) that make them resistant to or dependent upon fire. Most competing species, including maples, hemlocks, yellow-poplar, black gum (*Nyssa*), and white pine, are less resistant and decline under a regime of frequent burning (Beck 1990; McGee 1990; Walters and Yawney 1990; Wendel and Smith 1990; Harrod *et al.* 1998). Pines and oaks are relatively intolerant of shade and are most successful where disturbances kill competing vegetation (Abrams 1992; Williams 1998). Additionally, the pines require open, scarified microsites, such as those existing after fire, for optimal germination and seedling

establishment (Williams 1998). Southern pines appear to be most successful where burning is at least moderately intense, killing substantial portions of the dominant overstory trees (Harrod *et al.* 1998; Williams 1998). Oaks may thrive best under a regime of frequent, relatively light surface fires that kill shade-tolerant understory trees and reduce the cover of understory shrubs that compete with oak seedlings for light (Runkle 1990; Nowacki and Abrams 1992).

The presettlement dominance of oak-chestnut forests over most topographic positions in the southern and central Appalachians and other portions of the oak-chestnut region may imply that fire frequencies were high (Abrams 1992; Bratton and Meier 1998). Indeed, a fire history study in a presettlement-origin oak forest in central New Jersey revealed a mean fire interval of 14 years between 1641 and 1711 (Buell *et al.* 1954). Lightning-set fires currently occur too infrequently to have major influences over most of the landscape, and it is presumed that lightning-set fires were also uncommon in prehistoric times (Abrams 1992; Welch 1999). Most researchers have concluded that Indian-set fires were common and dominated the fire regime, although this is a controversial hypothesis (Buell *et al.* 1954; Russell 1983; Abrams 1992; Nowacki and Abrams 1992; Pyne *et al.* 1996; Bratton and Meier 1998; Williams 1998). Delcourt *et al.* (1986) demonstrated that Indian agriculture had significant influences on vegetation near settlements along the Little Tennessee River. However, it is not known whether Indian-set fires affected the more remote, more sparsely populated areas of the Appalachians. Williams (1998) suggested that lightning-set fires may have been more important than anthropogenic fires for maintaining table mountain pine stands. If neither lightning-set fires nor anthropogenic fires occurred frequently outside particularly fire-prone areas (e.g., near settlements or on dry ridgetops), burning may not explain fully the widespread dominance of oaks prior to Eureopean settlement.

European colonists adopted fire practices similar to those of Indians (Pyne *et al.* 1996). More severe burning followed large-scale industrial logging in the late 1800s and early 1900s,

leading to expansion of table mountain pine-pitch pine forests (Williams 1998). Successful fire-suppression began in the 1930s and appears to have had negative consequences for abundance of both pines and oaks (Abrams 1992; Nowacki and Abrams 1992; Williams 1998).

Lightning-set fires presently occur on Appalachian landscapes, but they are less frequent than anthropogenic fires. About 15 percent of all fires that occur in the Southern Appalachian Assessment (SAA) region are ignited by lightning (SAMAB 1996). A map of wildfires occurring between 1986 and 1993 on national forest lands in the SAA region reveals that both lightning-set and anthropogenic fires were more common in the southern part of the region than in the northern part (SAMAB 1996), but the analysis period may be too short to provide an accurate assessment of long-term spatial patterns. The map also implies higher fire frequency for the Blue Ridge than the Valley and Ridge, although this pattern is especially tenuous because the lower amount of national forest land in the Valley and Ridge makes interpretation of the pattern difficult.

Lightning-set fires are most common on low-elevation ridgetops, on slopes facing south to west, and in pine or pine-hardwood stands (Barden and Woods 1974; Bratton and Meier 1998). Barden and Woods (1974) estimated an average frequency of 6 lightning-set fires annually per 400,000 ha in the southern Blue Ridge of Tennessee and North Carolina. Mean fire size was 3.4 ha. However, lightning-set fires of up to 422 ha have occurred in the southern Blue Ridge (Bratton and Meier 1998). Anthropogenic fires contrast with lightning-set fires in several ways. They typically affect lower slopes and more mesic sites than lightning-set fires, occur during less humid weather, burn more intensely, and cover larger areas (Barden and Woods 1974; Bratton and Meier 1998). Average fire size is 5.4 ha in the Tennessee and North Carolina Blue Ridge, and the largest was a 20,000 ha burn near Johnson City, Tennessee, that occurred during a major drought in 1925 (Barden and Woods 1974).

It is possible that lightning-set fires were more important in presettlement forests than is evident from studies of the present fire regime. Without suppression, lightning fires would

probably burn larger areas. This would be especially likely if the initiating thunderstorm were followed by a period of sunny, less humid weather, a pattern that occurs commonly (e.g., following a cold front). During drought years, in particular, an episode of scattered thunderstorms could ignite fires that would eventually spread into very dry areas unaffected by thunderstorm rains, potentially burning thousands of hectares. Of course, on the modern landscape, such fires are prevented from spreading and developing into major events. Given the current level of suppression, which obscures the role of lightning-set fires, and the disagreement over the ubiquity of Indian-set fires, it is difficult to reach firm conclusions about "natural" or presettlement fire regimes in the Appalachians. What is clear is that lightning-set and anthropogenic fires probably occur too infrequently on the present landscape to be a major influence on forest dynamics in most sites.

Biotic disturbances – Biotic disturbances include a wide assortment of damaging agents, from fungi to insects to mammals, that kill or damage trees. The various agents of biotic disturbance cause greater losses throughout North American forests than any other type of disturbance (Haack and Byler 1993). Some of the most catastrophic biotic disturbances are associated with invasive exotic insects or fungi. For example, the chestnut blight fungus (*Cryphonectria parasitica*) killed all mature American chestnut (*Castanea dentata*) trees in the Appalachians during the early twentieth century. Previously, chestnut had been one of the most abundant tree species in the region, and the demise of chestnut led to compositional change. It appears that growth and abundance of oaks, pignut hickory (*Carya glabra*), and red maple, in particular, have increased in response to this disturbance (Stephenson 1974; McCormick and Platt 1980; Agrawal and Stephenson 1995). Numerous native species also kill trees. Many organisms specialize on one genus or species of trees and hence exert major influences on the direction of forest succession (Haack and Byler 1993). Anthropogenic influences, such as conversion of mixed-age stands to monocultures, planting timber species in high-stress environments outside

their native ranges, and releasing air pollutants, may also make forests more susceptible to biotic disturbance (Haack and Byler 1993).

The southern pine bark beetle (*Dendroctonus frontalis*) causes some of the most spectacular damage in forests of the southeastern United States. These beetles damage the cambium of southern pines, killing the trees. Trees stressed by competition, drought, or injury (e.g., from fire or lightning) are more vulnerable to bark beetle infestation than healthy trees (Schowalter *et al.* 1981; Lovelady *et al.* 1991; Williams 1998). Periodically, bark beetle populations expand to epizootic levels, during which healthy, normally resistant trees are killed (Lovelady *et al.* 1991). During these outbreaks, broad patches of dead pines can be observed. Beetle outbreaks increase the likelihood of catastrophic fire and hence pine regeneration by contributing heavy fuel loads (Schowalter *et al.* 1981). Without fire, bark beetles hasten succession to hardwood dominance (Williams 1998).

Vertebrates can cause significant levels of forest disturbance. Beavers (*Castor canadensis*) are one of the best examples, because they are able to fell large trees. Beaver foraging is restricted to narrow zones near streams. Within these areas, beavers cause major declines in forest density and basal area (Barnes and Dibble 1988; Johnson and Naiman 1990). Eventually, the abundance of preferred species, such as quaking aspen (*Populus tremuloides*), ashes (*Fraxinus*), hickories, and hackberry (*Celtis occidentalis*) declines, and composition shifts toward less palatable tree species, like basswood (*Tilia americana*), spruce (*Picea*), and fir (*Abies*) (Barnes and Dibble 1988; Naiman *et al.* 1988; Johnston and Naiman 1990). In some cases beaver-foraging is so heavy that zones near the stream are kept virtually clear of any forest vegetation (personal observation, Laurel Fork drainage basin, Highland County, Virginia). Beaver ponds themselves cause major compositional and structural change by flooding riparian areas. Beavers may eventually abandon a pond, permitting re-establishment of vegetation (Neff 1957).

Ungulate browsing can also cause significant vegetation changes by destroying seedlings of palatable tree species. Hanley and Taber (1980), for example, found that foraging by elk (*Cervus canadensis*) and black-tailed deer (*Odocoileus hemionus*) in Washington reduced shrub cover and increased the abundance of grasses and Douglas-fir (*Pseudotsuga menziesii*). Frelich and Lorimer (1985) predicted that preferential browsing of eastern hemlock seedlings by white-tailed deer (*Odocoileus virginianus*) in Michigan will result in conversion of hemlock-sugar maple stands to sugar maple stands within 150 years. Woodland grazing by livestock and wild ungulates probably contributed to oak dominance in the Appalachians by reducing the abundance of more palatable seedlings (Runkle 1990). Prior to their extinction, Pleistocene megafauna probably contributed to higher disturbance levels than those resulting from the activities of modern fauna. Seed predation by mammals, birds, and insects also influences reproductive success.

Biotic disturbances vary in frequency and intensity across the Appalachian region and within smaller landscapes. In the case of pathogens and insects, disturbance intensity is determined largely by the presence of host tree species. Spatial patterns of other disturbances (e.g., fire, ice storms) that increase vulnerability to insect or fungal attack, also influence patterns of biotic disturbance. Climate also influences patterns of biotic disturbance. The southern extremity of the Appalachian Mountains may suffer the most severe insect disturbances, because long growing seasons and mild winter temperatures permit several insect generations each year and rapid increases in population. Beavers are probably more common in some parts of the Appalachians than others, a consequence of dispersal and population growth patterns following near extirpation in the 1800s. Within a given landscape, beaver influences are probably less significant in the Appalachians than in the flatter terrain of other regions, where floodplains are wider. Disturbance by other browsers, such as white-tailed deer, is probably a function of

population density, which varies considerably throughout the southern Appalachian region (SAMAB 1996).

Dissertation organization

The following five chapters fall into three general groups. Chapters 2 and 3, which focus on disturbance patterns resulting from specific ice storms, comprise the first group. Chapter 2 addresses topographic patterns of ice storm damage resulting from two major events that affected southwestern Virginia in 1994. This assessment illuminates landscape-scale variability in ice damage that appears to be typical for the region. In Chapter 3, I examine ice storm damage to individual trees in six forests. Four of the forests I sampled were affected by the 1994 Virginia ice storms. The other forests were located in western Virginia and northern New York and were affected by two major ice storms that occurred fortuitously during my dissertation work in 1998.

Chapters 4 and 5 make up the second group. They employ different techniques to investigate ice storm climatology and characterize patterns of disturbance frequency resulting from ice storms. Chapter 4 discusses an attempt to use historic storm records to identify county-scale variations in ice storm frequency in the New River Valley, a major drainage basin of the southern Appalachian region. Chapter 5 presents an initial study on the use of tree-ring analysis to evaluate ice storm frequency and its variation at fine spatial scales.

Chapter 6, which applies insights gained from preceding chapters, describes the use of an individual-based forest succession model to help evaluate the effects of periodic ice storm disturbance on the forests that occupy the varied topography of an Appalachian landscape. I used a version of the model LINKAGES (Pastor and Post 1985) that I modified to simulate periodic disturbance by major ice storms.

Each chapter is written as a stand-alone paper. Chapter 2 is nearly identical to a paper published in *Physical Geography* (Lafon *et al.* 1999). Dan Graybeal and Ken Orvis are co-authors of this paper. Chapter 3 will be submitted to a vegetation/ecology journal. Chapter 4 was

published with minor differences in the *New River Symposium Proceedings* (Lafon 1999). Chapter 5 has been revised for resubmission following initial review at *Climate Research*. Jim Speer is co-author of this paper. Chapter 6 will be submitted to an ecological journal with Michael Huston as co-author.

Chapter 2

Patterns of Ice Accumulation and Forest Disturbance During Two Ice Storms in Southwestern Virginia

This chapter is a lightly revised version of a paper by the same name published in the journal *Physical Geography* in 1999 by Charles Lafon, Daniel Graybeal, and Kenneth Orvis:

Lafon, C.W., Graybeal, D.Y., and Orvis, K.H. Patterns of ice accumulation and forest disturbance during two ice storms in southwestern Virginia. *Physical Geography* 20:97 – 115.

Reprinted with permission from *Physical Geography*, Vol. 20, No. 2, pp. 97-115. © V.H. Winston & Son, Inc., 360 South Ocean Boulevard, Palm Beach, FL 33480. All rights reserved.

My use of "we" in this chapter refers to my co-authors and myself. My primary contributions to this paper include (1) selection of the topic and development of the problem into a work relevant to my study of ice storms as forest disturbances, (2) identification of the study areas and vegetation-sampling sites, (3) vegetation sampling and analysis, (4) most of the gathering and interpretation of literature, (5) most of the cartographic work, (6) pulling the various contributions into a single paper, and (7) most of the writing. Graybeal's main contributions were (1) analysis of synoptic-scale meteorological conditions associated with the two case-study ice storms, (2) writing related parts of the "Methods" section, (3) assisting with part of the vegetation-sampling, (4) producing initial drafts of some of the maps, and (5) helping me to clarify meteorological issues I did not understand initially. The main contributions of Orvis were (1) synthesizing and generating hypotheses on landscape-scale patterns of ice storm climatology, (2) initially pointing out the role of Appalachian cold air damming in ice storm climatology, and (3) providing critical insights on the presentation of the material in the paper. Further, I accomplished much of the development and refinement of the problem, particularly the identification of relevant literature, during a seminar on landscape climatology directed by Orvis. All three co-authors contributed to the vital section on topographic patterns in ice storm disturbance, although I list this under Orvis' contributions to underscore his predominant influence on the final appearance of the section.

Introduction

Disturbance is recognized as an important influence on such community parameters as species composition, species diversity, and vegetation structure (Loucks 1970; Huston 1979, 1994; Turner et al. 1997). Small-gap creation resulting from mortality of single canopy trees is generally considered to dominate disturbance regimes in the interior of the eastern forest region (Runkle 1990), but the weight of thick accumulations of freezing rain can bend, break, or topple trees over broad areas. Runkle (1990) concludes that more research is needed to assess the role of such intense, broad-scale disturbances in eastern forests and to determine the interplay between

topography and geographic patterns of disturbance. In this paper, we examine disturbance patterns in forests of southwestern Virginia that were affected by two major ice storms in 1994.

Ice storms occur more frequently in eastern North America than elsewhere on earth (Bennett 1959). The location and physiography of the continent permit occurrence of the extreme air mass contrasts necessary to produce freezing rain. In the Southeast, ice storms are typically associated with warm fronts (Gay and Davis 1993). Warm air advected (blown) over cold surface air creates a strong temperature inversion, and when the temperature of the warm layer is above freezing at its base, the precipitation falls as rain from the warm layer into the layer below. Freezing rain occurs where the surface cold layer is relatively shallow. Raindrops have insufficient time to refreeze and instead reach the surface in a supercooled state, freezing on impact into an icy coat (Ahrens 1991; Gay and Davis 1993). Huffman and Norman (1988) propose that freezing rain can also result from a supercooled warm rain process that involves coalescence of supercooled droplets in clouds with few ice nuclei available.

The frequency of ice storm disturbance varies spatially throughout North America. Maps presented by Bennett (1959) indicate that parts of the Midwest and Northeast experience the highest frequency of storms. The maps also portray a tongue of high frequency extending southward along the eastern Appalachians and western Piedmont, a pattern that probably reflects the influence of Appalachian cold air damming. Cold air damming occurs when cold air from a surface anticyclone over the Northeast flows toward the southwest and pools against the eastern slopes of the mountains, becoming entrenched as a shallow dome in Appalachian valleys and on the Piedmont (Richwien 1980; Bell and Bosart 1988; Michaels 1991).

An Appalachian cold air damming event is initiated when a surface high-pressure system moves eastward across the central United States. As the high approaches the northern Appalachians, northeasterly winds south of the center of the high begin to advect cold surface air from northeast to southwest along the eastern side of the mountains (Forbes *et al.* 1987). The

Coriolis force, which in the Northern Hemisphere deflects moving air to the right of its direction of movement, turns air from the east toward the mountains, causing adiabatic cooling and cold advection along the mountain slopes (Bell and Bosart 1988). Cooling and damming of air against the mountains creates a ridge of surface high pressure along the mountains that balances the Coriolis force and keeps air in the cold surface dome. The balance between the mountain-parallel pressure gradient force and the Coriolis force results in accelerated flow toward the southwest, causing continued cold-air advection from northeast to southwest (Bell and Bosart 1988). A low-level jet may develop parallel to the mountains in response to this orographically induced geostrophic balance (Bell and Bosart 1988). Once established, the shallow surface dome of high pressure in the eastern Appalachians and western Piedmont is maintained by the balance of forces within the dome, by continued cold advection from the northeast, by adiabatic cooling of air rising toward the mountains, by evaporative cooling as precipitation falls into the dry surface air from above, and by the establishment of an inversion above the cold dome that decouples the northeasterly flow within from the broader-scale southwesterly advection of warm air above (Forbes *et al.* 1987; Bell and Bosart 1988).

When air temperature in the cold dome is below freezing, rain falling through the dome from the warm, moist layer above may become supercooled, resulting in freezing rain. Cold air damming is probably responsible for important meso-β scale (Orlanski 1975) variations in ice storm climatology and, hence, disturbance regimes. The work of Michaels (1991), Gay and Davis (1993), and Konrad (1998) demonstrates that freezing rain and sleet occur more frequently in areas affected by Appalachian cold air damming than in surrounding regions.

Most parts of the southern Appalachians and adjacent Piedmont are subject to an average of 1.4 to 3.0 freezing rain events per year (Konrad, 1998). However, major storms that cause significant forest damage occur less frequently, and relatively little research has been conducted to characterize forest damage resulting from such events in the Appalachians. Abell (1934) and

Carvell *et al.* (1957) report briefly on damage in western North Carolina and eastern West Virginia, respectively. Whitney and Johnson (1984) examine disturbance in hardwood and pine forests affected by a major ice storm that struck southwestern Virginia in 1979. Nicholas and Zedaker (1989) identify effects of two ice storms in spruce-fir (*Picea-Abies*) forests of the Black Mountains, North Carolina. These studies indicate that species vary in their susceptibility and response to ice damage, and they suggest that ice storms have important consequences for tree form, stand dynamics, and forest composition in the Appalachians. The papers also report topographic variations in storm damage, but they provide little description of these patterns or the storm characteristics that may have contributed to their occurrence. Significant vegetation differences may develop across a landscape if ice storms repeatedly cause heaviest damage on particular topographic positions.

In this paper, we discuss multiple scales of ice accumulation and forest disturbance resulting from the 1994 storms in southwestern Virginia. We first examine synoptic-scale meteorology of the two 1994 storms. Second, we discuss topographic variations in forest damage. Heavy ice accretion was widespread during the storms (Shrader 1994; NCDC 1994c), but severe forest damage was mostly restricted to south- and east-facing mountain slopes, a pattern similar to that produced by a 1979 ice storm in southwestern Virginia (Whitney and Johnson 1984). Third, we quantify the level of canopy disturbance in several damaged stands. Finally, we compare patterns of damage associated with the 1994 events to those produced by several other ice storms.

Study Area

The Valley and Ridge physiographic province of southwestern Virginia is the focus of our research. The Valley and Ridge lies between the Blue Ridge to the southeast and the Appalachian Plateaus to the northwest. The province is characterized by long, roughly parallel, sandstone-capped ridges separated by valleys eroded into shales and limestones. Orientation of

structure and topography is typically northeast-southwest (Figure 2.1). The ridges are dissected in many sections by first-order streams, creating a landscape with spurs and hollows perpendicular to the main ridges. Oak (*Quercus*) forests are the primary cover type throughout much of the Appalachians, but composition varies considerably by topographic position. The chestnut blight fungus (*Cryphonectria parasitica*) invaded early in the twentieth century and killed all mature American chestnut (*Castanea dentata*), previously a major component of Appalachian forest canopies.

We sampled forest damage at nine sites in the Valley and Ridge province (Figure 2.1). Four sampling sites (B, C, D, and F) are located on the southeast side of Walker Mountain, where oaks are the primary canopy dominants. We sampled at five locations (A, E, G, H, and I) on nearby Little Walker Mountain. Sites A and E are located on east faces of spurs on the northwest side of the mountain, and oaks dominate the canopy at these sites. Site I is a table mountain pine (*Pinus pungens*) stand on the west face of a spur. Site G is a mixed mesophytic stand on an east-facing slope in a water gap, and site H is located in an oak-dominated forest on the southeast side of the mountain.

The crest of Walker Mountain is around 1125 to 1225 m elevation, and the top of Little Walker Mountain ranges between 900 and 1150 m. Relief in the study area varies between 120 and 485 m. Sampling sites are all located in the Jefferson National Forest between 730 and 940 m elevation. Hurricane Hugo damaged forests in the region during September 1989, but we used U.S. Forest Service air photos taken in 1990 to identify hurricane-damaged stands. We did not sample in locations that sustained significant hurricane damage. The ice storm of January 1979 (NCDC 1979b; Whitney and Johnson 1984) may have damaged some of the stands.

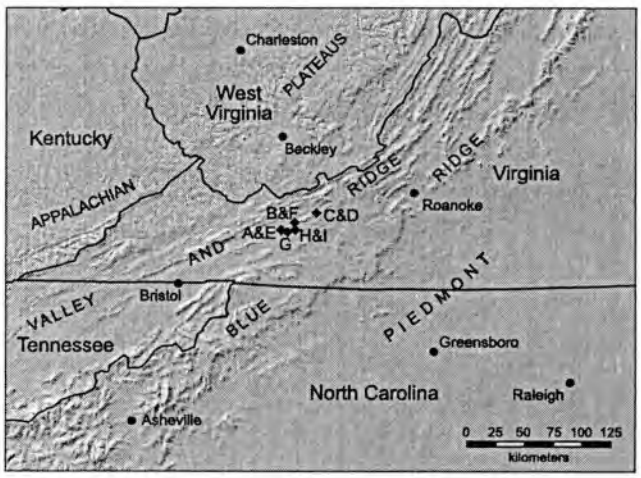

Figure 2.1. Study area. Labeled diamonds indicate the locations of forest damage sampling sites.

Methods

To assess the meteorology of the 1994 storms, which occurred 10 – 11 February and 1 – 3 March, we analyzed upper atmospheric and surface conditions. We obtained upper air patterns from NOAA-CIRES Climate Diagnostics Center (1998) and data for surface maps from NCDC (1994d). We also used these data sources to examine atmospheric conditions in more detail at Roanoke, Virginia, a first-order weather station approximately 100 km northeast of our forest sampling sites. We estimated the thickness of atmospheric layers over Roanoke by linear interpolation from isobaric surface maps obtained from NOAA-CIRES Climate Diagnostics Center (1998). We examined U. S. Forest Service air photos taken in May 1994 to investigate topographic variations in forest damage.

To characterize the degree of canopy disturbance within forest stands, we measured canopy cover and loss of basal area in damaged stands. We arranged three parallel transects, spaced 25 m apart and aligned with slope contours, at each of the nine sampling sites. Transects were 100 m in length. We defined transect midpoints by beginning at an arbitrary location near the top or bottom of each site. We chose a random compass direction within 45° of slope aspect and measured a random distance between 0 and 10 m along that bearing to define the midpoint of the upper or lower transect at the sampling site. We established remaining transects at 25 m intervals from the initial transect. At site G, one of the transects is only 90 m long, and we established only two transects at site H. At site C, we first established a transect endpoint, rather than a midpoint, to ensure that the endpoints did not fall on a nearby road. At site D, we used four 25 m long transects to sample the narrow, relatively mesic portion of a shallow hollow.

We measured canopy and subcanopy cover along each transect. We defined canopy trees as those with diameter at breast height (DBH) at least 25 cm, as suggested by Runkle (1992). We also measured cover of subcanopy trees (20 cm $\leq$ DBH $<$ 25 cm), because smaller trees were part

of the overstory in some places. We calculated percent canopy and subcanopy cover for each site, based on the proportion of transects covered by forest canopy or subcanopy.

We recorded DBH of each tree, including trees killed or injured by ice damage, with DBH at least 10 cm and whose base was within 5 m of a transect. At sites A, B, C, and D, we only included trees within 3 m of a transect. Using these individual-tree data, we calculated pre-storm basal area (m^2/ha) for each site. We then computed post-storm basal area by omitting all trees that had died from ice damage or that had boles bent, tilted, snapped, or broken by the ice.

Results and discussion

Synoptic-scale meteorological conditions

Prior to the 10 – 11 February ice storm, an upper air trough was centered over eastern Canada. The trough moved eastward and ushered in a large surface anticyclone, bringing persistent subfreezing temperatures to the Southeast. By 1200h UTC 10 February, a slight surface pressure trough had formed in the south-central Appalachians, and a coastal cyclone was developing in the western Gulf of Mexico (NOAA 1994). Associated with this surface low-pressure system, a deepening upper-level trough over the central U.S. was moving eastward, advecting warm air from the south and thickening the warm layer of air aloft over the study area (Figures 2.2A, C). The coastal cyclone had evolved two centers by 1200h UTC 11 February, one over Alabama and the other near Cape Hatteras (Figure 2.3A).

A shallow layer of cold surface air was dammed against the eastern sides of the mountains, creating a surface pressure ridge that is manifest in the map of surface isobars as a U-shaped pattern east of the mountains (Figure 2.3A). The relative locations of the upper air troughs described above are typical for Appalachian cold air damming events. The northern trough is far enough ahead of the southern trough that the cold surface air affects the damming region prior to coastal cyclonic development associated with the southern trough (Bell and Bosart 1988). The presence of the cold air dome is clearly evident in the potential temperature map for

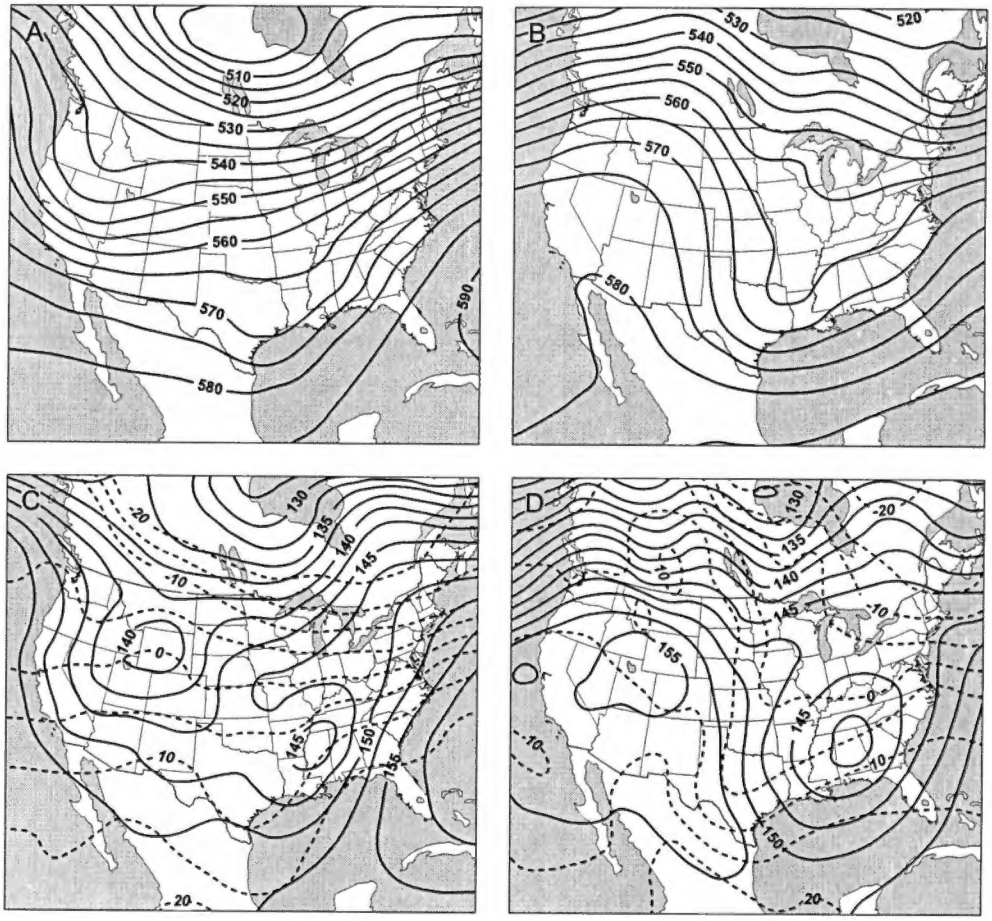

Figure 2.2. Meteorological conditions for (left) 11 February 1994 and (right) 2 March 1994: (A-B) 500 mb geopotential heights (dam); (C-D) 850 mb geopotential heights (dam, solid lines) and temperatures (°C, dashed lines). Mapped variables are daily averages.

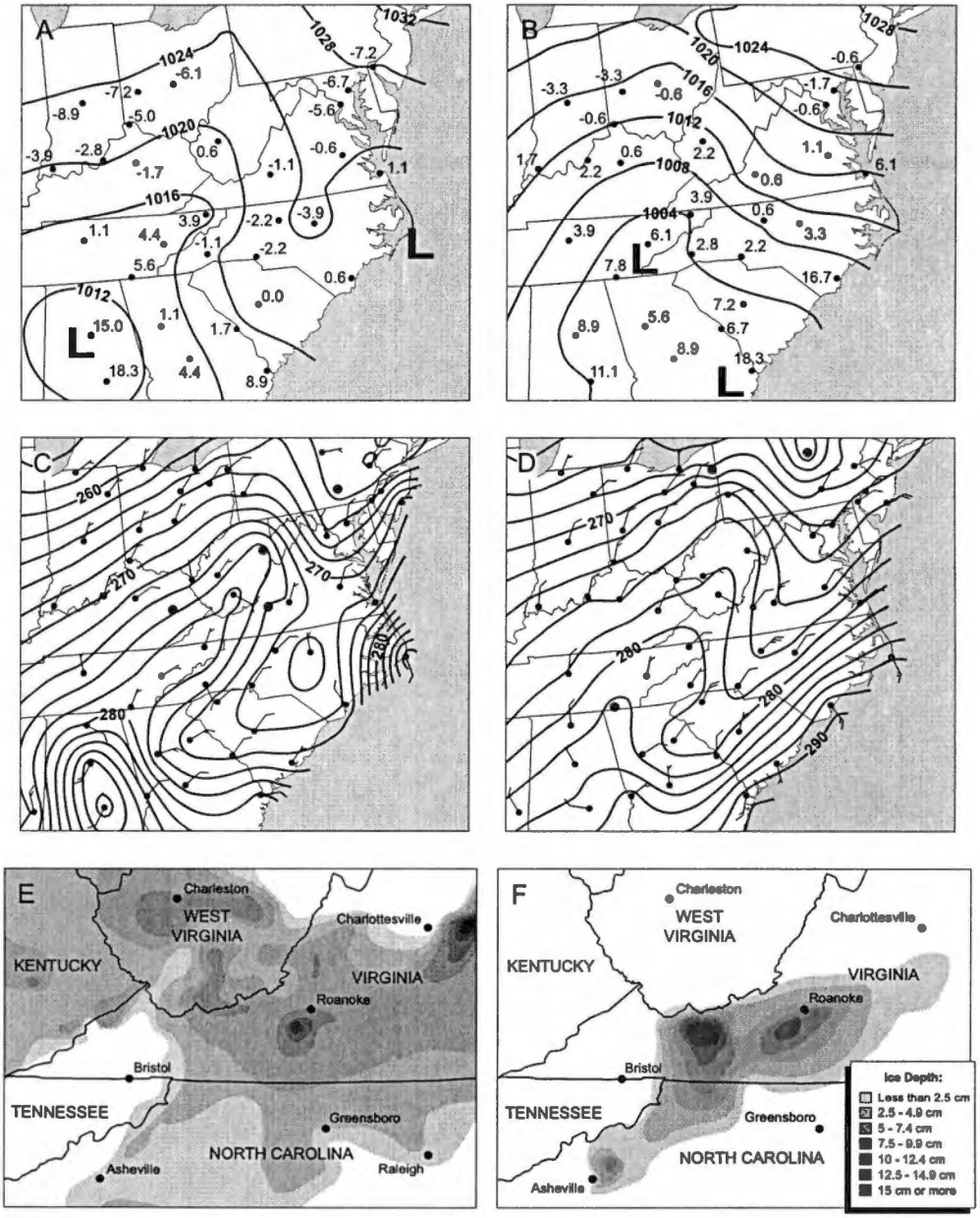

Figure 2.3. Surface meteorology and ice deposition for (left) 11 February 1994 and (right) 2 March 1994: (A-B) surface pressure (mb) and temperature (°C), 1200 UTC; (C-D) potential temperature (°K) and surface winds, 1200 UTC; and (E-F) total ice deposition (cm) per storm event.

11 February (Figure 2.3C), which also portrays northeasterly surface winds advecting cold air to the southwest. The cold air dome is well established where wind barbs are parallel to isentropes, and advection is occurring where they cross.

The storm brought heavy precipitation to the study area. Roanoke (elevation 358 m) recorded 61.2 mm liquid-equivalent precipitation on 10 February and 24.1 mm on 11 February, a storm total of 85.3 mm (NOAA 1994). The high precipitation total and relatively large variations in hourly precipitation amounts (NCDC 1994b) suggest convective precipitation may have occurred. Forbes *et al.* (1987) and Rauber *et al.* (1994) report convective cells associated with warm advection during ice storms.

The vertical temperature profile during the event supported freezing rain (Table 2.1), with a shallow layer of cold air near the surface overlain by a deep, warm layer. The thickness of 1300 m for the layer between 1000 and 850 mb was in the range reported for ice storms in the Southeast (Keeter and Cline 1991; Gay and Davis 1993; Table 2.2). Also, dew points at Roanoke were near dry-bulb temperatures, particularly during the latter half of the storm (Table 2.3), which discourages evaporative cooling and phase change of supercooled droplets while promoting retention of the liquid form and freezing rain (Ahrens 1991).

Surface winds at Roanoke during most of 10 February and into 11 February were persistently from the southeast before calming later (Table 2.3). Southeasterly surface winds prevailed throughout the storm at Beckley, West Virginia (elevation 765 m; NCDC, 1994d). The prevalence of southeasterly winds at the height of the event can be inferred for our field study area from the surface pressure field (Figure 2.3A) and the configuration of the 850 mb surface (Figure 2.2C). However, the inference of southeasterly winds from 850 mb conditions is tentative, because flow within the surface cold layer may have been largely decoupled from the flow above the inversion (Bell and Bosart 1988).

Table 2.1. Vertical profiles of temperature over Roanoke, VA, for each ice event.

	11 February		2 March	
Height	Elevation (m)	Temperature (°C)	Elevation (m)	Temperature (°C)
500 mb	5710	–13.5	5585	–17.5
700 mb	3075	1.0	2995	–3.0
850 mb	1500	3.0	1440	1.0
Surface	362	–1.1	362	0.6

Table 2.2. Thicknesses of key diagnostic layers of the atmosphere for each ice storm.

Atmospheric layer	Approximate thickness (m) over Roanoke, VA 11 Feb 1994	2 Mar 1994
1000 - 500 mb	5510	5455
850 - 700 mb	1575	1555
1000 - 850 mb	1300	1310

Table 2.3. Three-Hourly Surface Meteorological Conditions at Roanoke, VA, 10 – 11 February 1994 and 1 – 2 March 1994.

UTC time	0600	0900	1200	1500	1800	2100	0000	0300
Local time (EST)	0100	0400	0700	1000	1300	1600	1900	2200
10 February								
Temperature (°C)	1.7	0.0	–0.6	–3.9	–5.6	–6.7	–6.7	–6.1
Dew point (°C)	–5.6	–6.7	–3.9	–6.7	–7.2	–8.3	–7.8	–6.7
Wind direction	NW	NW	S	SE	SE	SE	SE	S
Wind speed (kt)	9	6	5	12	13	11	5	4
11 February								
Temperature (°C)	–3.9	–1.1	–1.1	0.0	0.0	0.6	0.6	0.6
Dew point (°C)	–4.4	–1.7	–1.7	–0.6	–0.6	–0.6	0.0	0.0
Wind direction	N	S	Calm	Calm	Calm	Calm	Calm	Calm
Wind speed (kt)	4	4	0	0	0	0	0	0
1 March								
Temperature (°C)	-2.2	-1.7	0.6	1.7	1.1	0	0	0
Dew point (°C)	-9.6	-6.7	-6.1	-7.8	-4.4	-0.6	-0.6	-0.6
Wind direction	Calm	Calm	S	S	N	Calm	SE	E
Wind speed (kt)	0	0	3	4	5	0	4	3
2 March								
Temperature (°C)	0	0	0.6	0.6	0.6	0	0	-0.6
Dew point (°C)	-0.6	-1.1	-1.1	-1.1	-0.6	-0.6	-0.6	-1.1
Wind direction	N	NE	NE	NE	NE	Calm	N	NE
Wind speed (kt)	5	9	11	12	6	0	7	7

The 10 – 11 February storm produced freezing rain, sleet, and snow throughout a large portion of the Southeast (NCDC 1994a). Figure 2.3E illustrates broad-scale patterns of relative storm severity in southwestern Virginia and surrounding regions. The map is based on published information about ice storm extent (NCDC 1994c; Jones *et al.* 1997) and ice depth (NCDC 1994a). Surface temperatures were above freezing in the Tennessee Valley, along the axis of the surface pressure trough (Figure 2.3A), which accounts for the lack of ice accumulation in eastern Tennessee and the southwestern corner of Virginia.

A similar progression of meteorological events occurred during the 1 – 3 March storm. Prior to development of the storm, an upper air trough over Canada brought a cold Canadian anticyclone to the eastern U.S. (NOAA 1994). A trough over the central U.S. on March 1 deepened strongly, forming a surface cyclone center off the southern Texas coast and bringing it to southern Georgia by 1200h UTC 2 March (Figures 2.2B, D, and 2.3B). Cold air was again entrenched along the mountains (Figures 2.3B, D). Along with a secondary low in eastern Tennessee, the system had brought 53.6 mm liquid-equivalent precipitation to Roanoke during the 48 hours prior to 1200h UTC 3 March (NOAA 1994). Hourly precipitation variations were less pronounced than during the February storm (NCDC 1994b). The eastward-moving trough aloft advected warm air from the south, resulting as before in a typical freezing rain vertical temperature profile (Table 2.1). Thicknesses of the 1000 – 500 mb, 1000 – 850 mb, and 850 – 700 mb layers were within the range reported for the Southeast (Keeter and Kline 1991; Gay and Davis 1993; Table 2.2).

Surface winds at Roanoke changed from southeasterly to northeasterly during the event (Table 2.3). At Beckley, southeasterly winds prevailed for most of the storm before shifting to easterly or northeasterly (NCDC 1994d). The surface pressure field suggests easterly or northeasterly winds for our study sites (Figure 2.3B), and 850 mb winds were probably southeasterly (Figure 2.2D). Figure 2.3F indicates the extent of ice deposition.

Topographic patterns of disturbance

Inspection of U. S. Forest Service air photos taken in May 1994 reveals that broad swaths of heavy damage exist on the southeast, windward, sides of major ridges. Northwest sides and valleys are generally free of substantial damage. Severe disturbance also exists on east-facing slopes of spurs perpendicular to the main ridgelines. The latter pattern is particularly evident on northwest (lee) sides of mountains, where distinct strips of severe damage along east faces of spurs alternate with relatively undamaged patches. Field inspection confirms the generality of these patterns. Damage boundaries are typically sharp, on the order of a few meters.

Landscape-scale patterns appear to be related to wind direction during the ice storms, with most severe damage occurring on windward slopes. Southeasterly winds prevailed during the February storm, and winds during the March storm varied from southeasterly to northeasterly. Several hypotheses might explain the observed topographic patterns of damage. These hypotheses can be classified into two general categories: (1) orographic effects on precipitation intensity and (2) variations in the proportion of rain that accretes as ice.

Plain orography, involving smooth forced ascent of air, is one mechanism that may enhance precipitation on mountain slopes, but this explanation is too simple to account for the observed patterns of ice damage. The scale of features is too small for significant lift, and the time interval during lift is too short for the condensation, coalescence, and falling necessary to produce rain. Also, because precipitation originates in the warm air aloft, the pattern of orography will be blurred by wind shear and downwind drift during droplet fall. Furthermore, during the 1994 ice storms, the warm air aloft flowed from the southwest (NOAA-CIRES 1998), not the southeast. The air aloft does not even encounter surface topographic features. The most probable result of broad-scale orographic lifting over both the mountains and the associated cold air dome is enhanced precipitation, particularly convection, over a large area.

The seeder-feeder mechanism enhances precipitation in moderate-sized mountains and low hills (Smith 1989) and may contribute to heavy ice damage on mountain slopes in the southern Appalachians. Condensation occurs in air that is forced over a mountain, and droplets falling from the upper-level (seeder) cloud grow in size as they fall through this lower (feeder) cloud. Patterns of rainfall enhancement in southern New England and Pennsylvania are consistent with seeder-feeder orography (Passarelli and Boehme 1983; Barros and Kuligowski 1998). However, the mechanism does not explain the sharp boundaries of heavy ice damage, because rain drops drift during fall, even through low clouds, and because feeder clouds would have to condense rapidly on the upwind side of a mountain and then re-evaporate immediately beyond the ridge top. In addition, seeder-feeder dynamics may be rendered less effective by a strong inversion, such as exists during an ice storm. Warm drops falling from above the inversion should tend to shrink by evaporation while the cold cloud droplets grow by condensation, offsetting the growth of the larger drops by collision.

Saturation-equivalent seeder-feeder orography is another possibility – saturation or super-saturation in air moving uphill enhances the effectiveness of precipitation falling from above. This hypothesis avoids the problem of condensation time. However, drift during fall remains an issue, and the thermodynamics of condensation will still not favor growth of the warm raindrops.

Sharp damage boundaries on both major ridges and spurs may result from greater raindrop interception rates on surfaces normal to raindrop fall vectors (windward slopes) than on surfaces more parallel to the fall vectors (lee slopes). Empirical and modeled results of Sharon (1980) and Poreh and Mechrez (1984), respectively, indicate that inclination of raindrop trajectories during wind promotes increased precipitation on the windward side of a ridge, which lies in the path of windblown rain. The lee side is sheltered from some of the hydrometeors and receives less precipitation. This process should be most effective for medium-sized drops heavy

enough to fall onto the windward slope but still light enough to be carried over the lee side, creating a rain shadow.

Two mechanisms could influence ice damage patterns by altering the proportion of rain that freezes to surfaces. The first of these involves variations in twig surface thermodynamics between windward and lee slopes. On a lee slope with little wind, high relative humidity, and insignificant horizontal temperature advection, cooling of twig surfaces by evaporation and advection may not exceed heat buildup by phase change, and ice may persist, grow slightly, or melt. However, such cooling may maintain or reduce temperatures of ice on windward branches, promoting ice accumulation. This process could produce sharp damage boundaries.

The second mechanism involves near-surface aerodynamics of falling droplets. Cooling, supercooling, or freezing of a water droplet is a function of the length of time the droplet spends falling through subfreezing air. The upward motion of air crossing a mountain should reduce raindrop fall velocities and increase the time available for droplets to become supercooled. Terminal velocity of water drops varies by drop size (Nieburger *et al.* 1982), and this process could affect the thermodynamic state at which droplets of certain sizes arrive at the surface. The larger the size of the droplet, the shorter the duration of fall, and the slower the rate of temperature change. Depending on the upslope/downslope component of flow and the mean and distribution of drop sizes, this mechanism could significantly affect the amount of time that droplets fall through the lower air mass, and hence the distribution of thermodynamic states of droplets when they contact the surface. Adiabatic cooling of lifting air would render this process more effective, because as air is warmed by falling drops, it is replaced by freshly cooled air. In sheltered locations with stagnant conditions, it is more likely that air would warm over time.

The near-surface aerodynamics mechanism may also contribute to the pattern of damage on lee-side spurs. Airflow patterns characterized by downvalley vortex roll, up east sides of spurs

and down west sides, are likely and could produce the pattern of heavy damage on east faces of lee-side spurs.

It is doubtful that one of these mechanisms alone produced the observed forest damage patterns in southwestern Virginia. Several processes, in combination, are probably responsible. For example, the seeder-feeder mechanism may have enhanced precipitation over the major ridges, and near-surface aerodynamics can help explain the pattern of damage on both southeast-facing mountain slopes and east faces of spurs. However, the sharp damage boundaries likely result from effects of rainfall angle or cooling of twig surfaces on windward slopes.

Stand damage

At the scale of individual stands, ice storm damage created large, interconnected gaps. Tangled piles of limbs and boles strewn through the stands indicate that the impact of falling trees often triggered damage in neighboring trees already strained by heavy ice loads. Compared to eastern hardwood forests disturbed by fine-scale gap dynamics, in which gaps are created at an annual rate of 0.5 – 2.0% of total land area (Runkle 1982; Lorimer and Frelich 1994), stands damaged by these recent ice storms are considerably more open (Figure 2.4). The lower transect (G-1) in Figure 2.4 is located in a section of the stand that sustained less ice storm damage, and it provides a contrast to the catastrophically disturbed areas above. Total overstory cover varies between 25% and 64% (Table 2.4). Ice damage contributed to substantial basal area loss, approximately 30 – 60%, in all sampled stands (Table 2.5). The disturbance will probably release many understory trees from suppression and cause long-term successional changes.

Site I, the table mountain pine stand, is located in a topographic position sheltered from severe ice storm disturbance. This fact accounts for the relatively moderate level of overstory damage at site I (Tables 2.4 and 2.5). The stand is on a west-facing spur on the northwest side of Little Walker Mountain. Storm damage is heaviest on slopes facing south or east, but table mountain pine stands are restricted to west-facing slopes. Southern pines, such as table mountain

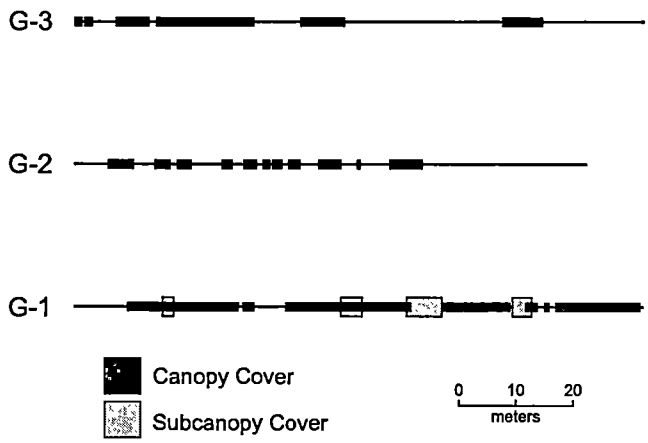

Figure 2.4. Overstory damage pattern at site G. Each line represents a 100 m transect, and bars represent portions of the transect covered by canopy or subcanopy. Transect G-2 is 90 m long.

Table 2.4. Percent cover data for each site.

Site	Canopy cover (%)	Subcanopy cover (%)	Total overstory cover (%)[a]
A	27	11	37
B	23	20	41
C	53	9	57
D	22	3	25
E	44	12	52
F	41	22	58
G	50	5	53
H	28	7	31
I[b]			64

[a]Cover of canopy and subcanopy trees (i.e., all trees with DBH ≥ 20 cm).
[b]At the table mountain pine stand (site I), where many canopy trees have small stems, we define all trees with DBH ≥ 10 cm as overstory.

Table 2.5. Basal area changes resulting from ice damage.

Sampling site	Pre-storm basal area (m^2/ha)	Post-storm basal area (m^2/ha)	Basal area loss (%)
		Overstory trees (stems with DBH ≥ 20 cm)	
A	18.5	7.7	58.4
B	21.8	15.0	31.3
C	32.2	24.7	23.3
D	32.2	20.8	35.4
E	24.4	15.6	36.2
F	24.0	17.2	28.3
G	36.3	18.1	50.3
H	23.1	8.9	61.4
I[a]	23.9	16.8	29.9
		Understory trees (stems with 10 cm ≤ DBH < 20 cm)	
A	5.1	2.7	46.0
B	9.1	3.7	59.3
C	5.1	2.5	50.4
D	4.8	2.8	40.8
E	3.5	1.8	50.1
F	7.4	2.4	67.8
G	4.5	1.7	63.3
H	2.9	0.7	75.6
		All trees combined (stems with DBH ≥ 10 cm)	
A	23.6	10.5	55.7
B	30.9	18.7	39.6
C	37.3	27.2	27.0
D	37.0	23.7	36.1
E	27.9	17.3	38.0
F	31.4	19.6	37.6
G	40.9	19.7	51.7
H	26.0	9.6	63.0
I	23.9	16.8	29.9

[a]At the table mountain pine stand (site I), where many canopy trees have small stems, we define all trees with DBH ≥ 10 cm as overstory.

pine, pitch pine (*Pinus rigida*) and Virginia pine (*P. virginiana*), are in fact highly vulnerable to ice damage (Whitney and Johnson 1984). Williams (1998) proposes that ice storms favor the conversion of table mountain pine-pitch pine stands to oak dominance. Perhaps ice storms have contributed to the spatial distribution of pine stands on the landscape.

Patterns of forest disturbance from other ice storms

The magnitude of damage we report is typical for major ice storms in the southern Appalachians. Rhoades (1918), Abell (1934), Carvell *et al.* (1957), Whitney and Johnson (1984), and Nicholas and Zedaker (1989) describe similar levels of forest disturbance in the mountains of South Carolina, North Carolina, Virginia, and West Virginia. In addition, two significant ice storms occurred in the southern Appalachians during 1998, causing damage in western Virginia and eastern Tennessee of magnitudes comparable to disturbance resulting from the 1994 storms (Lafon personal observation).

The topographic patterns of disturbance produced by the 1994 storms may also be typical in parts of the Appalachians. A major ice storm that affected portions of southwestern Virginia on 20 – 21 January 1979 produced heaviest damage on southeast exposures (Whitney and Johnson 1984). Meteorological conditions during the 1979 event were similar to those associated with the 1994 storms – a northern upper air trough contributed to cold air damming at the surface, followed by a southern trough that spawned coastal cyclogenesis and warm advection over the cold dome (NOAA 1979). Persistent southeasterly winds occurred at Roanoke (NCDC 1979c). Rhoades (1918) also reports heaviest damage on south- and east-facing slopes for a March 1915 ice storm in the Blue Ridge of North and South Carolina.

A recent (23 – 24 December 1998) ice storm produced a relatively similar topographic pattern of disturbance in the Great Smoky Mountains National Park, Tennessee. Cold air was widespread in the eastern United States during this event. Northeasterly and northerly winds prevailed at Knoxville, about 20 km northwest of the park (NCDC 1998). The main topographic

features have an east-west or northeast-southwest orientation, and limited field observation indicates that severe forest disturbance is confined to northeast faces of spurs and adjacent north-facing hollow bottoms on the north sides of ridges. It appears that less ice deposition occurred on south and southeast sides of ridges. However, southern pines sustained moderate losses on the southeast side of Chilhowee Mountain, a ridge just outside the park.

Aspect-related disturbance patterns have also been documented farther north, on the Allegheny Plateau of New York and Pennsylvania. An ice storm that occurred over 17 – 19 March 1936 caused greatest damage on slopes facing north or east (Downs 1938). East-facing slopes sustained the heaviest ice loads during a 27 – 30 December 1942 storm (Spaulding and Bratton 1946). A 3 – 4 March 1991 event produced more severe damage on north- and east-facing slopes than on other aspects (Seischab *et al.* 1993), and hourly weather data reveal that northeasterly winds prevailed throughout the storm at nearby Rochester, New York (NCDC 1991).

Two major ice storms that occurred in southern and eastern Wisconsin during March 1976 produced heaviest forest damage on northeast exposures (Bruederle and Stearns 1985). Winds were from the northeast, but Bruederle and Stearns (1985) attribute the topographic pattern to high wind velocity (up to 80.6 km/h), not to differences in ice accretion. Siccama *et al.* (1976) report that, in Connecticut, forests on a slope facing south-southwest sustained severe disturbance as a result of a grape vine (*Vitis*) infestation on that exposure. Ice accumulating on the vines increased the load borne by trees.

Elevational zonation in ice damage is another common topographic pattern. Most evidence indicates that ice accretion is typically heavier and occurs more frequently at higher elevations in the Appalachians (Abell 1934; Carvell *et al.* 1957; Bennett 1959; Williams 1960; Nicholas and Zedaker 1989; Konrad 1998). A February 1998 ice storm disturbed forests on all topographic positions above 825 m in the Blue Ridge of southwestern Virginia (Lafon personal

observation). In contrast, damage is sometimes most severe in valleys (Rhoades 1918; Boerner *et al.* 1986), and a January 1998 ice storm in the Adirondacks of New York caused disturbance on all topographic positions below about 750 m elevation (Lafon personal observation). The vertical temperature profile is likely the main factor determining which elevation zones sustain heaviest damage from a particular storm, but precipitation enhancement (e.g., seeder-feeder mechanism) probably also contributes to elevational patterns.

Summary and conclusions

This paper contributes to an understanding of how one agent of broad-scale disturbance affects Appalachian forests. Catastrophic fires and major windstorms occur infrequently in central hardwood forests, and fine-scale gap dynamics probably represent the primary mechanism driving canopy replacement in much of the region (Runkle 1990). However, forest damage sampling reveals that the 1994 ice storms caused major canopy and basal area losses in southwestern Virginia. Forests will undoubtedly require several decades to recover. The frequency of ice storm recurrence, a relatively unexplored topic, should determine the influence of ice damage on long-term stand dynamics. Where major ice storms recur on the order of 20 years, as is perhaps the case in parts of the Appalachians (Abell 1934; Whitney and Johnson 1984), these catastrophic events may be the primary component of the disturbance regime.

Cold air damming probably contributes to considerable differences in disturbance frequency throughout the Appalachian region. Cold air damming occurred during both storms in our study. The two storms are probably representative of meso-β scale spatial variations typical in many ice storms that affect the southern Appalachians, but our study area is located west of the regions most frequently affected by damming (e.g., the western Piedmont and Shenandoah Valley).

The 1994 storms also caused pronounced spatial variations in disturbance severity at the scale of landforms. Forests on south- or east-facing mountain slopes, the windward aspects,

sustained much heavier damage than stands at other sites, and several mechanisms could be responsible for this damage pattern. Such fine-scale patterns appear to be common during ice storms. If the same slope exposures or elevation zones in a given landscape consistently experience heavy ice accretion, substantial vegetation differences may develop between those sites and nearby portions of the landscape characterized by different ice storm climatologies. In southwestern Virginia, forests on south- and east-facing mountain slopes may be characterized by more frequent ice storm disturbance than stands at different topographic positions. Confinement of southern pine stands to lower elevations and west faces of spurs are vegetation patterns that may be partly explained by variations in the landscape climatology of ice storms.

Resolving spatial characteristics of ice storm disturbance will require much additional research on the climatology of freezing rain, particularly at finer scales. For example, Forbes *et al.* (1987) identify a low-level northeasterly jet near the top of the cold dome for a January 1980 ice storm associated with cold air damming. More work is needed to determine whether this situation is typical and to understand implications of the low-level jet for topographic patterns of disturbance in the mountains. Additionally, to interpret the role of ice storms as forest disturbances, it will be necessary to study forest responses along environmental gradients and under regimes of differing ice storm frequency. Variations in ice storm climatology probably contribute to numerous patterns of vegetation composition and diversity across different spatial scales.

Chapter 3

Forest Disturbance from Four Recent Ice Storms in Virginia and New York

Introduction

Periodic severe ice storms produce intense disturbances in deciduous forests of eastern North America that may have important consequences for long-term forest dynamics. Although fine-scale gap dynamics dominate disturbance regimes over much of the eastern forest region (Runkle 1990), ice storms subject these forests to broader-scale damage. Ice storm damage results when freezing rain accumulates heavily on trees, breaking limbs, bending or breaking stems, or toppling trees across entire slopes (Whitney and Johnson 1984; Seischab *et al.* 1993; Lafon *et al.* 1999).

The occurrence of freezing rain is dependent on the vertical structure of the atmosphere. When a sufficiently deep layer of warm air is advected over a relatively shallow surface cold layer, snow falling through the warm layer may melt. The raindrops become supercooled as they fall through the underlying cold layer and freeze on contact into an icy coat (Ahrens 1991; Gay and Davis 1993). On a global scale, ice storms most commonly occur in eastern North America (Bennett 1959), where extreme air mass contrasts can easily develop as a result of continental location and physiography.

Previous research on ice storm damage in southern Appalachian forests includes work by Carvell *et al.* (1957) in eastern West Virginia; by Whitney and Johnson (1984) and Warrillow and Mou (1999) in southwestern Virginia; and by Abell (1934) and Nicholas and Zedaker (1989) in western North Carolina. Boerner *et al.* (1986) characterized damage in an Appalachian Plateau watershed in Ohio. In the Northeast, Spaulding and Bratton (1946), Lemon (1961), and Seischab *et al.* (1993) worked in New York, Siccama *et al.* (1976) in Connecticut, Melancon and Lechowicz (1987) in southern Quebec, and Downs (1938) in New York and Pennsylvania.

Additional studies have been conducted in the midwestern and the southeastern United States (McKellar 1942; Bruederle and Stearns 1985; DeSteven and Matthiae 1991; Rebertus *et al.* 1997). Most of these studies focused on one forest type or a small area, but a few, particularly Whitney and Johnson (1984) and Seischab *et al.* (1993), reported ice storm effects among a number of species in several forest types. A number of these studies classify each affected tree into one of three or four categories, depending upon the severity of damage. From these papers it can be concluded that patterns of ice storm damage are influenced by several factors, including slope of the site, tree size, crown position, and interspecific differences in wood strength and canopy architecture. However, only one paper presents a multivariate approach to predict tree damage from ice storms. Seischab *et al.* (1993) obtained a multiple regression model to predict percent canopy damage from prevalence of unsound stems, stem diameter, and slope angle.

In this paper, I describe ice storm damage in six distinct forest types in the southern Appalachian Mountains of southwestern Virginia and the Adirondacks of northern New York. Two major ice storms affected southwestern Virginia in 1994, one on February 10 – 11 and the other on March 1 – 3. Another storm occurred on February 4 – 6, 1998. A major storm damaged Adirondack forests on January 4 – 9, 1998. In an earlier paper, my co-authors and I examined topographic-scale variations in ice storm damage resulting from the 1994 storms in Virginia (Lafon *et al.* 1999). We found that severe damage was restricted to east- and southeast-facing slopes, a pattern which appears to be common in the Appalachians. Damage from the 1998 storms was related to elevation, with severe damage confined to high-elevation forests in Virginia and to low-elevation stands in New York. Conspicuous aspect-related effects were not present in locations affected by the 1998 storms.

My objective in this paper is to characterize patterns of damage within ice-damaged stands and among individual trees in the stands. I examine canopy cover, pre-storm and post-storm species composition, interspecific variations in susceptibility to different types of damage,

tree and site factors that contribute to tree damage, and possible long-term consequences of ice storm disturbance for forest dynamics. A related objective is to create a multivariate model that can be used to predict damage characteristics of individual trees in order to incorporate simulations of ice storm disturbance into individual-based models of stand dynamics.

Study areas

Study sites in western Virginia are located in the Valley and Ridge physiographic province and in the Blue Ridge province (Figure 3.1). The Valley and Ridge sites were affected by both 1994 events. The Blue Ridge stands probably sustained minor damage from these storms, but major damage occurred during the February 1998 storm. Topography of the Valley and Ridge is characterized by long, roughly parallel ridges of resistant sandstones separated by valleys underlain by carbonates and shales. Structural and topographic trends generally exhibit a northeast-southwest alignment (Figure 3.1). In southwestern Virginia, valley elevations are mostly around 600 – 800 m above sea level, and ridgetops are typically between 900 and 1400 m. The major ridges are dissected to varying degrees by first-order streams running perpendicular to the main ridges.

The Blue Ridge is an upland underlain by metamorphic and igneous rocks. The southeastern edge of the Blue Ridge is an escarpment rising approximately 500 m above the Piedmont erosional surface. Typical elevations of the Blue Ridge crest in this section of Virginia are 800 – 1000 m, but farther south peaks exceed 2000 m.

The New York study sites are located in the northern part of the Adirondack Mountains (Figure 3.2). The Adirondacks are formed from metamorphic and igneous rocks that have been uplifted and exposed to surface processes, including Pleistocene glaciation (McMartin 1994). Much of the northern area of the Adirondacks is a hilly region between 400 and 800 m elevation. Elevations exceed 1600 m in the high peaks area to the south.

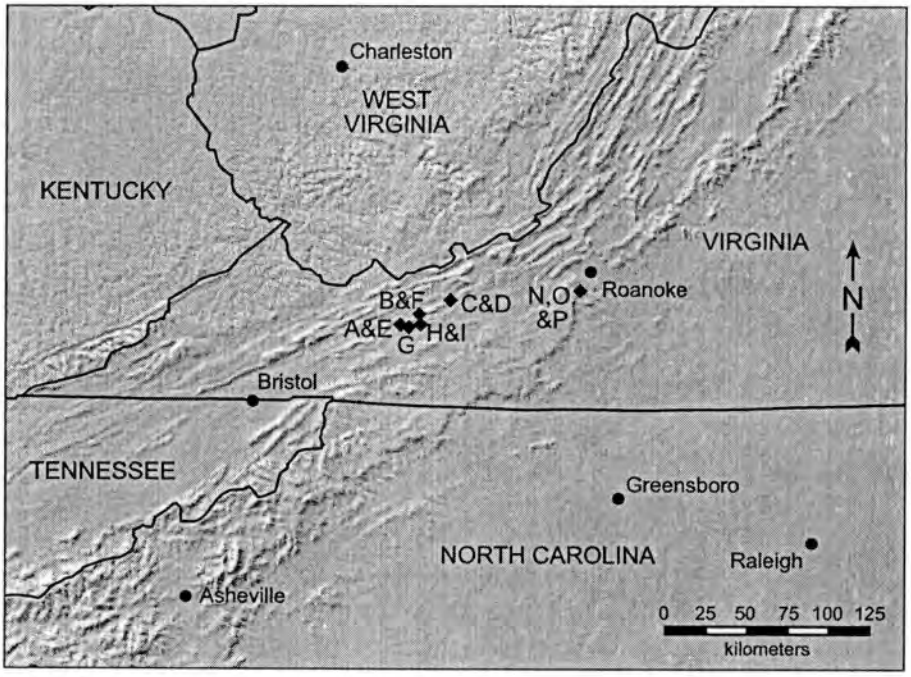

Figure 3.1. Study area – Virginia. Labeled diamonds indicate the locations of forest damage sampling sites.

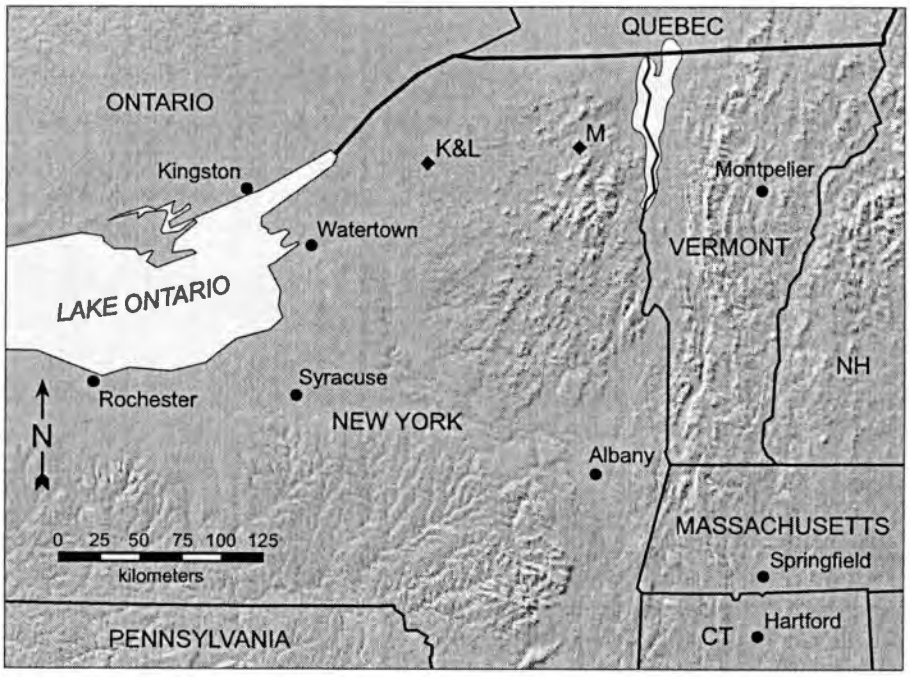

Figure 3.2. Study area – New York. Labeled diamonds indicate the locations of forest damage sampling sites.

Oak (*Quercus*) forests are the primary vegetation cover in much of the Appalachian region, but composition varies markedly across different topographic positions. Generally, mesophytic forests are concentrated on north-facing ravine slopes, concave slopes, and valley floors (Whittaker 1956; Hack and Goodlett 1960; Quarterman *et al.* 1972). Oak forests occupy broad, semi-mesic to semi-xeric zones, and southern pines (*Pinus*) are restricted to ridgetops, convex "noses," and recently disturbed sites. Conspicuous vegetation differences exist between north-facing and south-facing slopes, with that on south-facing slopes exhibiting a more xerophytic composition (Smith 1986). Imprints of human land use, including widespread timber harvest, farming and abandonment, and disease introduction, are evident in current forest composition and structure. In the early twentieth century, the exotic chestnut blight fungus (*Cryphonectria parasitica*) killed all mature individuals of American chestnut (*Castanea dentata*), a dominant species in Appalachian forests. Adirondack forests are dominated primarily by northern hardwood species at the low to middle elevations and by spruce (*Picea*) and fir (*Abies*) at higher elevations. Timber harvest is the primary human impact over much of the Adironacks (McMartin 1994).

Methods

Sampling Locations

Four of the six forest types I sampled are located in the Valley and Ridge province. I selected nine sampling sites within these four forest types (Figure 3.1, sites A – I). The sites are clustered on Jefferson National Forest lands on two adjacent ridges, Walker Mountain and Little Walker Mountain. Elevations at these sites are roughly 750 – 960 m, and slopes vary between 10° and 50°. The four general forest types are (1) oak forests dominated by chestnut oak (*Quercus prinus*), black oak (*Q. velutina*), and scarlet oak (*Q. coccinea*) on south-facing slopes; (2) oak forests dominated by chestnut oak, northern red oak (*Q. rubra*), and hickories (*Carya* spp.) on east-facing slopes of spurs that are located on the north side of Little Walker Mountain;

(3) a mesophytic assemblage in an east-facing slope of a ravine eroded through Little Walker Mountain; and (4) a table mountain pine (*Pinus pungens*) stand growing on the west face of a spur on the north side of Little Walker Mountain. I used aerial photographs taken for the U.S. Forest Service in 1990 to avoid sampling stands that had sustained major disturbance when remnants of Hurricane Hugo passed over southwestern Virginia in September 1989. A major ice storm affected parts of southwestern Virginia in 1979 (NCDC 1979b; Whitney and Johnson 1984), but dendrochronological evidence indicates that most of the study sites were not strongly affected (this dissertation Chapter 5).

The fifth forest type I sampled was yellow-poplar (*Liriodendron tulipifera*) forest. I sampled yellow-poplar stands at three sites along the crest of the Blue Ridge escarpment (Figure 3.1, sites N – P). I established the sampling sites on lands owned by the Blue Ridge Parkway. Elevations are around 840 – 880 m, and slopes are between 3° and 20°. It appears that Hurricane Hugo caused light forest disturbance along parts of the Blue Ridge escarpment. Ice storms in 1969, 1978, 1979, and 1983 may have affected these sites (NCDC 1969, 1978, 1979b, 1983).

Northern hardwoods dominated by sugar maple (*Acer saccharum*) comprise the sixth forest type. I established three sampling sites in northern hardwood forests in the Adirondacks (Figure 3.2) at elevations of 210 – 570 m. Slopes vary between 2° and 30°. There is evidence of some past disturbance at the Adirondack sites, including beech bark disease (the scale *Cryptococcus fagisuga* and fungus *Nectria coccinea faginata*).

None of the forests I sampled are truly old-growth stands, but I generally selected the most mature stands I could find. The oak-dominated forests and the mesophytic ravine stand, in particular, contain numerous large, old trees and appear to have an uneven age structure. Tree cores collected from one of the oak stands reveals the presence of 300-year old chestnut oak trees. The mesophytic ravine forest is dominated by eastern hemlock, a slow-growing, shade-tolerant species characteristic of old-growth stands (Godman and Lancaster 1990). Large hemlock trees,

possessing stems up to 79 cm in diameter at breast height (DBH), are common. Rugged terrain characterized by 25° to 50° slopes may have protected the site from heavy logging. Northern hardwood forests in the Adirondacks are also relatively old stands. The yellow-poplar stands along the Blue Ridge Parkway appear to be even-aged forests established on abandoned agricultural fields. The history and age structure of the table mountain pine stand are unclear without tree-ring analysis, but fire scars on some boles demonstrate that several fires have occurred since the stand was established.

Sampling Methods

To assess the level of forest disturbance, I collected data on canopy cover, tree damage, and basal area loss. I established three parallel transects in each stand, spacing them 25 m apart and aligning them with slope contours. Transects were 100 m long. I determined transect midpoints from an arbitrary starting point near the top or bottom of a site. I randomly selected a compass direction within 45° of the slope aspect, then measured a random distance of 0 – 10 m along that azimuth to determine the midpoint of the upper or lower transect at the site. I established remaining transects at intervals of 25 m from the original transect. I altered the sampling design (e.g., length or number of transects) at some sites to accommodate local conditions. Specifically, at one site I used four transects 25 m in length to sample an oak-dominated forest in a semi-mesic hollow on the south side of Walker Mountain. At one oak stand on the south side of Little Walker Mountain, I established only two transects. I used five transects at one of the Adirondack sites to characterize disturbance over a hillside with highly varied slope. I used only one or two 75-m transects at each of the Blue Ridge Parkway sites to keep the transects entirely within the borders of the narrow strip of land owned by the National Park Service.

I measured cover of overstory trees whose canopies intercepted the transects. I divided overstory cover into canopy and subcanopy components. I defined canopy individuals as trees

with DBH ≥ 25 cm, as suggested by Runkle (1992). I defined subcanopy trees as those with 20 cm ≤ DBH < 25 cm, measuring the cover of these trees because they comprised part of the overstory in some locations. For the table mountain pine stand, where many canopy individuals have small-diameter stems, I defined overstory trees as those with DBH ≥ 10 cm.

I measured DBH of all trees, including those killed or damaged by ice, with DBH ≥ 10 cm and whose base was located within 5 m of a transect, except at sites A – D, where I only measured trees within 3 m of the transect. I assigned each tree to one of seven damage categories: (1) little or no apparent damage, where less than 10% of the canopy was lost; (2) moderate canopy damage, where 10% to 50% of the canopy was removed; (3) major canopy damage, where more than 50% of the canopy was removed; (4) bent bole; (5) tilted bole; (6) broken bole; or (7) toppled bole. Some trees displayed two different types of damage, but one type typically dominated. Observations of damaged trees suggested that these seven damage categories were more useful for characterizing the damage characteristics unique to ice storm disturbance than are the simple ordinal categories (e.g., no damage, intermediate, severe) used in some other studies. Although the categories I used are ordered roughly by damage severity and are to that extent ordinal, they also distinguish different modes of damage that are difficult to characterize when damage types are aggregated into fewer ordered categories.

I also recorded whether or not each tree was dead or alive. I combined results for mockernut hickory (*Carya tomentosa*) and pignut hickory (*C. glabra*), because species-level identification of downed boles was not always possible. I also combined results for all ashes (*Fraxinus* spp.). Nomenclature follows Fernald (1950).

I collected data on seedlings and saplings in 10 m^2 circular plots positioned at 10 m intervals along each transect. Within each of the plots, I recorded the presence of each species represented as seedlings (seedlings or sprouts ≤ 1.5 m tall) or saplings (individuals ≥ 1.5 m tall and with DBH < 10 cm). I recorded slope angle and aspect at 20 m intervals along each transect.

Data Analysis

I calculated percent canopy, subcanopy, and total overstory cover remaining for each of the six forest types. I also calculated pre-storm and post-storm basal area (m^2/ha). Trees that had died prior to the ice storms were excluded from the calculations. To compute post-storm values, I omitted trees that had died from ice damage or that had been toppled.

To explore relationships of tree damage to tree and site attributes, I plotted patterns of tree damage frequency in relation to wood strength, DBH, and slope of the land surface. For wood strength I used modulus of rupture, a standard measure of wood strength that reflects the maximum load-bearing capacity of a piece of wood as it is bent. For each species I used modulus of rupture values for green specimens taken from the *Wood Handbook* of the U.S. Forest Products Laboratory (1974). I fitted regression lines to the scatter plots, taking apparent thresholds and nonlinear relationships into account where appropriate. Plots that show significant relationships ($P < 0.05$) are presented in the Results section.

I employed multinomial logistic regression (MLR) (SPSS 1999) to elucidate the combined influences of multiple factors on tree damage. MLR can be used to model the probability of several different values of a categorical dependent variable, whereas the more commonly used binary logistic regression method permits only two categories for the dependent variable. I simplified the seven damage categories into four categories for the logistic regression: (1) little or no apparent damage; (2) moderate or major canopy damage; (3) bent bole; and (4) tilted, broken, or toppled bole (Table 3.1). I used four predictor variables in the model, all of which were categorical variables (Table 3.1). The susceptibility ratings reflect that a species may be vulnerable to one type of damage but not another. For example, a species may commonly sustain heavy canopy damage but little stem damage (bending, tilting, breaking, or toppling). I considered this a more satisfactory way to categorize susceptibility than previously reported ordinal classifications that do not differentiate unique types of damage. I based susceptibility

Table 3.1. Damage categories and predictor variables used in multinomial logistic regression (MLR). MLR was used to model the probability of a tree being in each of the four damage categories, based on the values of the predictor variables.

Variable	Abbreviation	Categories	Value in logit equation	Sample size
Damage category		(1) Little or none		186
		(2) Canopy damage		700
		(3) Bent stem		145
		(4) Tilted, broken, or toppled stem		512
Diameter	DBH	(1) Less than 30 cm	1	1179
		(2) At least 30 cm	0	364
Slope	SLOPE	(1) Less than 22°	1	739
		(2) At least 22°	0	804
Canopy susceptibility	SUSCAN	(1) Low	1	711
		(2) High	0	832
Stem susceptibility	SUSSTEM	(1) Low	1	1279
		(2) High	0	264

class assignments (Table 3.2) primarily on whether more than half or less than half the individuals of the species sustained the respective damage type. I excluded species for which I had less than 25 individuals to insure that the susceptibility rating for each species was based on a sufficient number of trees to characterize susceptibility adequately. I omitted trees in the table mountain pine stand from this analysis, because the stand is located on a west-facing slope that was not exposed to heavy ice damage and would therefore not provide comparable susceptibility data. I also considered published susceptibility ratings from other studies when assigning susceptibility.

Results

Remnant overstory cover in ice-damaged stands varies between 27.6% in northern hardwood forests to 64.3% in the table mountain pine stand (Table 3.3). Figure 3.3 illustrates spatial patterns of canopy cover in three stands that represent the variability typical in ice-damaged forests. The storms caused considerable basal area loss, particularly in the Valley and Ridge sites (Table 3.4). Basal area changes shown in Table 3.4 reflect the loss of trees that were toppled or killed as a result of ice damage.

Post-storm species composition is similar to pre-storm composition (Table 3.4). Slight shifts in relative abundance occurred. Figure 3.4 depicts relative basal area (percent of total basal area comprised by a species) for seven major species in the four forest types sampled in the Valley and Ridge. The graphs show the distribution of species dominance among the four forest types, which are arranged along a gradient of presumed moisture availability. The graphs are analogous to those presented by Whittaker (1956) for tree species distributions along a moisture gradient in the Great Smoky Mountains. I omitted the Blue Ridge and Adirondack stands from the graphs because different climatic regimes, soils, and successional status limit their comparability with Valley and Ridge stands. Table 3.5 indicates which species are present as seedlings or saplings in disturbed stands.

Table 3.2. Susceptibility ratings for each of the common species used in the multinomial logistic regression analysis.

Species	Susceptibility to canopy damage	Susceptibility to stem damage
Acer rubrum	high	low
Acer saccharum	high	low
Betula alleghaniensis	high	high
Betula lenta	high	low
Carya spp.	low	high
Fraxinus spp.	high	low
Liriodendron tulipifera	high	low
Oxydendrum arborea	low	low
Pinus rigida	low	high
Quercus coccinea	high	low
Quercus prinus	low	low
Quercus rubra	low	high
Quercus velutina	high	low
Robinia pseudoacacia	low	high
Tilia americana	high	low
Tsuga canadensis	low	low

Table 3.3. Percent cover data for each forest type.

Forest type	Canopy cover (%)	Subcanopy cover (%)	Total overstory cover (%)	Number of sites	Total transect length (m)
Oak, S-facing slopes	35.7	14.1	46.4	5	1200
Oak, E-facing spurs	35.4	11.6	44.5	2	600
Mesophytic assemblage	50.1	5.3	52.8	1	290
Table mountain pine			64.3	1	300
Yellow-poplar	34.1	5.8	39.1	3	300
Northern hardwoods	22.9	6.1	27.6	3	1100

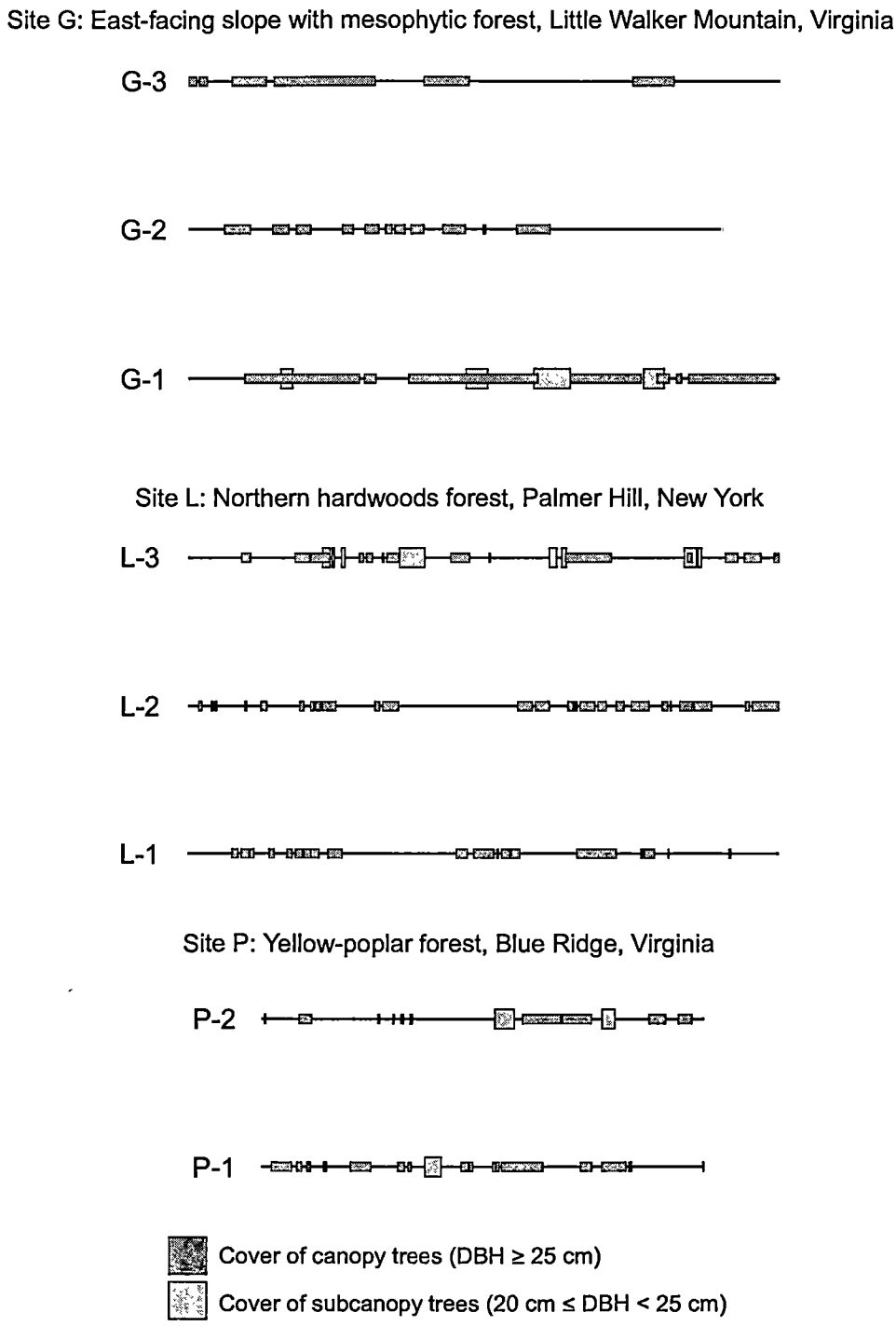

Figure 3.3. Patterns of overstory cover in three sampled stands. Each line represents a transect, and gray bars represent portions of the transects covered by foliage of canopy or subcanopy trees. In a stand with 100% of the overstory intact, the bars would completely obscure the line. Each transect is 100 m long, except G-2 is 90 m and P-1 and P-2 are 75 m.

Table 3.4. Pre-storm and post-storm basal area (m^2/ha) by species in each forest type. TMP = table mountain pine forest, OS = oak forests on south-facing slopes, OE = oak forests on east-facing slopes of spurs, M = mesophytic forest, YP = yellow-poplar forests, and NHD = northern hardwoods forests. Basal area changes reflect the loss of trees that were toppled or killed as a result of ice damage.

	Pre-storm						Post-storm					
Species	TMP	OS	OE	M	YP	NHD	TMP	OS	OE	M	YP	NHD
Acer pensylvanicum			0.02	0.04					0.02	0.04		
Acer rubrum	0.48	0.52	1.75	0.67	2.06	0.99	0.48	0.49	1.03	0.47	2.06	0.99
Acer saccharum		0.02	0.07	1.75		12.97		0.02	0.07	1.04		11.61
Undifferentiated *Acer*[1]		0.02				0.14						0.14
Amelanchier arborea	0.03	0.01	0.15				0.03	0.01	0.15			
Betula alleghaniensis				0.23	0.19	2.58				0.08	0.16	2.39
Betula lenta				1.43	2.80					0.56	2.80	
Betula papyrifera						0.33						0.33
Carya spp.		1.33	3.05	2.90	0.16			0.99	1.63	1.42	0.16	
Castanea dentata		0.03						0.03				
Cornus florida		0.03	0.02					0.02	0.02			
Fagus grandifolia						2.82						2.43
Fraxinus spp.					0.25	3.31					0.25	2.68
Liriodendron tulipifera		0.47		3.69	17.30			0.39		2.35	17.19	
Magnolia acuminata				0.37						0.37		
Nyssa sylvatica		0.53			0.28			0.51			0.28	
Ostrya virginiana						0.59						0.46
Oxydendrum arboreum		2.81						2.16				
Pinus pungens	18.12	0.18	0.25				12.51	0.12				
Pinus rigida	0.92	2.15					0.42	0.89				
Pinus strobus					1.00						0.87	
Undifferentiated *Pinus*[2]		0.06						0.06				
Prunus serotina						2.17						1.95

Table 3.4 (continued).

Species	Pre-storm						Post-storm					
	TMP	OS	OE	M	YP	NHD	TMP	OS	OE	M	YP	NHD
Quercus alba		1.95						1.47				
Quercus coccinea	0.67	2.58					0.53	1.54				
Quercus prinus	3.58	13.67	11.77	2.12	0.89		3.34	10.42	7.87	0.96	0.77	
Quercus rubra	0.11	0.34	8.95	5.32	2.89	0.20	0.11	0.22	5.53	4.29	2.89	0.20
Quercus velutina		4.91	0.03					3.42				
Undifferentiated *Quercus*[3]		0.33										
Rhododendron maximum				0.10						0.10		
Robinia pseudoacacia		0.16	0.10	0.62	1.42			0.04			1.25	
Sassafras albidum		0.04	0.03		0.50						0.47	
Tilia americana				1.37		1.48				0.78		1.47
Tsuga canadensis				20.11	0.05					9.52	0.05	
Ulmus rubra						0.01						0.01
Unidentified hardwoods		0.02	0.12	0.16								
Total basal area	23.91	32.17	26.31	40.88	29.78	27.59	17.42	22.80	16.32	21.98	29.19	24.66
Basal area change (%)							-27.1	-29.1	-38.0	-46.2	-2.0	-10.6

[1]Includes *Acer rubrum* and *A. saccharum* individuals not identified to species level.
[2]Includes *Pinus pungens* and *P. rigida* individuals not identified to species level.
[3]Includes red oak (*Quercus coccinea*, *Q. rubra*, and *Q. velutina*) individuals not identified to species level.

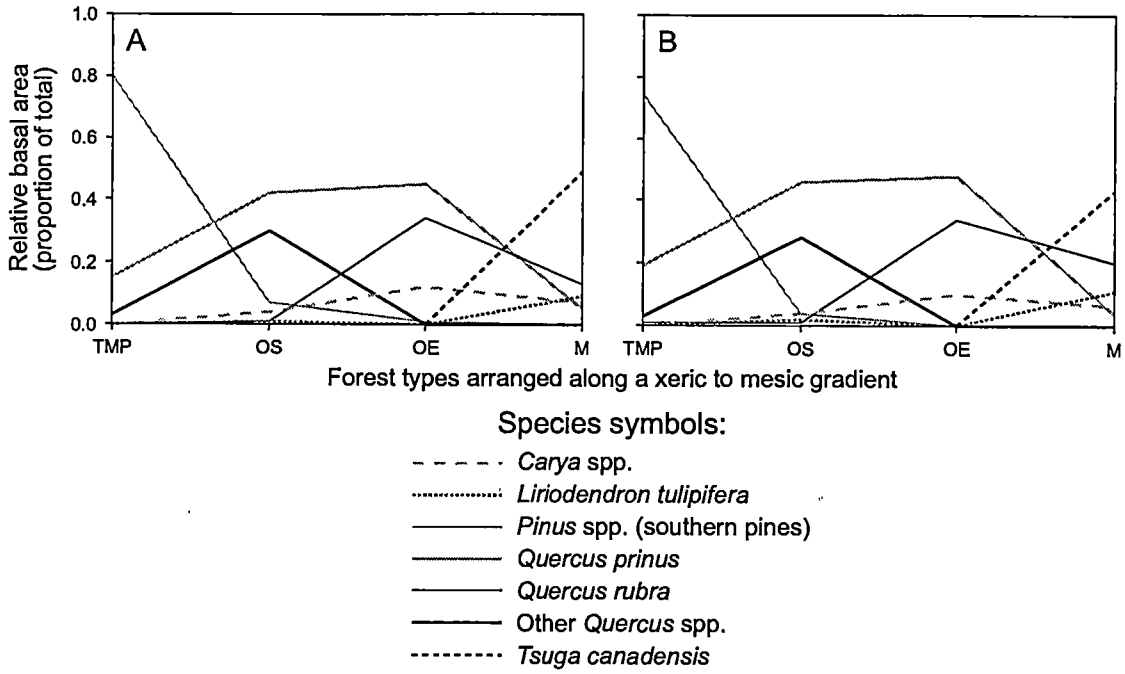

Figure 3.4. Patterns of species composition among the four forest types sampled in the Valley and Ridge province of Virginia: (A) pre-storm composition and (B) post-storm composition. The forest types are arranged along a presumed moisture gradient, from xeric on the left to mesic on the right. TMP = table mountain pine forest, OS = oak forests on south-facing slopes, OE = oak forests on east-facing slopes, and M = mesophytic ravine forest.

Table 3.5. Seedling and sapling frequencies in each forest type. TMP = table mountain pine forest, OS = oak forests on south-facing slopes, OE = oak forests on east-facing slopes of spurs, M = mesophytic forest, YP = yellow-poplar forests, and NHD = northern hardwoods forests.

	Seedlings (percent of plots)						Saplings (percent of plots)					
Species	TMP	OS	OE	M	YP	NHD	TMP	OS	OE	M	YP	NHD
Abies balsamea						5.0						
Acer pensylvanicum		2.3	42.4	35.5	3.1	39.7		1.5	40.9	25.8	3.1	5.0
Acer rubrum	45.5	51.9	80.3	64.5	31.3	52.1	6.1	18.0	3.0		21.9	
Acer saccharum				6.5		86.0						10.7
Undifferentiated *Acer*[1]			1.5									
Ailanthus altissima					9.4							
Amelanchier arborea	45.5	4.5	31.8	16.1	6.3		12.1	0.8	6.1	3.2		
Betula alleghaniensis				3.2		24.0				3.2		2.5
Betula lenta				25.8						12.9	6.3	
Betula papyrifera						1.7						
Undifferentiated *Betula*[2]					6.3							
Carya spp.		27.8	43.9	22.6	34.4			6.0	10.6	3.2	9.4	
Castanea dentata	12.1	10.5	1.5				3.0	12.8				
Castanea pumila		18.0						9.0				
Cornus florida	3.0	9.8	3.0	3.2	3.1	1.7		12.8	3.0			
Fagus grandifolia			1.5			36.4						
Fraxinus spp.				3.2	53.1	33.1						
Hamamelis virginiana	3.0	1.5	1.5	3.2	6.3			0.8	1.5	3.2	3.1	
Kalmia latifolia	84.8	15.8	1.5		3.1		54.5	9.8				
Lindera benzoin				3.2								
Liriodendron tulipifera		2.3	3.0	54.8	40.6			0.8		3.2	18.8	
Magnolia acuminata				16.1	3.1							
Nyssa sylvatica	6.1	22.6	4.5	6.5	12.5							
Ostrya virginiana			6.1			16.5			3.0			5.0
Oxydendrum arboreum		13.5	1.5					12.8				
Pinus pungens	3.0		15.2				18.2		3.0			
Pinus rigida		1.5						0.8				
Pinus strobus	3.0	1.5		12.9			6.1	3.0				

Table 3.5 (continued).

Species	Seedlings (percent of plots)						Saplings (percent of plots)					
	TMP	OS	OE	M	YP	NHD	TMP	OS	OE	M	YP	NHD
Prunus serotina		3.0			6.3	49.6					3.1	
Populus grandidentata						2.5						
Quercus alba	6.1	7.5	1.5					1.5		3.2		
Quercus coccinea	45.5	29.3					18.2	1.5				
Quercus ilicifolia	36.4											
Quercus marilandica	36.4											
Quercus prinus	27.3	59.4	62.1	3.2			9.1	17.3	7.6			
Quercus rubra	63.6	11.3	84.8	25.8	53.1	7.4		6.8	1.5	3.2		
Quercus velutina	18.2	37.6	4.5		9.4		3.0	7.5				
Undifferentiated *Quercus*[4]	3.0	1.5										
Rhododendron calendulaceum	15.2	20.3										
Rhododendron maximum	18.2	0.8		19.4			15.2	0.8		3.2		
Robinia pseudoacacia		3.8	9.1	6.5	25.0			6.0		9.7	6.3	
Sassafras albidum	27.3	91.0	6.1	12.9	34.4		9.1	50.4			6.3	
Tilia americana				3.2	3.1	4.1						
Tsuga canadensis				9.7					1.5	9.7		
Ulmus rubra												0.8
Vaccinium spp.	90.9	85.0	51.5					0.8				
Viburnum acerifolium	9.1											

[1]Includes *Acer rubrum* and *A. saccharum* individuals not identified to species level.
[2]Includes *Betula alleghaniensis* and *Betula lenta* individuals not identified to species level.
[3]Includes *Pinus pungens* and *P. rigida* individuals not identified to species level.
[4]Includes red oak (*Quercus coccinea*, *Q. rubra*, and *Q. velutina*) individuals not identified to species level.

Mortality is related both to damage category and time since damage (Figure 3.5). Severely damaged trees have experienced higher mortality than less damaged individuals. Stands that were sampled longer after disturbance (i.e., the Valley and Ridge sites) exhibit higher mortality than those sampled in the growing season immediately following storm damage.

My results demonstrate considerable interspecific variation in susceptibility to damage. To compare observed damage for major species to the ordinal damage classifications of other studies, I combined my seven damage categories into the following three classes: (1) none/minor – trees with little or no damage (damage category 1), (2) intermediate – trees with ≤ 50% canopy loss or with bent or tilted boles (damage categories 2, 4, and 5), and (3) severe – trees with > 50% canopy loss or with broken or toppled boles (damage categories 3, 6, and 7) (Table 3.6). These classes reflect the patterns of tree mortality and damage shown in Figure 3.5. I also included in Table 3.6 a column with category 3 – 7 damage for comparison to the results of Whitney and Johnson (1984), who conducted a study of ice storm damage in southwestern Virginia. Their "severely damaged" category includes trees with bent and tilted boles as well as those with heavy canopy damage, broken stems, or toppled boles (i.e., categories 3 – 7 of my study).

Percent mortality is positively related to the percent of trees in the severe damage class ($P < 0.05$, Figure 3.6) but does not show a significant relationship to the alternative category 3 – 7 class. This indicates that the severe damage class defined by damage categories 3, 6, and 7 is probably more appropriate for comparing susceptibility among species.

It may be more useful to consider susceptibility of trees to different types of damage, rather than simply to characterize the vulnerability of a species to all damage types. For example, classifying the susceptibility of each species into two broad damage categories, canopy *versus* stem, elucidates interspecific patterns of damage not otherwise evident. Some species, such as yellow-poplar, typically experience canopy damage, whereas other species (e.g., black locust) are characterized by stem damage (Figure 3.7). I omitted data for the table mountain pine forest from

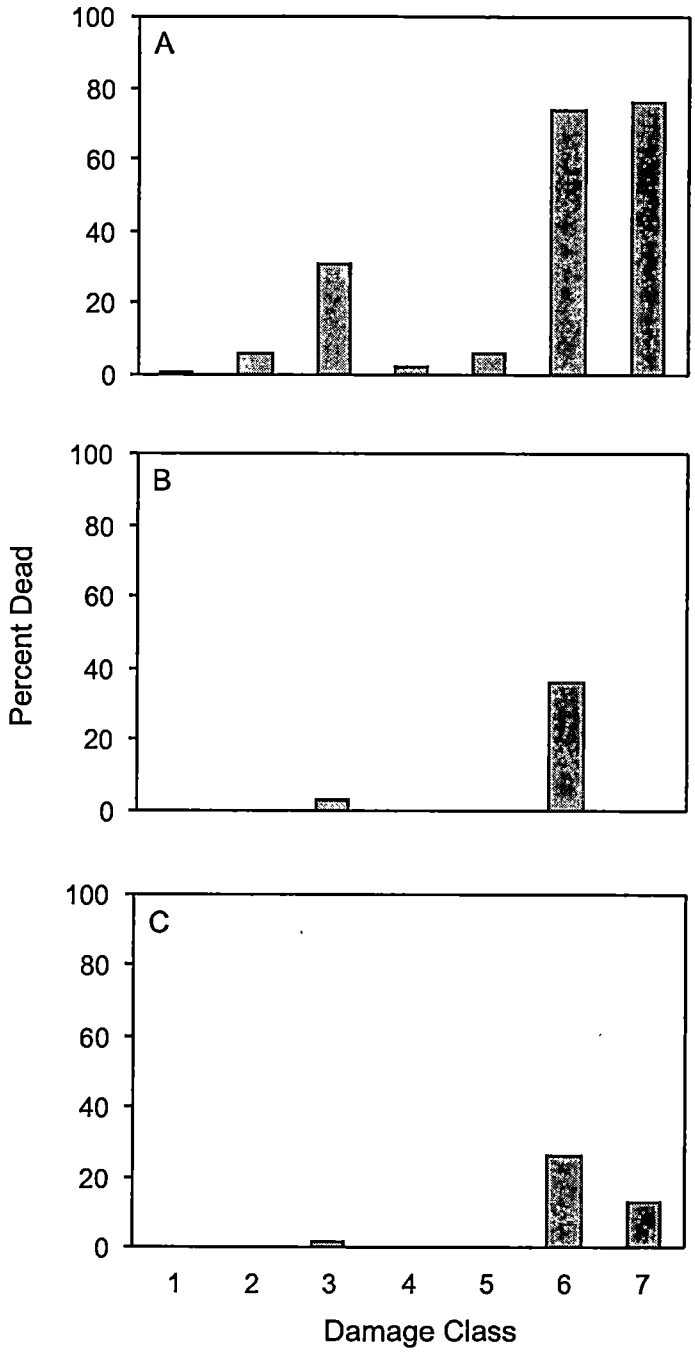

Figure 3.5. Percent of trees in each damage class that were dead at the time of sampling in stands disturbed by the recent ice storms: (A) the 1994 ice storms in Virginia, (B) the 1998 ice storm in Virginia, and (C) the 1998 ice storm in New York.

Table 3.6. Interspecific differences in tree damage. Only species with data for ≥ 25 individuals are included, and the table mountain pine site is omitted from the analysis.

Species	Sample size	Damage by category (% of trees)				Mortality
		None/minor	Intermediate	Severe	Class 3-7	
			VIRGINIA			
Quercus prinus	326	25.3	40.3	34.4	43.1	18.7
Carya spp.	89	23.6	37.1	39.3	60.7	20.2
Quercus coccinea	50	10.5	47.4	42.1	47.4	42.0
Acer rubrum	83	20.7	31.5	47.8	58.7	10.8
Betula lenta	27	3.7	48.1	48.1	74.1	18.5
Quercus rubra	79	22.5	25.0	52.5	58.8	46.8
Oxydendrum arboreum	129	7.0	39.5	53.5	80.6	20.2
Tsuga canadensis	60	20.0	20.0	60.0	68.3	41.7
Quercus velutina	87	5.7	33.3	60.9	65.5	36.8
Pinus rigida	30	12.8	17.9	69.2	71.8	76.7
Liriodendron tulipifera	75	1.3	28.0	70.7	73.3	5.3
Robinia pseudoacacia	27	11.1	7.4	81.5	88.9	55.6
			NEW YORK			
Ostrya virginiana	34	8.8	35.3	55.9	70.6	11.8
Fagus grandifolia	128	8.6	34.4	57.0	71.1	6.3
Acer saccharum	174	2.3	30.5	67.2	73.6	7.5
Fraxinus spp.	40	0.0	17.5	82.5	87.5	7.5
Betula alleghaniensis	30	6.7	10.0	83.3	86.7	6.7

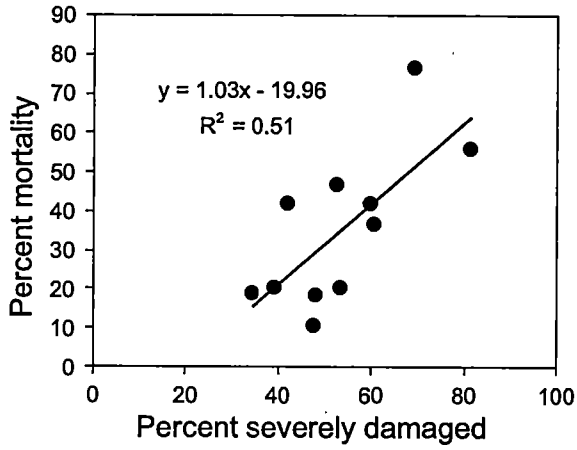

Figure 3.6. Relationship of mortality to percent of individuals severely damaged for eleven species in the Virginia sites. *Liriodendron tulipifera* is excluded from the graph due to its extremely high damage and low mortality.

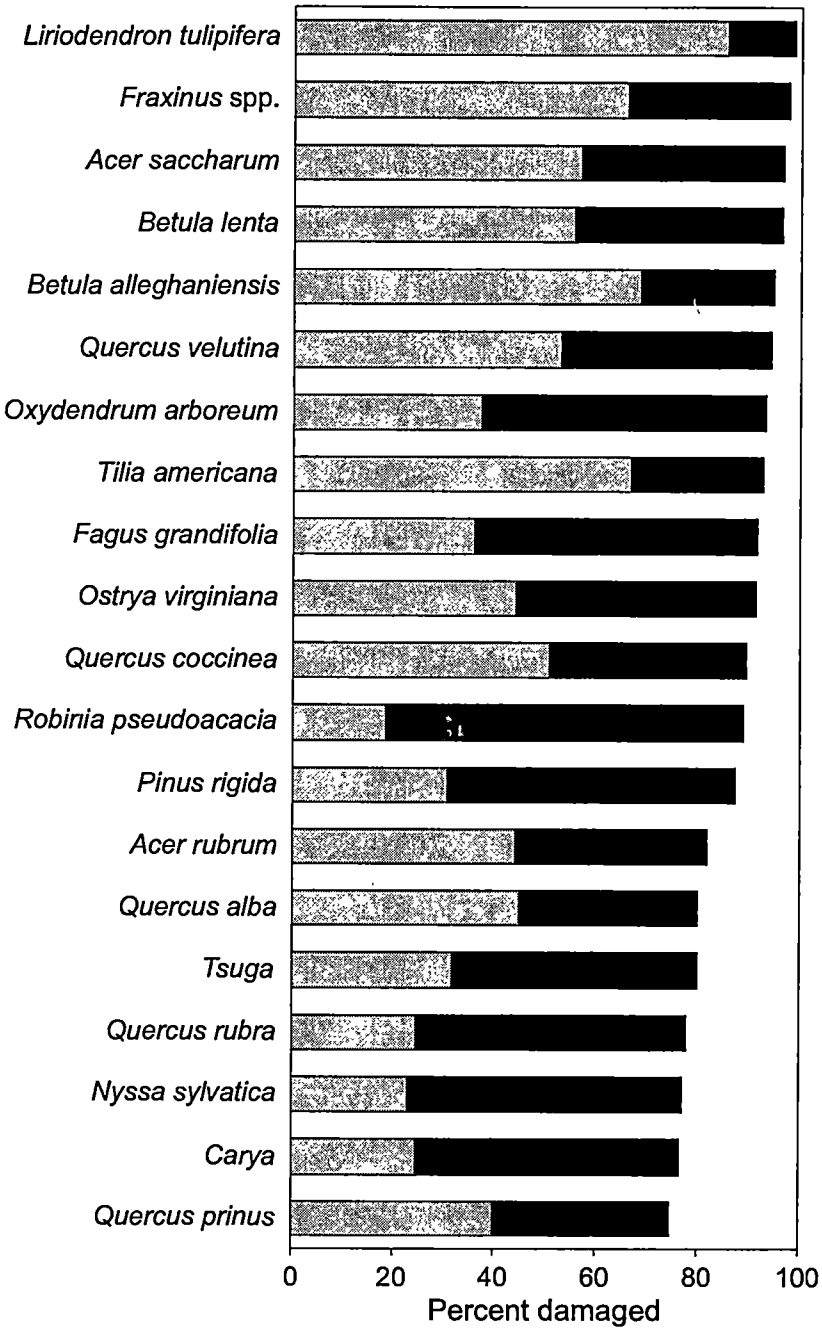

Figure 3.7. Percent of individuals of common species exhibiting canopy damage and stem damage. Gray portions of bars represent canopy damage (moderate or major), and black portions represent stem damage (bent, tilted, broken, or toppled stems).

analyses of interspecific differences in damage characteristics. The stand was growing on a west-facing slope that was apparently not exposed to as high a level of ice accumulation as other sites (Lafon *et al.* 1999). Although pine stands on west-facing slopes sustained moderate ice storm damage, damage to hardwoods in these stands was minor. The low level of hardwood damage relative to the damage sustained by individuals of the same species growing on other aspects implies that west-facing slopes were sheltered from the processes that led to heavy disturbance on east- and southeast facing slopes. Inclusion of data from this site probably would have caused misrepresentation of the relative susceptibility of some species to ice storm damage.

Wood strength is one factor that may affect the susceptibility of a tree to ice storm damage, but my results indicate that the relationship is not straightforward. Of all trees, only toppled trees (category 7) exhibit a significant relationship between modulus of rupture and percent damaged ($P < 0.01$, Figure 3.8).

Stronger relationships exist between DBH and damage (Figure 3.9). To construct these plots, I grouped trees into twelve DBH classes (Table 3.7) and calculated the percent of stems in each of these classes that sustained the given damage type. Significant relationships ($P < 0.01$ or better) exist for all but tilted trees.

Tree damage characteristics are also related to slope (Figure 3.10). These graphs are analogous to those in Figure 3.9. Slope was divided into seven classes (Table 3.7). Based on the slope of the site on which the tree was growing, I assigned each tree to one of these seven classes.

In addition to slope, soil properties may also affect damage characteristics. Figure 3.11 presents a comparison of damage between Walker Mountain and Little Walker Mountain on sites of similar slope angle (20° – 29°). Despite similar slopes, bole breakage and toppling (damage categories 6 and 7) are more prevalent on Little Walker Mountain, where, according to the soil survey of Wythe County, Virginia, soils are generally thinner than on Walker Mountain (Gall and Edmonds 1992). I did not measure soil depth at my study sites.

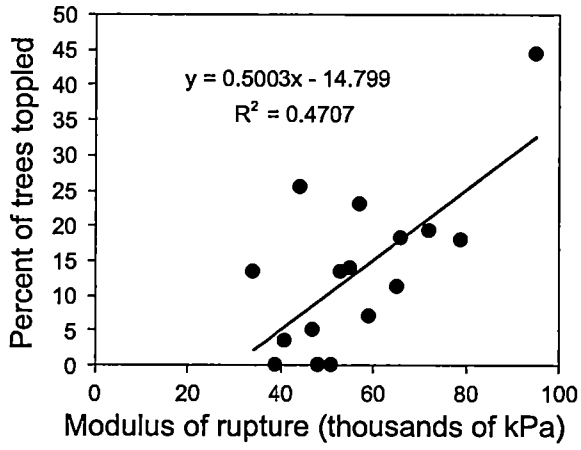

Figure 3.8. Percent of trees with each modulus of rupture that was toppled.

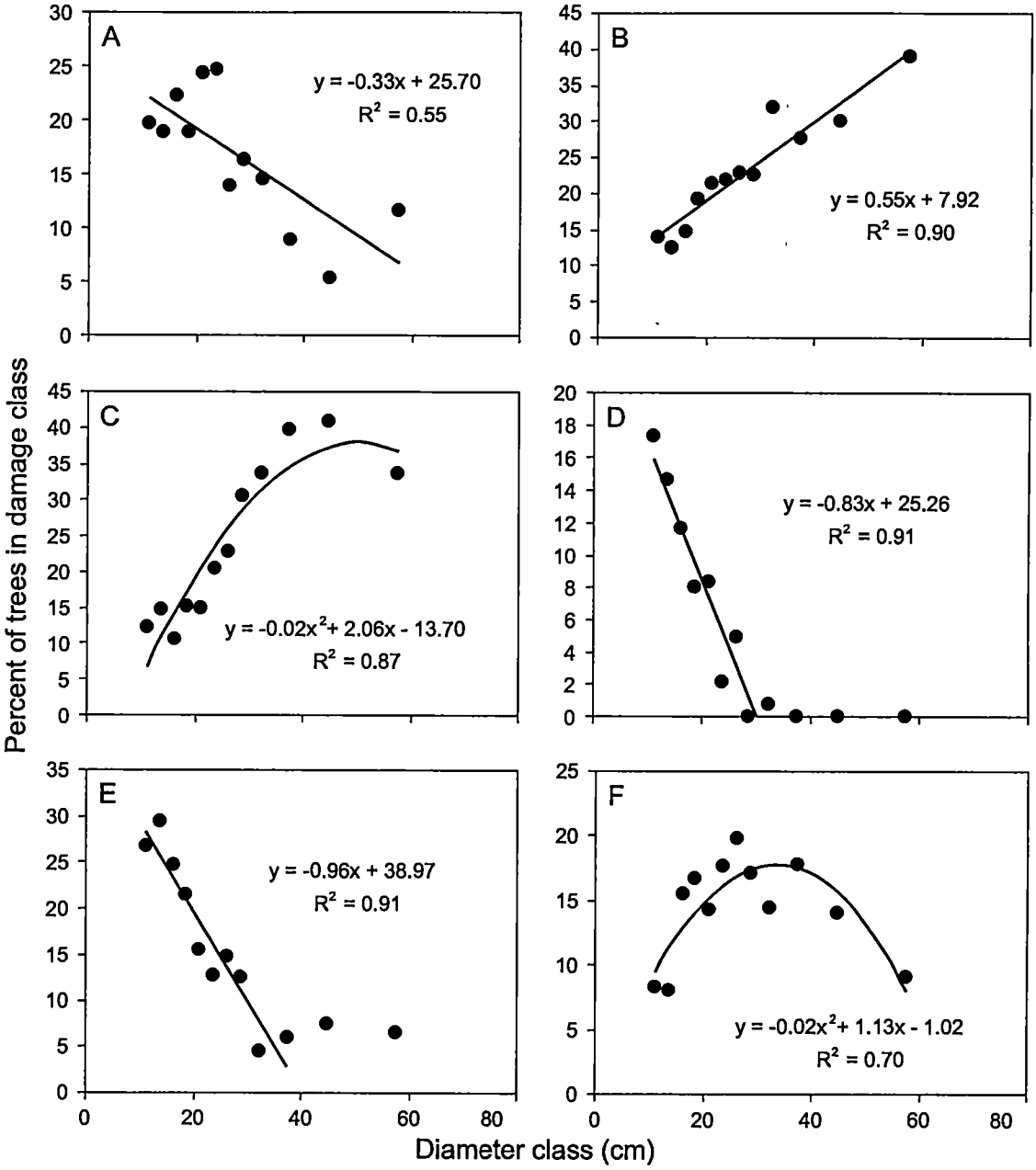

Figure 3.9. Percent of trees in each DBH class with each of the following damage types: (A) little or no damage, (B) moderate canopy damage, (C) major canopy damage, (D) bent stems, (E) broken stems, and (F) toppled stems.

Table 3.7. DBH and slope classes used in scatterplots.

DBH classes (cm)	Slope classes (degrees)
10.0-12.4	2-9
12.5-14.9	10-14
15.0-17.4	15-19
17.5-19.9	20-24
20.0-22.4	25-29
22.5-24.9	30-34
25.0-27.4	35-50
27.5-29.9	
30.0-34.9	
35.0-39.9	
40.0-49.9	
50.0-88.8	

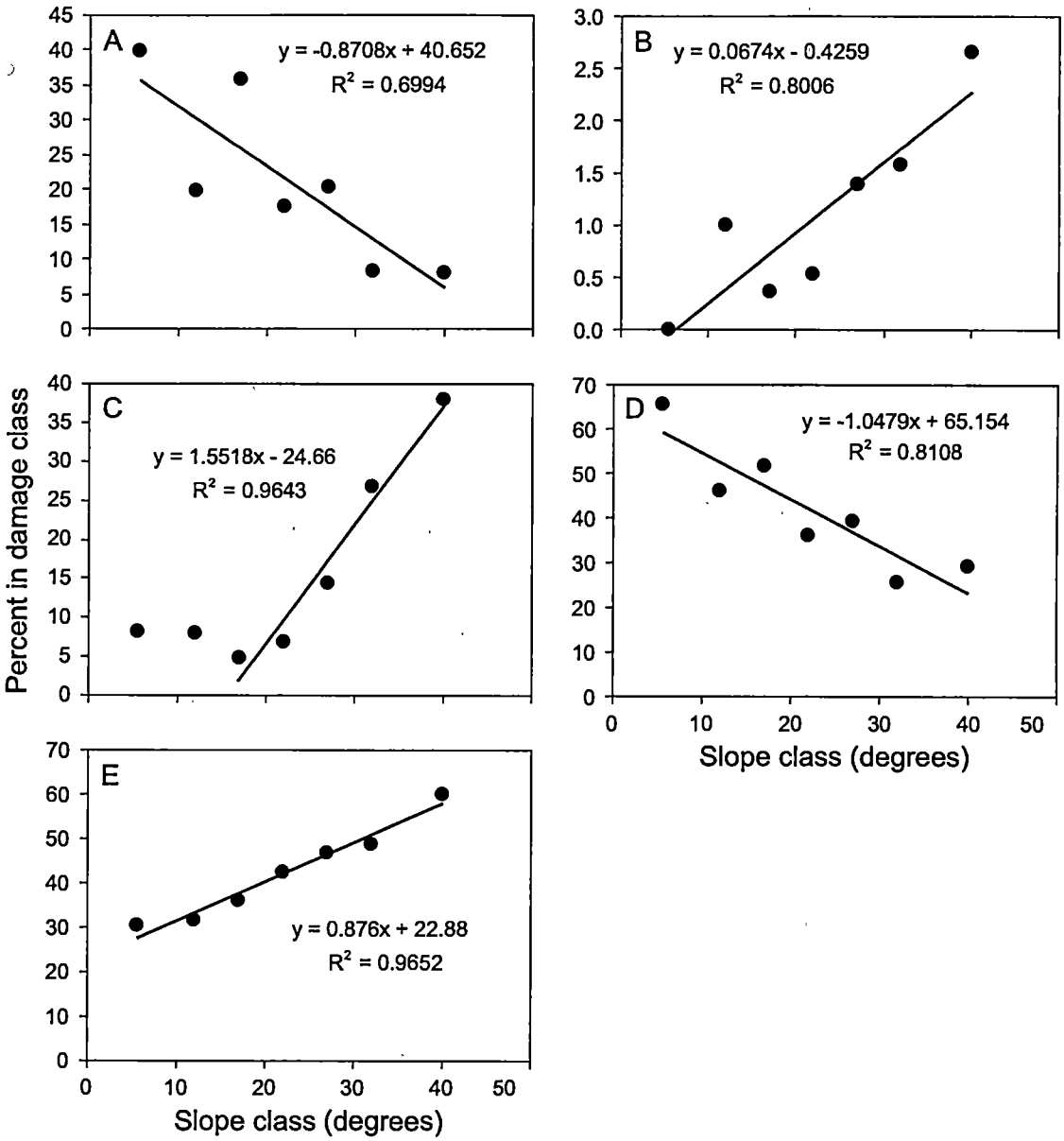

Figure 3.10. Percent of trees on slopes of each class with each of the following damage types: (A) major canopy damage, (B) tilted stems, (C) toppled stems, (D) any level of canopy damage, and (E) any type of stem damage.

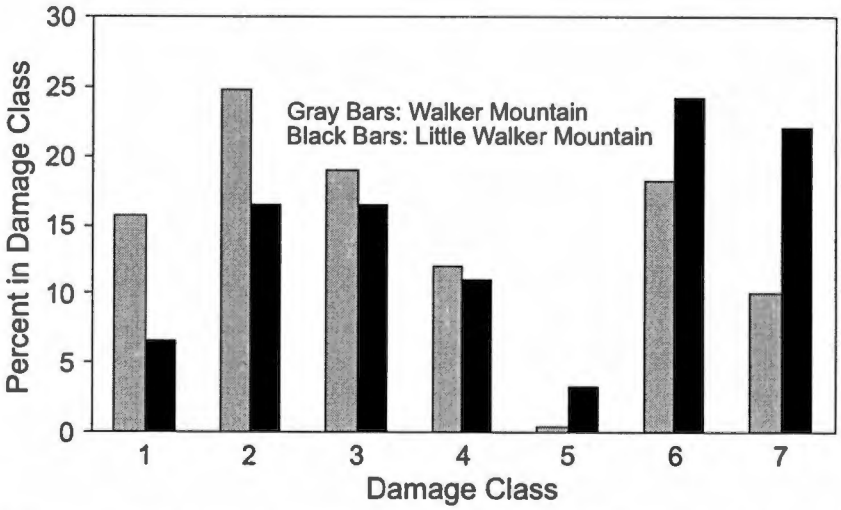

Figure 3.11. Percent of trees in each damage class on Walker Mountain and Little Walker Mountain. All trees were growing on sites with similar slope (20°– 29°).

Although individual species and sites are combined in the scatter plots, few major discrepancies are apparent when patterns are examined for individual species. For damage category 1 (little or no damage), sourwood (*Oxydendrum arboreum*) and table mountain pine exhibit significant positive relationships ($P < 0.05$) between DBH and damage. For damage category 6 (broken boles), hickory has a significant positive relationship ($P < 0.05$) between DBH and damage when the largest two diameter classes are not included in the analysis. Hickory also exhibits a significant positive relationship ($P < 0.05$) between DBH and percent in damage category 7 (toppled trees), a trend which may be inconsistent with the relationship in Figure 3.9F.

Results of the MLR provide a means to predict the probability of tree damage from the combined influence of several factors. MLR involves estimating the logit for each category of the dependent variable (Johnston 1980; SPSS 1999). A logit is the natural log of the odds of being in one category compared to being in a baseline category. Assigning damage category 4 as the baseline category, I obtained the following equations for estimating logits for the four damage categories:

$$u_1 = -1.650 - 0.314(\text{DBH}) + 0.09155(\text{SLOPE}) + 1.135(\text{SUSCAN}) + 0.230(\text{SUSSTEM})$$

$$u_2 = 0.200 - 1.225(\text{DBH}) + 0.846(\text{SLOPE}) - 0.04642(\text{SUSCAN}) + 0.777(\text{SUSSTEM})$$

$$u_3 = -5.193 + 3.161(\text{DBH}) + 0.830(\text{SLOPE}) - 0.652(\text{SUSCAN}) + 0.258(\text{SUSSTEM})$$

$$u_4 = 0$$

where u_i = estimated logit for the damage category and the predictor variables are as shown in Table 3.1. Categories for the predictor variable DBH were chosen to reflect the relationships between stem diameter and tree damage shown in Figure 8. All variables were significant at $P < 0.0005$, although not for all equations. A *chi*-square analysis was not conducted, because it is not an appropriate measure of model fit for results such as these, in which some of the cells in the

contingency table have predicted values less than five (Griffith and Amrhein 1991). However, examination of predicted frequencies indicates that they match observations quite well.

To estimate the logit for a given tree, each binary variable would be assigned a value of zero or one (Table 3.1). After calculating the logit for each damage category, according to the attributes of the tree, the following equation is used to determine the probability of being in a given damage category:

$$P(u_i) = \frac{e^{u_i}}{\sum_{k=1}^{j} e^{u_k}}$$

where $P(u_i)$ is the probability of damage category i and j is the number of damage categories (SPSS 1999).

After obtaining these results, I refined the MLR analysis to model tree damage probabilities in the most heavily disturbed forest patches separately from those in less disturbed patches. In dense forest stands, the fall of one tree may strike neighboring trees, triggering their fall or breakage (Lafon *et al.* 1999) and creating multiple-tree gaps that alternate with less damaged patches where such multiple-tree events were not initiated (Figure 3.3). This stand-level effect may reduce the utility of a single MLR model for characterizing tree damage across both heavily damaged and less damaged patches. The purpose of the refined MLR analysis was to enhance modeling of tree damage probabilities by accounting for damage triggered by falling neighbors in heavily disturbed patches. Such impact-triggered damage would not be predictable from characteristics of individual trees alone.

To identify heavily disturbed and less disturbed forest patches, I divided each transect into 25-m segments and defined the segment as heavily disturbed if at least 45% of the trees along the segment had sustained category 4 damage (tilting, breaking, or toppling). The 45% threshold was chosen based on a histogram showing that 45% represented a reasonable natural break in my data set that also retained a sufficient number of segments in both the heavily disturbed and less disturbed categories to permit statistical analysis.

The proportion of total transect length occupied by heavily disturbed segments increases with increasing slope angle (Figure 3.12, $P < 0.001$). MLR analysis for these heavily disturbed transects yielded the following equations for estimating logits, with damage category 4 as the baseline category:

$u_1 = -2.633 - 0.569(\text{DBH}) + 1.84(\text{SUSCAN})$

$u_2 = -0.007846 - 1.065(\text{DBH}) - 0.212(\text{SUSCAN})$

$u_3 = -4.244 + 2.186(\text{DBH}) + 0.449(\text{SUSCAN})$

$u_4 = 0.$

Probability of category 4 damage is lower in less disturbed segments. Logits for these segments are calculated as follows, with damage category 4 as the baseline category:

$u_1 = -0.639 - 0.355(\text{DBH}) + 0.986(\text{SUSCAN})$

$u_2 = 2.201 - 1.293(\text{DBH}) - 0.357(\text{SUSCAN})$

$u_3 = -18.291 + 17.557(\text{DBH}) + 0.408(\text{SUSCAN})$

$u_4 = 0.$

The variables are significant at $P < 0.0005$. Again, *chi*-square analyses were not conducted because of small predicted values for some cells of the contingency tables, but inspection of the results revealed that predicted frequencies generally match observations closely. Splitting the data into two groups necessitated the elimination of two variables, SLOPE and SUSSTEM, that were included in the original MLR equations. However, the effect of slope can be accounted for by the relationship graphed in Figure 3.12.

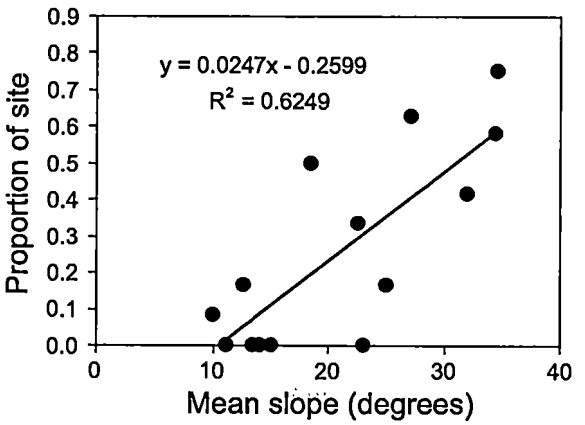

Figure 3.12. Proportion of total transect length at each site occupied by heavily damaged segments, as a function of mean slope of the site. Each segment is 25 m long, and a heavily damaged segment is defined as one in which at least 45% of all trees were broken or toppled.

I excluded the table mountain pine forest from the multinomial logistic regression analyses, because not enough data are available to conduct a detailed analysis of tree damage probabilities. Results presented in Table 3.8 reflect general patterns of damage in the stand.

Discussion

Forest damage patterns

All four ice storms were major events that removed substantial basal area or created large canopy gaps. Ice storm damage of similar magnitude has been reported in the Appalachians, the Northeast, and the Midwest (Rhoades 1918; Downs 1938; Whitney and Johnson 1984; Bruederle and Stearns 1985; Seischab *et al.* 1993). Dendrochronological and historical records suggest that similar events have occurred about 2 – 4 times during the past century on southeast-facing slopes of the Valley and Ridge province in southwestern Virginia (this dissertation Chapter 5). These events are a major component of the disturbance regime in an area where other large disturbances, such as stand-replacing fires, are thought to be uncommon.

Some forest types sustained greater basal area reductions than others, although canopy openness is high in all forest types. Yellow-poplar stands are particularly notable for the tendency of nearly all individuals to experience severe canopy loss without bending, tilting, breaking, or toppling of boles. The straight bole, symmetrical shape, and relatively weak wood of a yellow-poplar tree allows the bole to stand erect while branches are stripped off by the weight of ice. Many of the damaged yellow-poplars will probably recover, permitting continued yellow-poplar dominance. Whitney and Johnson (1984) documented low mortality of yellow-poplar the second growing season after an ice storm that inflicted major damage to most individuals of the species. My limited data on yellow-poplar trees damaged by the 1994 storms indicates that 25% of trees with severe canopy damage died by 1997 – 98, but observations in additional stands suggest that mortality may generally be lower.

Table 3.8. Damage characteristics at site I, the table mountain pine stand on a west-facing slope.

Major tree group	Percent in damage class							Mortality (percent)
	1	2	3	4	5	6	7	
Conifers	48.8	7.6	4	3.6	0	34.4	1.6	42.0
Hardwoods	53.8	23.1	1.9	5.8	0	11.5	3.8	11.5

Basal area loss was also relatively low in the northern hardwood stands, despite major canopy loss. However, it is unlikely that all these species will respond as yellow-poplar. Many of the surviving, heavily damaged trees will probably succumb over the next few growing seasons. In fact, in the Valley and Ridge forests, where I sampled several years after disturbance, nearly a third of all trees with severe canopy damage are dead (Figure 3.5). Trees with broken or toppled boles exhibited higher mortality rates. Relatively few bent or tilted trees have died, but mortality will probably increase as competition for light from dominant canopy trees becomes more pronounced during forest recovery. Additionally, bent and tilted trees may sustain heavy damage in future ice storms.

Characterizations of interspecific variations in susceptibility to storm damage generally agree with other studies (Table 3.6, Figure 3.7). For example, hickories and chestnut oak are usually rated low in susceptibility, whereas pitch pine is highly susceptible (Whitney and Johnson 1984; Seischab *et al.* 1993; Warrillow and Mou 1999). My results differ most from others in the finding of considerable ash and black locust damage, although Abell (1934) also reported heavy damage to black locust in the mountains of western North Carolina. Reasons for these differences are not apparent. For black locust, the high degree of damage may reflect my sampling on steep slopes, where toppling is common. Black locust had a higher percentage of trees toppled (44.4%) than any other species. The species has strong wood and may be more resistant to damage in gently sloping terrain.

My results also underscore the high susceptibility of yellow-poplar to ice storm damage. Some have reported major damage in this species (Carvell *et al.* 1957; Whitney and Johnson 1984), but others consider it resistant (Lemon 1961; Warrillow and Mou 1999). These divergent findings may in part reflect the inadequacy of a simple ordinal damage-classification scheme. My results show that nearly all yellow-poplar trees were damaged, but that canopy damage was predominant (Figure 3.7), as discussed above. This damage pattern may permit most yellow-

poplars to survive ice storms despite heavy damage. The different ratings for the species also reflect different sampling schemes. To obtain reasonably comparable data for different species, I located all but one of my sampling sites in parts of the landscape that were exposed to heavy ice accumulation. The table mountain pine site, which I analyzed separately, is the exception. Whitney and Johnson (1984) also selected stands in such locations, which probably accounts for the similarity of their results to mine. However, Warrillow and Mou (1999) sampled over different landscape positions, some of which sustained heavy damage from the 1994 storms and others which did not. In the Valley and Ridge province of Virginia, yellow-poplar is largely confined to valley bottoms and lower slopes, but heavy damage from the 1994 ice storms occurred farther up the slopes (Lafon *et al.* 1999). Sampling yellow-poplar stands on sites that were not exposed to heavy damage leads to the conclusion that yellow-poplar is less susceptible to ice damage than other species, when in fact it is more so. To provide a more appropriate characterization of yellow-poplar susceptibility, I sampled along the crest of the Blue Ridge escarpment, where yellow-poplar is an important species and where the 1998 ice storm caused major damage.

Another dichotomy exists in opinions about the relative susceptibility of conifers as compared to hardwoods. Dyer (1983), Whitney and Johnson (1984), Boerner *et al.* (1986), and Warrillow and Mou (1999) found that conifers generally sustained heavier ice storm damage than hardwoods in Appalachian forests. Studies in northern forests reported low to moderate damage in conifer species (Downs 1938; Carvell *et al.* 1957; Lemon 1961). These varied findings appear to reflect differences among different conifer species, rather than differences between hardwoods and conifers. Southern pine species are highly vulnerable to ice storm damage. The high wintertime surface area of evergreen conifers permits heavy ice loads to accrete (Lemon 1961), which, combined with relatively weak wood, probably accounts for heavy damage in southern pines. My results indicate that southern pines are among the most susceptible trees. Pitch pine

(*Pinus rigida*) had the highest mortality of any species in Table 3.6. Table 3.8 demonstrates that pines sustained relatively high levels of damage, even on a site sheltered from the heaviest ice accumulation. The resistance of northern conifers, despite their evergreen habit, probably reflects their conical forms, straight boles, flexible limbs, and other adaptations to heavy snow or ice (Lemon 1961). I found moderate damage levels among hemlock, a species for which there is little disagreement about susceptibility (Lemon 1961; Boerner *et al.* 1986; Seischab *et al.* 1993). Hemlock is probably best considered low or moderate in susceptibility to ice damage. My field observations in New York reveal that spruce and fir sustained little damage, although I did not assess conifer damage quantitatively. White pine (*Pinus strobus*) also appeared to be one of the most resistant species in New York, but in Virginia some white pines suffered heavy limb loss (personal observation). Geographic differences in wood strength or other characteristics may make white pine more resistant to ice damage in the northern part of its range than farther south.

Despite an intuitive expectation that wood strength accounts for much of the interspecific variation in susceptibility to ice damage, my data provide little evidence for such relationships. The only significant relationship is for toppled trees, which probably indicates that strong trees resistant to breaking or bending are likely instead to be pulled down completely. Other researchers also report poor relationships of tree damage to modulus of rupture (Lemon 1961; Bruederle and Stearns 1985). Susceptibility of a species to ice damage probably involves a complex suite of attributes related both to wood strength and canopy architecture. Again, yellow-poplar provides an example of how individual tree characteristics influence damage patterns – weak wood, straight boles, symmetrical canopies, and rapid recovery rates allow individual trees to survive an ice storm by sacrificing much of their canopies. In contrast, some of the species characterized by stem damage experienced higher levels of mortality (e.g., black locust, pitch pine; Figure 3.7, Table 3.6). Decay may also affect the susceptibility of a species to damage (Seischab *et al.* 1993). For example, both scarlet oak and northern red oak sustained heavier

damage than chestnut oak, despite their greater published wood strength (U.S. Forest Products Laboratory 1974). The lower resistance of these two oak species to heartwood decay (McQuilkin 1990) may effectively reduce their average bole strengths. In addition, the red oaks are more susceptible than white oaks to the oak decline disease complex involving the root fungus *Armillaria mellea*, which weakens roots and contributes to toppling during disturbances (Greenberg and McNab 1998).

Stem diameter is a readily quantified tree attribute that is strongly related to damage (Figure 3.9). Generally, significant damage becomes more frequent with increasing size, a result consistent with findings of Seischab *et al.* (1993) and Rebertus *et al.* (1997). Dominant canopy trees more frequently sustain damage than smaller trees, but the damage is less likely to cause immediate loss of these trees from the stand. Small trees are characterized by bending or breakage of boles. Downs (1938) also reported high rates of bending and breaking in small stems. Trees become more susceptible to toppling as they grow into medium diameter trees, and canopy damage is characteristic of larger trees. Again, these results agree with those of Downs (1938), who found a positive relationship between stem diameter and canopy damage. These patterns probably reflect the increasing strength of stems and root systems as trees mature.

The tendency of trees growing on hillslopes to lean downhill (Phipps 1974; Mills 1984) probably influences damage patterns. Few canopy-size individuals on steep slopes in my study areas have vertical boles. Leaning trees are probably unbalanced prior to an ice storm, which increases their susceptibility to damage, particularly toppling. Interspecific differences, such as wood strength and length of tap roots, undoubtedly affects vulnerability to toppling, but slope angle appears to exert a major influence. My results show a strong positive relationship between slope angle above a threshold of 20° and percent of trees toppled by ice (Figure 3.10C). Seischab *et al.* (1993) likewise demonstrated a positive correlation between slope angle and percent of trees toppled by a major ice storm in western New York. Generally, my results indicate that stem

damage (category 4 – 7 damage) becomes increasingly common as slope angle increases, and that canopy damage is more common at sites having lower slope angles (Figure 3.10).

Individual tree attributes, such as diameter and wood strength, are important influences on damage patterns, but ice storm disturbance is also a stand-level phenomenon, particularly in steeply sloping terrain. Tangled limbs and boles piled in damaged stands indicate that falling trees often triggered damage among neighboring trees that were approaching their own weight-bearing thresholds (Lafon *et al.* 1999), an occurrence that becomes more common with increasing slope (Figure 3.12). The resulting disturbance pattern consists of large gaps alternating with less damaged sections (Figure 3.3)

Boerner *et al.* (1986) found the damage resulting from the impact of neighboring trees unpredictable. They analyzed trees with direct ice storm damage separately from those with secondary damage. They detected relationships between individual-tree parameters and direct ice damage but concluded that secondary damage caused by the fall of surrounding trees was unpredictable. I also tried to determine whether damage to each individual was direct or secondary but frequently found such distinctions impossible. It could not always be assumed that limbs or boles on the bottom of a debris pile had been broken or toppled by the fall of overlying trees. In fact, a tree on the bottom of such a pile may actually have fallen first. Nearby trees upset by the impact of this falling tree may not have toppled until several minutes later, eventually falling on top of the tree that initially triggered the multiple-tree fall (Ken Orvis personal communication). Stand-scale effects may make prediction less precise, but my analyses elucidated strong relationships nonetheless.

My results also suggest that soil depth may influence damage, although I did not sample soil depth myself. Bole breakage and toppling are more common on Little Walker Mountain than on Walker Mountain, where soils are generally deeper (Gall and Edmonds 1992). This pattern is consistent with the finding of Seischab *et al.* (1993) that toppling was more prevalent on shallow,

sandy, or gravelly soils. The relationship of toppling to soil depth is probably a consequence of less supportive root systems in thin soils. Enhanced stem breakage in these sites may result when falling trees strike neighboring trees. Further exploration of this topic would be useful. Variations in toppling rates among different soils could have implications for both vegetation dynamics and erosion rates (Mills 1984).

The multinomial logistic regression analyses reflect the combined influences of multiple factors on damage characteristics of a tree. Additional damage sampling in disturbed stands would probably allow construction of a more detailed model containing additional categories for the predictor and dependent variables. Nonetheless, significant relationships exist between the variables I chose, and the predicted frequencies provide good matches with observations. The multivariate approach may prove more useful for some applications than the simpler bivariate analyses. Incorporating these results into an individual-based forest-succession model will permit evaluation of long-term consequences of repeated ice storm disturbance on forest dynamics (this dissertation Chapter 6).

Implications of the ice storms for long-term forest dynamics

The importance of disturbance in regulating species composition and diversity has been widely recognized in recent decades (Loucks 1970; Huston 1979, 1994; Turner *et al.* 1997). Disturbance is thought to maintain species diversity, especially in mesic sites where competition for light is high, by reducing the abundance of superior competitors and thereby preventing competitive exclusion (Connell 1978; Huston 1979; Sousa 1979; Pickett and White 1985; Smith and Huston 1989). Without disturbance, shade-tolerant species would ultimately dominate mesophytic forests, forming self-replacing stands from which other species are excluded. Although most species grow best on mesic sites, competition in favorable sites displaces species distributions toward suboptimal conditions. The consequence is zonation in species abundance along moisture gradients (Huston 1994; Smith and Huston 1989). Zonation should become more

pronounced over the course of succession, unless disturbances interfere. Zonation in tree species abundance is evident on southern Appalachian landscapes (Whittaker 1956; McCormick and Platt 1980), including my study area (Figure 3.4). The absence of extreme dominance in my study sites (Figure 3.4), especially in the mature mesophytic forest, probably reflects the role of past natural or anthropogenic disturbances in preventing competitive exclusion.

The presence of species as seedlings in stands from which they are not present as larger trees indicates that the most recent ice storms may further diminish the zonation pattern. Post-disturbance seedling distributions are presumably closer to the "physiological niches" of the species, whereas canopy composition reflects "ecological niches." Both white pine and ash seedlings occur in the mesophytic ravine forests, and table mountain pine seedlings are present in oak forests on east-facing slopes (Table 3.5). None of the three species, which exhibit low to intermediate shade-tolerance, is currently present in larger size classes of these forests (Table 3.4).

Ice storm disturbance probably has unique consequences for forest dynamics in each of the forest types I sampled. In the mesophytic ravine forest on Little Walker Mountain, disturbance should delay competitive exclusion and allow continued existence of shade-intolerant species. Maintenance of yellow-poplar and other shade-intolerant species in southern Appalachian mesophytic forests is attributed largely to periodic disturbance (Barden 1980; Lorimer 1980; Busing 1995). The heavy ice storm disturbance at the ravine site removed approximately half the basal area of the dominant, shade-tolerant eastern hemlock (Table 3.4) and will likely permit recruitment of intolerant species from the seedling and sapling levels (Table 3.5). The presence of yellow-poplar, hickories, oaks, sweet birch, and black locust (Table 3.4) in the overstory suggests that the forest has been influenced previously by ice storms or other disturbances. Similarly, periodic ice storms in the Adirondacks probably allow the persistence of opportunistic, light-demanding species, such as black cherry (*Prunus serotina*) and bigtooth

aspen (*Populus grandidentata*), that would otherwise be excluded from late-successional communities dominated by sugar maple.

Ice storm disturbance in the old-field yellow-poplar forests of the Blue Ridge may enhance yellow-poplar dominance. Whitney and Johnson (1984), who observed low mortality in ice-damaged yellow-poplar and abundant post-storm yellow-poplar reproduction, hypothesized that periodic ice storms might perpetuate the "pioneer" yellow-poplar community. Nearly pure stands of yellow-poplar are unusual in natural landscapes. They typically originate on abandoned farmland (Beck 1990) and therefore were probably scarce on presettlement landscapes. Now that the stands are established, however, the rapid growth rates and high fecundity of yellow-poplar (Beck 1990) may indeed promote its continued dominance in stands affected periodically by ice storms or other major canopy disturbances. A few other species, including red maple, northern red oak, ashes, and hickories, may also be favored by ice storm damage at my study sites (Table 3.5). However, yellow-poplar generally grows more rapidly than other southern Appalachian species (Beck 1990) and appears to be the most likely beneficiary of ice storm disturbance. Both eastern hemlock (*Tsuga canadensis*) and Carolina hemlock (*Tsuga caroliniana*) are present on the Blue Ridge and may eventually invade the stand, but expansion of the introduced hemlock wooly adelgid (*Adelges tsugae*) throughout the region makes the continued, long-term presence of either species unlikely (SAMAB 1996). Seedlings of the exotic tree *Ailanthus altissima* are present (Table 5). This shade-intolerant species exhibits extremely fast growth (Miller 1990) that enables it to outcompete yellow-poplar on abandoned farmland and form patches composed purely of *Ailanthus* (personal observation). However, *Ailanthus* trees are short-lived and do not attain the heights of yellow-poplar (Miller 1990), making it unlikely that the species will become a significant competitor in established yellow-poplar stands.

Results from the oak-dominated forests of the Valley and Ridge indicate that ice storms may be a major component of disturbance regimes in Appalachian oak forests. The relatively

high resistance of oaks, particularly chestnut oak, to ice damage permitted slight increases in oak dominance, although the absolute abundance of oaks decreased (Table 3.4, Figure 3.4). Additionally, the dominant oaks and hickories are present in the seedling and sapling classes (Table 3.5) and among the understory trees that will probably fill many of the canopy openings. Diversity may be enhanced in oak forests if periodic canopy disturbances reduce the abundance of chestnut oak and northern red oak sufficiently to prevent competitive exclusion of other oaks, hickories, and black locust.

Disturbance regimes characteristic of upland oak forests are not well understood (Lorimer 1980; Runkle 1990). Some authors have suggested that past burning brought about the widespread oak dominance that characterizes Appalachian landscapes (Runkle 1990; Abrams 1992; Nowacki and Abrams 1992; Bratton and Meier 1998; Delcourt and Delcourt 1998; Harrod *et al.* 1998). Reduced fire frequency on present landscapes may lead to successional replacement of oaks by shade-tolerant species, such as red maple and sugar maple, that are more abundant than oaks in forest understories (Abrams 1992; Nowacki and Abrams 1992). My results show that red maple, in particular, is a common understory tree in oak forests (Table 3.5). However, oak seedlings and saplings occur even more frequently than those of red maple. Given the sprout origins of many seedling-size individuals I recorded, the rapid growth rates of oak sprouts and advance oak seedling reproduction (Johnson 1990; McQuilkin 1990; Rogers 1990; Sander 1990a, 1990b), the high survival rates of oak seedlings, and the increase in understory light levels following canopy disturbance, there is little reason to doubt that oaks will continue to dominate these forests. Whitney and Johnson (1984) found increased oak regeneration in southwestern Virginia oak forests following ice storm disturbance, and they concluded that oak dominance would be maintained. It appears that canopy disturbance by periodic ice storms may be a major factor in the maintenance of oak-dominated forests, especially where fires occur infrequently.

Oaks are among the most valuable of hardwood species, both in ecological and economic terms, and further research is merited on the role of disturbance in oak-forest dynamics.

The table mountain pine forest I sampled is located on a topographic position sheltered from major ice storm disturbance (Lafon *et al.* 1999). The importance of the dominant species would otherwise likely have been reduced severely. Southern pines appear particularly vulnerable to ice damage, as evidenced by severe decline or complete loss of table mountain and pitch pines from oak-dominated stands exposed to heavier ice accumulation. Whitney and Johnson (1984) reported that three species of southern pines – table mountain pine, pitch pine, and Virginia pine – suffered heavy losses during the 1979 ice storm in western Virginia. Except on extremely xeric sites, where table mountain pine may form self-replacing populations, hardwoods are currently replacing table mountain pine in the southern Appalachians (Williams and Johnson 1990; Williams 1998). Williams (1998) proposed that ice storm disturbance promotes the conversion of table mountain pine-pitch pine stands to oak dominance. Indeed, oak regeneration is abundant in the table mountain pine stand I sampled (Table 3.5). Periodic burning is the primary natural disturbance that favors table mountain pine dominance (Williams 1998). However, an increase in table mountain pine seedlings following heavy ice storm damage may be adequate to maintain the pre-storm composition on some xeric sites (Whitney and Johnson 1984).

In my study area, table mountain pine seedlings invaded oak stands on the relatively dry, upper slopes of east-facing spurs following the 1994 ice storms (Table 3.5). Nearby pine stands on the tops and west faces of the spurs provided seed sources. As long as a seed source is available, heavy ice storm disturbance appears to create conditions favorable for the maintenance of table mountain pine on subxeric sites from which it would otherwise be excluded. Mineral soil and thin litter, which are necessary for table mountain pine seedling survival (Williams and Johnson 1992), are present in patches on the floor of disturbed forests. Availability of mineral soil and high light levels, combined with slow recovery of oak populations on subxeric sites,

should permit establishment and growth of scattered table mountain pine individuals even where fire occurs infrequently.

Topographic differences in ice storm disturbance may enhance *beta* diversity (Whittaker 1975) on the forested landscape and contribute to such well-known vegetation patterns as aspect-related differences in forest composition. If the same forest patches are subjected repeatedly to disturbance, they may develop distinctive characteristics that preserve the imprints of disturbance. Mesophytic forests exposed to periodic ice storm disturbance are probably characterized by higher species diversity than those on sheltered sites, where shade-tolerant species should strongly dominate. In oak-dominated forests, ice storms may favor maintenance of oak populations, whereas red maple or other shade-tolerant species may replace oaks on sheltered sites. Ice storms may also contribute to the confinement of table mountain pine-dominated stands to west-facing slopes.

Disturbance boundaries associated with topography are often sharper than the topographic changes themselves. These sharp boundaries reflect locations in which thresholds of tree stress were exceeded. Such abrupt boundaries may accentuate topographic patterns in species composition and diversity.

Conclusions

Major ice storms represent significant canopy disturbances that have important consequences for forest dynamics in eastern forests. Consistent with previous studies, my results demonstrate that a number of factors influence tree damage characteristics. These factors include tree size, wood strength, canopy architecture, and site variables such as slope and soil depth. The use of multinomial logistic regression allowed me to model the combined influences of several variables on tree damage.

Discerning the role of ice storms in forest dynamics will require additional work to find sites characterized by varying ice storm frequency and to assess differences in vegetation

characteristics among those sites. Forest stand simulation models provide another useful way to evaluate long-term forest processes. Development of a multivariate approach for estimating ice storm damage among individual trees is an important component necessary for modeling long-term dynamics of forests affected by repeated ice storm disturbances.

Ice storms are only one of several disturbance agents that impact Appalachian forests. Small gaps created by individual tree mortality are thought to dominate disturbance regimes over much of the eastern hardwood region (Runkle 1990), but larger disturbances, such as ice storms, hurricanes, strong thunderstorm winds, tornadoes, debris slides, fires, and insect outbreaks, also occur. In fact, these larger disturbances may have more influence than frequent individual tree-falls on forest dynamics in some parts of the Appalachians and Adirondacks. In southwestern Virginia, several major ice storms and the remnants of Hurricane Hugo have struck the same parts of the landscape over the past two decades. Air photo interpretation and field reconnaissance suggest that Hurricane Hugo damage was most severe on southeast-facing slopes, some of the same sites damaged by the subsequent ice storms. These sites may be repeatedly struck by ice storms and hurricanes. Easterly, southeasterly, or northeasterly winds are probably typical during ice storms (Konrad 1998; Lafon *et al.* 1999), which are usually associated with warm fronts (Gay and Davis 1993), contributing to heaviest ice accumulation on slopes facing these directions (Lafon *et al.* 1999). In north temperate regions, hurricane damage is greatest to the right of the storm track, where counterclockwise flow around the cyclone is aligned with the direction of storm movement (Foster and Boose 1995). Slopes facing east to southwest are therefore exposed to the highest winds (Foster 1988).

Natural gap-forming disturbances are important for maintaining the presence of shade-intolerant species in eastern forests. Black locust, table mountain pine, white pine, yellow-poplar, oaks, and hickories, all of which exhibit relatively low shade-tolerance, have become established in southwestern Virginia forests damaged heavily by the recent ice storms, hurricane, or both.

The role of these disturbances may be especially significant in wilderness areas in which anthropogenic disturbances are restricted. In Kimberling Creek Wilderness Area, a few kilometers north of my sampling sites, disturbance of a mature oak forest by Hurricane Hugo and the subsequent ice storms has stimulated reproduction and rapid growth of black locust and other shade-intolerant species, including herbaceous plants, which would otherwise be scarce or absent.

Feedback may exist among different types of disturbance. Glitzenstein and Harcombe (1988) speculated that tornado damage in southeastern Texas would increase the likelihood of fire by supplying flammable woody debris and causing increased growth of fine live fuels in the understory. Bratton and Meier (1998) found that some of the most severe historic fires in the Chattooga River basin of the southern Blue Ridge occurred in forests disturbed by previous windstorms. Ice storms also supply large quantities of woody debris that probably increase the likelihood of a major fire. Typically, fires in Appalachian hardwood forests are relatively light, burning litter and understory vegetation. The presence of tree limbs and boles would increase the magnitude of a fire, if ignition occurs. Ice storm disturbance may also increase vulnerability to wind damage by opening the forest and exposing individual trees to higher winds. Further, ice storm damage provides entry sites for insects and diseases. Thus, in addition to their direct effects, ice storms likely initiate a range of other mortality-causing disturbances that help maintain forest diversity.

Chapter 4

Spatial Patterns of Ice Storm Occurrence in the New River Valley of North Carolina, Virginia, and West Virginia

This chapter is very similar to a paper published in 1999 in the *New River Symposium Proceedings:*

Lafon, C.W. 1999. Spatial patterns of ice storm occurrence in the New River Valley. *New River Symposium Proceedings, April 15-16, 1999, Boone, North Carolina.* New River Gorge National River, Glen Jean, West Virginia. Pages 68 – 87.

Introduction

Spatial variations in ice storm frequency or magnitude may contribute to differences in vegetation characteristics among locations with different ice storm climatologies. In this paper, I investigate spatial patterns in ice storm frequency in the New River Valley of North Carolina, Virginia, and West Virginia. The New River drainage basin comprises a large portion of the southern Appalachian region, and variations in ice storm climatology throughout the basin are representative of patterns across the broader region. Appalachian cold air damming (Richwien 1980; Bell and Bosart 1988; Michaels 1991) is a particularly important influence on ice storm climatology in the Appalachian region. Research of Michaels (1991), Gay and Davis (1993), and Konrad (1998) indicates that the occurrence of sleet and freezing rain is more frequent in the eastern Appalachians and western Piedmont, which are influenced by cold air damming, than in other nearby regions.

My purpose is to use information reported by the National Climatic Data Center (NCDC) in its monthly *Storm Data* publication to estimate fine-scale patterns of ice storm frequency and severity in the New River Valley. Several factors, including cold air damming and topographic structure, may contribute to spatial variations in ice storm frequency in the area. Unfortunately, few quantitative data about freezing rain are collected at weather observation stations, and little is known about patterns of ice storm occurrence at fine spatial scales. *Storm Data* is one of the only sources of information about ice storm occurrence outside of major cities.

Study area

My research is focused on the North Carolina, Virginia, and West Virginia counties situated partially or entirely within the New River drainage basin. I also include in my analyses all counties bordering these New River Valley counties (Figure 4.1). The study area is characterized by considerable topographic variation. The southeastern edge of the area (North Carolina counties of Caldwell, Wilkes, and Surry, and Virginia counties of Patrick, Franklin, and Bedford) is located on the gently rolling Piedmont province. Elevations are mostly around 300 m above sea level. The Blue Ridge rises sharply above the Piedmont to elevations around 750 – 1000 m, and several peaks in the Blue Ridge exceed 1500 m. Four North Carolina counties (Avery, Watauga, Ashe, and Allegheny), both Tennessee counties, and three Virginia counties (Grayson, Carroll, and Floyd) are in the Blue Ridge. Portions of adjacent counties are also in the Blue Ridge. All the remaining counties of Virginia, except for Buchanan County, are located primarily in the Ridge and Valley province. Pendleton County, West Virginia, is also in the Ridge and Valley. The Ridge and Valley province consists of numerous mountains and valleys oriented roughly parallel to one another. Elevations generally range between 600 and 1400 m. The rest of the counties in the study area are located in the Appalachian Plateaus province, a region of dissected plateaus. Elevations are generally 300 – 1100 m, with some areas reaching nearly 1500 m.

Methods

I used the monthly *Storm Data* reports to map patterns of ice storm frequency in the study area. I consulted the winter (October – April) issues of *Storm Data* for each year from 1986 – 1998 to identify ice storms in any county in the study area. The publication provides qualitative descriptions of significant weather events occurring in each state. For each event, *Storm Data* lists the National Weather Service (NWS) forecast zones affected by the storm. From 1986 until late-1993, each state was divided into only a few forecast zones, with several counties per zone. I

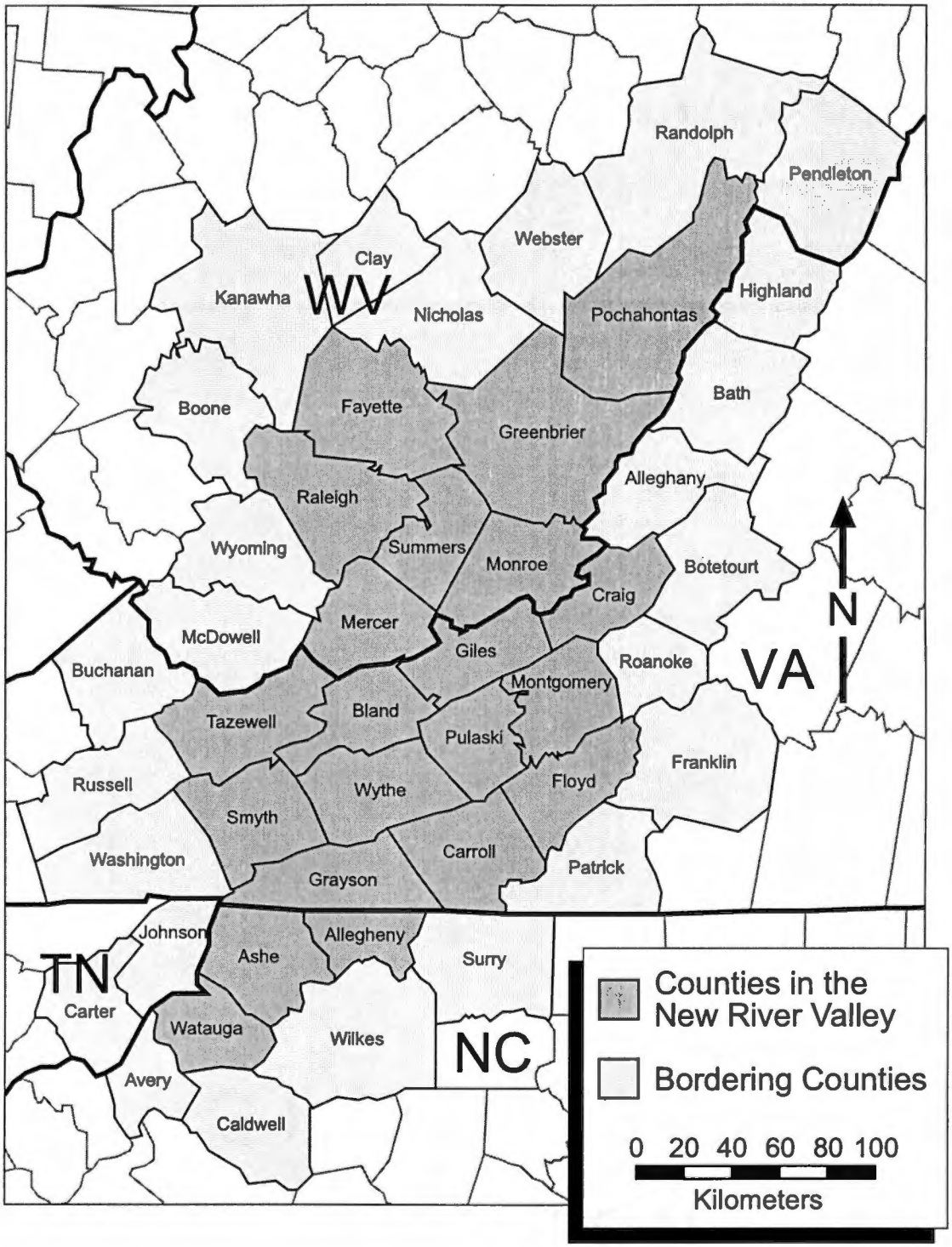

Figure 4.1. Counties in the study area.

recorded the occurrence of each ice storm for all counties in an affected zone, unless the description provided more detailed information about the location of the storm. In fact, it was frequently possible to determine which individual counties in a forecast zone experienced an individual event.

In late-1993, NWS redefined its forecast zones, creating a forecast zone for each county in the study area. The change permits better spatial resolution of ice storm occurrence for the last five winters, beginning with an event that affected parts of North Carolina and Virginia in December 1993. One consequence of the change in forecast zones is that it was necessary to divide Greenbrier County, West Virginia into two halves for data analysis. Prior to 1993, the eastern half of the county was in one forecast zone and the western half in another.

I used the descriptions in *Storm Data* to classify each ice storm into one of three categories of severity – minor, moderate, or major. Unless significant tree or transmission line damage was noted in a description, I classed the storm as minor. For storms in which tree or line damage occurred, I classified only storms causing major power disruptions or severe forest damage as major events. Otherwise, they were considered moderate storms. Use of *Storm Data* to identify such variations in spatial patterns of ice storm occurrence requires a degree of subjective assessment.

Storm Data lacks a Virginia report for February 1994, when a major ice storm struck much of the study area. I used a report compiled by Jones *et al.* (1997) from newspaper accounts to identify the Virginia counties affected by the storm during that month.

After compiling a record of all ice storms identified by *Storm Data*, I summed by county the number of events in each severity category. I then mapped spatial patterns of frequency for storms of each level of severity.

Results

The frequency of ice storms exhibits pronounced spatial variation over relatively short distances for the 12.5 winters occurring January 1986 – March 1998. Minor ice storms occurred most frequently in the northeastern section of the study area (Figure 4.2A), with the greatest number (fourteen) in Highland County, Virginia. The northwestern section of the study area experienced the lowest number of storms. For moderate storms, eastern counties again exhibit the highest number of events, but the maximum frequency is farther south, in the Blue Ridge counties of Floyd and Carroll, Virginia (Figure 4.2B). The pattern for major storms is relatively similar to that for moderate events (Figure 4.2C).

When moderate and major storms are combined (Figure 4.3A), the resultant pattern indicates that, during the period 1986 – 1998, storms of at least moderate severity occurred most frequently in the east-central portion of the study area, with a maximum in Floyd and Carroll Counties. The highest frequency of all events (all three severity classes combined) was along the eastern edge of the study area, and the lowest frequency was along the northwestern margin (Figure 4.3B).

In an attempt to resolve spatial patterns at the finest possible scale, I created another set of maps using data for the last five winters only, during which storm data were reported for individual counties. As in Figure 4.2A, the patterns in Figure 4.4A indicate that minor ice storms occurred most frequently along the eastern edge of the study area and least frequently along the western edge. However, the Blue Ridge and Piedmont of North Carolina are more conspicuous for high frequency than in Figure 4.2A. In addition, the pattern of low ice storm frequency along the western margins of the study area is more pronounced. This latter pattern is particularly noticeable in southwest Virginia, where the western counties (Washington, Russell, and Buchanan) had previously been grouped in the same forecast zones as counties to the east (e.g., Giles, Floyd, and Montgomery).

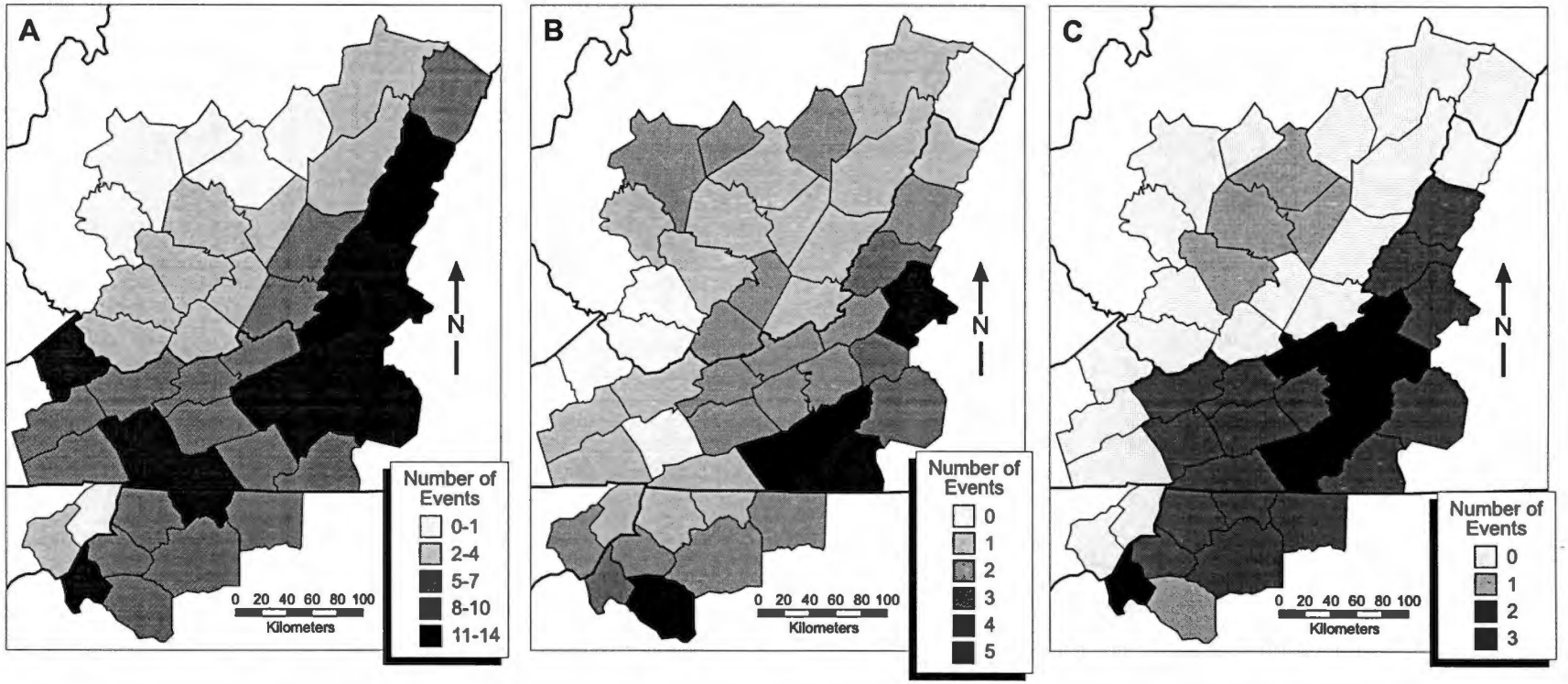

Figure 4.2. Number of freezing rain events per county, January 1986-March 1998: (A) minor ice storms, (B) moderate ice storms, and (C) major ice storms.

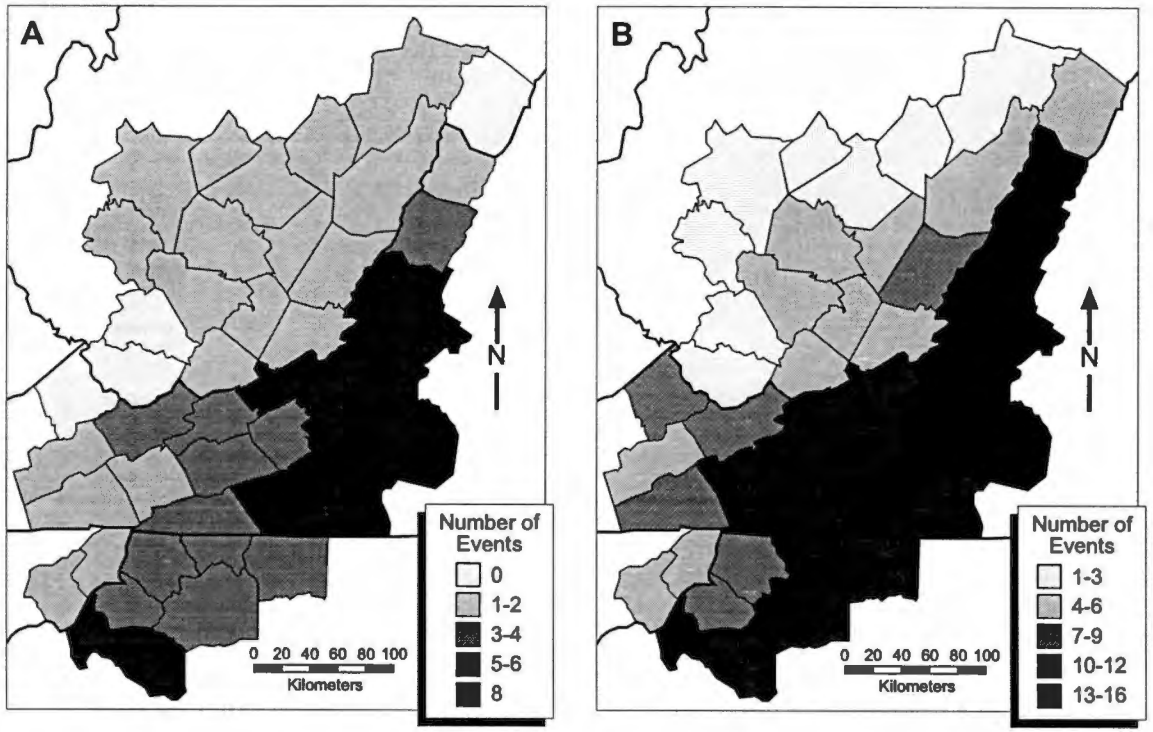

Figure 4.3. Number of freezing rain events per county, January 1986-March 1998: (A) moderate and major ice storms and (B) all ice storms.

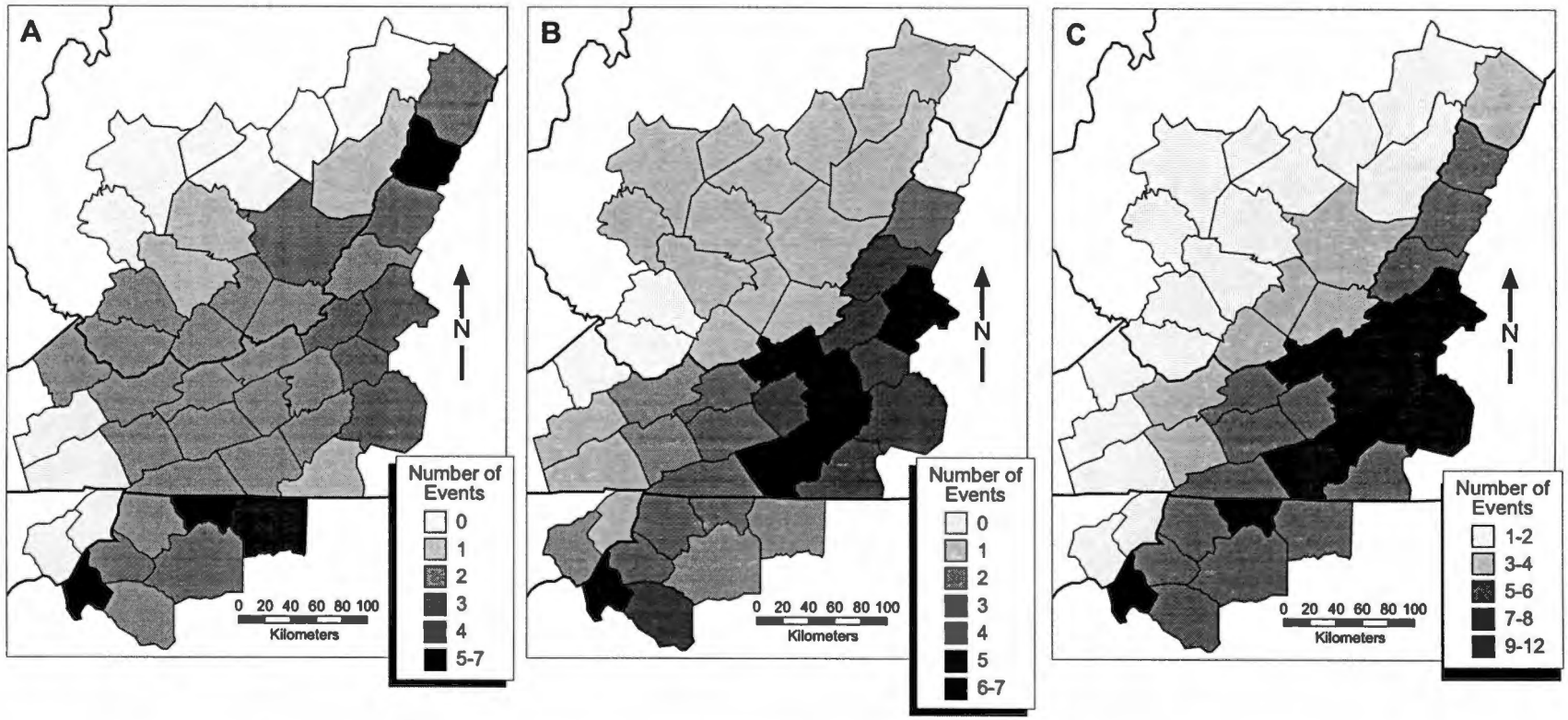

Figure 4.4. Number of freezing rain events per county, December 1993-March 1998: (A) minor ice storms, (B) moderate and major ice storms, and (C) all ice storms.

The pattern of moderate and major storms (Figure 4.4B) is similar to that mapped previously (Figure 4.3A). Highest frequency of these events occurs in the east-central portion of the study area and extends southward into North Carolina along the Blue Ridge. The Virginia Blue Ridge (Floyd and Carroll Counties) experienced the greatest number of events. When ice storms of all three severity levels are combined for the last five winters, a striking pattern emerges, with high frequency in the east and low frequency in the west (Figure 4.4C). The east-central portion of the region, in particular, exhibits a high frequency.

Discussion

The most useful maps are those that depict total number of ice storms (Figures 4.3B and 4.4C) and those that portray the combined number of moderate and major events (Figures 4.3A and 4.4B). The former maps (total number of storms) demonstrate an east to west gradient in freezing rain frequency, a pattern almost certainly influenced by cold air damming. Other factors may also contribute to the pattern. For example, elevations are generally lower on the western edge of the study area than in the central and eastern portions, and during some storms these elevational differences may promote rain in the west and freezing rain in the east. Another consideration is that snow occurred in West Virginia during several of the events that produced freezing rain farther east, indicating that the surface cold layer was deeper in the west than the east during those events. Resolution of all factors responsible for the observed patterns would require detailed analyses of meteorological conditions during each storm.

The maps of moderate and major storms combined are the most important results of this research. These storms cause the most severe forest disturbance, power outages, and travel hazards. Also, *Storm Data* likely contains more complete reports for these storms than for minor events that attract less attention. The same mechanisms discussed above, particularly cold air damming, are likely responsible for the patterns of moderate and major storms. However, fine-scale variation within the region affected by cold air damming indicates that several other factors

also influence the spatial distribution of significant icing. High frequency along the Blue Ridge (especially Floyd and Carroll Counties) suggests that elevation may be an important determinant of the location of heavy ice accumulation. Most published information about ice storms indicates that ice accumulation is usually heavier and occurs more often in high elevations of the Appalachians than in adjacent valleys (Abell 1934; Carvell *et al.* 1957; Bennett 1959; Williams 1960; Konrad 1998). The Blue Ridge pattern may reflect the role of both low temperatures and orographic precipitation enhancement at high elevations.

In some cases, the storm record for an individual state is missing from the monthly *Storm Data* report. Some of the mapped patterns may be exaggerated or obscured as a result of these missing records. Of the four states in my study area, records are most complete for North Carolina and least complete for West Virginia. Fewer records are missing for recent years than for the earlier years. To assess the possibility that variations in information completeness influences the mapped patterns, I identified cases in which a monthly report is missing from one state and an ice storm occurred in adjacent parts of a neighboring state. It appears from this examination that missing records do not significantly affect the patterns I have mapped. One moderate-intensity event occurred in North Carolina during December 1989, for which a Virginia report is missing, and two minor events occurred in Tennessee during this month. It appears that the inclusion of these events for Virginia would only augment the pattern of high ice storm frequency already identified for Virginia. Two minor events in Virginia during January and March 1989 may have affected southeastern West Virginia, for which data on both months are missing. Including these events would probably identify a sharper distinction in minor event frequency between eastern and central West Virginia.

Subjectivity involved in interpreting the information reported in *Storm Data* undoubtedly results in some errors. It was difficult to define county-level spatial extents for some events. Additionally, it was often necessary to classify a single storm as a minor event in some counties

and a moderate event in others, or as a moderate event in some and a major storm in others. All such decisions could produce inaccuracies. However, the orderly patterns of mapped ice storm frequency and their agreement with mechanisms known to influence freezing rain occurrence suggest that the maps provide reasonably accurate portrayals of ice storm occurrence patterns.

A final problem affecting the identified patterns is that the length of record may be too short to provide definite conclusions about spatial patterns. The entire data record covers only 12.5 winters, and county-level reports have been issued for only five of those winters. The general patterns I have mapped, particularly the east to west gradient, probably agree favorably with long-term patterns in ice storm frequency. However, some of the finer-scale patterns, such as the high frequency in Floyd and Carroll counties, may not persist over longer time intervals. Additional research, perhaps employing extensive newspaper reports, would be necessary to identify spatial patterns for a longer period.

Conclusions

Understanding spatial variations in ice storm recurrence may provide insights about patterns of forest composition and diversity across the New River Valley. This paper uses qualitative descriptions found in *Storm Data* to identify patterns of ice storm frequency and severity over a region for which few quantitative data exist. Results suggest strongly that cold air damming exerts an important degree of control on ice storm climatology in the study area. The maps indicate that freezing rain occurs more frequently in the eastern half of the study area than in the western half. Finer-scale variations within this general pattern probably reflect the role of other factors, such as elevational differences in temperature and precipitation. It would be useful to extend this analysis to longer time intervals, if possible, and to larger geographic regions.

Chapter 5

Using Dendrochronology to Identify Ice Storm Events in Oak Forests of Southwestern Virginia

This chapter is based on a paper written by Charles Lafon and James Speer and reviewed for possible publication in the journal *Climate Research.* A revised version of this paper will be resubmitted to *Climate Research*:

Lafon, C.W. and Speer, J.H. Using dendrochronology to identify ice storm events in oak forests of southwestern Virginia.

My use of "we" in this chapter refers to my co-author and myself. My primary contributions to this paper include (1) working with Speer to develop the project, (2) co-directing the fieldwork, (3) preparing and measuring samples, (4) most of the data analysis, and (5) most of the writing. Speer's main contributions were (1) conceiving the project, (2) co-directing the fieldwork, (3) guiding me in the use of dendrochronological techniques, and (4) assisting with data analysis and writing.

Introduction

Vegetation disturbances have important consequences for species composition and diversity (Loucks 1970; Huston 1994). In the forests of eastern North America, major ice storms produce heavy amounts of rain that freeze on tree surfaces, breaking limbs, bending or breaking boles, and toppling trees over broad areas (Whitney and Johnson 1984; Seischab *et al.* 1993). Canopy tree losses on the order of 50% are common in heavily damaged stands (Downs 1938; Seischab *et al.* 1993; Lafon *et al.* 1999). Where they occur frequently, ice storms represent one of the most significant agents of forest disturbance. Ice storms also disrupt traffic, damage utility lines, and cause other economic losses. Recent major ice storms in the southeastern and northeastern United States contributed to a number of deaths and caused several billion dollars in damage (Lott and Sittel 1994; Lott *et al.* 1998).

The frequency and severity of ice storms vary spatially at several scales. Globally, ice storms occur most frequently in eastern North America, where conditions are favorable for the extreme air mass contrasts necessary for freezing rain to occur (Bennett 1959). Freezing rain typically results when warm, moist air is advected over a subfreezing surface layer, creating an

inversion (Stewart and King 1987; Gay and Davis 1993; Rauber *et al.* 1994). If the temperature above the inversion is above freezing, rain falls from this warm layer and then becomes supercooled as it travels through the underlying cold air. Generally, freezing rain occurs where the cold layer is not deep enough to permit raindrops to freeze before striking the surface. The supercooled drops freeze on impact to form a layer of ice (glaze) on trees, roads, utility lines, and other surfaces (Ahrens 1991; Gay and Davis 1993). In clouds with few ice nuclei, a supercooled warm rain process may also produce freezing rain in the absence of an inversion (Huffman and Norman 1988).

Within North America, the midwestern and northeastern United States generally experience the highest frequencies of freezing rain (Bennett 1959; Eagleman 1983). The eastern Appalachian Mountains and the western Piedmont are also subject to frequent ice storms, a consequence of Appalachian cold air damming (Bennett 1959; Gay and Davis 1993; Konrad 1998). Cold air damming involves the establishment of a shallow dome of cold surface air over the eastern Appalachians and the Piedmont. This condition arises when cold air from a surface anticyclone situated over the Northeast flows toward the southwest and becomes trapped against the eastern slopes of the mountains (Richwien 1980; Bell and Bosart 1988). Cold advection, upslope flow, and evaporative cooling may help maintain the presence of the cold surface layer (Forbes *et al.*1987). When air temperatures in the surface dome are below freezing, rain falling through this subfreezing air from a warmer layer above becomes supercooled and freezes on impact with surface objects (Michaels 1991).

Patterns of ice storm damage often exhibit pronounced topographic influences in hilly or mountainous terrain. In eastern North America, slopes facing east, north, northeast, or southeast appear especially susceptible to heavy ice accumulations (Rhoades 1918; Downs 1938; Spaulding and Bratton 1946; Whitney and Johnson 1984; Seischab *et al.* 1993; Lafon *et al.* 1999). These are typically the windward aspects during an ice storm. The aspect-related differences in ice

accretion may result from topographic effects on precipitation intensity on windward slopes (Sharon 1980; Poreh and Mechrez 1984; Smith 1989; Lafon *et al.* 1999) or from influences of wind on twig surface temperatures and raindrop fall velocities (Lafon *et al.* 1999). In the Appalachian Mountains, elevational zonation in glaze damage is also common. Most evidence suggests that ridgetops are subject to more frequent ice storms or more severe ice storm damage than adjacent lowlands (Abell 1934; Carvell et al 1957; Bennett 1959; Williams 1960; Anthes 1976; Nicholas and Zedaker 1989; Konrad 1998). Vertical temperature profile is probably the primary influence on elevational patterns of ice accretion. Below-freezing temperatures may exist immediately below the inversion while temperatures above and/or below that layer are slightly above freezing, a condition that favors accretion of the supercooled drops at particular elevations, e.g., on the ridges but not in the valleys, or vice versa. Orographic effects on precipitation intensity may also influence elevational patterns of ice storm damage.

Despite observations of topographic variations in ice storm damage, little work has been conducted to quantify fine-scale spatial patterns in ice storm frequency or severity. A dearth of pertinent climatic data hampers efforts to estimate these fine-scale patterns. First-order National Weather Service (NWS) stations report weather type hourly, making it possible to identify the occurrence and duration of freezing rain events but not their magnitude. Gay and Davis (1993) used data from first-order stations to map patterns of freezing rain and sleet frequency in the southeastern U.S. However, first-order weather station records do not permit quantitative assessments of the frequency of major, forest-damaging events, because ice accretion is not reported. Further, first-order stations are too sparsely distributed to permit resolution of topographic variations in ice storm frequency. Konrad (1998) used daily climatic data collected at cooperative weather stations to estimate patterns of ice storm frequency at a relatively fine spatial scale in the Appalachians. Cooperative stations form a denser network than the first-order stations, but Konrad's technique still does not provide a way to identify fine-scale topographic

variations in the frequency of ice storm disturbance. Record-length constraints also limit the usefulness of instrumental climatic data. Climate records at most stations are only a few decades long, but recurrence-interval analyses for relatively infrequent events like major ice storms require longer data chronologies. Descriptive accounts, such as newspaper articles, provide longer records but do not furnish sufficiently detailed information for reconstructing long-term histories of ice storm disturbance at fine spatial scales.

We report here the results of a preliminary analysis designed to determine whether it is possible to distinguish a tree-ring signal resulting from ice storm disturbance in Appalachian hardwood forests. Discerning such a tree-ring signal would permit researchers to reconstruct the history of ice storm events that have affected a forest stand and to characterize fine-scale spatial variations in ice storm climatology. Tree-ring analysis, or dendrochronology, involves matching ring-width patterns between trees to develop a chronology of factors affecting tree growth. Dendrochronology provides a means to study patterns of climate at finer spatial scales than other records permit (Phipps 1982). Dendrochronology is useful for extending temporal records of rainfall and temperature variations, droughts, forest fires, insect defoliations, and other events (Stahle *et al.* 1985; Baisan and Swetnam 1990; Swetnam and Betancourt 1990; Graumlich 1993; Swetnam and Lynch 1993; Speer *et al.* in press). Dendrochronology is also commonly used in studies of fire history, because it is possible to date fire scars on trees that survive a blaze and to identify even-aged cohorts of early-successional trees that colonize after a fire. Fine-scale spatial patterns of fire extent and fire frequency can be inferred by sampling trees growing on different topographic positions or dispersed throughout a watershed (Arno 1976; Romme and Knight 1981; Baisan and Swetnam 1990).

A few researchers have investigated relationships between ice storm occurrence and tree-ring width in conifers. Travis *et al.* (1989) and Travis and Meentemeyer (1991) included ice storms in regression models they developed to predict ring width in loblolly pine (*Pinus taeda*)

and shortleaf pine (*P. echinata*) in Georgia and South Carolina. The reduced growth resulting from ice damage accounted for 10 – 19% of ring-width variance in addition to the 25 – 39% explained by standard temperature and precipitation variables. Travis and Meentemeyer (1991) concluded that ice storm damage reduces radial growth only during the growing season immediately following the storm. This result may in part reflect the fact that trees showing no structural damage from ice were selected for the study. In contrast, Belanger *et al.* (1996) reported that loblolly pine damaged by a 1983 ice storm in Georgia still exhibited slower radial growth than adjacent undamaged trees when they studied the trees five years later. Felin and Rivest (1983) showed that ice storm damage contributed to reduced ring widths for several years in black spruce (*Picea mariana*) and balsam fir (*Abies balsamea*) in Quebec.

No previous research has been published specifically on the effects of ice storm disturbance on tree rings in hardwood species, but dendrochronology has been used to identify major canopy disturbance events in hardwood forests from the periods of abruptly increased radial growth that follow (Lorimer 1980; Lorimer and Frelich 1989). Such growth patterns generally indicate release of understory trees from competition with canopy individuals killed or damaged by a disturbance. Remaining canopy trees may also exhibit increased growth following the loss of neighboring competitors, although their response is not as dramatic as that of understory trees (Lorimer and Frelich 1989).

We hypothesized that, as in conifers following ice storm damage, and hardwoods following canopy disturbance, canopy damage to hardwood species by ice storms would produce marked changes in radial growth. To investigate this possibility, we conducted a dendrochronological study of chestnut oak (*Quercus prinus*) and black oak (*Q. velutina*) at two sites in southwestern Virginia where major ice storms had occurred at known dates in recent years. These species are abundant over a wide range of topographic positions in upland forests of

the Appalachian Mountains, and we hoped they could prove useful for studies of ice storm history.

Study area

Two stands were selected, both on mountain slopes in southwestern Virginia. Three recent ice storms caused major forest disturbance in this area. The first of these occurred on 20 – 21 January 1979. The other two occurred in 1994, one on 10 – 11 February and the other on 1 – 3 March. Data reported by NCDC (1979a, 1979b, 1994a, 1994c) imply that ice accreted to depths of 2.5 cm or more during all three events. Widespread forest damage occurred and was most severe on east- and southeast-facing slopes (Whitney and Johnson 1984, Lafon *et al.* 1999). A full discussion of the meteorological events that produced the storms can be found in Lafon *et al.* (1999).

One study site is located on the southeast side of Gap Mountain, Montgomery County, Virginia, near the eastern end of the mountain at an elevation between 790 – 825 m (2600 – 2700 ft.) (Figure 5.1). Whitney and Johnson (1984) described disturbance in this stand following the 1979 ice storm. The storms of 1994 also affected the stand. Field observation of downed boles indicates that the most severe damage from the 1979 storm occurred at a lower elevation than the most severe 1994 damage. We focused on the portion of the stand affected by the 1979 event.

Our second study site is about 60 km southwest of the first one, on the southeast side of Walker Mountain, Bland County, Virginia, at an elevation between 850 – 915 m (2800 – 3000 ft.) (Figure 5.1). Disturbance at this site was described by Lafon *et al.* (1999) after the forest was damaged by the ice storms of 1994. Both the Gap Mountain and Walker Mountain sites are located in the Jefferson National Forest.

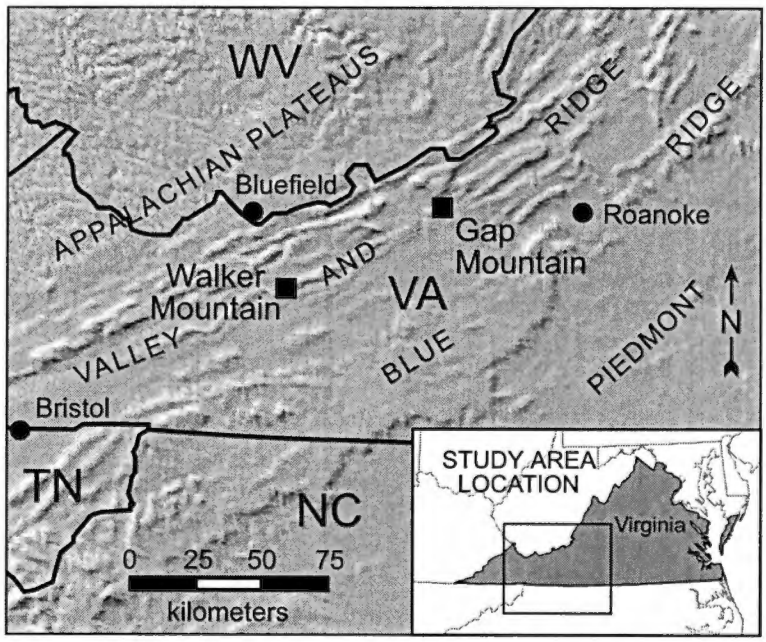

Figure 5.1. Location of the Gap Mountain and Walker Mountain study sites in southwestern Virginia.

Methods

We cored fifteen canopy trees at each of the two study sites during September 1998. Swedish increment borers were used to collect two cores at breast height from opposite sides of each tree. We also cut cross-sections from five downed trees at each site, using a chain saw. The zones of 1994 ice storm damage were evident from recently toppled boles and relatively fresh canopy damage. At Gap Mountain, the presence of toppled, decaying boles marked the zone in which heavy storm damage occurred in 1979. Trees were selected for sampling within the zones of major disturbance on the basis of tree age. We sampled older trees, regardless of damage level, to obtain the longest possible records.

We mounted the cores on standard wooden core mounts and then sanded the cores and cross-sections with progressively finer sandpaper (up to 400-grit) to obtain a smooth surface on which each ring is distinct. We constructed skeleton plots (Stokes and Smiley 1968) for ten trees at each site to develop a master chronology for the site. Significant marker rings from the master chronology were used to crossdate the remaining specimens. This approach permits identification of false or missing rings in a specimen and ensures correct dating of every ring.

We measured the rings from each pair of cores and from two radial transects on each cross-section using a Velmex measuring stage accurate to 0.02 mm. We then ran the COFECHA program (Holmes 1986) on our results to verify and refine our chronology. COFECHA generates a master chronology from the measured ring widths of all samples, correlating each series with the master chronology and identifying potential dating problems. We then used the ARSTAN program (Cook and Holmes 1986) to standardize the individual series using a fifty-year cubic smoothing spline, producing standardized growth chronologies. ARSTAN matches a smoothing spline to each core and then divides the measured ring width by the splined value, yielding a chronology with normalized variance and a mean of one. This technique removes age-related growth trends and long-period variation due to climate, permitting meaningful comparisons

among trees of different ages and growth rates. Use of a fifty-year smoothing spline retains 50% of the variance over a fifty-year period and 99% of the variance over sixteen years, removing long-term trends while retaining virtually all annual- to decadal-scale variation. Based on reported effects of ice storm damage on conifer ring-widths (Felin and Rivest 1983; Belanger *et al.* 1996), we anticipated that any ice storm signal would be primarily subdecadal, so that a fifty-year spline would be appropriate. We also used ARSTAN to average the paired chronologies from each tree into a single chronology.

In order to make any signal related to ice storms more visible, we first removed from our data sets as much of the noise related to background climate as possible. It would be ideal to sample trees growing in moist bottomland sites, because these trees exhibit minimal response to climatic variation (Fritts 1976). However, mountain slopes such as our study sites typically possess shallow, dry soils. Trees growing on such sites exhibit significant interannual ring-width variation due to changes in moisture availability (Fritts 1976). We employed stepwise regression to develop climate-response models, one for each tree chronology, of the ring-width variability associated with climate (methodology after Fritts 1976). In their study of ice storm effects on tree growth in southern pines, Travis and Meentemeyer (1991) also used stepwise regression to account for the climate signal, using as independent variables monthly temperature and precipitation.

This approach is similar to insect-outbreak analysis in which chronologies from non-host tree species are used to subtract the climate signal from host species and thereby clarify the influences of insect defoliation on ring width (Swetnam *et al.* 1985; Swetnam and Lynch 1993). We chose to create a unique climate-response model for each tree, instead of applying the same model for all trees, because individual trees vary in their responses to climate (Phipps 1982).

We used ring-width index generated with ARSTAN as the dependent variable for each of our climate-response models. Preliminary analysis revealed that Palmer Drought Severity Index

(PDSI), which integrates effects of temperature and precipitation on evapotranspiration, was a more satisfactory predictor of ring width in oaks than were simple temperature and precipitation (see Appendix). Independent variables for stepwise regression were monthly PDSI values for NOAA's Virginia Climate Division 5 region (NCDC 1999) for fifteen months prior to September of the year of ring formation. Our study sites are located at relatively high elevations in the eastern part of Virginia Climate Division 6, and ring-width indices show a closer relationship to PDSI values from Division 5 immediately to the northeast (Figure 5.2). PDSI is frequently used in dendrochronology and is often strongly correlated with tree-ring indices in eastern North America (Stahle *et al.* 1985; Jenkins and Pallardy 1995). Significance levels for variable entry and retention were set to 0.05 and 0.10 respectively.

We created climate-response models from climate data for the period 1930 – 1978. Weather records indicate that this period was relatively free of major ice storm disturbances that might create growth patterns unrelated to PDSI. The climate response models for Gap Mountain generally satisfied regression assumptions. However, skewed error distributions for some of the Walker Mountain series necessitated the creation of new climate-response models for that site, based on the years 1936 – 1978 only.

Ring-width index exhibited a significant relationship ($P < 0.05$) with PDSI in most trees (Table 5.1). Ring-width index is most commonly related to PDSI in July of the year of ring formation. Other growing season months (May or June) were also significant contributors in several cases. Adjusted R^2 (R^2 adjusted by sample size and the number of variables in the model) is reported because simple R^2 tends to overestimate the performance of the regression model (SPSS 1999).

The climate-response models generally explained 15 – 40% of the variance in ring-width indices. This is typical of climate reconstructions in the eastern U.S. (Travis *et al.* 1989; Travis and Meentemeyer 1991; Grissino-Mayer and Butler 1993), where radial growth is less tightly tied

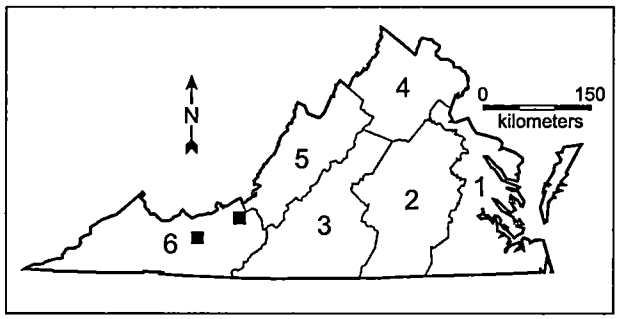

Figure 5.2. National Climatic Data Center climate divisions for Virginia. The black squares in division 6 indicate the locations of the two study sites.

Table 5.1. Results of regression analysis. The dependent variable is standardized ring width for each tree. The independent variables are monthly PDSI values. Variables ending in "py" indicate a month from the year previous to the year of ring formation.

Tree	Regression equation	Adjusted R^2	Significance
	Gap Mountain – chestnut oak		
A	y = 0.901 + 0.08688jul – 0.05071apr	0.260	0.000
B	y = 0.998 + 0.09038jan – 0.07213nov_py	0.222	0.001
C	y = 1.011 + 0.02832jul – 0.05945jul_py + 0.04063aug_py	0.243	0.001
D	y = 0.982 + 0.03436jul	0.275	0.000
E	y = 0.952 + 0.04107jul	0.182	0.001
F	y = 0.987 + 0.05214jun	0.222	0.000
G	no model		
H	y = 0.990 + 0.03061jul	0.172	0.002
I	y = 0.967 + 0.07881jul – 0.03906nov	0.243	0.001
J	no model		
K	y = 0.982 + 0.05680jul – 0.03368mar	0.442	0.000
	Gap Mountain – black oak		
L	y = 1.048 + 0.06428jul	0.184	0.001
M	y = 0.991 + 0.04264jul	0.152	0.003
N	y = 0.987 + 0.04165jul + 0.07532aug_py – 0.05426jul_py	0.453	0.000
O	no model		
P	y = 1.033 + 0.02665jan	0.066	0.041
Q	y = 1.077 + 0.05097jul	0.165	0.004
R	y = 1.061 + 0.03392dec_py	0.092	0.019
S	no model		
T	y = 1.022 + 0.09434aug_py – 0.07116jul_py	0.171	0.008
	Walker Mountain – chestnut oak		
A	y = 1.000 + 0.05776jun	0.178	0.003
B	y = .996 + 0.02540may	0.081	0.036
C	no model		
D	y = .991 + 0.02879jul	0.257	0.000
E	y = 1.021 + 0.02717aug_py	0.102	0.021
F	y = 0.977 + 0.05050jul	0.417	0.000
G	no model		
H	no model		
I	y = 0.996 + 0.05520jul	0.283	0.000
J	y = 0.999 + 0.04180jul	0.352	0.000
K	no model		
	Walker Mountain – black oak		
L	y = 1.018 + 0.05043jun	0.197	0.002
M	y = 0.984 + 0.05749oct_py	0.313	0.000
N	no model		
O	y = 1.006 + 0.04795may + 0.03814sep_py	0.326	0.000
P	no model		
Q	no model		
R	y = 0.983 + 0.03124jan + 0.02772sep_py	0.352	0.000
S	y = 0.977 + 0.06496nov_py + 0.04313jun	0.440	0.000
T	y = 1.020 + 0.04494jul	0.192	0.002

to moisture availability than in the more arid western U.S. (Phipps 1982). Our results imply that moisture availability during a critical period of several weeks in late spring to early summer strongly influences radial growth at our sites. July PDSI generally provides the best representation of this influence; however, the varied responses of individual trees indicates that the critical period spans more than one month and may vary from year to year.

We used the models to predict climate ring-width response indices for all years from 1896 – 1998. Subtracting the predicted indices from the observed ARSTAN values for each tree yielded a "climate-free" chronology whose variability is relatively disassociated from background climate and therefore more clearly signals other factors that affect ring width.

To allow identification of earlier ice storms, in addition to those of 1979 and 1994, we compiled a list of significant ice storms that may have affected our study sites during the period covered by our chronologies. We obtained information on these storms from the National Climatic Data Center (NCDC) publication *Storm Data and Unusual Weather Phenomena*. This monthly publication and its predecessors provide qualitative state-by-state descriptions of major weather events, including ice storms, back to 1914. We noted records of ice storms or heavy, wet snowstorms that caused damage to trees or utility lines. In some months, the storm record for an individual state is missing from the *Storm Data* report. For months in which the Virginia report is missing we checked reports for surrounding states to identify ice storms that may have affected our study area. Similar information was obtained for the pre-1914 period from monthly weather descriptions published in *Monthly Weather Review*. We verified the occurrence of all storms by searching for storm descriptions on the appropriate dates in *The Roanoke [Virginia] Times and World News*. Qualitative descriptions, particularly the sketchy reports of early years, are often inadequate for determining spatial extent of storm damage, but we recorded all events that may have affected our study sites.

Results

Tree-ring analysis revealed a bipartite ice storm signal. The climate-free ring-width indices are graphed in Figures 5.3 and 5.4. In some trees, radial growth declined following ice storm damage. Other trees experienced increased growth. Tree-ring series at either Gap Mountain or Walker Mountain ending before 1998 are from cross-sections cut from trees toppled by one of the ice storms. Also, remnants of Hurricane Hugo downed at least one of our sample trees in 1989 (chronology P, Figure 5.4).

Some chestnut oak chronologies (especially chronologies B, C, and H, Figure 5.3) from the Gap Mountain site record decreased growth for 1979, the year of a major ice storm, but long suppressions are not evident in this species. Several chestnut oaks exhibit increased growth for a few years after the 1979 ice storm. The 1979 storm is not recorded, at least as a major event, at Walker Mountain (Figure 5.4). Decreases and increases in radial growth following the 1994 storms are evident among chestnut oak at both study sites, particularly Walker Mountain.

Among the black oaks, two at Gap Mountain had decade-long growth suppressions beginning in 1979 (chronologies L and R, Figure 5.3), and several experienced decreased growth during the year of the storm. The 1994 storms triggered growth decreases and increases in several trees (Figures 5.3 and 5.4), but the 1994 signal is not as pronounced as that for the 1979 event. Black oak shows a stronger signal than chestnut oak for the 1994 storms at Gap Mountain (Figure 5.3). However, at Walker Mountain black oak records a weaker signal of the 1994 storms than chestnut oak (Figure 5.4). Visual inspection of our samples clearly reveals these suppression and release patterns in many of the cores and cross-sections we obtained.

To objectively quantify the dual pattern of suppression and release that appeared to constitute the ice storm signal in our results, we calculated trends of decrease and increase in the climate-free ring-width indices by comparing the index for each year to the mean for the previous five years. We arbitrarily defined a significant decrease as one in which climate-free ring-width

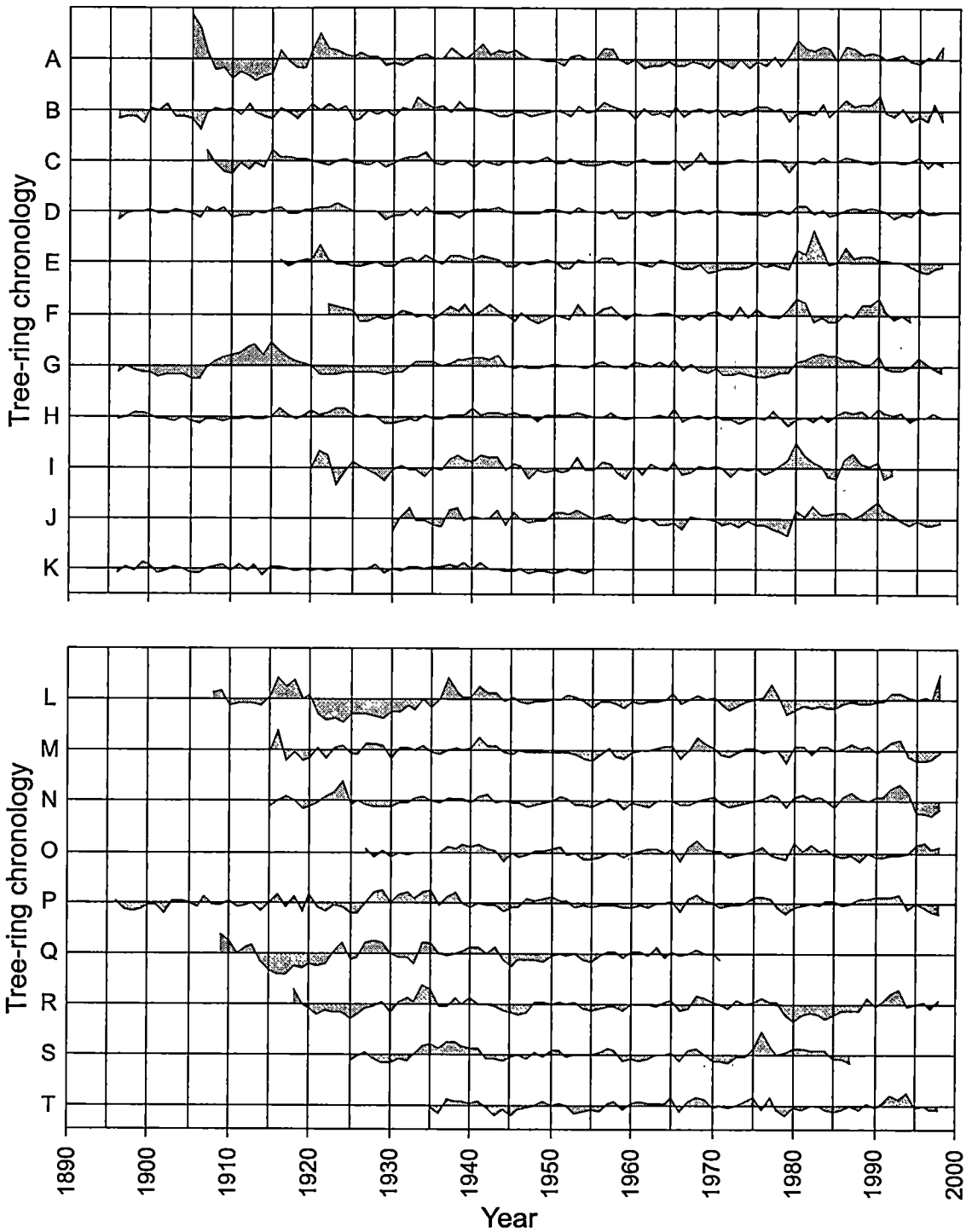

Figure 5.3. Climate-free chronologies for chestnut oak (top) and black oak (bottom) at the Gap Mountain site.

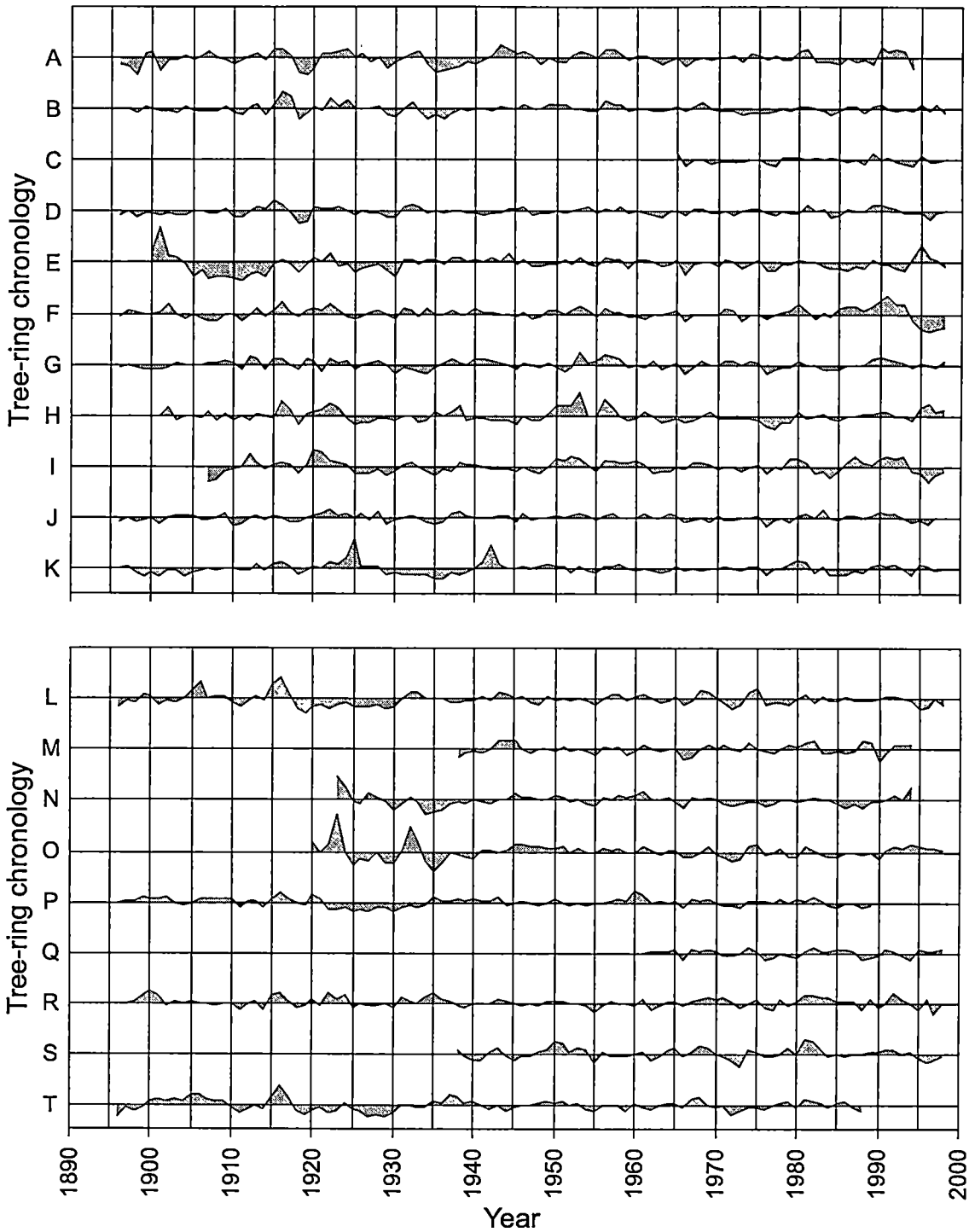

Figure 5.4. Climate-free chronologies for chestnut oak (top) and black oak (bottom) at the Walker Mountain site.

index declines at least 40%, and a significant increase as an enlargement of at least 50% over the mean for the previous five years. These thresholds capture the signals of the 1979 and 1994 ice storms but exclude most of the noise during the same period that is not associated with known ice storms. Figure 5.5 graphs the percent of trees experiencing significant growth increase and decrease each year. Suppressions and releases associated with the 1979 and 1994 ice storms show clearly.

Climatic records indicate that several other ice storms and heavy snowstorms occurred in the vicinity of the study sites during the years covered by our tree-ring chronologies (Table 5.2). The graphs in Figure 5.5, which encompass the period covered by ten or more parallel chronologies, show responses to several known events. Small sample size precludes interpretation of the suppression and release patterns in the early years of the Gap Mountain chronologies. It appears that the January 1918 and November 1920 ice storms are clearly recorded in the Walker Mountain and Gap Mountain chronologies, respectively. Other events, such as a 1911 snowstorm or ice storm, the 1934 snowstorm, or the 1984 ice storm correspond to possible signals as well. There are no indications that the major ice storms of 1978 or 1998 affected either site. The tree-ring chronologies do record a few possible signals not associated with known events in Table 5.2, for example the suppression patterns of 1925, 1943, and 1972 (Figure 5.5).

Comparing the known ice storm events in Table 5.2 with Figures 5.3 – 5.5 suggests that in many trees, suppression begins during the growing season immediately following disturbance, whereas the initiation of release frequently lags the disturbance by a year or more. This pattern my constitute an additional diagnostic tool for identifying ice storms in tree-ring chronologies.

Occurrence of the major ice storms is also reflected in patterns of between-tree ring-width variance (Figure 5.6). Increased variance following an ice storm is a consequence of differential response of trees to the disturbance. The 1921 and 1979 signals are especially clear

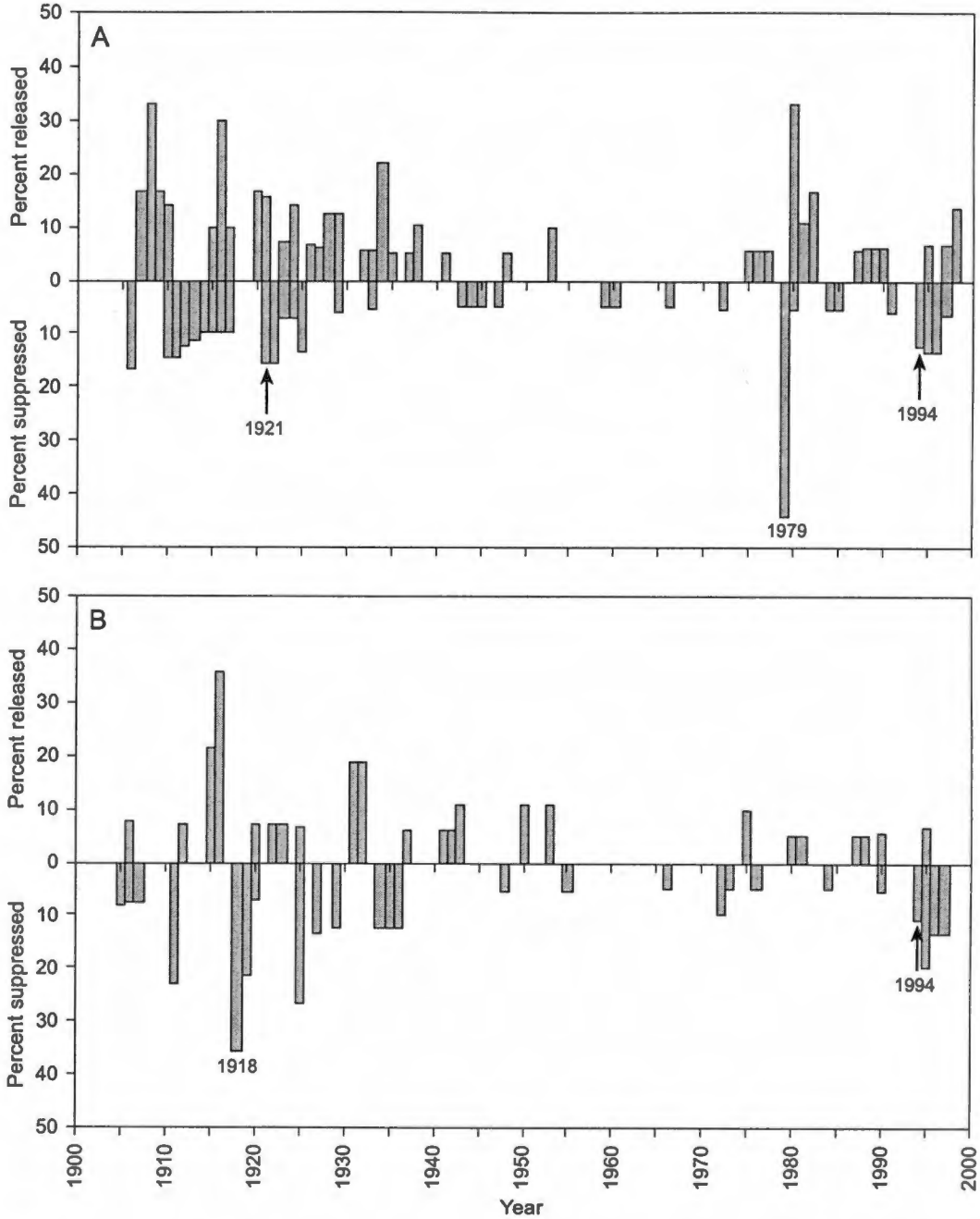

Figure 5.5. Percent of trees exhibiting significant growth decrease or increase each year for (A) Gap Mountain and (B) Walker Mountain. These chronologies cover the period with at least ten trees available. Years of major ice storms known to affect the stands are labeled (1979 and 1994). Also labeled are possible signals of earlier major ice storms (1918 and 1921).

Table 5.2. Record of ice storms occurring during the period spanned by tree-ring chronologies (1901-1998). The year assigned to each event is the first growing season represented after the storm occurred. Sources of information are abbreviated as follow: MWR = *Monthly Weather Review*, RT = *The Roanoke Times and World News*, SD = *Storm Data and Unusual Weather Phenomena* or predecessor.

Year	Remarks
1906	Ice damage to orchards in VA and NC in January 1906, but damage may have been restricted to the Piedmont (MWR).
1911	Four inches of sleet in Wytheville on March 7, 1911 (MWR). Heavy snow in Roanoke, but melted rapidly as it fell and only accumulated 2 inches (RT).
1918	Heavy "sleet" storms throughout VA on Jan. 11-15, 1918 and Jan. 27-30, 1918 (SD). RT reports most of Southeast suffered from sleet or glaze, but no information specific to western VA.
1920	Several moderate ice storms in VA in Jan. 1920 (SD).
1921	A major ice storm in western VA on Nov. 14-16, 1920 (SD, MWR). Signal may partially reflect Jan. 1920 event.
1932	Heavy snow on Mar. 8, 1932 damaged telegraph lines, mostly north and east of Roanoke (SD, RT).
1934	Heavy snow in SW VA on Feb. 25-26, 1934, accompanied by sleet, freezing rain, and thunderstorms, caused timber and power line damage (SD, RT).
1962	Wet snow on Oct. 20, 1961 damaged trees and power lines in parts of SW VA (SD). Not so heavy at our study sites (RT).
1969	Moderate to major ice storm on Jan. 20-21, 1969 caused considerable damage to trees and utility lines at high elevations. Rain at low elevations, snow in Shenandoah Valley (SD).
1971	Heavy snow on April 6-7, 1971 damaged trees and power lines in western VA (SD), but RT does not mention line damage.
1974	Heavy snow Dec. 10, 1973 damaged power lines, mostly near Rich Creek (SD, RT).
1975	Heavy snow, sleet, rain, and wind damaged trees and power lines in western VA on Dec 1-2, 1974. Most damage apparently east of our sites, toward Roanoke (SD, RT).
1978	Major ice storm in western VA on Mar. 27, 1978. Heavy damage was restricted to elevations above 915 m (3000 ft.) (SD, RT).
1979	Major ice storm on Jan. 20-21, 1979 (SD, RT).
1984	Major ice storm on Dec. 21-22, 1983 in western, northern, and central VA. Much power line damage in Roanoke vicinity, less to the west (SD, RT). Wet snow on Feb. 23, 1984 damaged trees and power lines near Bluefield (SD, RT).
1994	Major ice storms on Feb. 10-11, 1994 and Mar. 1-3, 1994 (SD, RT).
1998	Major ice storm on Feb. 4-6, 1998 caused heavy forest damage above 850 m (2800 ft.) in western VA, mainly east of our study sites (SD, RT).

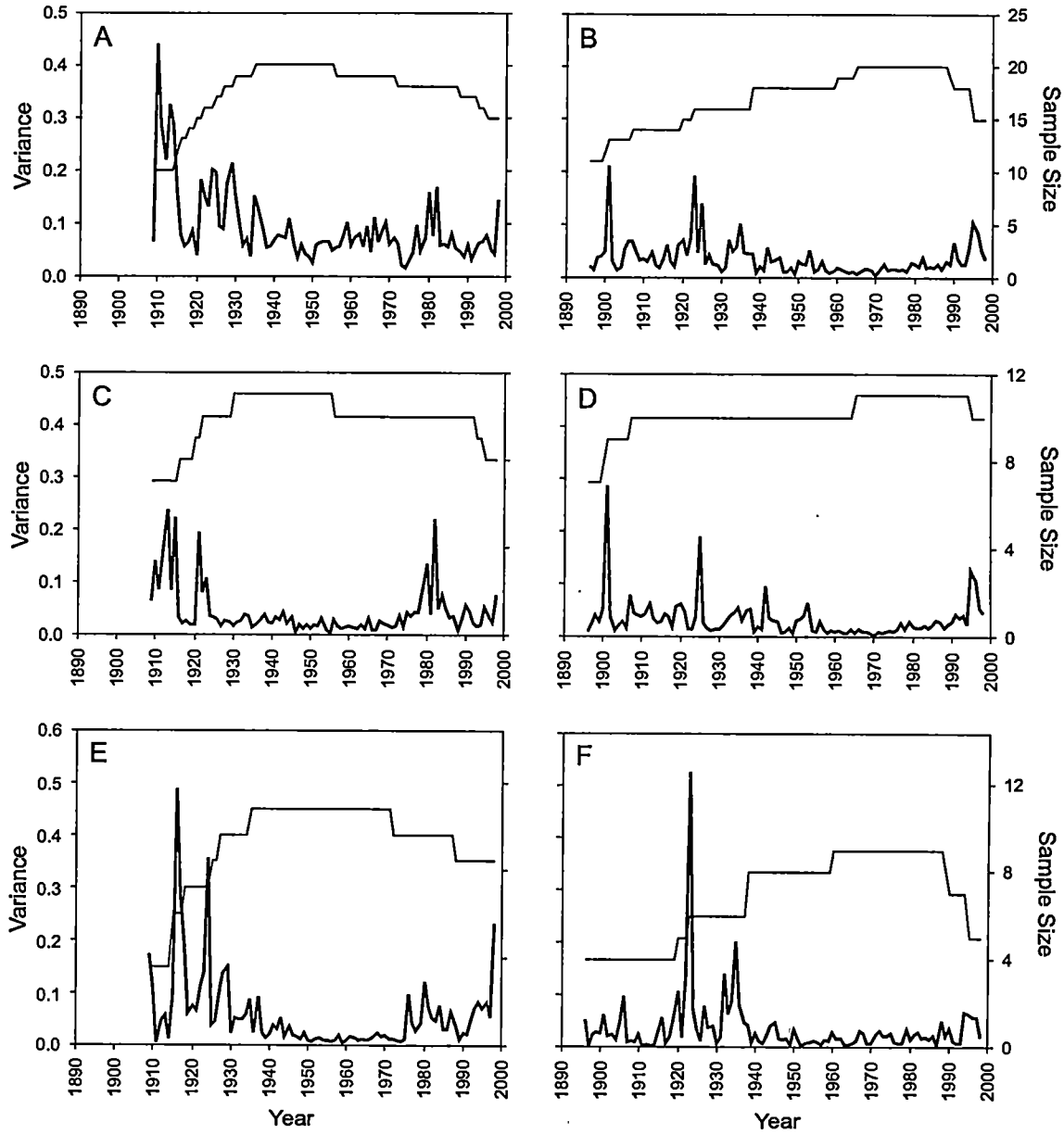

Figure 5.6. Between-tree variance of climate-free ring-width index (heavy line) and sample size (thin line) for (left) Gap Mountain and (right) Walker Mountain series: (A,B) chestnut oak and black oak combined, (C,D) chestnut oak, and (E,F) black oak.

for Gap Mountain, and the 1994 event is readily evident in the Walker Mountain graph. Chestnut oak variance seems to show the ice storm signal more clearly than black oak variance.

To reconstruct a record of ice storms prior to the availability of PDSI or other climate data, it would be necessary to identify periods of release and suppression from the unmodified ring-width indices (ARSTAN values), rather than from climate-free ring-width indices. The graphs in Figure 5.7 were created using the same thresholds of growth decrease or increase used previously, but without subtracting the climate signal. The patterns are noisier than those presented in Figure 5.5, but major ice storm events are nonetheless discernible.

Discussion

Climate-response models

Climate subtraction clarifies the ice storm signal and should be used when climate data are available. However, climate subtraction does not appear necessary for distinguishing major ice storms. It should be feasible, then, to establish a history of ice storms prior to availability of climatic data. For analyzing extremely dry sites (e.g., ridgetops) where the climate signal may obscure any ice storm signal, it may be useful to create a tree-ring based climate reconstruction from other sites expected to be less prone to ice damage. Nash *et al.* (1975) employed such an approach, using a regional climate reconstruction to adjust for climate in their study of air pollution effects on tree growth near a pollution source. However, it may not be necessary to perform a complete climate reconstruction. Identification of extreme drought periods, which could be confused with suppressions related to ice storms, might be sufficient.

The ice storm signal

The ice storm signal consists of opposing patterns. First, severely damaged trees lose much of the support structure for leaves, causing a sharp decline in radial growth, which remains low for several years. These results are similar to those reported for pines in the Appalachian Piedmont (Belanger *et al.* 1996) and for spruce and fir in Quebec (Felin and Rivest 1983).

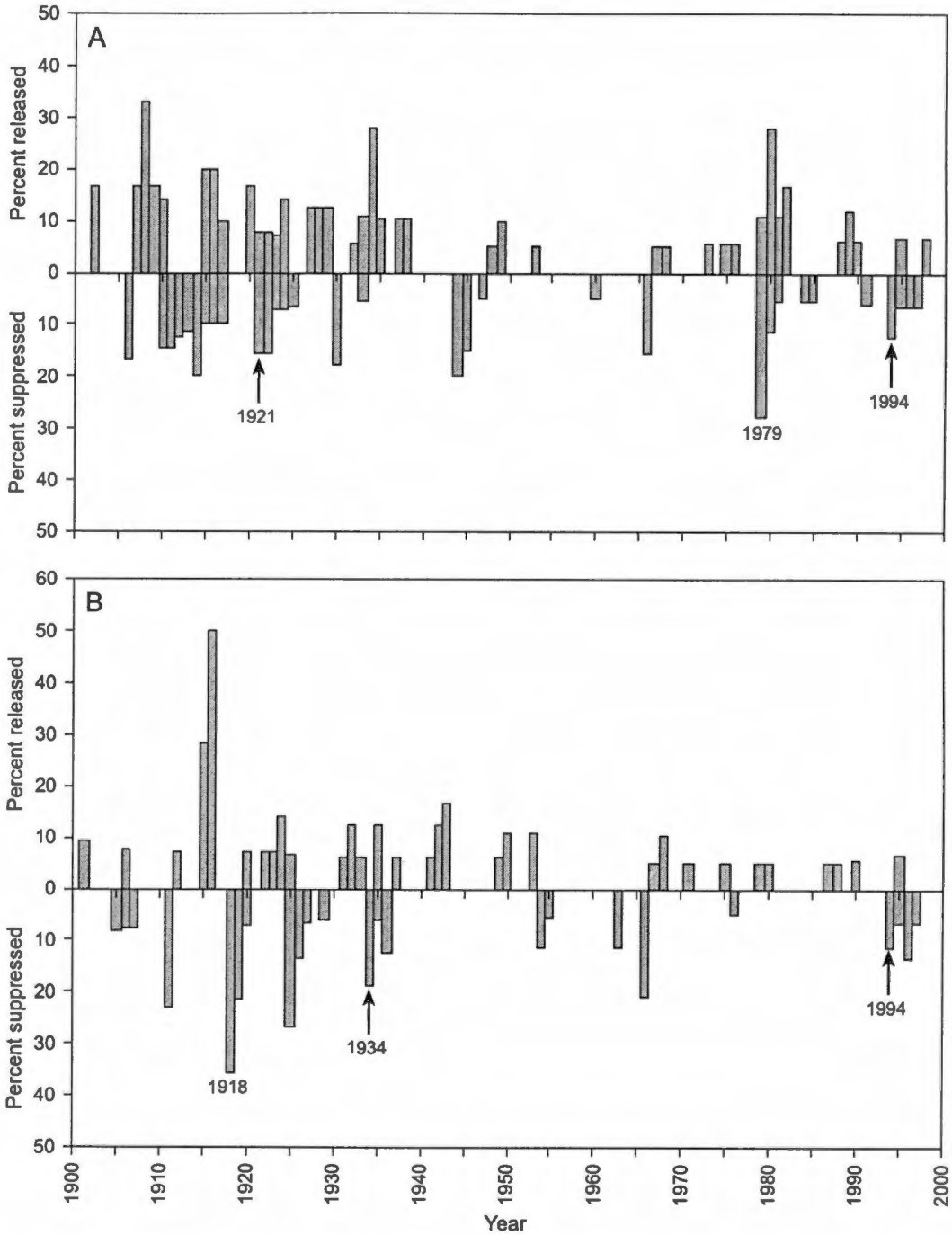

Figure 5.7. Percent of trees exhibiting significant growth decrease or increase each year for (A) Gap Mountain and (B) Walker Mountain chronologies based on tree-ring series without the climate signal subtracted. The chronologies cover the period with at least ten trees available. Years of major ice storms known to affect the stands are labeled (1979 and 1994). Also labeled are possible signals of earlier major ice storms (1918 and 1921) and a snowstorm (1934).

Second, many trees, even some with moderate damage, experience increased radial growth following an ice storm. This signal is a response to release from competition with neighboring trees that were damaged or removed. The degree of canopy damage caused by the 1979 and 1994 ice storms created dramatic increases in light availability. These two conflicting responses, one toward suppression and one toward release, probably offset each other in some damaged trees and weaken the ice storm signal. For example, at Walker Mountain, the 1994 ice storms broke out approximately half the canopy of tree R, but tree rings provide little evidence of the damage (Figure 5.4).

As a model for using our growth reduction and increase thresholds to distinguish ice storms from other events in tree-ring chronologies, we arbitrarily defined three criteria for selecting potential ice storm years: (1) the growth-reduction threshold is exceeded in at least 10% of trees during the first year of a suppression, (2) evidence of growth reduction continues for at least two consecutive years, and (3) the growth-increase threshold is exceeded by at least 5% of trees within two years of the beginning of a suppression in other trees. These criteria provided good matches with known major ice storms. Ignoring the pattern at the beginning of the chronology, only the years 1921, 1979, and 1994 are selected as potential ice storm years at Gap Mountain. Similarly, only 1918 and 1994 meet the criteria in the Walker Mountain chronologies. All four years correspond with major ice storms reported in Table 5.2.

The above method does not describe duration of a suppression or release. This is because it compares each ring-width index with the mean width for the previous five years, and five years into a suppression (or release) would compare a ring only with other suppressed (or released) rings. The graphs in Figure 5.8 convey the duration of the five signals identified above. These graphs reflect the following criteria. First, for each "ice storm" year, we identified the number of years that a tree exceeding the growth-reduction threshold (40% decline) maintained a ≥ 20% reduction relative to the five years preceding the initial year of suppression. Second, to capture

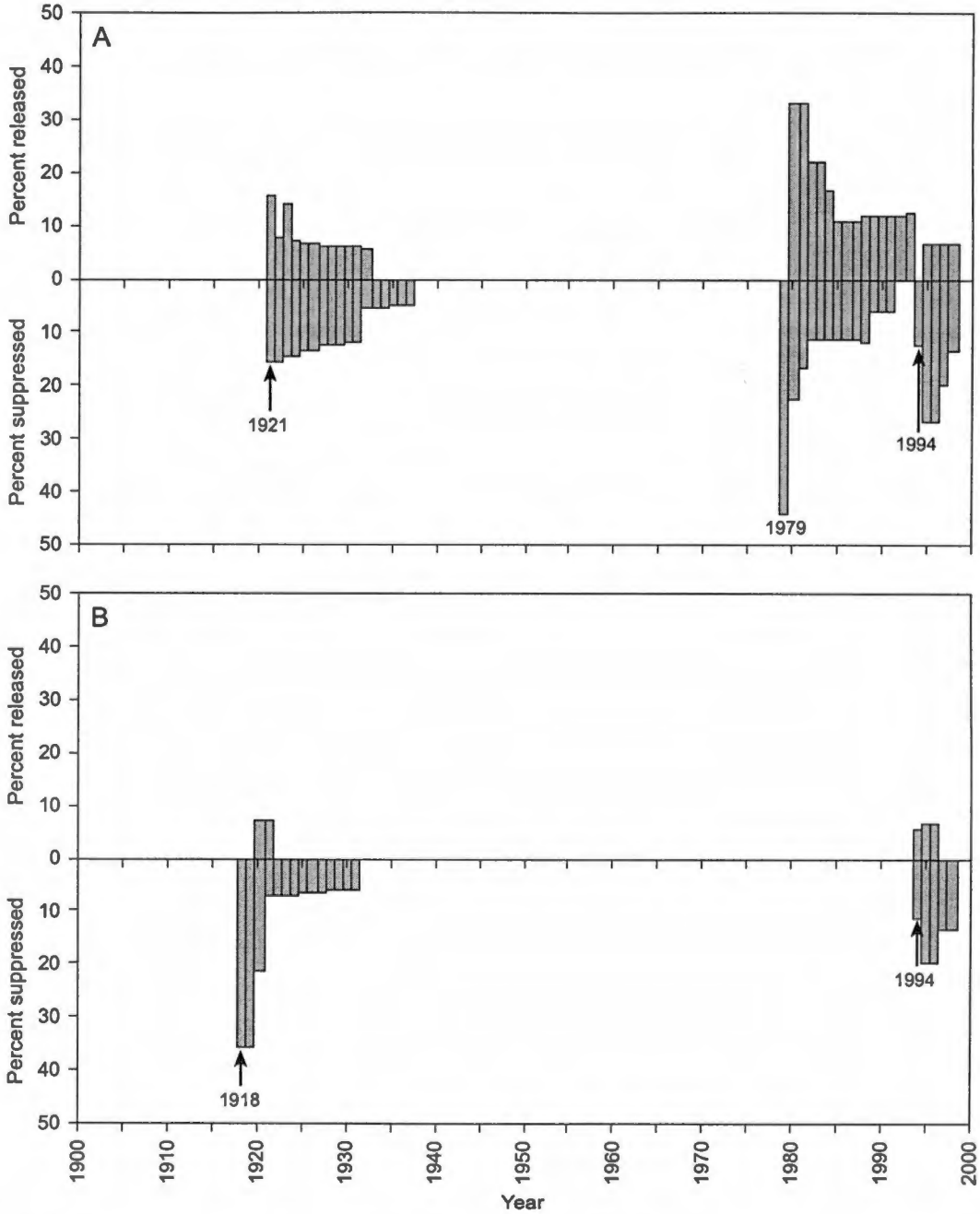

Figure 5.8. Percent of trees at (A) Gap Mountain and (B) Walker Mountain whose growth exceeded thresholds for decrease or increase in climate-free ring-width index relative to the five years prior to the identified ice storms, which are labeled. Thresholds required for maintaining a release or suppression are half as high as those required to initiate one.

lagged suppressions, we identified reductions of ≥ 40% beginning the year after a storm year and as before identified length of time that growth was reduced by ≥ 20%. Third, for each ≥ 50% growth increase occurring within two years of the beginning of the suppression, we determined the period in which ≥ 25% increase was maintained, relative to the five pre-release years. Where a suppression or release continued until the next ice storm, the end of the signal was truncated. When these same criteria are applied for selecting potential ice storm years without subtracting the climate signal, the same five years are identified, with the addition of 1934 for Walker Mountain. The 1934 signal corresponds with a heavy snowstorm (Table 5.2).

The dual signal has not been reported in dendrochronological studies of ice storms in conifers. However, it is probably common among hardwoods, which respond rapidly to reduced competition. Thresholds of growth increase and decrease appear particularly useful for identifying ice storm occurrences. However, the thresholds we used may not be appropriate for all species and study sites. Trees growing in highly productive stands, for example, may show stronger release patterns and more rapid rates of recovery from injury. Nonetheless, it is likely that a similar set of criteria could be developed to distinguish ice storms from other events, which would create different ratios of suppressed to released trees. Windstorms, for example, may trigger release but rarely suppression, whereas drought probably reduces growth of all trees.

The widespread, heavy canopy damage characteristic of severe ice storm disturbance does not appear common in wind-damaged forests, except in the case of extreme winds associated with tornadoes and the most powerful hurricanes (Reilly 1991; Whigham *et al.* 1991). Hurricane damage is reported to produce a dual tree-ring signal, similar to ice storms, in coastal sites that experience winds strong enough to strip limbs from trees (Doyle and Gorham 1996; Reams and Van Deusen 1996). However, in inland forests such wind speeds rarely occur, and severe canopy damage is much less common than uprooting (Foster 1988; Greenberg and McNab 1998) so that growth release appears to be the predominant tree-ring signal (Merrens and Peart

1992). Catastrophic disturbance resulting from downbursts or other severe thunderstorm winds is typically in the form of toppling, bending, or snapping (Dunn *et al.* 1983; USFS 1999; Peter Fischer personal communication). Bent or snapped trees that recover from wind damage may exhibit a period of suppression following the storm, but release is likely to be the predominant signal in such a stand. Literature on tornado disturbance is limited, but it is clear that a variety of damage types, including crown damage, can result (Held and Winstead 1976; Glitzenstein and Harcombe 1988). Severe canopy damage only occurs locally, and in any case, tornadoes are infrequent in the Appalachians (Kelly *et al.* 1978; Eagleman 1983; Leathers 1993). Further, spatial patterns of ice storm disturbance across a landscape differ from those caused by windstorms. An ice storm typically affects specific elevation zones over a broad area, whereas tornadoes and downbursts are local rather than regional and devastate long, straight, narrow corridors of forest oriented west-to-east, southwest-to-northeast, or northwest-to-southeast (Glitzenstein and Harcombe 1988; Wilkinson 1993; Peter Fischer personal communication). These differences in disturbance pattern should permit researchers to distinguish between the two disturbance types. Clearly, the influence of wind on Appalachian forests merits further research. It would be instructive to conduct a dendrochronological study in an Appalachian oak forest affected by a major windstorm to characterize the signal produced by such an event.

Wet snow can accumulate heavily on tree limbs and may produce an "ice storm" signal in Appalachian forests. Forest damage resulting from a February 4, 1998 snowstorm resembled moderate ice storm damage in forests on the Cumberland Plateau of Tennessee (Lafon personal observation). The storm chronology presented in Table 5.2 includes several such events, but the clearest ice storm signals (1918, 1921, 1979, and 1994) all appear to be associated with major ice storms.

Severe drought can substantially reduce growth, but droughts are limited in duration. The typical drought signal in our oak cores consists of a single narrow ring, rather than several

consecutive narrow rings such as those associated with ice storm damage. Nonetheless, a drought signal may last up to five years (Lorimer and Frelich 1989). Subtracting the climate signal diminishes the drought signal, making it unlikely that a drought would be confused with an ice storm. Under unusual circumstances, a drought signal could conceivably be mistaken for an ice storm signal in the absence of climate reconstruction. For example, a drought lasting several years, combined with a major windstorm, might produce a dual signal of suppression and release. However, the landscape pattern of a drought-windstorm combination would undoubtedly be different than that of an ice storm.

One consideration is that the signature of ice storm disturbance may change over time within a forest stand, as trees mature and change in susceptibility to particular types of ice damage. Trees become more susceptible to canopy damage as they age (Downs 1938; this dissertation Chapter 3). Nonetheless, sufficient numbers of trees were damaged by the 1918 and 1920 events to generate suppression patterns despite the younger tree ages. Many of the trees, at 10 – 30 cm in diameter in 1920, were large enough to be damaged by ice storms. Young trees are especially susceptible to bending and breaking (Downs 1938; this dissertation Chapter 3), and those that survive such an event may experience years of reduced radial growth. Young tree canopies are also damaged when larger trees fall on them.

Canopy and understory trees respond differently to enhanced light levels after a disturbance. Radial growth of understory trees that were previously suppressed by deep shade often increases by 100% or more, but canopy trees respond less dramatically (Lorimer and Frelich 1989). This may help explain differences between the 1979 and 1994 signals at Gap Mountain. The 1979 storm damaged many trees, but typically the growth declines persisted for only a year or two, after which substantial growth increases occurred (Figure 5.3). Chestnut oaks exhibited particularly strong responses. This pattern suggests that growth in many of the sampled trees was suppressed by shade from taller individuals prior to the 1979 storm. By 1994, the

smaller trees had gained canopy positions and were hence more vulnerable to damage and less responsive to increased light. Differences in response to the 1979 and 1994 storms probably also reflect spatial variations in damage severity. The 1994 storm caused more damage at elevations slightly above our sampling site, which was in the zone of severe damage from the 1979 storm. Despite variations in the signal produced by the different storms, all the major storm signals were similar enough to be distinguished from other ring-width patterns, indicating that comparable and identifiable ice storm signals are produced at different stand ages.

Directions for future research

Our results suggest that dendrochronology merits attention as a technique for studying fine-scale spatial variations in ice storm damage and for extending the length of the ice storm record. This study also points toward directions for additional work. First, response to disturbance varies greatly between trees – from long suppressions, to little change in growth, to major release – and this complex signal is more difficult to interpret than a simpler one, such as uniform suppression. Collecting a greater number of samples per study site would help solve this problem and would also help to overcome noise associated with unrelated events that affect individual trees but not the entire stand. Second, it appears that some species are better recorders of ice storm disturbance than others. Several additional oak species, as well as pignut hickory (*Carya glabra*), red maple (*Acer rubrum*), and yellow-poplar (*Liriodendron tulipifera*) are widely distributed in Appalachian hardwood forests and may be useful in research on ice storm climatology. Variations in response among stands of different ages and productivity levels also merit attention.

Our Gap Mountain chronologies record clear signals of major ice storms during three winters – 1920 – 21, 1979, and 1994 – the last of which had two events. Walker Mountain forests were apparently affected by a 1918 event, for which climatic records are sketchy, and by the 1994 storms. Our dendrochronological evidence and the independent storm records imply that ice

storm frequency varied temporally over the twentieth century. Neither source indicates that a major ice storm occurred in this region between the early 1920s and the late 1960s, and it appears that a remarkably high number of major ice storms occurred during the last twenty years. These results differ from those of Travis and Meentemeyer (1991), who described several "major" or "severe" ice storms on the South Carolina and Georgia Piedmont during the mid-twentieth century. Additional sampling is needed to determine whether other ice storms or heavy snowstorms are recorded in our study area. In particular, it would be useful to locate older trees that may provide records of ice storms occurring during or prior to the early 1900s and to establish chronologies for stands growing on sites of different elevation, aspect, and slope.

Summary

Major ice storms cause widespread forest disturbance and disrupt human society. Studies of forest disturbance indicate that ice storm severity varies among topographic positions. Windward slopes and high elevations may be particularly prone to ice storm damage. Instrumental climatic data are not suitable for estimating these fine-scale patterns, but ice storms produce a tree-ring signal that shows promise for analyzing fine-scale spatial variations and for extending the length of the ice storm record. Previous dendrochronological studies of ice storm effects on coniferous species demonstrated that canopy damage from ice storms contributes to reduced ring width following the event. In this study we found a dual signal in chestnut oak and black oak that consists of growth decreases and increases following an ice storm. Growth reductions result from canopy damage, and growth increases reflect the response of trees to reduced competition with other individuals that have been broken or killed.

The dual signal differentiates ice storm damage from other types of disturbance in Appalachian forests. Like many tree-ring signals in eastern forests, the signal is relatively subtle. However, the results of this study demonstrate that the occurrence of major ice storms can be identified quantitatively using thresholds of ring-width decrease and increase. Changes in ring-

width variance also show promise as a tool for recognizing the occurrence of ice storms. Increased variance following an ice storm reflects the varied response of different trees to the event. More investigation is needed to determine whether other species are more suitable for ice storm research and to document how the ice storm signal differs among forests of different ages and productivity levels. Successful resolution of these issues will enhance study of fine-scale spatial variations in the climatology of major ice storms.

Chapter 6

Modeling Influences of Ice Storm Disturbance on Forest Dynamics in an Appalachian Landscape

Introduction

Major ice storms are an important agent of forest disturbance in eastern North America. Ice storm disturbance occurs when heavy loads of freezing rain accumulate on trees, bending, breaking, or toppling them (Downs 1938; Whitney and Johnson 1984; this dissertation Chapter 3). Ice storms typically affect forests over a broad area, with heavy damage confined to specific elevation zones or aspects (Ashe 1918; Downs 1938; Whitney and Johnson 1984; Seischab *et al.* 1993; Lafon *et al.* 1999). Ice storm disturbance is more intense than the small-gap creation that dominates disturbance regimes in much of the central hardwood forest. Tree mortality and canopy loss on the order of 50% are typical in heavily disturbed forests (Downs 1938, Seischab *et al.* 1993, Lafon *et al.* 1999; this dissertation Chapter 3). Several investigations of ice storm damage have been conducted following major events (Downs 1938; McKellar 1942; Siccama *et al.* 1976; Whitney and Johnson 1984; Bruederle and Stearns 1985; Boerner *et al.* 1986; Seischab *et al.* 1993; Rebertus *et al.* 1997; Warrillow and Mou 1999; this dissertation Chapter 3), but little is known about their long-term consequences for tree species composition and diversity. In this chapter, I use an individual-based stand simulation model to assess implications of periodic ice storm disturbance for forest dynamics along a topographic moisture gradient in a southern Appalachian landscape.

Appalachian forests are characterized by striking topographic patterns of tree species composition and diversity. Mesophytic species, including yellow-poplar (*Liriodendron tulipifera*), magnolias (*Magnolia* spp.), sugar maple (*Acer saccharum*), and eastern hemlock (*Tsuga canadensis*) are concentrated in valley floors, on concave slopes, and on north-facing ravine slopes (Whittaker 1956; Hack and Goodlett 1960; Quarterman *et al.* 1972). Oaks

(*Quercus*) dominate broad side-slope zones, and southern pines (*Pinus*) are restricted to convex "noses," ridgetops, and recently disturbed sites. Whittaker (1956) analyzed the distribution of tree species along a topographic moisture gradient in the Great Smoky Mountains of Tennessee and North Carolina. His study portrayed a unique spatial distribution for each species, with abundance peaking at some point along the gradient. Typically, the entire distribution of a species is restricted to a portion of the moisture gradient, resulting in compositional zonation along the gradient. Whittaker concluded that the distribution of species independently, rather than as parts of species associations, supported the individualistic concept of Gleason (1926).

Most species grow best on sites with abundant resources, despite observed zonation patterns (Huston 1994). The observed patterns suggest that competitive displacement toward suboptimal conditions is a major control on species distributions (Smith and Huston 1989; Huston 1994). Smith and Huston (1989) employed an individual-based model of forest succession to show that such distribution patterns could result from competition for light among a suite of hypothetical species with different levels of tolerance to shade and drought. Their work was based on the hypothesis that species whose rapid growth, high fecundity, or large size provide superior competitive abilities at high resource levels exhibit characteristics that preclude such responses at lower levels. Conversely, species tolerant of low resource levels are incapable of rapid growth when resource levels are increased. An additional constraint on the hypothetical species of Smith and Huston was that those with attributes permitting tolerance of low light could not tolerate drought, and *vice versa*. Consequences of these physiological tradeoffs include competitive displacement of slow-growing, drought-tolerant species toward the xeric end of the moisture gradient, and dominance by shade-tolerant species during late-succession in mesic sites. Further, species distributions along the moisture gradient become increasingly confined over the course of succession as competition becomes more pronounced toward mesic sites. The work of

Smith and Huston (1989) and Huston (1994) represents an elaboration of the dynamic equilibrium model of Huston (1979).

Smith and Huston (1989) and Huston (1994) predicted that disturbances disrupt the approach to competitive exclusion during plant succession, reducing the degree of species zonation along gradients, permitting reproduction of shade-intolerant species in old stands, and promoting higher species diversity in mesic sites. However, disturbance may also reduce diversity, particularly in less productive stands, if the disturbance rate or magnitude is so high that populations of some species do not recover between disturbances (Huston 1979).

My research applies the theoretical framework and individual-based modeling approach of Smith and Huston (1989) to understanding spatial distributions and temporal dynamics of actual species across southern Appalachian landscapes affected by ice storm disturbance. Individual-based models have been used primarily to evaluate the role of small gaps resulting from single-tree mortality, although they have also been employed to assess larger disturbances such as hurricanes in Puerto Rico (Doyle 1981) and removal of all mature American chestnut (*Castanea dentata*) trees by blight in eastern Tennessee (Shugart and West 1977). A primary difference between my work and most other applications of individual-based models is that it seeks to predict successional patterns for multiple sites across a varied landscape, rather than for a single homogeneous site.

Description of the model

The work reported here employs FORICE, a descendant of the JABOWA and FORET models (Botkin *et al.* 1972; Shugart and West 1977). The FORET model of Shugart and West (1977) simulates the birth, growth, and death of individual trees on a 1/12 ha plot. Pastor and Post (1985) enhanced the ability of the model to simulate ecosystem functions by adding subroutines that simulate the dynamics and effects on tree growth of litter return and decomposition, nitrogen-cycling, and soil-water balance. They have used their model version

(LINKAGES) to predict possible changes in carbon and nitrogen cycles, as well as forest species composition, resulting from climate change in northeastern Minnesota (Post and Pastor 1996). Huston (1994) made additional modifications to LINKAGES to simulate disturbance, atmospheric nitrogen deposition, and the influences of humidity, wind, and insolation on soil moisture. I further modified the model to simulate ice storm dynamics and also altered the way the model handles temperature and moisture constraints. I call my version of the model FORICE. Following are changes I have made in various model subroutines, discussed in the order in which the subroutines are called. The program is written in FORTRAN and is available for public use.

Subroutine TEMPE

This subroutine calculates growing season degree days, based on monthly temperatures during the growing season. The model previously simulated monthly temperatures from monthly temperature means and standard deviations supplied by the user, but it now reads actual monthly temperatures from the file TEMP.DAT, recycling the data until all years of the simulation are complete. This modification results in a more realistic representation of the effects of climatic variability, which may not follow a normal distribution.

Subroutine MOIST

This subroutine calculates the proportion of the growing season during which moisture is insufficient for tree growth (defined as – 15 bars). As in TEMPE, I have changed the model to read actual monthly precipitation totals from the file PPT.DAT, instead of estimating it from means and standard deviations. Reading in actual climate data increased the proportion of the growing season with drought by up to an order of magnitude, which in part reflects the combined effects of simultaneous anomalies in temperature and precipitation. An additional change to this subroutine simulates the effect of topography in redistributing moisture across the landscape. The user inputs the topographic index of the watershed model TOPMODEL (Beven and Kirkby 1979; Quinn *et al.* 1995) for the site, and MOIST alters water input accordingly. This is accomplished

by calculating a precipitation multiplier based on the relationship found by Garten *et al.* (1994) between topographic index and soil moisture percent at Walker Branch Watershed, Tennessee. MOIST uses this multiplier to enhance monthly precipitation for all sites with topographic index exceeding 5.0, which includes all sites downslope of ridgetops. Valley bottoms receive the greatest moisture augmentations. This simple approach does not account for the complex variations in soil attributes, such as depth and transmissivity, and water runoff characteristics throughout a watershed, but such data are not typically available. Use of a hydrologic model, such as TOPMODEL (Beven and Kirkby 1979), to account for topographic effects on soil moisture would provide more appropriate estimates in watersheds for which sufficient parameterizations are available.

A final modification to subroutine MOIST is that it no longer initializes soil water content to field capacity (FC) each January. This alteration permits a drought to continue uninterrupted between consecutive years.

Subroutine GMULT

Subroutine GMULT computes multipliers used in subroutines BIRTH and GROW to reduce the performance of each tree according to factors (e.g., temperature or moisture) that limit growth. My first modification changes the influence of temperature on tree growth. Previously, growth of each species was permitted to occur only within a minimum and maximum number of annual growing degree days, with a peak of optimum growth halfway between the maximum and minimum. This parabolic function was based on observed influences of instantaneous temperature on tree growth (Fitter and Hay 1981; Botkin 1993) but does not accurately describe the relationship between growth and heat sum over a growing season (Schenk 1996; Loehle 1998). Loehle (1998) demonstrated that, in fact, maximum sapling height growth rates for species in eastern North America typically increase above a minimum number of growing degree days and ultimately level off. Loehle (1998) argued that southern range limits of north temperate

species are not determined by high temperatures but by competition from faster-growing species whose growth is unencumbered by adaptations to cold. Based on the work of Loehle, I created an asymptotic function to calculate the degree day growth multiplier, selected arbitrarily so that tree growth is 0.95 of optimum when the minimum growing degree day requirement of a species is exceeded by 1000 (Figure 6.1).

My second modification to GMULT is the inclusion of a crowding growth factor that reduces growth as the plot becomes more densely stocked. Each tree species is assigned to one of three categories to simulate the species' effect on relative stocking (Figure 6.2), an indicator of stand density (Stout *et al.* 1987; Colbert and Sheehan 1995). The relationships depicted in Figure 6.2 reflect that some species (e.g., oaks), have larger crowns, given the same stem diameter, than others (e.g., yellow-poplar). The proportional contributions of all trees in the plot are summed to estimate relative stocking, or RSTOCK, on the plot. RSTOCK is then used to calculate a crowding growth multiplier (CROWDGF) used in subroutines GROW and BIRTH to diminish rates of growth and seedling establishment. I chose CROWDGF arbitrarily so that growth is reduced to 0.75 of optimum when the plot is stocked at 100% (Figure 6.3). Busing (1991) and Colbert and Sheehan (1995) employed similar approaches to simulate effects of crowding in Appalachian forests. In their model of the effects of gypsy moth (*Lymantria dispar*) defoliation in Allegheny hardwood forests, Colbert and Sheehan (1995) also reduced growth to 0.75 at 100% stocking.

Subroutine ICEDIST

Subroutine ICEDIST assigns each tree to an ice damage category during an ice storm year. Ice storm years are selected randomly in the main program, and all plots are affected by each ice storm. The user selects mean ice storm recurrence interval via the variable ZFREQ in the input file INPUT.DAT. ZFREQ is the reciprocal of the mean recurrence interval.

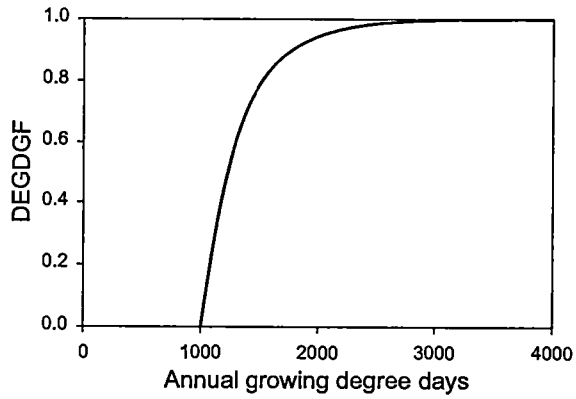

Figure 6.1. Function used to calculate growing degree day growth multiplier (DEGDGF), based on the minimum annual growing degree days tolerated by the species. All species have a curve of the same shape. The function shown is for a species that requires at least 1000 growing degree days per year.

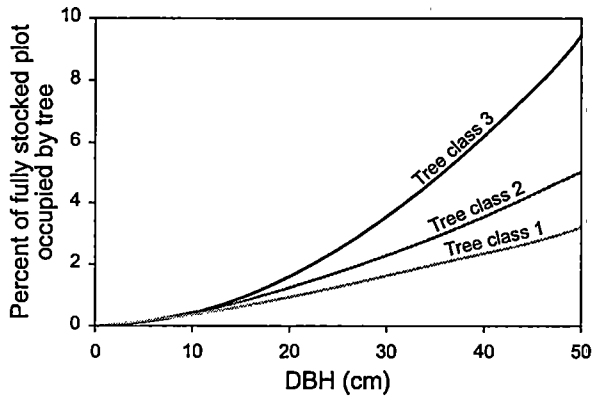

Figure 6.2. Functions to calculate the effect of each tree on relative stocking. Each species is assigned to one of the three classes. The three different classes reflect that trees of some species have larger crowns, given the same stem diameter, than others.

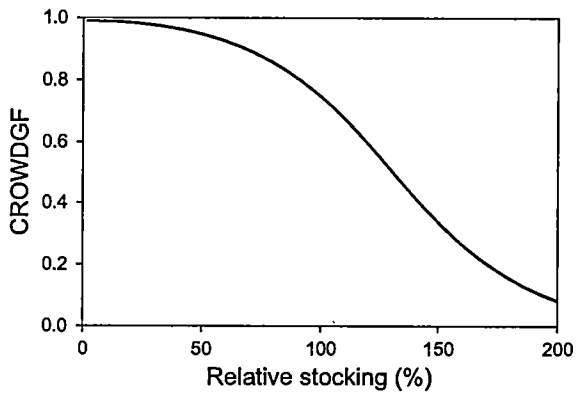

Figure 6.3. Function used to calculate crowding growth multiplier (CROWDGF) based on relative stocking of the stand.

ICEDIST simulates the fine-scale patchiness in damage severity that characterizes ice storm disturbance (this dissertation Chapters 2 and 3). In an ice-damaged stand, large, multiple-tree gaps are interspersed with less damaged patches. These large gaps apparently form when a falling tree strikes neighboring ice-laden trees, triggering additional breakage and toppling (Lafon *et al.* 1999). According to results of a regression analysis reported in Chapter 3 of this dissertation (Figure 3.11), the proportion of stand area occupied by such heavily damaged patches increases with increasing slope angle. To reflect this relationship, ICEDIST randomly assigns plots to severely damaged patches or less damaged patches during each ice storm year, with probability of being in a severely damaged patch increasing with slope.

ICEDIST uses tree attributes to assign each tree to one of four categories of ice storm damage: (1) little or no damage (up to 15% canopy loss), (2) canopy damage (greater than 15% canopy loss), (3) bent stem, or (4) broken or toppled bole (i.e., tree is killed immediately). The probability of a tree being in each category is based on its diameter and the susceptibility of the species to canopy damage. The relationship is modeled according to results of multinomial logistic regression analysis reported in Chapter 3. First, stem diameter is assigned to one of two categories. If diameter is less than 30 cm, IDIAM = 1, else IDIAM = 0. Each species is classified as exhibiting low or high susceptibility to canopy damage (value of 1 or 0, respectively, for variable ISUSCAN). Logits for the four damage categories are estimated via equations of Chapter 3. For plots in heavily damaged patches, the following equations apply:

$$UA = -2.633 - 0.569*IDIAM + 1.84*ISUSCAN(I)$$

$$UB = -0.007846 - 1.065*IDIAM - 0.212*ISUSCAN(I)$$

$$UC = -4.244 + 2.186*IDIAM + 0.449*ISUSCAN(I)$$

$$UD = 0.$$

Probability of category 4 damage is lower in less damaged patches. Logits for these plots are calculated as follows:

UA = – 0.639 – 0.355*IDIAM + 0.986*ISUSCAN(I)

UB = 2.201 – 1.293*IDIAM – 0.357*ISUSCAN(I)

UC = – 18.291 + 17.557*IDIAM + 0.408*ISUSCAN(I)

UD = 0.

Each logit is used to estimate probability of a particular category of damage:

PROBSUM = EXP(UA) + EXP(UB) + EXP(UC) + EXP(UD)

PROB1 = EXP(UA)/PROBSUM

PROB2 = EXP(UB)/PROBSUM

PROB3 = EXP(UC)/PROBSUM

where PROB1, PROB2, and PROB3 are the probabilities of category 1, 2, and 3 damage, respectively. It is unnecessary to calculate the probability of category 4 damage, as this would be redundant.

Damage to southern pines is modeled differently. Based primarily on results of Whitney and Johnson (1984) that show exceptionally heavy damage to southern pines, these species are assigned to a unique stem damage susceptibility class. The probabilities of the first three categories of damage for southern pines are

PROB1 = 0.200

PROB2 = 0.040

PROB3 = 0.010

leaving the probability of category 4 damage at 0.75.

FORICE also provides the option to simulate less severe damage on xeric sites where southern pine dominance is typical. Pine-dominated stands on west-facing slopes may be sheltered topographically from heavy ice accretion (Williams and Johnson 1990; Lafon *et al.* 1999). Trees on sheltered sites, for which less ice-damage data are available, are assigned the following probabilities, based on damage patterns in a table mountain pine (*Pinus pungens*) stand on a west-facing slope (this dissertation Chapter 3):

For southern pines,

PROB1 = 0.488

PROB2 = 0.116

PROB3 = 0.036.

For all other species,

PROB1 = 0.538

PROB2 = 0.250

PROB3 = 0.058.

Based on these probabilities, the damage type (IDAMAGE(J)) for each tree J is selected randomly. Canopy damage and killing are performed in subroutines BIRTH and KILL. However, trees in category 3 are "bent" in ICEDIST. Bending involves the reduction of canopy height to .50 of the height predicted from stem diameter. Bent trees recover by an increment of .02 per year, and this height multiplier is stored in array BENT(J). BENT(J) is incremented until its value reaches 1.0, simulating the possibility that if a bent tree can persist long enough in the subcanopy level it may eventually send a new shoot into the canopy. Currently, the model allows all species to recover in this manner, although little is known about the long-term effects of bending on trees of any species.

Subroutine BIRTH

Subroutine BIRTH adds new seedlings and saplings to the plot, based on species fecundity and environmental conditions (e.g., light availability). The first part of BIRTH calculates leaf biomass through all levels of the canopy to determine light availability (proportion of full sunlight) at the forest floor. Ice storm damage increases light availability by removing foliage biomass and killing trees. During an ice storm year, trees in damage category 1 (little or no damage) sustain random foliage biomass loss between 0.0 and 0.15 (i.e., loss of up to 15% of foliage biomass). Category 2 (canopy-damaged) trees lose random proportions of foliage biomass greater than 0.15. Category 3 (bent) trees, although reduced in height, lose none of their canopy biomass. The entire canopy of each category 4 (killed) tree is removed before light availability is calculated. The proportion of foliage biomass remaining after ice storm damage is stored in array CANPCT(K).

Canopy recovery occurs in the years following an ice storm. The rate of canopy recovery varies according to damage level. Tree-ring analysis of several black oak (*Quercus velutina*) and chestnut oak (*Q. prinus*) trees damaged by ice storms reveal that the ratio of post-storm to pre-storm radial increment (hereafter "relative diameter increment") increases linearly following an

ice storm, until recovery is complete (Figure 6.4). Tree-ring chronologies used in this analysis are from the study reported in Chapter 5. Only chronologies showing long periods of post-storm suppression were used to estimate recovery rates, thus avoiding an overestimate due to the confounding effect of reduced competition from neighboring trees.

About 5% of pre-storm ring width is added to relative diameter increment during each year of recovery. The rate of recovery in radial increment does not appear to be related to initial canopy damage, nor does it change as the canopy recovers. However, my data suggest that the absolute size of the ring width varies by canopy damage level. The trees used in the dendrochronological analysis were classified as having severe canopy damage (remaining canopy < 0.5 original canopy) or moderate canopy damage (remaining canopy ≥ 0.5 but < 0.85 original canopy). Following an ice storm, relative diameter increment is approximately 0.2 in severely damaged trees and about 0.45 in moderately damaged trees. I graphed relative diameter increment in relation to remnant canopy proportion (Figure 6.5), assuming the trees had remnant canopy amounts at the midpoint of their damage categories (i.e., 0.25 and 0.675 for severely and moderately damaged trees, respectively). Switching the axes to make canopy percent a function of relative diameter increment yields the graph in Figure 6.6.

I used the relationship shown in Figure 6.6 to model annual canopy recovery. For a heavily damaged tree, represented by the steeper slope on the left of the graph, 0.085 is added yearly to the remaining canopy of a heavily damaged tree. Once canopy biomass has recovered to 0.675 its potential biomass, annual canopy increment slows to about 0.03. This function implies greater carbon allocation to canopy recovery, relative to diameter growth, in the most heavily damaged trees.

The model of canopy recovery used here is based on data from only a few damaged trees. Additional dendrochronological analyses, incorporating more species, are needed to clarify rates of canopy and diameter recovery and their variation among species. Currently, BIRTH uses the

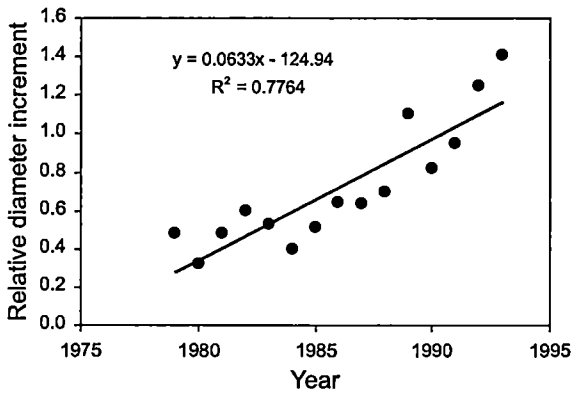

Figure 6.4. Recovery of relative diameter increment for a black oak (*Quercus velutina*) damaged by an ice storm in 1979.

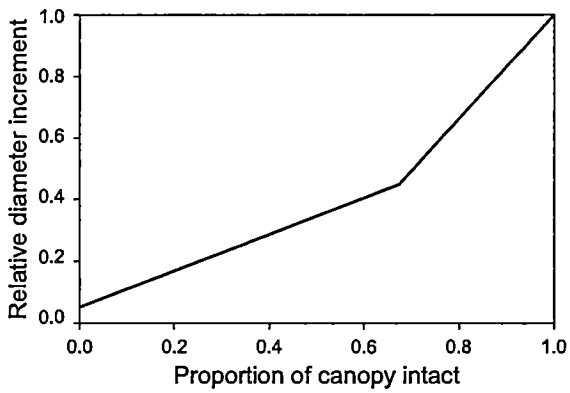

Figure 6.5. Relationship between canopy damage and relative diameter increment, based on results of tree-ring analysis. Initially, relative diameter increment for trees with severe canopy damage is about 0.2, and that for trees with moderate canopy damage is about 0.45.

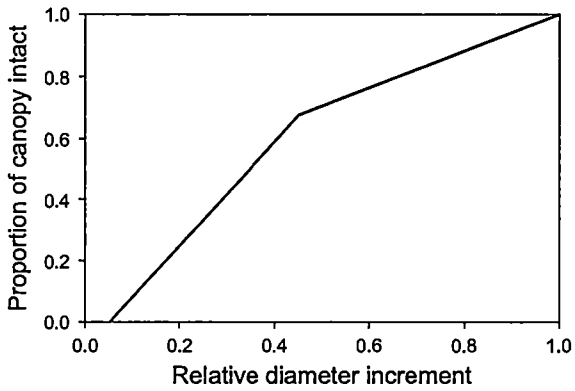

Figure 6.6. Same relationship as shown in Figure 6.5, with axes switched to make intact canopy proportion a function of relative diameter increment.

G parameter of each species, relative to that of black and chestnut oak, to simulate interspecific differences in recovery rates. G, which is assigned in file INPUT.DAT, is used in subroutine GROW to regulate how rapidly a tree achieves most of its growth. Larger values of this parameter result in more rapid growth at a young age (Botkin 1993). BIRTH divides G by 245, the average G value for black oak and chestnut oak, and multiplies this proportion by annual canopy increment. This produces more rapid recovery for fast-growing species like yellow-poplar, a result consistent with field observations.

Subroutine GROW

This subroutine calculates annual diameter increment for each tree by reducing optimal growth according to resource availability. First, GROW estimates available light, based on the leaf biomass of taller trees. An available light growth multiplier (ALGF) is calculated to simulate the effect of light availability on tree growth. GROW chooses different multipliers for species in different shade-tolerance classes. The original version of LINKAGES employed two shade-tolerance classes (Pastor and Post 1985), and Huston and Smith (1987) increased the number to three (tolerant, medium, and intolerant). I have increased the number to five, where 1 = very tolerant, 2 = tolerant, 3 = medium, 4 = intolerant, and 5 = very intolerant. Species were assigned to tolerance classes based on Baker (1949) and Burns and Honkala (1990). The new ALGF functions are graphed in Figure 6.7A.

I assign small trees (those with stem diameter no more than 5 cm) different light multipliers than larger trees of the same species to simulate the higher shade tolerance of young trees (Daniel *et al.* 1979). The functions for these trees are shown in Figure 6.7B. The bottom curve of Figure 6.7A has been removed and a new function added at the top, hence a small tree of a given tolerance class is assigned the next higher ALGF function than would be used for a larger tree of the same class. A new species parameter, ITOLSEED, has been added to the model to determine which ALGF function to use for small trees. Seedling shade-tolerance of a few species

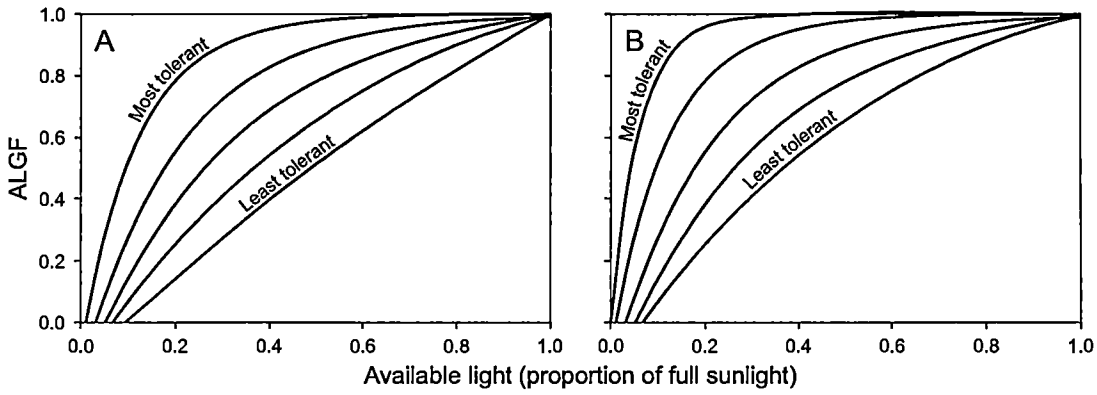

Figure 6.7. Functions used to calculate available light growth multiplier (ALGF) for each tree, according to its shade-tolerance rating. Each species was assigned to one of the five shade-tolerance classes. The growth-response for each class is shown for (A) large trees (DBH > 5 cm) and (B) seedlings (DBH ≤ 5 cm).

has been adjusted more than one level above that of larger individuals. For example, mockernut hickory is shade-tolerant as a seedling (ITOLSEED = 2) but becomes intolerant as it matures (ITOL = 4) to reflect the tolerance rating of Smith (1990). Seedling ALGF functions are also used in subroutine BIRTH to reduce the number of seedlings that are recruited.

Next, a canopy damage growth factor CANDAMGF is calculated to simulate reduced diameter growth in trees sustaining canopy damage during an ice storm. CANDAMGF is defined according to the functions graphed in Figure 6.5. Like the other growth multipliers, CANDAMGF has a value ranging from 0 to 1. Trees that were bent during an ice storm (damage category 3) have fully intact canopies, but their growth may be reduced by increased shading from taller trees. To model this effect, the height of each tree is multiplied by BENT(J), which was calculated in subroutine ICEDIST.

To determine diameter increment for a tree, GROW first calculates its potential diameter increment (DNCMAX), based on its current diameter and species-specific growth parameters. Next, the minimum growth multiplier is chosen from among the multipliers for available light, soil moisture, soil nitrogen, and growing degree days. This minimum is itself multiplied by CROWDGF and CANDAMGF before being multiplied by DNCMAX to calculate realized diameter increment (DINC).

I have altered some of the species-specific parameters that affect growth rates. First, I changed parameter G to reflect information on height growth reported in Burns and Honkala (1990). Previously, all species had growth curves of the same shape, so that with optimal conditions a tree reached two-thirds its maximum size at half its maximum age (Botkin *et al.* 1972). Defining all tree growth curves by the same shape was an arbitrary decision governed by a lack of data for differentiating species (Botkin 1993). Indeed, information on maximum growth-rates is still limited, and I used the approach of Botkin *et al.* (1972) to estimate G for a few species with particularly sketchy data and for several species of minor importance in

southwestern Virginia. White pine (*Pinus strobus*) presents an unusual case because its growth rate is exceptionally high, but seedling growth is slow for the first 8 – 10 years (Wendel and Smith 1990). I accounted for this pattern by using G = 60 to calculate growth of white pine seedlings less than 10 years old. For older trees, G = 450.

I used distribution patterns reported by Whittaker (1956) for tree species of the Great Smoky Mountains to calculate new drought tolerance values for all species. Variable D3 represents the proportion of the growing season that a species can withstand drought and is used in calculating SMGF(I) for each species. Previously, Pastor and Post (1985) had estimated this parameter from geographic ranges of species. Using temperature and precipitation data for Gatlinburg, Tennessee, adjacent to the Great Smoky Mountains, I ran FORICE for several points along the Whittaker moisture gradient and calculated the mean proportion of growing season drought days estimated by subroutine MOIST for each point (Table 6.1).

I chose the points shown in Table 6.1 because their appropriate location on the moisture gradient could be determined with relative certainty. Each point was given a representative soil moisture capacity, slope, aspect, and topographic index. I obtained soil moisture capacity estimates from the soil survey of Blount County, Tennessee (Elder *et al.* 1959). I created an ARC/INFO AML program to calculate the topographic index of Beven and Kirkby (1979) from 30 m Digital Elevation Models (DEMs) of the Great Smoky Mountains. The algorithm permits multiple flow direction from each grid cell and uses sub-grid cell interpolation to estimate contour length (Quinn *et al.* 1995).

My results using Gatlinburg climate data demonstrated a strong relationship characterized by exponentially increasing drought with distance along the gradient graphed by Whittaker. I fitted a logistic curve to the drought data, arbitrarily assigning an upper limit of 0.9 (Figure 6.8). The relationship is significant at $P < 0.0005$, with $R^2 = 0.93$. I used this relationship to estimate drought tolerance for each major species whose distribution and abundance was graphed along

Table 6.1. Simulated site and soil parameters along the Great Smoky Mountains moisture gradient.

Topographic position	Distance along gradient (mm)[a]	Slope (degrees)	Topo-graphic index	Predicted growing-season drought	Soil parameters: Depth (cm)	Field capacity (cm/cm)	Wilting point (cm/cm)	Soil series
Upper slope to ridge transition	54.5	0	5.00	0.401	30	0.370	0.270	Ramsey
Upper slope, south-facing	52.0	27	5.60	0.315	30	0.370	0.270	Ramsey
Lower slope, north-facing	41.6	22	6.25	0.091	45	0.370	0.270	Ramsey
Sheltered slope, south-facing upper end	32.6	22	6.25	0.006	90	0.370	0.220	Allen/ Jefferson
Sheltered slope, south-facing lower end	19.0	11	7.50	0.002	100	0.370	0.200	Allen/ Jefferson
Shallow cove	13.5	1	11.75	0.004	100	0.370	0.200	Hamblen/ Barbourville

[a] Distance along the moisture gradient as graphed by Whittaker (1956).

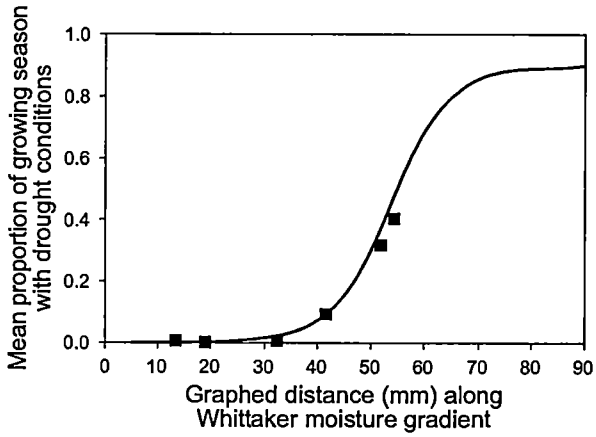

Figure 6.8. Proportion of growing season with unfavorable moisture conditions, as a function of distance along the moisture gradient graphed by Whittaker (1956). Black squares represent points along the gradient for which drought was modeled. The line shows the logistic function fitted to those points.

the moisture gradient (Whittaker 1956). I defined the drought-tolerance (D3) of each species according to modeled drought at the estimated upper limit of the distribution of each species on the moisture gradient. The only exceptions to this method are that I increased D3 for pignut hickory (*Carya glabra*) to a value equal to that of chestnut oak, and raised drought-tolerance of mockernut hickory (*Carya tomentosa*) proportionately. Whittaker (1956) found pignut hickory on moderately dry sites in the Smokies, but the species occurs on some of the most xeric sites in the Valley and Ridge of southwestern Virginia (McCormick and Platt 1980).

I used climate data from Mt. LeConte, a high peak in the Smokies, to parameterize drought-tolerance for three species abundant only at high elevations – red spruce (*Picea rubens*), American beech (*Fagus grandifolia*), and yellow buckeye (*Aesculus octandra*). High-elevation sites are moister, and only the driest ridgetops showed unfavorable moisture levels for any portion of the growing season. Drought-tolerance estimates for high-elevation species were interpolated linearly from distance along the gradient.

Subroutine KILL

Subroutine KILL kills trees by age-dependent mortality and supplies litter to subroutine DECOMP, where it is decomposed. Leaf litter is supplied annually, according to the biomass of leaves on trees in the plot and to the foliage retention time (array FRT(I)) of each species I. FRT is one year for deciduous species and greater than one year for evergreen trees. Huston (1994) added a disturbance algorithm that kills trees at random intervals, according to disturbance intensity and frequency probabilities defined by the user. I added logging disturbance that removes all trees over a given size in all plots the same year. The purpose is to simulate logging that occurred in eastern forests during the late 1800s and early 1900s. Extensive timber harvest contributed to changes in species composition and other attributes (Foster *et al.* 1992; Foster *et al.* 1998; Fuller *et al.* 1998). A stand developing on a logged site would differ from one established on bare soil because advance regeneration would be present, favoring species that might not

occur in old agricultural fields, and because soil organic matter and nutrient levels would be greater.

When a tree dies, all the biomass of the tree, including foliage, is returned as litter. Litter decomposition occurs over a period years, based such factors as litter quality, soil water-holding capacity, and climate (Pastor and Post 1985). Annual foliage production (FOLW) is multiplied by FRT(I) to determine the number of years of foliage production to return. To account for the fact that a killed tree may have had canopy damage from a recent ice storm and would therefore return less foliage than an undamaged tree, foliage return is multiplied by CANPCT(K), the proportion of canopy that is intact. The resultant equation is

FOLW = FOLW*FRT(I)*CANPCT(K).

This equation is not appropriate for trees killed outright during an ice storm (category 4 trees), which would occur during the leaf-off season of deciduous trees. For ice-killed trees, FOLW is multiplied by FRT(I) – 1, so that a deciduous tree returns no foliage and an evergreen returns the production of one year less than FRT(I). The equation for ice-killed trees, then, is

FOLW = FOLW*FOLRET*CANPCTPY(K)

Where FOLRET = FRT(I) – 1. CANPCTPY(K) is the proportion of canopy intact the previous year. This value is used because an evergreen tree killed during the winter by an ice storm would possess only the proportion of canopy that was present during the previous growing season.

Annual leaf litter return from trees damaged, but not killed, by an ice storm is also simulated. Leaf return for the current year is reduced according to the amount of canopy that was lost in the storm (i.e., is multiplied by CANPCT). Further, winter foliage of evergreen trees

sustaining canopy loss the previous winter is also returned, according to the proportion of canopy that was removed.

Applying FORICE

I used the model to simulate temporal and spatial patterns of forest dynamics for a landscape in the Valley and Ridge province of southwestern Virginia (Figure 6.9), in the vicinity of ice storm damage sampling sites reported in Chapter 3 of this dissertation. Walker Mountain and Little Walker Mountain dominate topography in this landscape (Figure 6.10). I used the ARC/INFO AML described above to calculate topographic index for each 30-m cell in the DEM. I used the topographic index to stratify the landscape into five topographic classes, including ridgetops, three slope positions, and valleys (Table 6.2). I modeled the three slope positions for both north-facing and south-facing slopes. Ridgetops and valleys were modeled as level sites. Simulated soils represent soils characteristic of these topographic positions (Gall and Edmonds 1992). The proportion of the growing season characterized by drought conditions increases in increments of approximately 0.1 between each modeled site type (Table 6.2). Temperature and precipitation data for Wytheville, Virginia were obtained from NCDC (1995). A longer climate record exists for Wytheville than for most other sites in southwestern Virginia and may provide a reasonably good representation of climatic conditions over several southwestern Virginia counties. Of course, altitudinal variations limit the suitability of any single station for describing climate over the region. Table 6.3 lists species parameters used in the model.

For each topographic position, I simulated three different types of canopy disturbance, in addition to age-related tree mortality, during a 700-year long run for 10 plots. First, random, low-frequency disturbance (e.g., thunderstorm winds) was simulated by causing mortality of approximately 50% of all trees between 10 and 300 cm DBH at an average frequency of once every 200 years. Second, logging in year 300 killed all trees with DBH at least 15 cm. Third, I modeled each site with ice storm disturbance and without. Ice storms occurred at a mean rate of

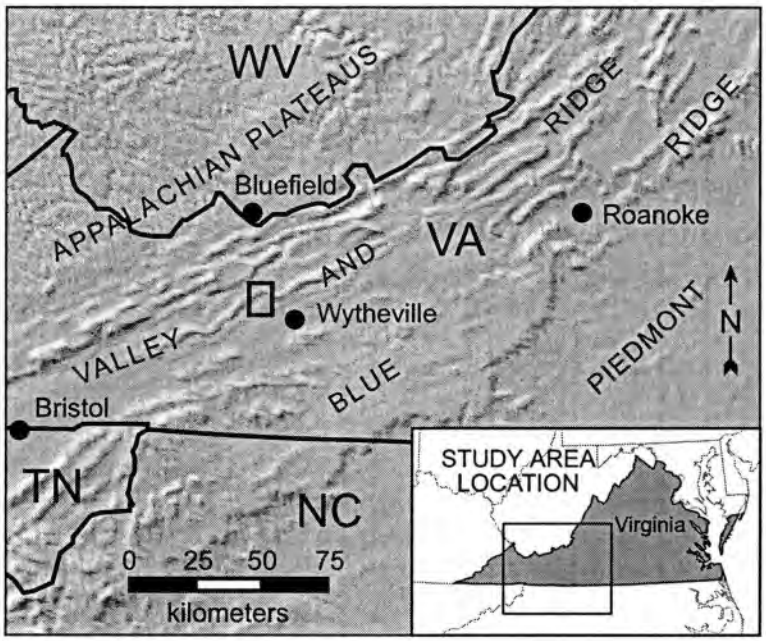

Figure 6.9. Valley and Ridge landscape of southwestern Virginia for which forest dynamics were simulated. Small rectangle northwest of Wytheville indicates the location of the specific landscape modeled. Climate data for Wytheville were used in the simulations.

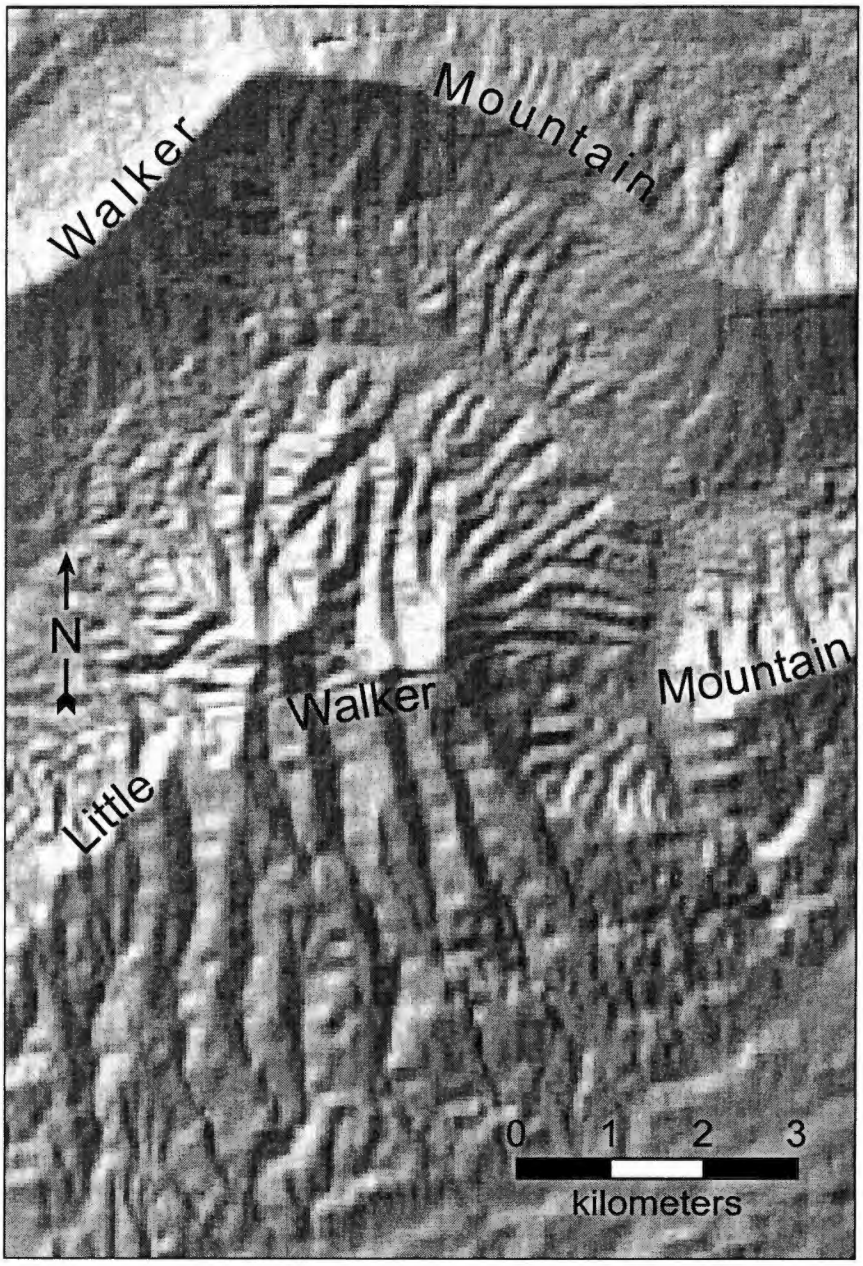

Figure 6.10. Landscape on which forest modeling was focused. The location of this study area is indicated in Figure 6.10.

Table 6.2. Input data for the site types for which simulations were conducted.

Topographic position	Aspect (degrees)	Slope (degrees)	Topo-graphic index	Growing season drought	Soil parameters: Depth (cm)	Field capacity (cm/cm)	Wilting point (cm/cm)	Soil series
Ridgetop	None (0)	0	4.5	0.717	30	0.370	0.285	Weikert
Upper slope	South (180)	20	5.0	0.584	45	0.370	0.280	Weikert
	North (0)	20	5.0	0.474	45	0.370	0.280	Weikert
Mid-slope	South (180)	30	5.5	0.423	70	0.370	0.304	Berks
	North (0)	30	5.5	0.296	70	0.370	0304	Berks
Lower slope	South (180)	25	6.63	0.206	100	0.370	0.295	Berks
	North (0)	25	6.63	0.117	100	0.370	0.295	Berks
Valley	None (0)	0	10.0	0.000	160	0.370	0.184	Gullion
Ravine	East (90)	35	7.5	0.052	100	0.370	0.270	Tran-sition[a]

[a] Soil is transitional between Berks and Gullion.

Table 6.3. Selected parameters for species used in the model. DMIN = minimum number of growing degree days required (base temperature = 5.56° C); HTMAX = maximum height (m); DIAMAX = maximum stem diameter (m); ITOL = shade-tolerance (1 = very tolerant, 5 = very intolerant); ITOLSEED = shade-tolerance of individuals with stem diameter ≤ 5 cm; AGEMAX = maximum age (years); G = growth-rate regulator; SPRTND = multiplier reflecting tendency of species to sprout; MPLANT = maximum number of seedlings recruited annually; D3 = maximum proportion of growing season species can tolerate drought; ISUSCAN = susceptibility to canopy damage during an ice storm (0 = high, 1 = low; simulation of damage to southern pines does not use this variable); ITREAREA = measure of amount of canopy space required by tree of a given stem diameter (1 = low, 2 = medium, 3 = high). Species nomenclature follows Fernald (1950).

Species	DMIN	HTMAX	DIAMAX	ITOL	ITOLSEED	AGEMAX	G	SPRTND	MPLANT	D3	ISUSCAN	ITREAREA
Acer rubrum	458	38	1.50	2	2	150	223.1	9	250	0.826	0	2
Acer saccharinum	936	37	1.20	2	2	130	375.0	0	250	0.007	0	2
Acer saccharum	603	37	0.90	1	1	400	240.0	3	250	0.001	0	3
Aesculus octandra	2333	40	1.55	3	3	300	117.1	1	250	0.100	0	2
Betula alleghaniensis	519	35	1.45	3	3	350	250.0	3	500	0.002	0	2
Betula lenta	1756	24	1.50	4	3	265	325.0	3	500	0.015	0	2
Carpinus caroliniana	1419	18	0.90	3	3	150	111.5	2	100	0.280	0	2
Carya cordiformis	1547	30	0.90	4	3	200	300.0	1	100	0.013	1	2
Carya glabra	1963	37	1.20	3	2	300	300.5	2	100	0.716	1	2
Carya ovata	1692	40	1.20	3	3	300	300.5	3	100	0.242	1	2
Carya tomentosa	2142	30	0.90	4	3	500	300.0	1	100	0.220	1	2
Celtis laevigata	2660	24	1.00	3	3	200	108.5	2	100	0.280	1	2
Cornus florida	2023	17	0.50	1	1	125	250.0	3	250	0.579	0	2
Fagus grandifolia	1165	37	1.35	1	1	370	225.0	2	100	0.018	0	3
Fraxinus americana	1165	36	1.80	4	3	300	295.0	2	250	0.038	0	1
Juglans cinerea	1641	30	0.90	4	4	75	353.9	1	50	0.180	0	2
Juglans nigra	2076	46	1.80	4	4	300	435.0	1	50	0.280	0	2
Juniperus virginiana	1384	37	1.20	4	4	300	108.3	0	100	0.350	1	1
Liriodendron tulipifera	1677	61	3.70	4	4	300	650.0	2	500	0.383	0	1
Magnolia acuminata.	1963	30	1.20	3	3	150	575.0	3	250	0.083	0	2
Nyssa sylvatica	1929	36	1.20	3	3	300	400.0	1	50	0.718	1	2
Ostrya virginiana	1384	24	0.60	1	1	100	213.3	2	100	0.300	0	2
Picea rubens	1165	33	1.35	2	2	400	145.0	0	100	0.091	1	1

Table 6.3 (continued).

Species	DMIN	HTMAX	DIAMAX	ITOL	ITOLSEED	AGEMAX	G	SPRTND	MPLANT	D3	ISUSCAN	ITREAREA
Pinus echinata	2617	42	1.05	4	4	250	325.5	2	500	0.850	–	1
Pinus pungens	1929	30	0.95	4	4	250	245.0	0	500	0.870	–	1
Pinus rigida	1825	30	1.10	4	4	200	260.0	2	500	0.873	–	1
Pinus strobus	903	60	2.50	3	2	450	485.0	0	500	0.857	0	1
Pinus virginiana	2026	35	0.80	4	4	250	220.0	0	500	0.893	–	1
Platanus occidentalis	1842	51	2.50	3	3	300	148.4	2	250	0.001	0	2
Populus grandidentata	1148	30	0.75	5	5	70	377.2	2	250	0.250	1	2
Prunus pensylvanica	274	15	0.30	5	5	50	269.6	0	500	0.250	0	1
Prunus serotina	1342	40	1.20	5	5	250	350.0	3	500	0.039	0	1
Quercus alba	1415	46	2.45	3	2	600	300.0	2	100	0.656	1	3
Quercus coccinea	1821	30	1.20	5	5	400	385.0	2	100	0.813	0	3
Quercus marilandica	2493	15	0.50	3	3	400	34.7	2	100	0.890	0	3
Quercus prinus	1906	30	1.85	3	2	300	400.0	3	100	0.716	1	3
Quercus rubra	763	50	1.50	3	3	400	350.0	3	100	0.666	1	2
Quercus stellata	2204	30	1.20	4	4	400	66.9	2	100	0.761	1	3
Quercus velutina	1607	45	1.20	3	3	200	325.0	2	100	0.716	0	3
Robinia pseudoacacia	1720	25	0.75	5	5	100	460.0	3	500	0.656	1	2
Tilia americana	763	45	1.35	2	2	200	235.0	3	100	0.004	0	2
Tilia heterophylla	2111	27	0.90	2	2	200	305.0	3	100	0.004	0	2
Tsuga canadensis	693	53	2.15	1	1	800	150.0	0	250	0.485	1	1
Ulmus alata	2985	30	0.50	3	3	125	208.6	1	250	0.250	0	2

three times per century. This frequency agrees with evidence from tree-ring chronologies and historic records for parts of southwestern Virginia (Chapter 5), including a site on Walker Mountain north of Wytheville. FORICE chooses ice storm years randomly, based on mean frequency, and simulates ice storm disturbance during the same years for all plots in the run. I accounted for fire on dry sites by reducing white pine and red maple reproduction to 1% and 10% of optimum, respectively, on ridgetops, upper slopes, and middle slopes. Both species are easily damaged by fire, and frequent burning may completely eliminate white pine (Wendel and Smith 1990). Although my focus is not on fire ecology, this crude measure was necessary to prevent white pine and red maple from so dominating successional patterns on dry sites that oak and southern pine dominance were prevented. Burning affected xeric sites in the Appalachians in the past (Welch 1999), probably contributing to the commonly observed patterns of pine and oak dominance (Harrod *et al.* 1998). Harrod *et al.* (1998) concluded that without fire, species composition of stands on dry slopes and ridgetops currently dominated by southern pines and oaks would shift toward white pine, red maple (*Acer rubrum*), black gum (*Nyssa sylvatica*), and eastern hemlock.

I also conducted four simulations to model unique conditions on specific sites. First, to reflect tree damage patterns in xeric southern pine-oak sites on topographic positions sheltered from heavy ice accretion, I modeled the three most xeric site types with the sheltered-site option described above in the discussion of subroutine ICEDIST. West-facing slopes typically occupied by these forests appear less prone to heavy ice accumulation than east-facing slopes (Williams and Johnson 1990; Lafon *et al.* 1999), but pines can sustain moderate damage levels nonetheless (Chapter 3). Second, to simulate stand dynamics on unburned dry sites, I modeled south-facing upper and middle slopes with optimal levels of white pine and red maple reproduction. Third, I ran the model for a mesic site on the steep, east-facing slope of a ravine for comparison to forest conditions in a similar site sampled as part of the field study reported in Chapter 3. Fourth, I

simulated ice storm disturbance in valley sites at a lower average frequency of 100 years to simulate the possibility that valleys are less frequently affected by major ice storms than adjacent mountain slopes at higher elevations (Lafon *et al.* 1999).

I obtained Forest Inventory and Analysis (FIA) plot data for several counties in western Virginia from the U.S. Forest Service web site (www.srsfia.usfs.msstate.edu/wo/wofia.htm) for comparison with model results (Figure 6.11). All the counties appear to be affected by ice storms at relatively high frequencies (Lafon 1999). I selected only stands at least 75 years old. Maximum ages were around 130 years. Based on topographic characteristics, each plot was considered either exposed to or sheltered from major ice accumulations. Criteria for exposed plots included (1) slope at least 35%, or approximately 20°, and (2) aspect at least 45° but no more than 180°. All other plots were classed as sheltered.

Results

Simulated temporal dynamics along the topographic moisture gradient

Graphs shown in this section indicate predicted temporal trends in species composition and richness for the post-logging period (years 300 – 700). Results for no-ice simulations are plotted on the left, and those for with-ice simulations are shown on the right. Results are graphed at 25-year intervals. Also, to demonstrate immediate effects of the disturbances, results are also shown for each ice storm year and each year preceding an ice storm.

FORICE predicts dominance by southern pines, primarily table mountain pine and pitch pine (*Pinus rigida*), on dry ridgetops and upper south-facing slopes (Figures 6.12 and 6.13). However, oaks sustain less ice damage and are more abundant than pines on south-facing upper slopes influenced by ice storms (Figure 6.13B). In the most xeric sites, species richness is low, and ice storms reduce richness further (Figures 6.12C, D).

Forests of chestnut oak, pignut hickory, and a mix of other oaks are predicted to dominate moderately xeric sites on north-facing upper slopes and south-facing mid-slope sites (Figures

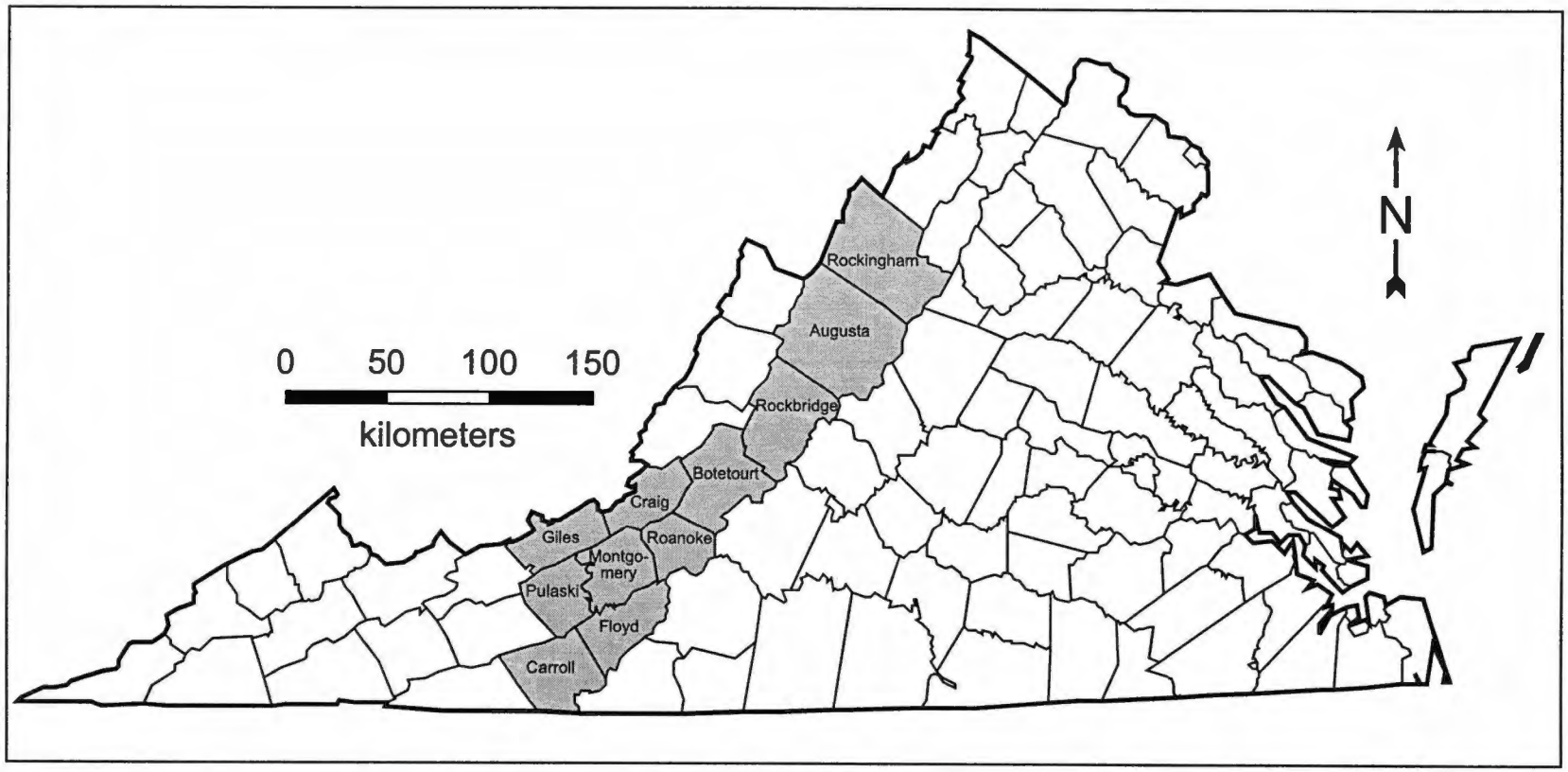

Figure 6.11. Virginia counties for which Forest Inventory and Analysis (FIA) data were obtained and analyzed.

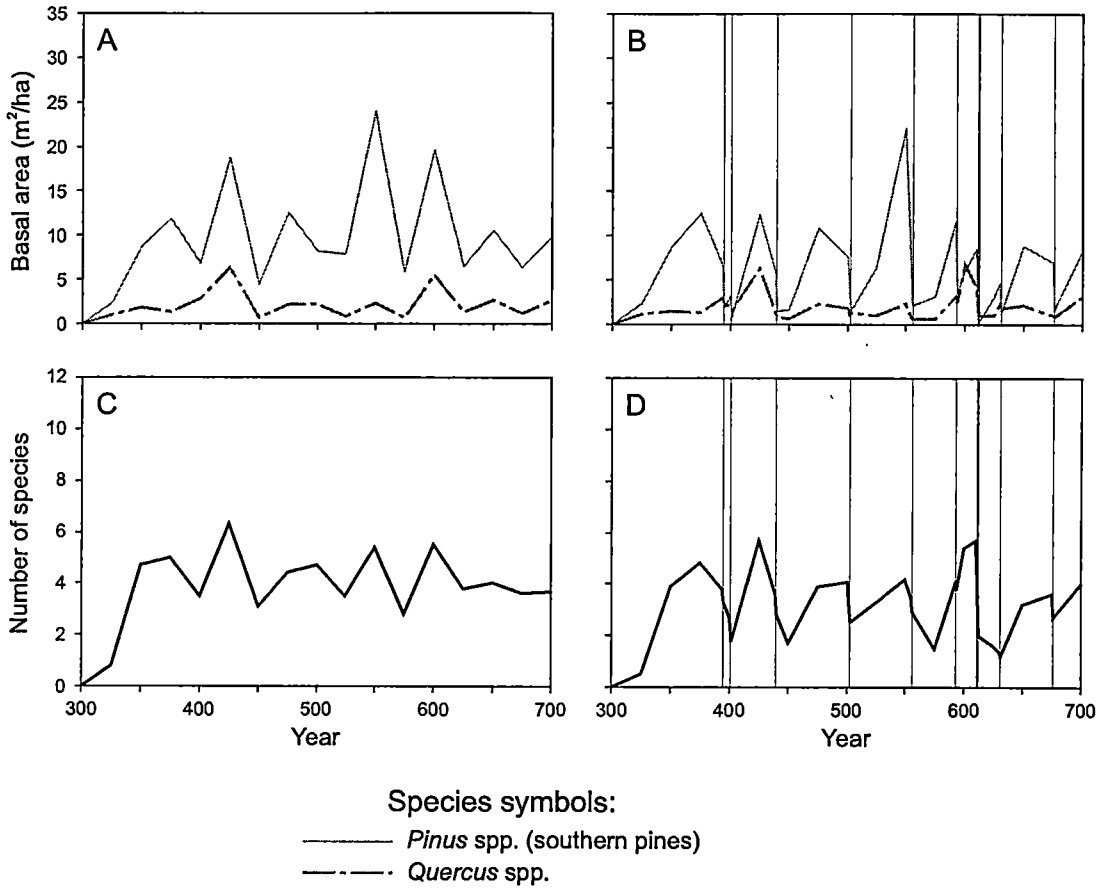

Figure 6.12. Simulated temporal dynamics of forests on ridgetops: (A,B) species composition, (C, D) species richness. No-ice simulations are graphed on the left, and with-ice simulations on the right. Vertical lines indicate years in which ice storm disturbance was simulated.

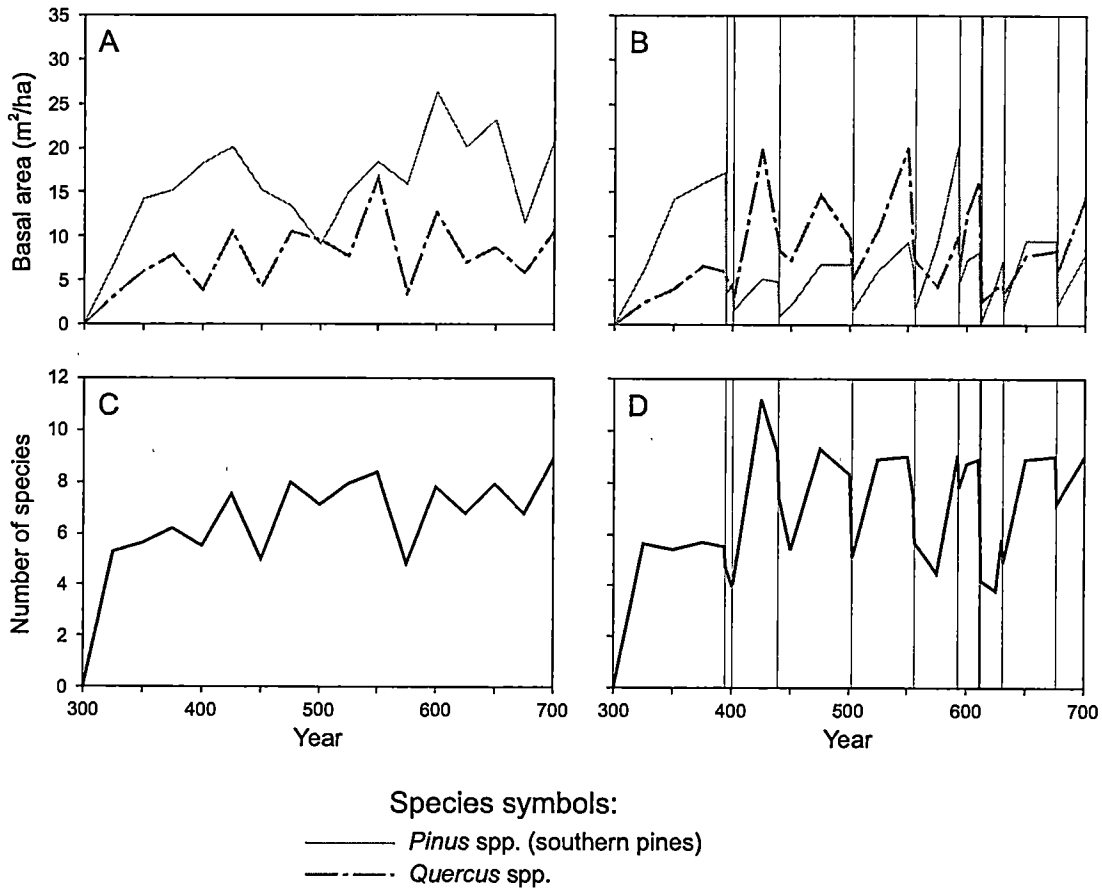

Figure 6.13. Simulated temporal dynamics of forests on south-facing upper slopes: (A,B) species composition, (C, D) species richness. No-ice simulations are graphed on the left, and with-ice simulations on the right. Vertical lines indicate years in which ice storm disturbance was simulated.

6.14 and 6.15). These species ultimately exclude southern pines, but periodic ice storm disturbances permit maintenance of pines in low numbers. Species richness is relatively high and appears to be enhanced by ice storm disturbance.

Black locust (*Robinia pseudoacacia*) dominates early-successional assemblages on north-facing mid-slope sites but is rapidly excluded (Figure 6.16). The species appears periodically in low numbers following ice storm disturbance in older stands. Chestnut oak, northern red oak (*Quercus rubra*), and pignut hickory are the dominant species, and ice storms contribute to more equitable abundance and slightly higher species richness.

On south-facing lower slopes, black locust and yellow-poplar share dominance in early succession but are rapidly excluded by northern red oak and hemlock without ice storm disturbance (Figure 6.17A). Periodic ice storms preclude hemlock dominance, permitting shared dominance by northern red oak and chestnut oak, and they favor the appearance of yellow-poplar and locust at low levels in older stands. Ice storms enhance species richness considerably (Figure 6.17C, D).

A similar succession of yellow-poplar to hemlock occurs on the more mesic north-facing lower slopes in the absence of ice storms, except that a northern red oak stage does not occur (Figure 6.18A). Ice storms prevent competitive exclusion of other species by hemlock (Figure 6.18B). They permit long-term maintenance of several species, including chestnut oak, yellow-poplar, and cucumber magnolia (*Magnolia acuminata*), contributing to much higher species richness (Figure 6.18C, D).

Yellow-poplar is highly abundant in mesic valley sites. However, sugar maple competition is too intense for long-term maintenance of yellow-poplar, even when ice storms occur (Figure 6.19). Ice storms do permit the existence of some species, such as cucumber magnolia, that would not otherwise persist, thus enhancing species richness.

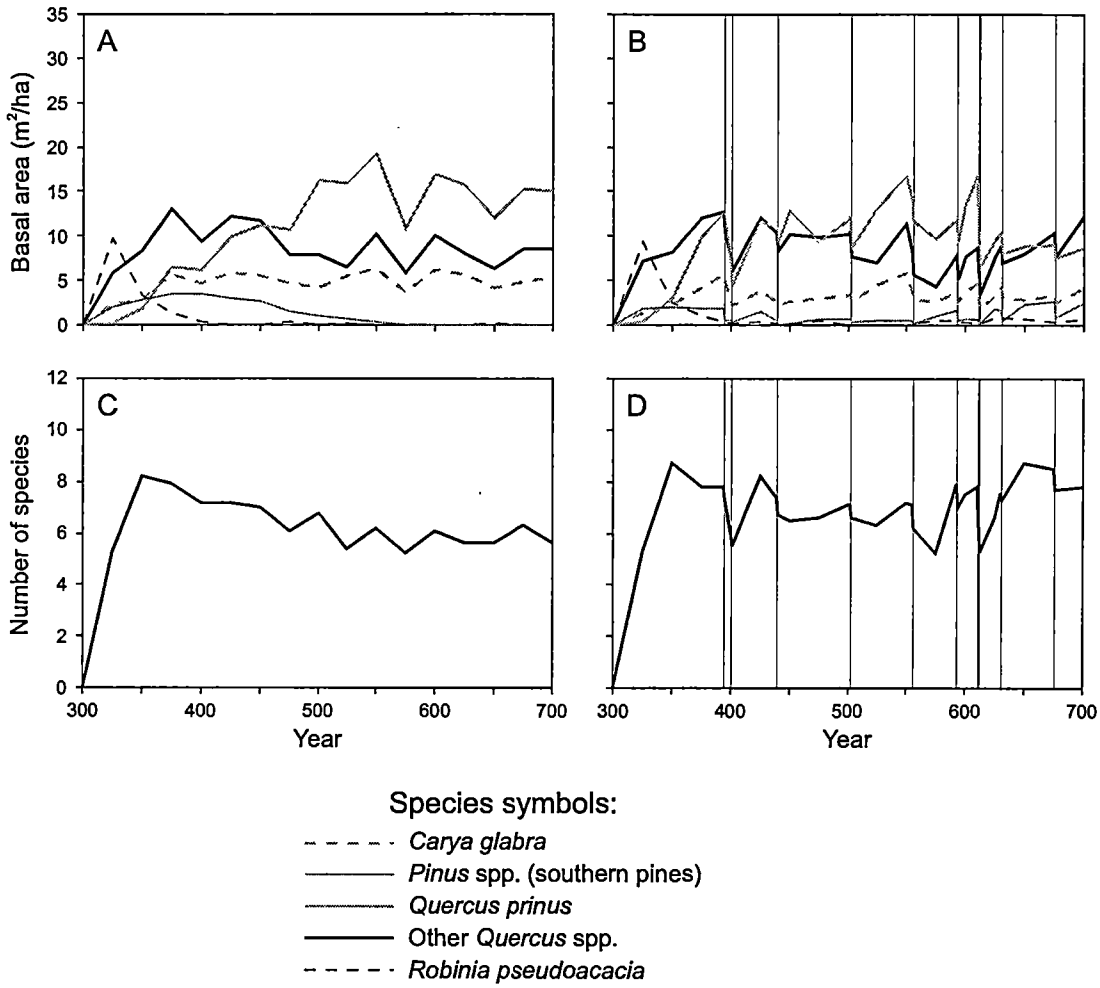

Figure 6.14. Simulated temporal dynamics of forests on north-facing upper slopes: (A,B) species composition, (C, D) species richness. No-ice simulations are graphed on the left, and with-ice simulations on the right. Vertical lines indicate years in which ice storm disturbance was simulated.

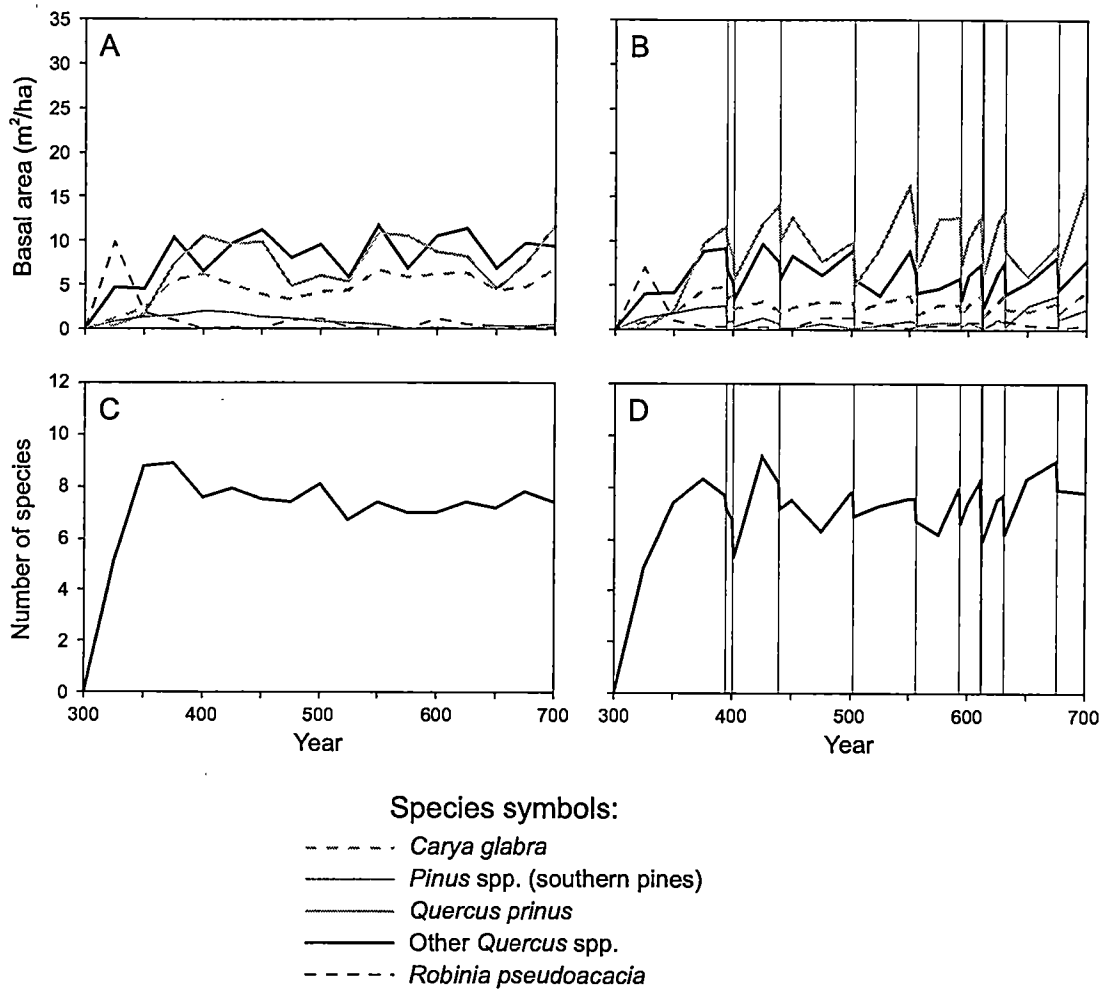

Figure 6.15. Simulated temporal dynamics of forests on south-facing middle slopes: (A,B) species composition, (C, D) species richness. No-ice simulations are graphed on the left, and with-ice simulations on the right. Vertical lines indicate years in which ice storm disturbance was simulated.

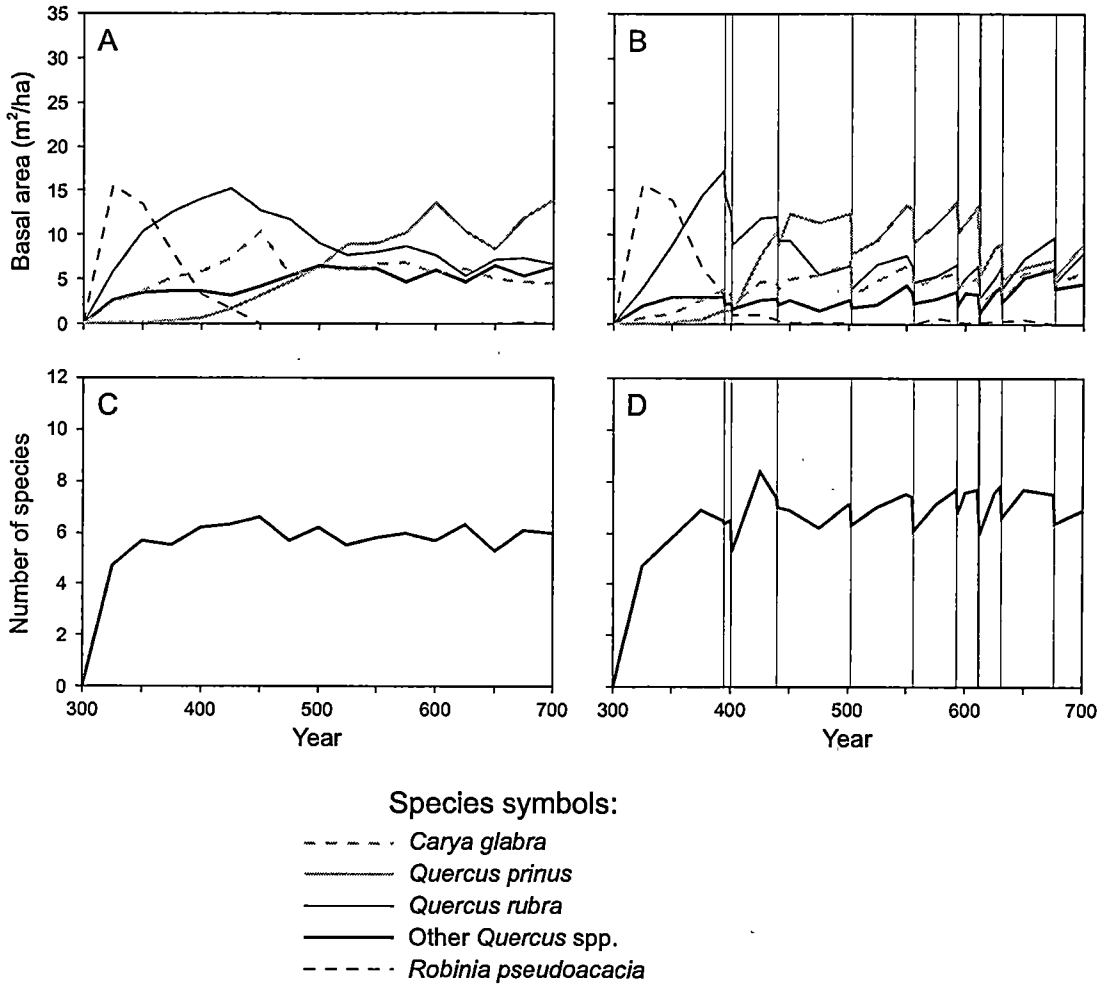

Figure 6.16. Simulated temporal dynamics of forests on north-facing middle slopes: (A,B) species composition, (C, D) species richness. No-ice simulations are graphed on the left, and with-ice simulations on the right. Vertical lines indicate years in which ice storm disturbance was simulated.

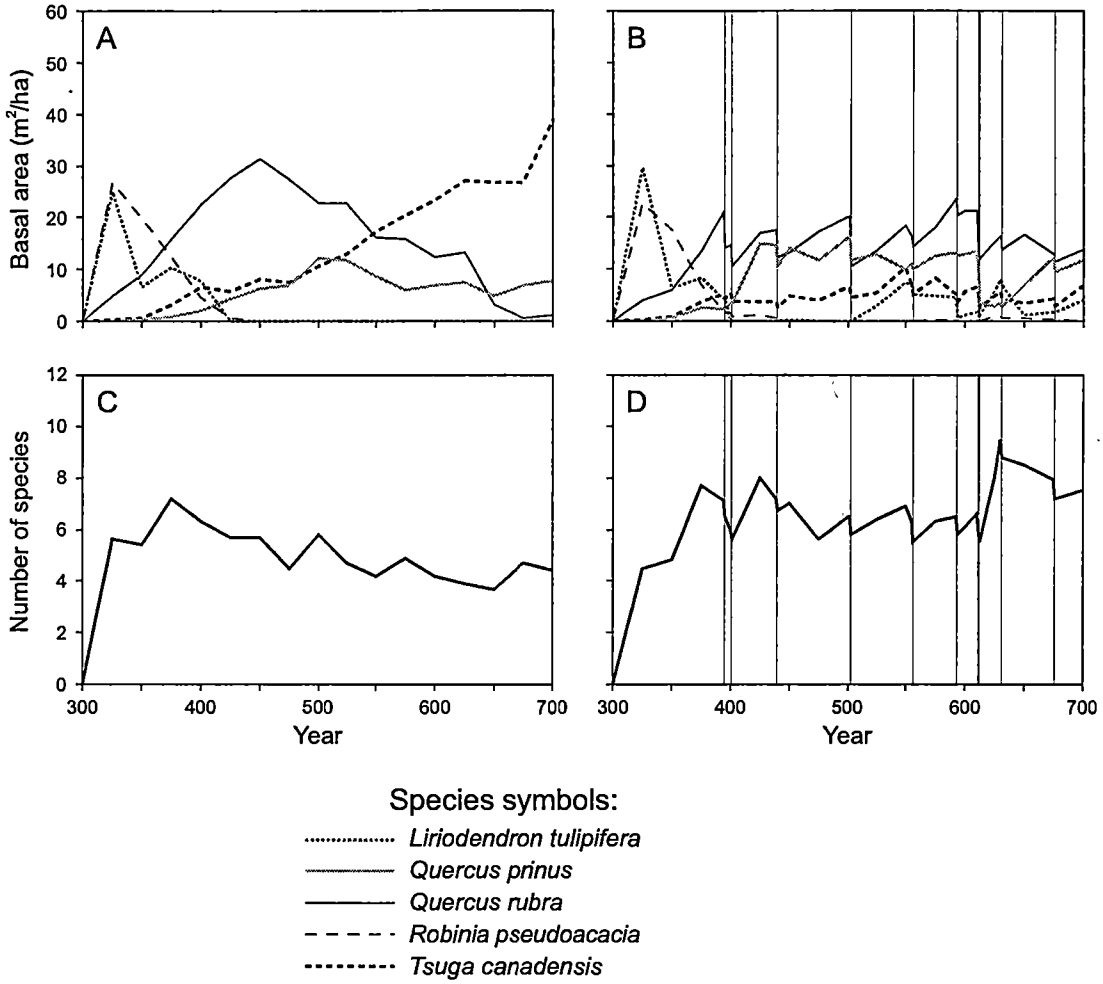

Figure 6.17. Simulated temporal dynamics of forests on south-facing lower slopes: (A,B) species composition, (C, D) species richness. No-ice simulations are graphed on the left, and with-ice simulations on the right. Vertical lines indicate years in which ice storm disturbance was simulated.

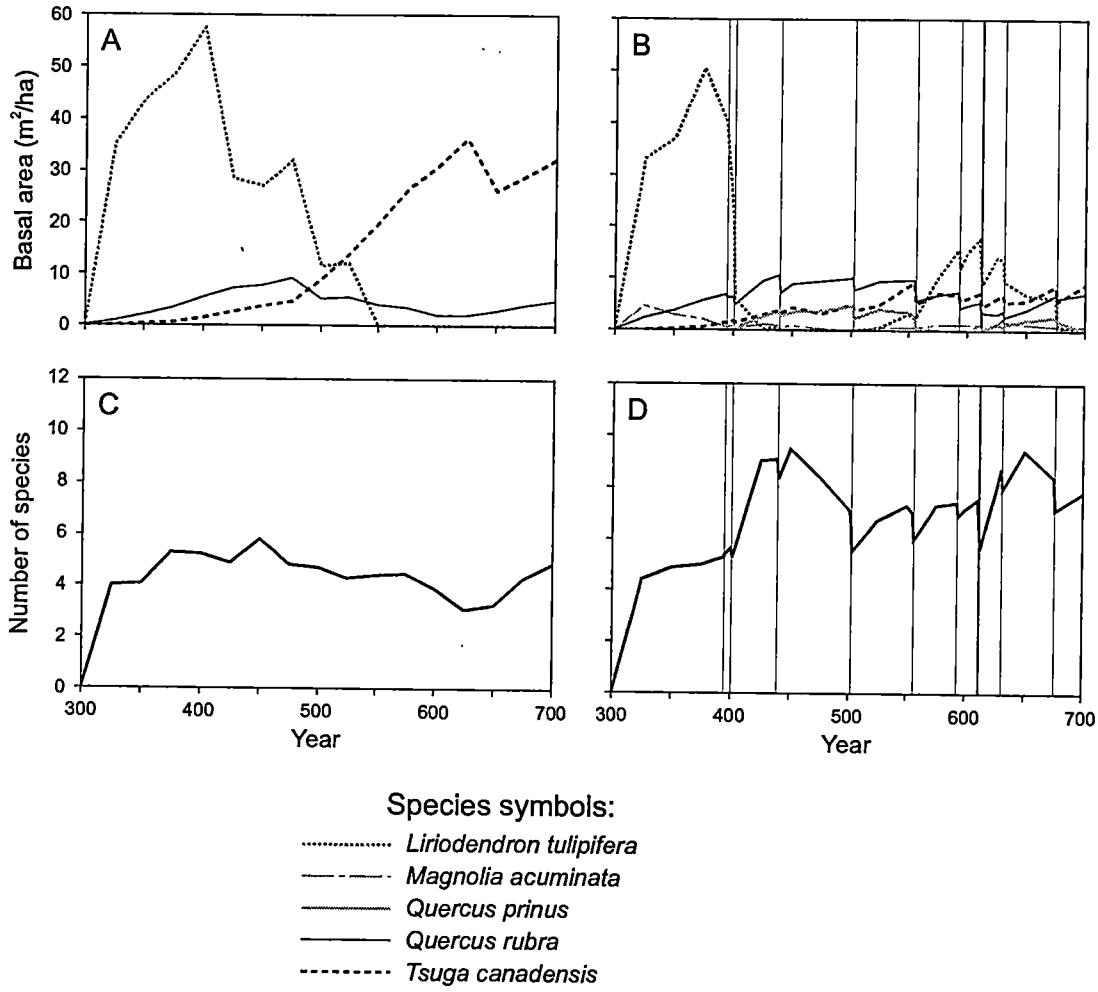

Figure 6.18. Simulated temporal dynamics of forests on north-facing lower slopes: (A,B) species composition, (C, D) species richness. No-ice simulations are graphed on the left, and with-ice simulations on the right. Vertical lines indicate years in which ice storm disturbance was simulated.

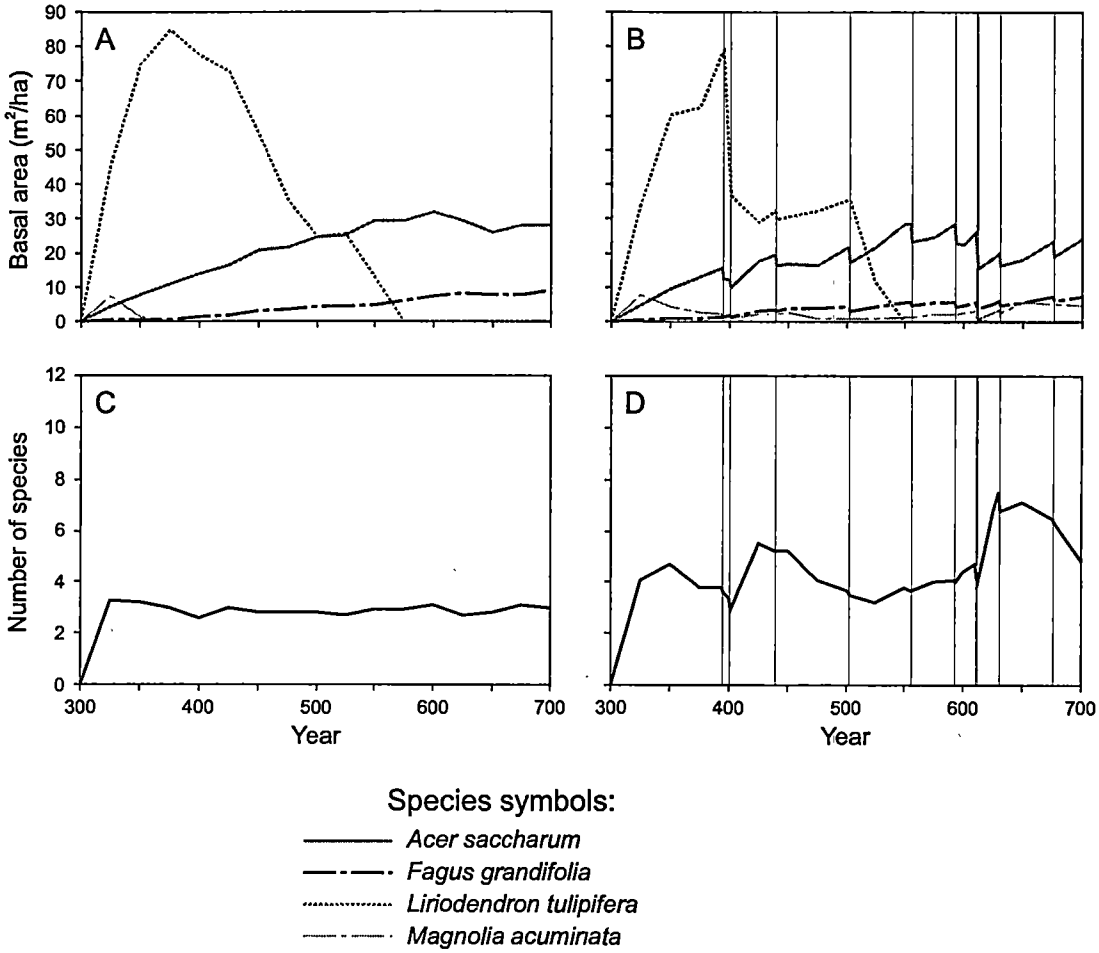

Figure 6.19. Simulated temporal dynamics of forests in valleys: (A,B) species composition, (C, D) species richness. No-ice simulations are graphed on the left, and with-ice simulations on the right. Vertical lines indicate years in which ice storm disturbance was simulated.

Special simulations for specific sites

Simulations of moderate ice storm damage on xeric sites sheltered from heavy ice accumulation yield patterns intermediate between those resulting from the no-ice and heavy-ice simulations (Figure 6.20). On south-facing upper slopes, pines and oaks share dominance evenly (Figure 6.20C), whereas pines are more abundant than oaks without ice disturbance (Figure 6.13A) and oaks are more abundant on sites exposed to heavy ice accumulation (Figure 6.13B). On north-facing upper slopes, sheltered sites do not exhibit long-term maintenance of pine and locust (Figure 6.20E), as occurs at exposed sites (Figure 6.14B).

In the absence of fire, southern pine dominance on xeric, south-facing upper slopes eventually shifts to white pine dominance, and southern pines may eventually be excluded (Figure 6.21A). Ice storms contribute to more rapid loss of southern pine dominance (Figure 6.21B). However, they also prevent excessive dominance by white pine and may allow long-term persistence of southern pines at moderate levels. Species richness is high in ice-damaged stands (Figure 6.21D). On moderately dry, south-facing middle slopes, white pine dominates for a period (Figure 6.22A) but declines as the trees age, with composition shifting to oak and hickory. Ice storms prevent extreme white pine dominance but permit its reproduction and maintenance in the stands over longer periods (Figure 6.22B), contributing to high species richness (Figure 6.22D). White pine never becomes a dominant species in unlogged stands on these same sub-xeric sites, regardless of ice storm disturbance (Figure 6.23). However, ice storms promote low levels of white pine occurrence in these stands (Figure 6.23B).

Mesic ravine slopes provide excellent conditions for growth of yellow-poplar. Without periodic disturbance, however, the species is not maintained, and dominance shifts to hemlock (Figure 6.24). Ice storms contribute to exceptionally high species richness. At the highly mesic valley sites, less frequent ice storms do not enhance richness substantially (Figure 6.25B). More

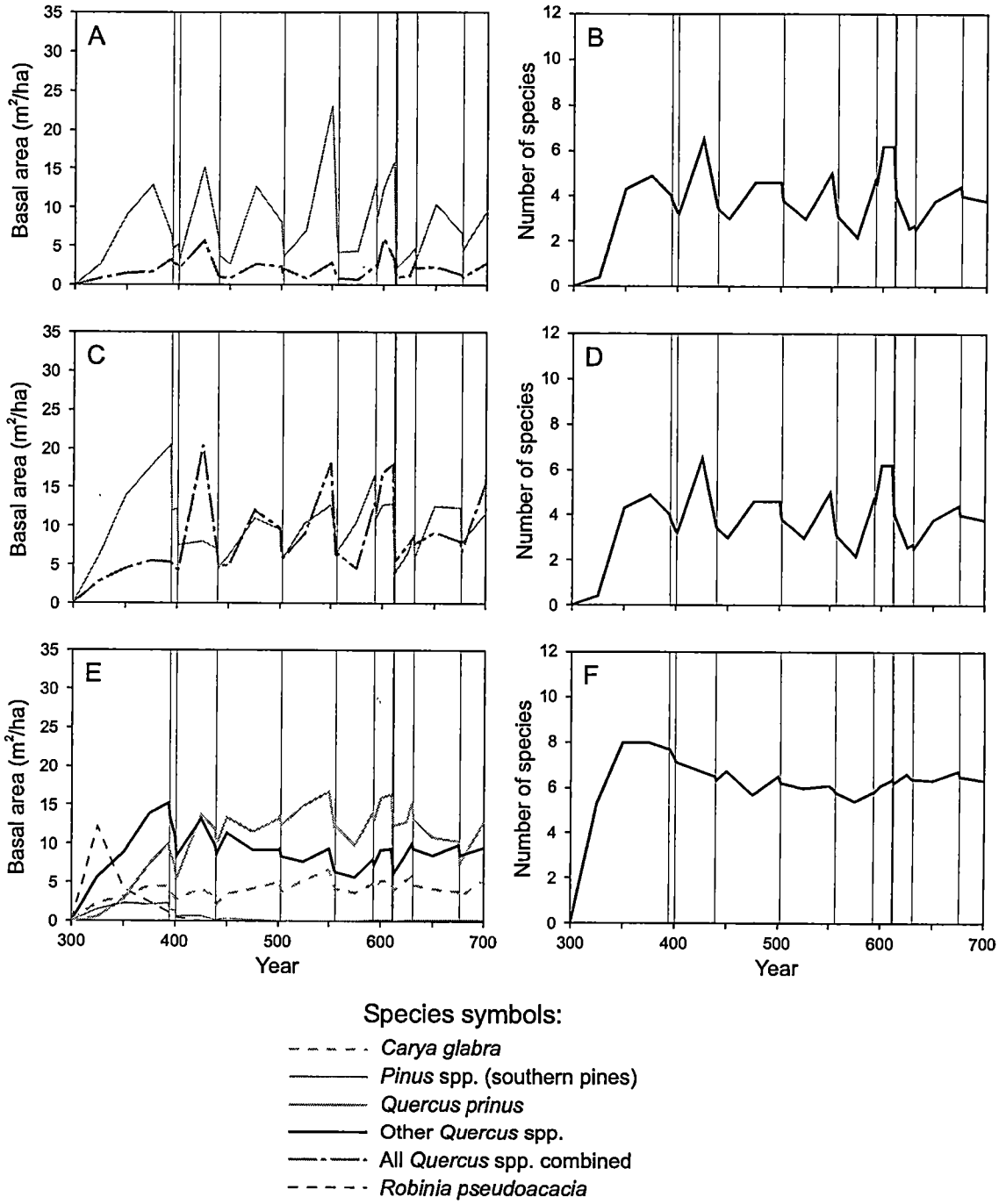

Figure 6.20. Simulated temporal dynamics of species composition (left) and species richness (right) for forests on xeric sites disturbed by ice storms but sheltered from heavy ice accumulation: (A,B) ridgetops, (C,D) south-facing upper slopes, (E,F) north-facing upper slopes.

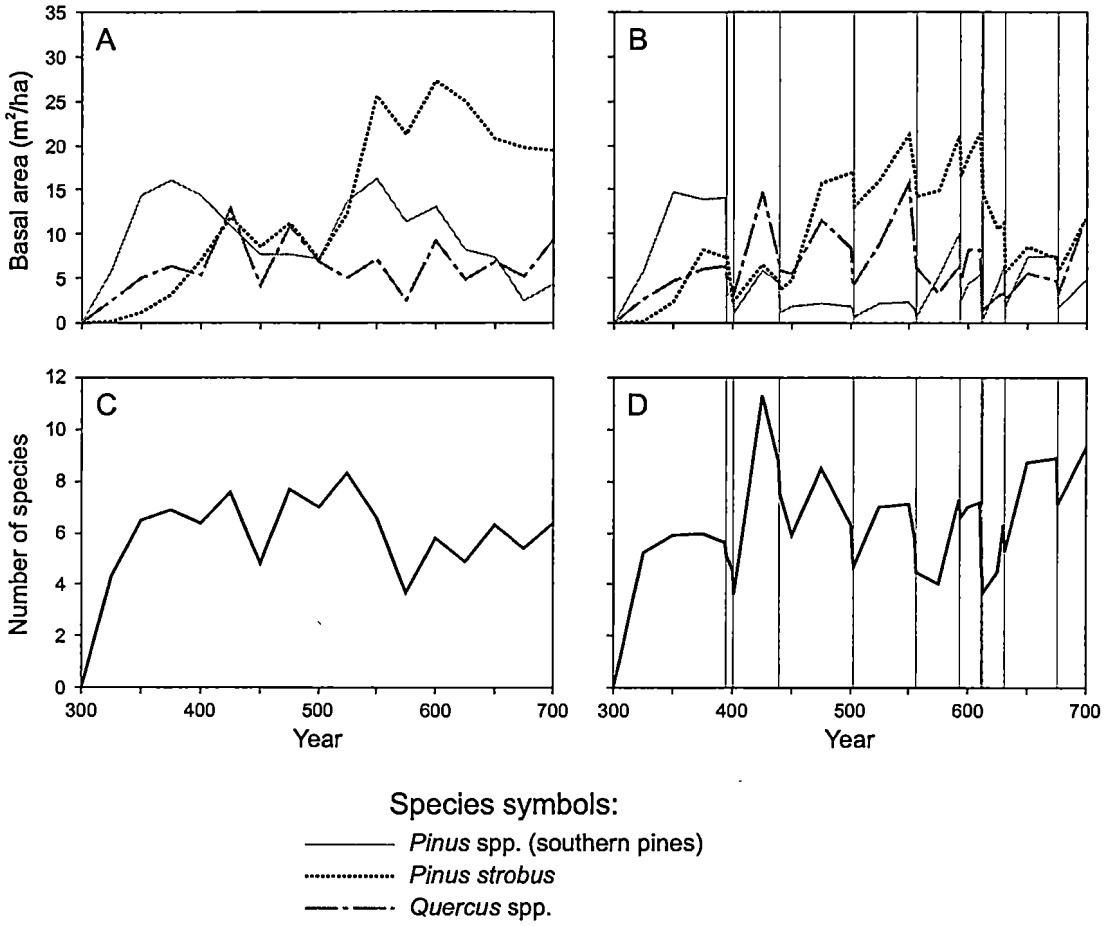

Figure 6.21. Simulated temporal dynamics of forests on south-facing upper slopes without fire: (A,B) species composition, (C, D) species richness. No-ice simulations are graphed on the left, and with-ice simulations on the right. Vertical lines indicate years in which ice storm disturbance was simulated.

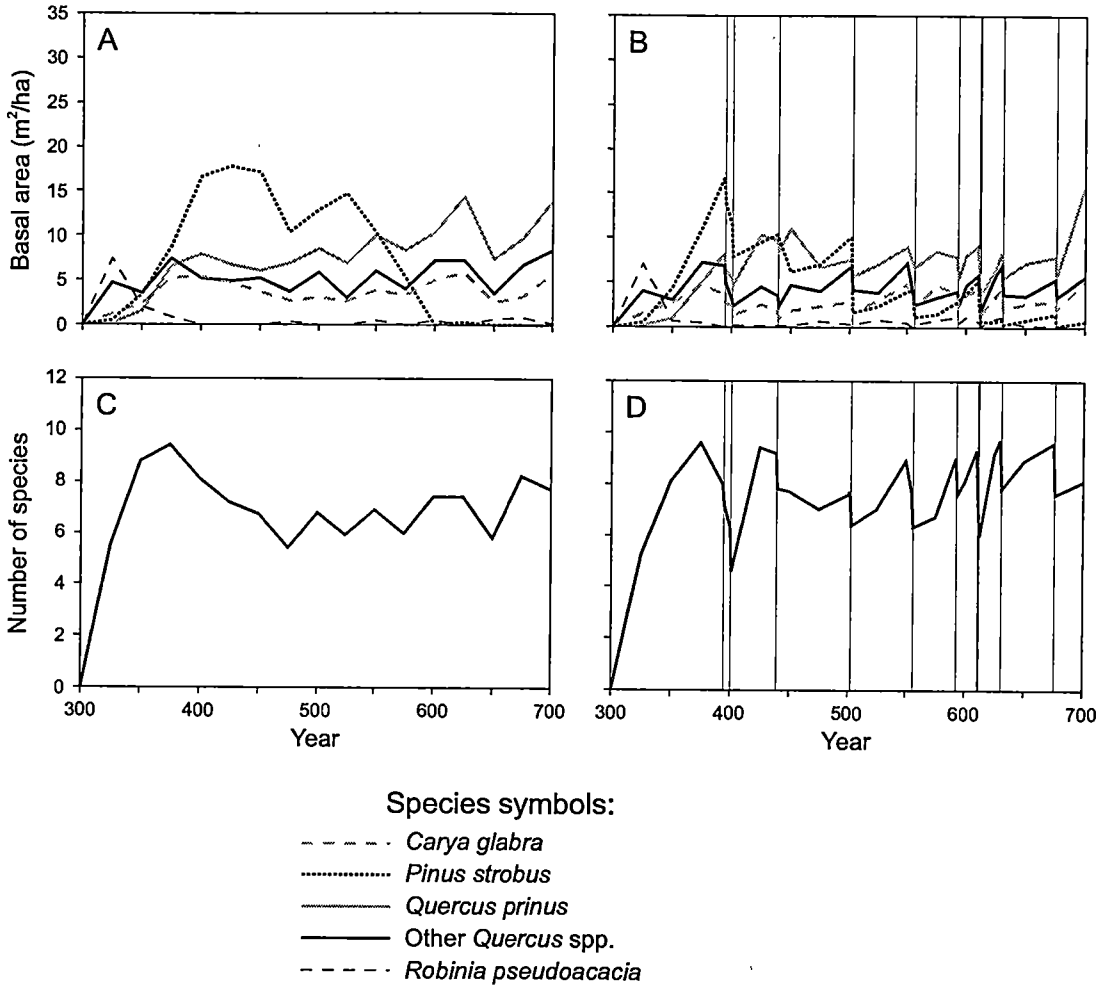

Figure 6.22. Simulated temporal dynamics of forests on south-facing middle slopes without fire: (A,B) species composition, (C, D) species richness. No-ice simulations are graphed on the left, and with-ice simulations on the right. Vertical lines indicate years in which ice storm disturbance was simulated.

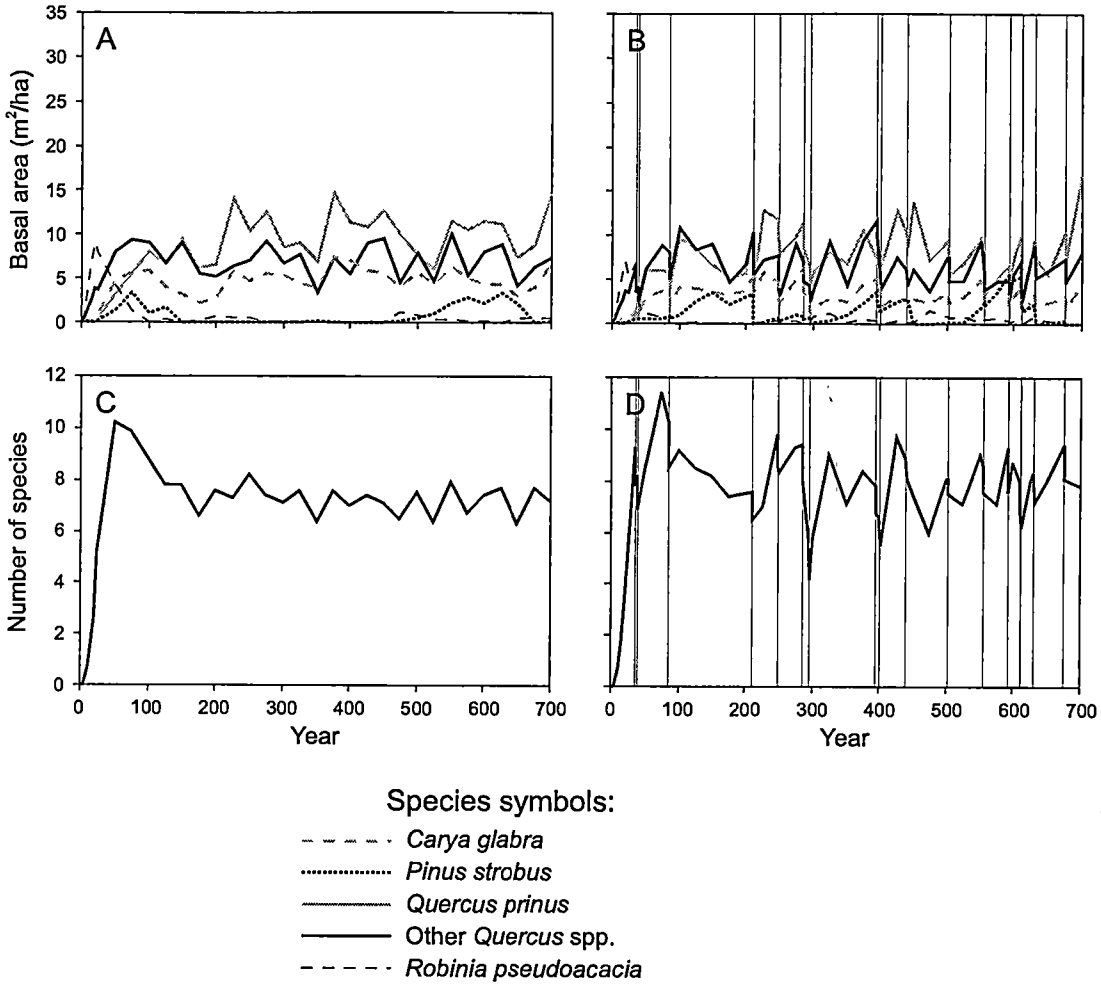

Figure 6.23. Simulated temporal dynamics of forests on unlogged south-facing middle slopes without fire: (A,B) species composition, (C, D) species richness. No-ice simulations are graphed on the left, and with-ice simulations on the right. Vertical lines indicate years in which ice storm disturbance was simulated.

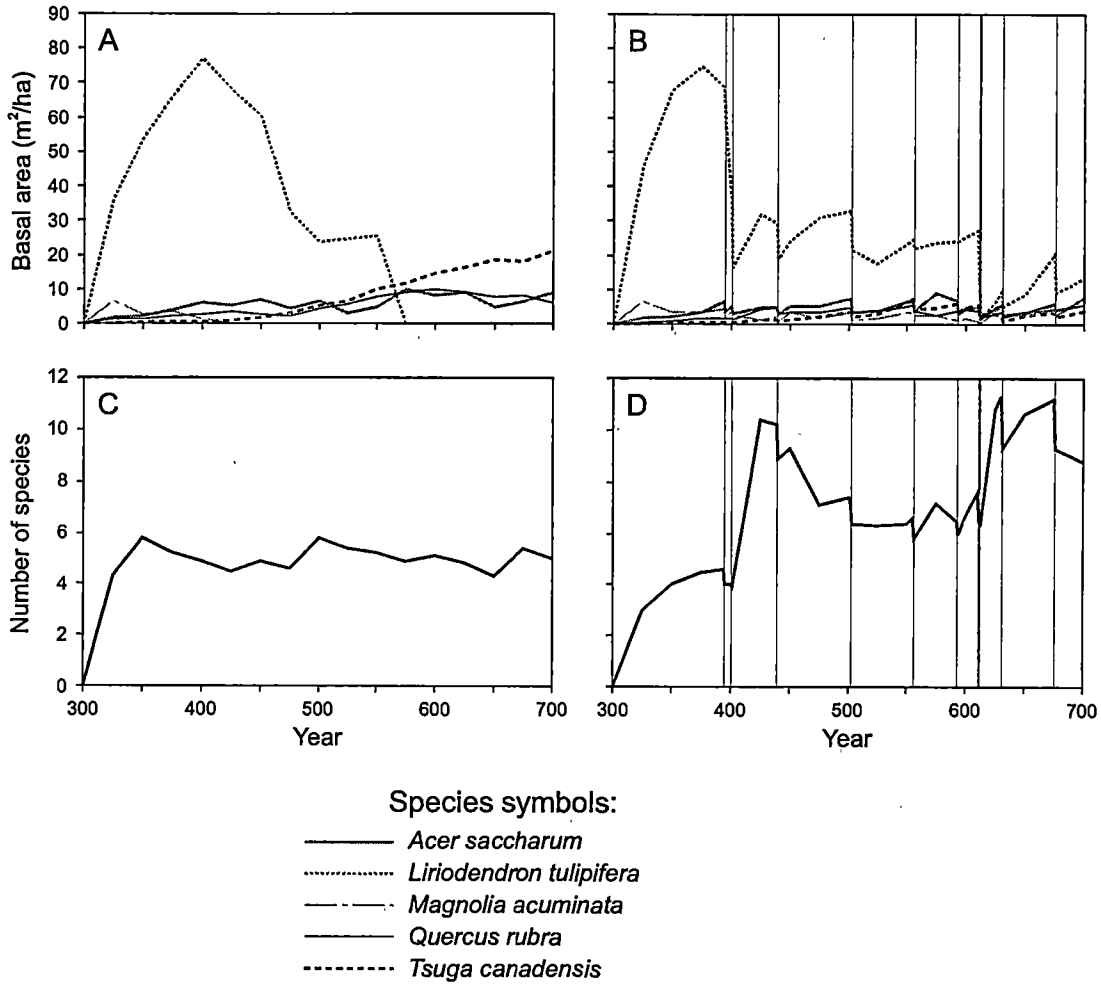

Figure 6.24. Simulated temporal dynamics of forests on mesic east-facing ravine slopes: (A,B) species composition,(C, D) species richness. No-ice simulations are graphed on the left, and with-ice simulations on the right. Vertical lines indicate years in which ice storm disturbance was simulated.

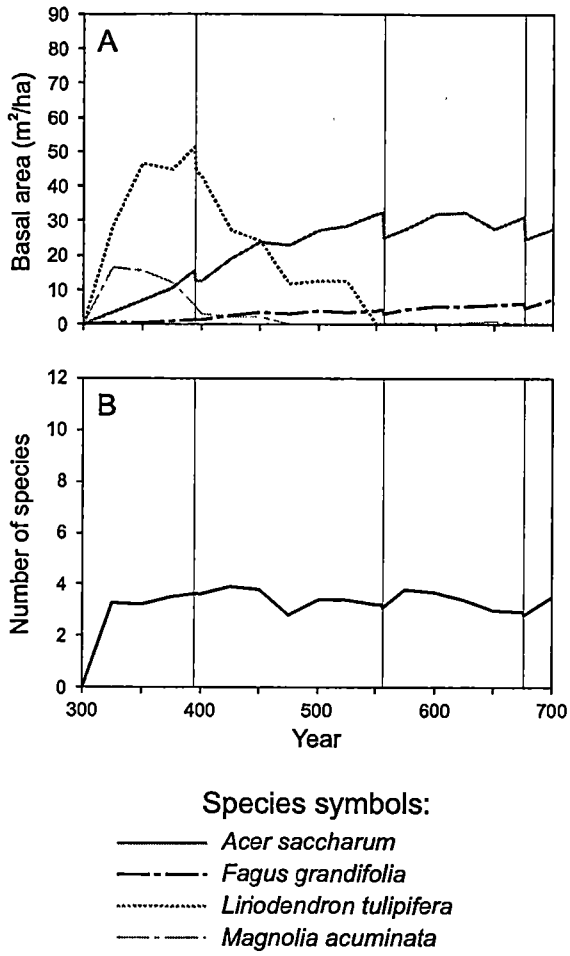

Figure 6.25. Simulated temporal dynamics of forests in valleys subjected to ice storms at a mean frequency of 100 years: (A) species composition and (B) species richness. No-ice simulations are graphed on the left, and with-ice simulations on the right. Vertical lines indicate years in which ice storm disturbance was simulated.

frequent ice storm disturbance is necessary for the maintenance of even moderate richness levels (Figure 6.19D).

Spatial patterns of abundance and diversity

Species distribution patterns presented in Figure 6.26A-D are analogous to those of Whittaker (1956) and Smith and Huston (1989). Figure 6.26 provides snapshots of species composition and richness along the entire moisture gradient at two points in succession. These graphs are based on standard model runs and do not include the special cases described in the previous section. Graphs on the left portray patterns at 100 years, and those on the right show conditions at 400 years. The top four graphs provide relative basal area calculated from the summed basal area of a species over all plots divided by the total for all species over all plots. The younger stands (Figure 6.26A, C) are characterized by pine-dominance on the dry end and yellow-poplar dominance on the mesic extreme, with chestnut oak and northern red oak relatively important over the middle of the gradient. The primary difference between the no-ice and with-ice simulations at this age is that yellow-poplar dominance is less pronounced in the disturbed sites, permitting greater importance of chestnut oak and northern red oak in mesic sites. Additionally, peaks of dominance appear to be shifted slightly toward the xeric end of the gradient.

Without ice storm disturbance, yellow-poplar is absent from the entire gradient by 400 years (Figure 6.26B). The gradient is divided more finely into distinct zones of pronounced dominance than was the case at 100 years. Stands exposed to ice storm damage, however, do not display conspicuous zonation patterns (Figure 6.26D), except at the extreme ends of the gradient.

Species richness exhibits a unimodal distribution along the moisture gradient at 100 years (Figure 6.26E) and generally shows slightly higher levels in stands undisturbed by ice storms. At 400 years, richness peaks near the xeric end of the gradient and declines toward the mesic end

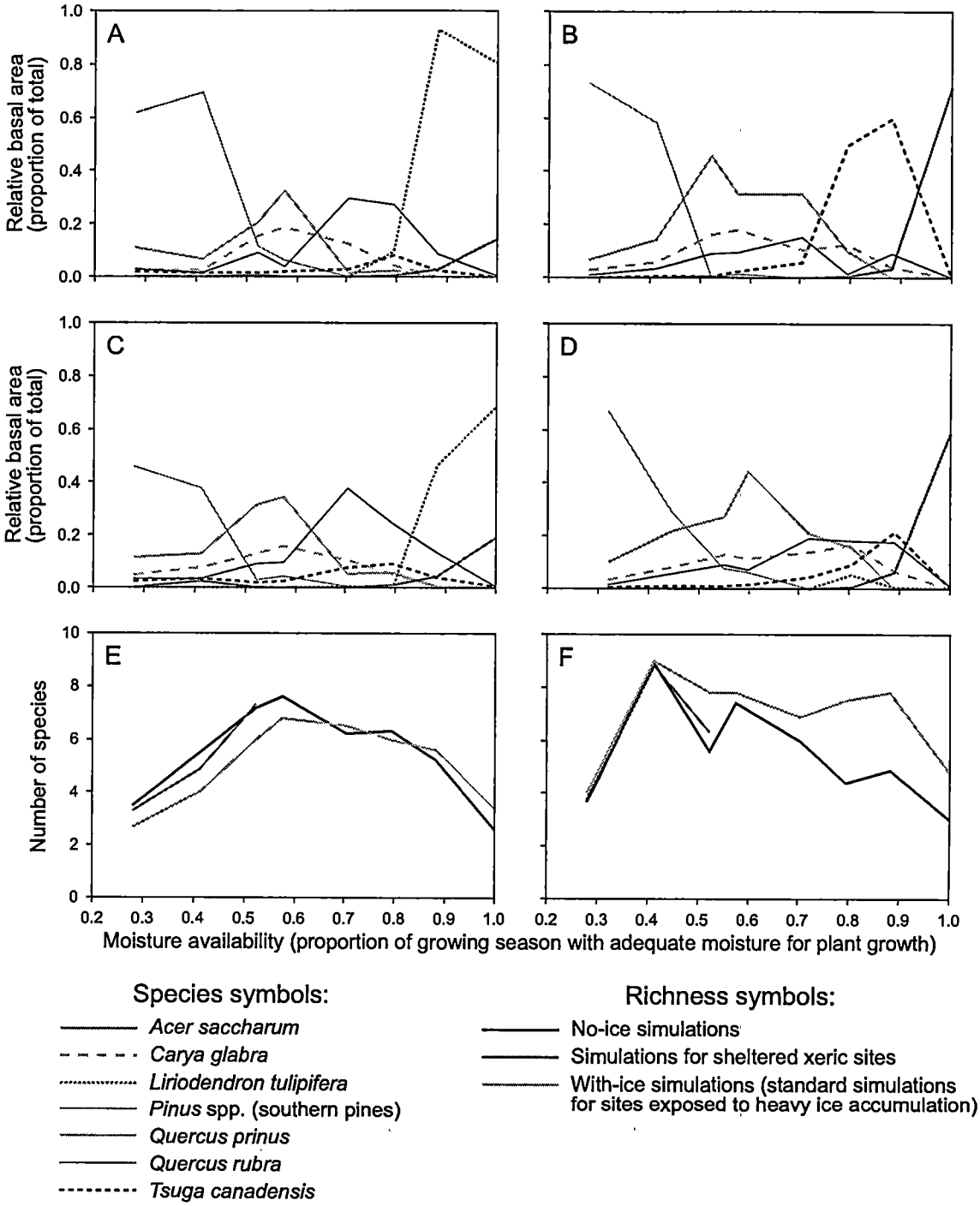

Figure 6.26. Simulated patterns of species composition and richness along the topographic moisture gradient for 100-year old forests (left) and 400-year old forests (right): (A,B) predicted species composition without ice storm disturbance, (C,D) predicted species composition with ice storm disturbance, and (E,F) predicted species richness.

(Figure 6.26F). The decline is less pronounced in ice-disturbed stands than in undisturbed forests.

Modeled patterns of composition and richness along the moisture gradient can be mapped readily to an actual landscape, using a DEM. As an example, Figure 6.27A shows locations of modeled forests with a mesophytic composition. The green zones show grid cells with topographic index exceeding 6.5, for which modeling results indicate species composition would include hemlock, yellow-poplar, sugar maple, northern red oak, beech, and other mesophytic and semi-mesophytic species (Figures 6.17 – 6.19, 6.24-6.25). The magenta zones in Figure 6.27B indicates locations of mesophytic forests that may be exposed to periodic heavy ice storm disturbance. Specifically, these are steeply sloping sites (at least 15°) with a southerly to northeasterly exposure (aspect between 45° and 180°). High tree species richness is likely in parts of the landscape identified in this map.

FIA plots

Graphs in Figure 6.28 indicate species distributions along a gradient of increasing Site Index (SI). Due to small sample size, all plots with SI ≥ 80 were assigned a value of 90, the approximate median value. Additionally, there were only three plots with SI = 30, but these were graphed separately nonetheless. The most significant patterns evident from these graphs include predominance of southern pines in the least productive sites, dominance of chestnut oak over a broad portion of the gradient, and increasing importance of yellow-poplar toward productive stands. Mean richness increases with increasing productivity and exhibits similar levels in both exposed and sheltered stands.

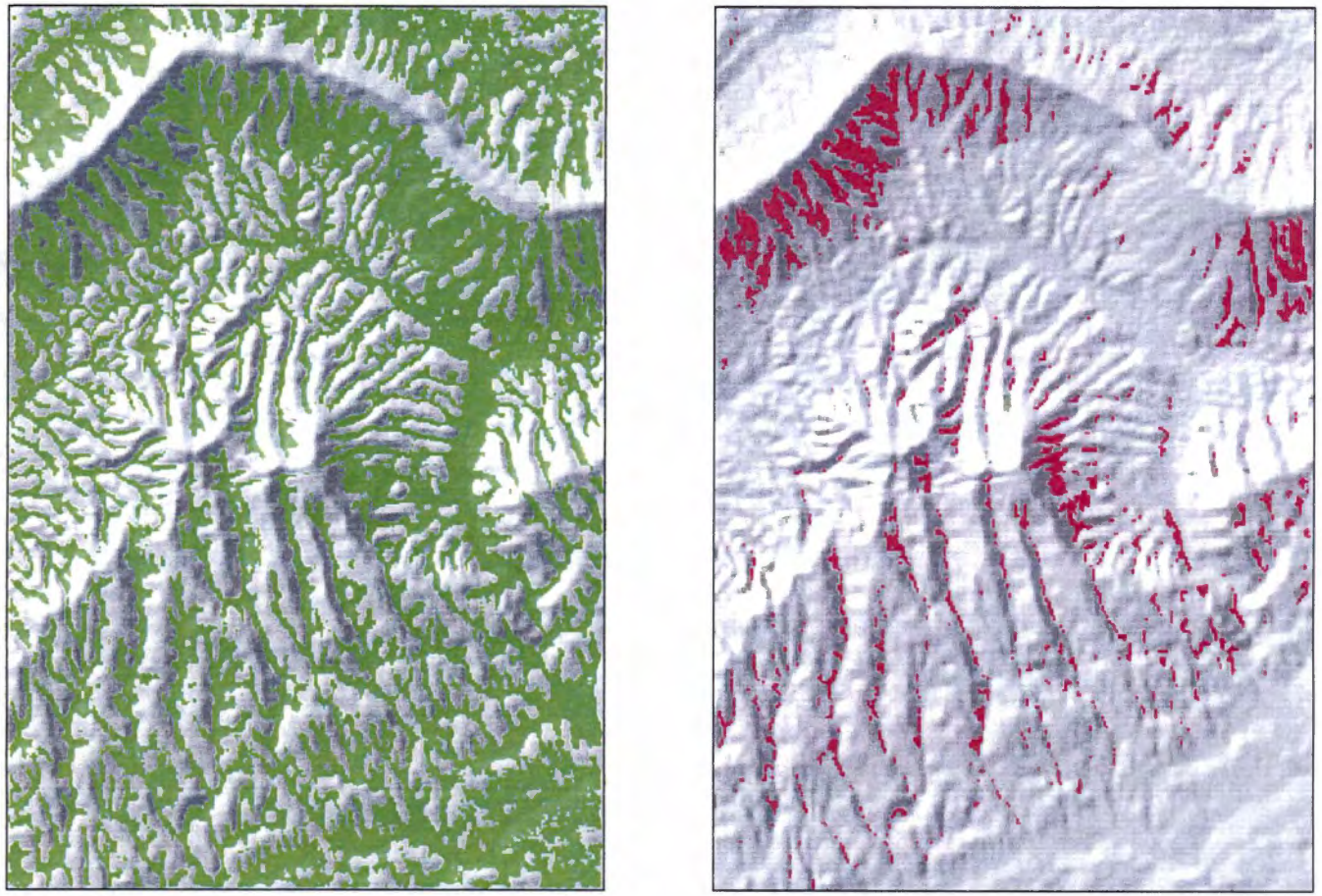

Figure 6.27. Spatial distribution of modeled forest characteristics. (A) predicted locations of mesophytic forests; (B) predicted locations of mesophytic forests exposed to periodic heavy ice storm disturbance. These maps depict the same landscape shown in Figure 6.10.

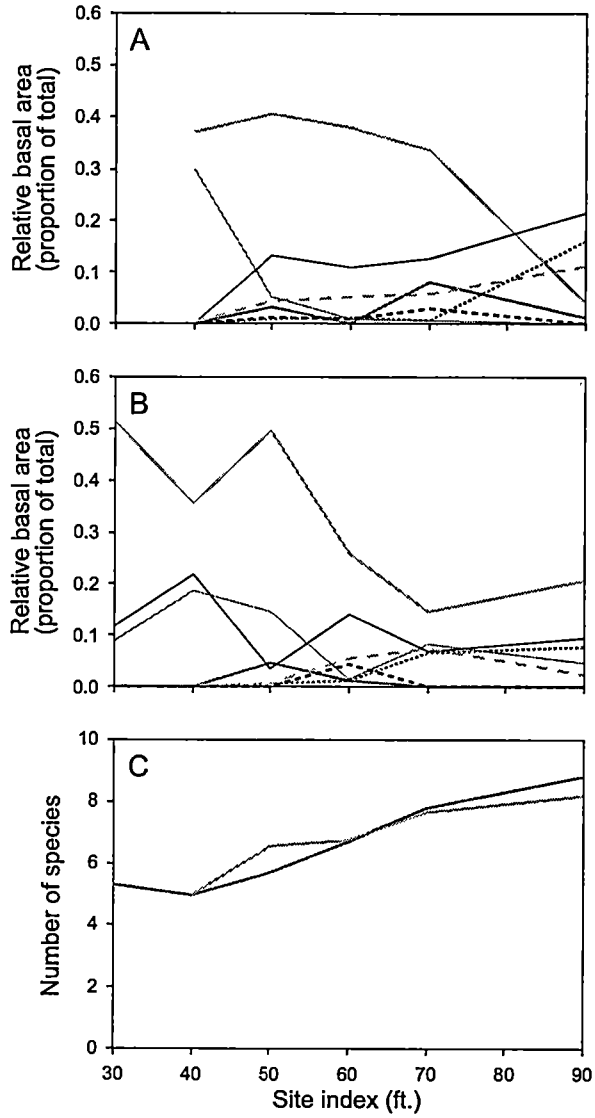

Species symbols:

- *Acer saccharum*
- *Carya* spp.
- *Liriodendron tulipifera*
- *Pinus* spp. (southern pines)
- *Quercus prinus*
- *Quercus rubra*
- *Tsuga canadensis*

Richness symbols:

- Richness on sites considered to be sheltered from heavy ice accumulation
- Richness on sites considered to be exposed to heavy ice accumulation

Figure 6.28 . Patterns of species composition and richness for Forest Inventory and Analysis (FIA) plots arranged along a gradient of site index. Site index is shown in units of feet, as recorded by the U.S. Forest Service. The plots are located in stands approximately 100 years old (75 - 100 years old). (A) composition of stands considered to be exposed to heavy ice storm damage, (B) composition of stands considered to be sheltered from heavy ice storm damage, and (C) species richness.

Discussion

General patterns of succession and zonation – without-ice simulations

The modeling approach employed here produced temporal and spatial patterns in forest composition and diversity that are typical for the southern Appalachians and consistent with predictions of the dynamic equilibrium model (Huston 1979, 1994). Simulated temporal dynamics include minimal successional change on dry ridgetop sites, black locust dominance in early succession followed by rapid mid-successional locust decline and oak dominance over sub-xeric to sub-mesic sites, and succession of yellow-poplar to hemlock or sugar maple dominance in mesic locations. These patterns are common on Appalachian landscapes (Whittaker 1956; Crownover 1983; Clebsch and Busing 1989).

Species richness rises rapidly in early succession at all sites and then levels off or declines. Field studies of secondary forest succession in the eastern United States demonstrate similar patterns of increasing richness in early succession followed by gradual decline as shade-intolerant species are eliminated (Hibbs 1983; Sakai and Sulak 1985; Clebsch and Busing 1989). Model results suggest that fine-scale gap dynamics may be sufficient to maintain moderate richness levels in actual stands.

An examination of simulated successional trends underscores the pervasive influence of anthropogenic disturbance in southern Appalachian forests. For example, modeling results suggest that the nearly pure stands of yellow-poplar that often characterize early succession in mesic sites (Clebsch and Busing 1989; Beck 1990; Busing 1995) are largely a product of human land clearing (Figures 6.17 – 6.19). This shade-intolerant species is not typically dominant in older forests. Likewise, white pine and black locust are especially common in early-successional forests developing on formerly cleared land (Figures 6.16 and 6.22; Clebsch and Busing 1989; Huntley 1990; Wendel and Smith 1990).

Predicted spatial patterns along the moisture gradient include pine dominance on xeric ridgetops, oak stands over a broad range of sub-xeric to sub-mesic sites, yellow-poplar/hemlock on lower slopes, and yellow-poplar/sugar maple in valley bottoms (Figure 6.26). In the oak zone, the peak in chestnut oak dominance occurs at more xeric sites than that for northern red oak. These patterns reflect quite accurately the typical compositional variations across Appalachian landscapes (Whittaker 1956; Hack and Goodlett 1960; Stephenson 1974; Clebsch and Busing 1989; Figure 6.28; this dissertation Chapter 3). Succession to white pine on unburned xeric sites is also typical (Harrod *et al.* 1998). Variations from commonly observed patterns in the region include a virtual absence of sweet birch (*Betula lenta*), yellow birch (*Betula alleghaniensis*), and basswood (*Tilia*) from mesic sites. The extremely high basal area of yellow-poplar at the most mesic sites (Figures 6.18, 6.19, 6.24) is probably unrealistic. In addition, yellow-poplar is much more abundant on the modeled mesic ravine slope than in the actual ravine site discussed in Chapter 3 of this dissertation (Table 3.4). This discrepancy may reflect a need for better parameterization of yellow-poplar in the model or the possibility that heavy browsing by herbivores such as white-tailed deer (*Odocoileus virginianus*) has reduced yellow-poplar seedling levels severely in the actual ravine site. It is also likely that my field study site is not as mesic as the modeled one. Indeed, my field results are similar to simulation results for the slightly less mesic north-facing lower slope (Figure 6.18), particularly when ice storm disturbance is simulated. The northern red oak-hemlock dominance and presence of chestnut oak, yellow-poplar, and cucumber magnolia resemble the composition of the stand I sampled (this dissertation Chapter 3, Table 3.4).

These simulated spatial patterns indicate that vegetation zonation similar to that predicted by Smith and Huston (1989) for hypothetical species constrained by adaptations to drought and shade can be reproduced for actual species. Consistency between modeled and actual distributions along the moisture gradient suggest that the proposed tradeoffs in growth-rate,

shade-tolerance, and drought-tolerance exert major control over patterns of species distribution on the landscape. Increased zonation in older forests (Figure 6.26B) also agrees with predictions of Smith and Huston. In addition, the attainment of realistic compositional patterns without the use of a parabolic growing degree day function supports the hypothesis that cold-adapted species are excluded from warmer climates by their slow growth rates and their inability to compete successfully with more rapidly growing species of warmer climates (Loehle 1998).

Spatial patterns in species composition are associated with variations in species richness. The unimodal relationship of richness to moisture availability in 100-year old forests (Figure 6.26E) matches observed patterns of plant species richness along moisture gradients (Dix and Smeins 1967; Kutiel and Danin 1987) and agrees with the predicted consequences of intense competition in productive stands and slow growth rates in unproductive sites (Huston 1979). Declining species richness along the moisture gradient at older sites also agrees with the dynamic equilibrium model, which predicts that low competition in unproductive stands leads to high diversity levels, given sufficient time for a number of species to become established and grow to larger sizes.

Predicted influences of ice storm disturbance

The predicted influence of ice storms is least pronounced at xeric sites, where the species present are drought-resistant and relatively intolerant to shade. The most important effect of ice storms in some xeric sites (but not the most extremely xeric) may be the conversion of pine stands to greater oak dominance (Figure 6.13B), as suggested by Williams (1998). This effect would probably be more pronounced if the model included the ericaceous shrubs *Kalmia* and *Vaccinium*, which often form relatively dense understory cover on xeric sites and may compete with pine seedlings for light. Conversely, ice storms appear to favor modest levels of pine regeneration in sub-xeric sites, contributing to broader distributions for the species even if their dominance is reduced by ice storms. Ice storms appear to contribute to greater importance of

oaks, particularly chestnut oak and northern red oak, over broad portions of the landscape (Figure 6.26C, D *versus* 26A, B). These results suggest that ice storms may be important components of disturbance regimes in some upland oak forests, for which disturbance dynamics are poorly understood (Lorimer 1980; Runkle 1990). Generally, ice storm disturbance appears to have its most significant consequences in mesic sites, where the dominance of shade-tolerant species is reduced, permitting the maintenance of shade-intolerant trees that would otherwise be excluded. Some of the shade-intolerant species typical of these sites, such as yellow-poplar, require relatively large gaps to maintain a presence in old-growth stands (Runkle 1990; Busing 1995). Ice storms provide large, multiple-tree gaps, particularly on steep sites (e.g., ravine slopes) where toppling and stem-breakage are common.

By disrupting competitive relationships, ice storms contribute to increased species richness in old-growth forests (Figure 6.26). Increased richness in mesic sites is consistent with predictions of the dynamic equilibrium model. According to the model, higher disturbance levels are required to maintain diversity in productive stands than in less productive ones. Although richness declines toward mesic sites, even in ice-damaged stands, the decline is more gradual than in undisturbed forests (Figure 6.26F). Prior to major anthropogenic disturbance, ice storms and other large canopy disturbances (e.g., hurricanes) were probably important for the maintenance of several shade-intolerant species, such as black locust and yellow-poplar, on Appalachian landscapes. These events will undoubtedly have an important role in the dynamics of maturing forest vegetation of wilderness areas and national parks, where anthropogenic disturbances are restricted. An important contrast to the tendency for ice storms to increase species richness is that lower diversity results when ice storms are simulated on the most xeric sites (Figure 6.12 D), reflecting the inability of some species to recover between successive disturbances in these less productive stands (Huston 1979).

Zonation is also reduced in old-growth forests (Figure 6.26D), particularly over middle portions of the gradient, a result that agrees with the dynamic equilibrium model. Hemlock dominance is dramatically lower in disturbed stands, permitting greater importance of oaks and pignut hickory toward the mesic end of the gradient. The zone of chestnut oak is not affected as severely as the hemlock zone, relative to undisturbed stands, indicating that the same disturbance regime can produce differing influences along the gradient. Both chestnut oak and hemlock are relatively resistant to ice storm damage, but the slow-growing, shade-tolerant hemlock occupies a mesic zone where several faster-growing species recover rapidly following disturbance. The result is more equitable abundance levels among species and the maintenance of higher species richness. Chestnut oak dominates in a more xeric zone where interspecific differences in growth rates are less pronounced.

Implications of ice storms for landscape-scale forest patterns

Modeling results indicate that in sections of the Appalachians where ice storms are a dominant element of the disturbance regime, highest species richness may occur on mesic, east-facing ravine slopes (Figure 6.24D). These sites provide adequate resources for growth of numerous species, and their steep slopes contribute to large patches of severe damage. Adjacent valley sites are characterized by much lower diversity, a consequence of both high moisture levels and lower levels of ice storm disturbance. Even if ice storms affect valleys as frequently as slopes, their effects on vegetation are less severe because forests on gentle slopes are not as prone to severe toppling and stem breakage. Relatively xeric upper slope sites are also predicted to have some of the most diverse forests on the landscape, a result of less intense competition at these unproductive sites.

Fine-scale topographic patchiness in ice storm disturbance may contribute to high *beta* diversity (Whittaker 1975) between those patches exposed to repeated heavy disturbance and those where ice storm disturbance rarely occurs. According to model predictions, especially

pronounced compositional differences are expected between ice-prone and sheltered sites near the mesic end of the moisture gradient (Figures 6.17; 6.18; 6.26B, D). A periodically disturbed forest on a mesic southeast-facing site may consist of a diverse oak-hemlock-hickory assemblage. A nearby stand growing on a site with a similar moisture regime but that is sheltered from frequent ice storm disturbance may be characterized by strong hemlock dominance. Thus, ice storms may be partly responsible for such classic vegetation patterns as north-slope *versus* south-slope compositional differences that are usually attributed to differences in moisture regimes.

Modeling results suggest that differences between sites characterized by differing ice storm climatologies may become more conspicuous as stands mature (Figure 6.26). The 100 year old stands exhibit less differences in zonation and richness patterns between the no-ice and with-ice scenarios than do the 400 year old stands.

Conclusions

This research indicates that individual-based forest succession models can simulate temporal and spatial patterns of forest composition and diversity that generally agree with observed patterns. This modeling approach also yields predictions that are consistent with theories of vegetation dynamics. Further, the specific model used here, FORICE, shows promise for contributing to a better understanding of the role of major ice storms as forest disturbances. FORICE results suggest that ice storm damage functions as an intermediate-level disturbance that promotes increased diversity over most of the moisture gradient. However, the effects of ice storm disturbance vary among sites. One reason for this variability is that physical damage levels are greater on steep slopes than on more gentle slopes and among some species than others. Another reason is that different levels of forest productivity result in variations in recovery rates among stands, a premise of the dynamic equilibrium model of Huston (1979). On the most xeric sites, ice storm damage may be too severe to be classified as an "intermediate" disturbance, whereas on the mesic valley sites a heavier level of damage would be needed to boost species

richness to high levels. High species richness resulting from especially severe damage on steep ravine slopes reflects the higher magnitude of disturbance necessary to produce "intermediate-level" damage in productive stands.

A number of problems exist in the functioning of the model, and these need to be addressed in order to provide a better research tool. The most important need is for more adequate information on the parameters of each species. Different handling of sprout growth, as opposed to seedling growth, is another need. Sprouts should grow more rapidly than seedlings. Regeneration by sprouting is especially important in Appalachian hardwood forests, and incorporating differential growth rates into the model could lead to better evaluations of the ecological roles of ice storms and other damaging agents. Adding understory herbs and shrubs, such as *Rubus*, *Kalmia*, and *Vaccinium*, as well as a full complement of native tree species would simulate more realistic conditions. Field observations indicate that heavy understory growth stimulated by canopy disturbance may have important consequences for forest dynamics, particularly in mesic sites where the abundance of shade-intolerant species may be reduced considerably by ground-level shading. Additional data on recovery of canopy biomass and diameter increment would permit a more accurate assessment of the influence of ice storms. Finally, enhanced understanding of climatological patterns at several spatial scales, particularly between topographic positions, would be useful for simulating moisture and temperature levels across a complex landscape. Better knowledge of variations in ice storm climatology at these same spatial scales is also necessary for further advances in modeling the effects of this type of disturbance. Ecosystem modeling, combined with field study and climate modeling, sheds light on the role of major natural disturbances. Modeling also provides a means to evaluate forest responses to climatic change under regimes of increasing or decreasing disturbance frequencies.

Chapter 7

Conclusions

This study illuminates patterns and consequences of major freezing rain events in forested landscapes of the Appalachian Mountains. Relatively little previous work has been conducted to understand the role of ice storms in disturbance regimes of eastern North American forests, despite their significant ecological and economic effects. To characterize their role adequately requires a consideration of patterns and processes that occur at widely contrasting spatial scales. For example, the nature and consequences of ice storm disturbance are affected by damage characteristics and physiology of individual plants, topographic variations in soil moisture availability and ice accumulation, and atmospheric processes operating at synoptic and even global scales. A variety of techniques are necessary for understanding ice storms and their influences on vegetation. In this study, field damage sampling, analysis of meteorological data, interpretation of historic storm records, tree-ring analysis, and computer simulations of forest dynamics were all employed to gain insights into the role of ice storms. Results of the various analyses shed new light on a major component of natural disturbance regimes in the Appalachians and demonstrate the potential utility of these methods for further research on ice storms and other types of disturbance.

The work reported here, combined with other research on ice storms, suggests that patterns of ice storm disturbance and the responses of forests to these disturbances are predictable over several spatial scales. At a global scale, ice storms are primarily a phenomenon of eastern North America. Within this region, the northeastern and midwestern United States appears to be affected most frequently. Sections of the Appalachians and Piedmont affected by cold air damming also experience frequent ice storms. Available data suggest that within a given landscape in the Appalachians, east-facing slopes are most prone to heavy ice accumulation. This topographic pattern could result from several processes enhancing ice accumulation on windward

slopes. Ice storm disturbance is typically confined to a relatively narrow elevation range but may occur within that range across a region hundreds of square kilometers in area. Higher elevations may be affected more frequently than lower slopes and valleys. Dendrochronological results and historic storm data imply that southeast-facing slopes in parts of southwestern Virginia have been affected by two to four major ice storms over the last century.

Slope angle influences the level of disturbance occurring within a forested landscape. Trees growing on steep slopes are more likely to be toppled than those on gentler slopes. High toppling rates on steep sites contribute to large, multiple-tree gaps, because falling trees strike neighbors and trigger additional damage. Soil depth may also influence disturbance patterns, with trees on thin soils more prone to toppling than those rooted in deeper soils.

Tree species vary in their susceptibility to ice storm damage. Some species possess attributes that make them particularly vulnerable to canopy damage. For example, the weak wood and straight boles of yellow-poplar trees make limb breakage likely. Conversely, the strong limbs of some oaks, hickories, and black locust increase their resistance to breakage but make them more vulnerable to uprooting during a major ice storm. Other characteristics of individual trees also influence susceptibility to certain types of damage. Tree size, in particular, exerts a strong influence on damage characteristics. Small trees are typically bent or broken, whereas larger trees often sustain canopy damage. Toppling is most common among medium-sized individuals.

Modeling results suggest that ice storms have several consequences for tree species composition and richness in forested landscapes of the southern Appalachians. In the most xeric sites, ice storm damage is effectively a more severe disturbance than in mesic sites, because low forest productivity impedes recovery between ice storms. Repeated ice storm disturbance in xeric sites may reduce species richness relative to richness in similar, but less ice-prone, sites. Over a broad sub-xeric to sub-mesic zone, ice storms appear to contribute to slightly higher species

richness and to favor oak dominance. This result may indicate a particularly important role for ice storm disturbance in oak-forest dynamics. Forest sampling reported in Chapter 3 confirms that oak regeneration in ice-damaged stands is generally more widespread than that for any other species. On mesic sites, where shade-tolerant species typically dominate old-growth forests, ice storm disturbance may enhance species richness substantially by permitting the maintenance of shade-intolerant species like yellow-poplar. My results suggest that this effect is especially important on steep, east-facing ravine slopes, where mesic conditions prevail and where ice storm damage is most severe. Ice storm frequency and magnitude are probably too low to enhance species richness considerably in highly productive valley-bottom stands.

Ice storm disturbance appears similar to hurricane disturbance in intensity and scale. Both types of events cause disturbances intermediate in intensity between single-tree mortality and the complete canopy removal associated with tornadoes, downbursts, catastrophic geomorphic events, or severe fires. Ice storms and hurricanes typically affect broader areas of the landscape and occur much more frequently than some of the more catastrophic events. However, whereas hurricanes create discrete canopy gaps with some trees remaining inside (Greenberg and McNab 1998), ice storm disturbance is better characterized as variable thinning of large patches of forest. Effects of these two disturbance agents on forest composition and diversity may be similar. However, oaks are among the species most resistant to ice damage but are most vulnerable to hurricane damage (Greenberg and McNab 1998). If not followed by abundant oak regeneration, hurricanes may be less favorable than ice storms for oak dominance.

Spatial patterns of ice storm and hurricane disturbance exhibit some similarities. Both appear to occur more commonly in eastern parts of the Appalachian region, a consequence of cold air damming for ice storm climatology and of proximity to the Atlantic coast for hurricane climatology. They also commonly affect similar topographic positions (southeast-facing slopes). However, each also disturbs forests sheltered from the other. In southwestern Virginia, for

example, Hurricane Hugo and the 1994 ice storms disturbed forests on the broad southeast-facing sides of major ridges. However, little or no hurricane damage is evident on the east-facing slopes of spurs and ravines, where heavy ice damage occurred.

Some disturbance patterns associated with fire may also be similar to those of ice storms. For example, both types of disturbance cause less damage to oaks than other species and appear to favor oak regeneration and dominance. However, fires differ in that they often cause heavier understory loss than canopy disturbance. Spatial patterns of fire and ice storm frequency may have some similarities, particularly in the Blue Ridge of North Carolina, where both types of disturbances occur relatively frequently. Major geomorphic disturbances are more catastrophic than ice storm disturbances but affect smaller areas. At broad spatial scales, zones of high ice storm and flood/debris slide frequency overlap. Both occur most frequently in the Blue Ridge and parts of the Ridge and Valley, and both cause more severe forest damage in steeply sloping terrain. At finer scales, the two types of disturbance may typically affect different parts of the landscape (e.g., floodplains *versus* slopes).

Likewise, beavers disturb only valley floor and adjacent lower slope forests, stands where ice storm damage is apt to be less severe relative to that occurring on nearby mountain slopes. Spatial patterns of insect and pathogen occurrence probably reflect those of ice storms and other disturbances. Tree injury renders the trees less resistant to insect or fungal attack.

Based on the current state of knowledge, it is reasonable to conjecture that disturbance frequencies and intensities are much higher in some parts of the Appalachian region than in other sections. The Blue Ridge and some sections of the Valley and Ridge appear to have particularly high disturbance rates. Ice storms, hurricanes, floods, debris slides and possibly fires all reach their maximum frequencies in this area (this dissertation Chapter 1). East-to-west vegetation differences probably reflect variations in disturbance frequency and magnitude across the region. For example, the more widespread oak dominance over the Blue Ridge and Valley and Ridge

than in the Appalachian Plateaus (Braun 1950) may result in part from differences in disturbance regimes.

Intermediate-intensity disturbances (i.e., ice storms and hurricanes) appear to occur quite frequently in eastern parts of the Appalachian region. In fact, these events probably occur frequently enough to function as the primary agents of disturbance in parts of the Blue Ridge and Valley and Ridge, particularly on steep southeast-facing slopes. More catastrophic events may occur too infrequently to have major influences on vegetation dynamics, and frequent small gap creation may not be intense enough to produce significant changes during the intervals between ice or hurricane damage. Determining the relative importance of ice storms *versus* hurricanes would require a study of the long-term climatology of these events. Ice storms are probably more significant in stands growing on sites sheltered from hurricane winds. Such sites include east-facing ravine slopes and east-facing slopes of spurs that are not located near the top of a major ridge.

Feedbacks among the various disturbances probably amplify the effects of individual disturbance events. For example, ice storm damage increases the likelihood of insect or disease outbreaks, which in turn increase susceptibility to damage from subsequent ice storms or windstorms. All these disturbances contribute to heavier fuel loads, enhancing the likelihood of severe fire.

Much additional work will be necessary to provide a thorough understanding of ice storms and their ecological consequences. Ice storm climatology remains largely unexplored in a quantitative manner, particularly at fine spatial scales. Landscape climatological modeling using a physiographic approach similar to that used by Orvis (1992) to predict patterns of convective precipitation in Arizona may help resolve topographic variations in ice storm climatology in the Appalachians. The dendrochronological results reported in this dissertation indicate that further

tree-ring analyses using additional species from more sites could provide a longer record of fine-scale patterns than any other available source.

Difficulties encountered in attempting to decipher fine-scale variations in ice storm climatology underscore a need for more detailed data collection over a dense network of weather stations. This need is particularly acute in the topographically diverse Appalachian region, where meteorological records from a few first-order weather stations located in valleys may not adequately represent conditions at higher elevations. A need also exists for research to assess the likelihood that changes in ice storm frequency may result from alterations in global climate.

Additional field sampling in damaged stands would be helpful for interpreting patterns of damage within stands. Although several field studies, including mine, have been conducted to quantify and characterize forest damage resulting from major ice storms, additional data would permit refinement of the multivariate approach I have employed to predict damage probabilities. Ice storm damage resulting from storms that occurred in the Northeast, Virginia, and the Great Smoky Mountains during 1998 is still reasonably fresh and provides good opportunities for additional study. Incorporating results of more field sampling would enhance the ability of FORICE to simulate the disturbance patterns unique to ice storms. Including better simulations of other types of disturbances and ecological processes, such as fire, hurricanes, human land-use imprints, and topographic variations in precipitation and soil moisture, would also enhance the utility of FORICE. Finally, field sampling of vegetation in stands with known ice storm histories is needed to evaluate predictions of FORICE and of the dynamic equilibrium model (Huston 1979).

References

Abell, C.A. 1934. Influence of glaze storms upon hardwood forests in the southern Appalachians. *Journal of Forestry* 32:35 – 37.

Abrams, M.D. 1992. Fire and the development of oak forests. *BioScience* 42:346 – 353.

Agrawal, A. and Stephenson, S.L. 1995. Recent successional changes in a former chestnut-dominated forest in southwestern Virginia. *Castanea* 60:107 – 113.

Ahrens, C.D. 1991. *Meteorology Today: An Introduction to Weather, Climate, and the Environment.* 4th edition. West, St. Paul, Minnesota.

Anthes, R.A. 1976. Variations in temperatures and freezing conditions between mountaintops and valleys in central Pennsylvania. *Weatherwise* 29:178 – 183.

Arno, S.F. 1976. *The Historical Role of Fire on the Bitterroot National Forest.* USDA Forest Service, Research Paper INT-187. Intermountain Forest and Range Experiment Station, Ogden, Utah.

Ashe, W.W. 1918. Note on the preceding. *Monthly Weather Review* 46:374.

Baisan, C.H. and Swetnam, T.W. 1990. Fire history on a desert mountain range: Rincon Mountain Wilderness, Arizona, U.S.A. *Canadian Journal of Forest Research* 20:1559 – 1569.

Baker, F.S. 1949. A revised tolerance table. *Journal of Forestry* 47:179 – 181.

Barden, L.S. 1980. Tree replacement in a cove hardwood forest of the southern Appalachians. *Oikos* 35:16 – 19.

Barden, L.S. and Woods, F.W. 1974. Characteristics of lightning fires in southern Appalachian forests. *Proceedings Annual Tall Timbers Fire Ecology Conference* 13:345 – 361.

Barnes, W.J. and Dibble, E. 1988. The effects of beaver in riverbank forest succession. *Canadian Journal of Botany* 66:40 – 44.

Barros, A.P. and Kuligowski, R.J. 1998. Orographic effects during a severe wintertime rainstorm in the Appalachian Mountains. *Monthly Weather Review* 126:2648 – 2672.

Beck, D.E. 1990. *Liriodendron tulipifera* L.: yellow-poplar. Pages 406 – 416 in Burns, R.M. and Honkala, R.M., tech. coords. *Silvics of North America.* USDA Handbook 654, Vol. 2. Washington, DC.

Belanger, R.P., Godbee, J.F., Anderson, R.L., and Paul, J.T. 1996. Ice damage in thinned and nonthinned loblolly pine plantations infested with fusiform rust. *Southern Journal of Applied Forestry* 20:136 – 142.

Bell, G.D. and Bosart, L.F. 1988. Appalachian cold-air damming. *Monthly Weather Review* 116:137 – 161.

Bennett, I. 1959. *Glaze: Its Meteorology and Climatology, Geographical Distribution, and Economic Effects.* U.S. Army, Quartermaster Research and Engineering Command, Natick, Massachusetts. Technical Report EP-105.

Beven, K.J. and Kirkby, M.J. 1979. A physically-based variable contributing area model of basin hydrology. *Hydrological Science Bulletin* 24:43 – 69.

Blum, B.M. 1966. Snow damage in young northern hardwoods. *Journal of Forestry* 64:16 – 18.

Boerner, R E.J., Runge, S.D., and Cho, D. 1986. Localized ice storm damage in an Appalachian Plateau watershed. *American Midland Naturalist* 119:199 – 208.

Botkin, D.B. 1993. *Forest Dynamics: An Ecological Model.* Oxford University Press, Oxford.

Botkin, D.B., Janak, J.F., and Wallis, J.R. 1972. Some ecological consequences of a computer model of forest growth. *Journal of Ecology* 60:849 – 872.

Bratton, S.P. and Meier, A.J. 1998. The recent vegetation disturbance history of the Chattooga River watershed. *Castanea* 63:372 – 381.

Braun, E.L. 1950. *Deciduous Forests of Eastern North America.* The Blakiston Company, Philadelphia.

Brinkman, W.A.R., Baumann, D.D., Beck, E.M., Krane, S.W., Murphy, A.H., Sims, J.H., and Visvader, H.J. 1975a. *Severe Local Storm Hazard in the United States: A Research Assessment.* Institute of Behavioral Science, The University of Colorado, Boulder.

Brinkman, W.A.R., Huszar, P.C., Baker, E.J., Baumann, D.D., and Sims, J.H. 1975b. *Hurricane Hazard in the United States: A Research Assessment.* Institute of Behavioral Science, The University of Colorado, Boulder.

Brokaw, N.V.L. and Walker, L.R. 1991. Summary of the effects of Caribbean hurricanes on vegetation. *Biotropica* 23:442 – 447.

Bruederle, L.P. and Stearns, F.W. 1985. Ice storm damage to a southern Wisconsin mesic forest. *Bulletin of the Torrey Botanical Club* 112:167 – 175.

Buell, M.F., Buell, H.F., Small, J.A. 1954. Fire in the history of Mettler's Woods. *Bulletin of the Torrey Botanical Club* 81:253 – 255.

Burns, R.M. and Honkala, R.M., tech. coords. 1990. *Silvics of North America.* USDA Handbook 654, Washington, DC.

Busing, R.T. 1991. A spatial model of forest dynamics. *Vegetatio* 92:167 – 179.

Busing, R.T. 1995. Disturbance and the population dynamics of *Liriodendron tulipifera*: simulations with a spatial model of forest succession. *Journal of Ecology* 83:45 – 53.

Canham, C.D. and Loucks, O.L. 1984. Catastrophic windthrow in the presettlement forests of Wisconsin. *Ecology* 65:803 – 809.

Carvell, K.L., Tryon, E.H., and True, R.P. 1957. Effects of glaze on the development of Appalachian hardwoods. *Journal of Forestry* 55:130 – 132.

Clark, G.M. 1987. Debris slide and debris flow historical events in the Appalachians south of the glacial border. Pages 125 – 138 in Costa, J.E. and Wieczorek, G.F., eds. *Reviews in Engineering Geology*, vol. 7. Geological Society of America, Boulder, Colorado.

Clark, G.M., Ryan, P.T., Jr., and Drumm, E.C. 1987. Debris slides and debris flows on Anakeesta Ridge, Great Smoky Mountains National Park, Tennessee. Pages 18 – 19 in Schultz, A.P. and Southworth, C.S., eds. *Landslides of Eastern North America*. U.S. Geological Survey Circular 1008. U.S. Government Printing Office, Washington, DC.

Clebsch, E.E.C. and Busing, R.T. 1989. Secondary succession, gap dynamics, and community structure in a southern Appalachian cove forest. *Ecology* 70:728 – 735.

Colbert, J.J. and Sheehan, K.A. 1995. *Description of the Stand-Damage Model: Part of the Gypsy Moth Life System Model*. USDA Forest Service, General Technical Report NE-208. Radnor, Pennsylvania.

Connell, J.H. 1978. Diversity in tropical rainforests and coral reefs. *Science* 199:1302 – 1310.

Cook, E.R. and Holmes, R.L. 1986. User's manual for program ARSTAN. Pages 50 – 56 in Holmes, R.L., Adams, R.K., and Fritts, H.C., eds. *Tree-Ring Chronologies of Western North America: California, Eastern Oregon, and Northern Great Basin*. Chronology Series 6. Laboratory of Tree-Ring Research, University of Arizona, Tucson.

Cremeans, D.W. and Kalisz, P.J. 1988. Distribution and characteristics of windthrow microtopography on the Cumberland Plateau of Kentucky. *Soil Science Society of America Journal* 52:816 – 821.

Croker, T.C. 1958. Soil depth affects wind-firmness of longleaf pine. *Journal of Forestry* 56:432.

Crownover, R.N.S. 1983. *Forest Communities of House Mountain, Knox County, Tennessee and Their Relationships to Site and Soil Factors*. M.S. Thesis, University of Tennessee, Knoxville.

Daniel, T.W., Helms, J.A., and Baker, F.S. 1979. *Principles of Silviculture*. 2nd ed. McGraw-Hill Book Company, New York.

Delcourt, P.A. and Delcourt, H.R. 1998. The influence of prehistoric human-set fires on oak-chestnut forests in the southern Appalachians. *Castanea* 63:337 – 345.

Delcourt, P.A., Delcourt, H.R., Cridlebaugh, P.A., and Chapman, J. 1986. Holocene ethnobotanical and paleoecological record of human impact on vegetation in the Little Tennessee River Valley, Tennessee. *Quaternary Research* 25:330 – 349.

DeSteven, D., Kline, J., and Matthiae, P.E. 1991. Long-term changes in a Wisconsin *Fagus-Acer* forest in relation to glaze storm damage. *Journal of Vegetation Science* 2:201 – 208.

Dix, R. and Smeins, F. 1967. The prairie, meadow, and marsh vegetation of Nelson County, North Dakota. *Canadian Journal of Botany* 45:21 – 58.

Downs, A.A. 1938. Glaze damage in the birch-beech-maple-hemlock type of Pennsylvania and New York. *Journal of Forestry* 36:63 – 70.

Doyle, T.W. 1981. The role of disturbance in the gap dynamics of a montane rain forest: and application of a tropical forest succession model. Pages 56 – 73 in West, D.C., Shugart, H.H., and Botkin, D.B., eds. *Forest Succession Concepts and Applications*. Springer-Verlag, New York.

Doyle, T.W. and Gorham, L.E. 1996. Detecting hurricane impact and recovery from tree rings. *Radiocarbon* 14:405 – 412.

Dunn, C.P., Guntenspergen, G.R., and Dorney, J.R. 1983. Catastrophic wind disturbance in an old-growth hemlock-hardwood forest, Wisconsin. *Canadian Journal of Botany* 61:211 – 217.

Dyer, K.W. 1983. *Community change two decades following a catastrophic ice storm in the Marshall Forest of Northwest Georgia*. M.S. Thesis, University of Tennessee, Knoxville.

Eagleman, J.R. 1983. *Severe and Unusual Weather*. Van Nostrand Reinhold Company, New York.

Elder, J.A., Bacon, S.R., Flowers, R.L., Love, T.R., Phillips, J.A., Thompson, G.M., and Tucker, D.A. 1959. *Soil Survey: Blount County, Tennessee*. USDA Soil Conservation Service, in cooperation with Tennessee Agricultural Experiment Station and Tennessee Valley Authority. US Government Printing Office, Washington, DC.

Eschner, A.R. and Patric, J.H. 1982. Debris avalanches in eastern upland forests. *Journal of Forestry* 80:343 – 347.

Felin, B. and Rivest, J. 1983. An application of dendrochronology to the determination of the recurrence of severe ice storms. Pages 217 – 224 in *Atmospheric Icing of Structures: Proceedings of First International Workshop: 1 – 3 June 1982, Hanover, NH*. US Army Corps of Engineers, Cold Regions Research and Engineering Laboratory, Hanover, New Hampshire. CRREL Special Report 83-17.

Fernald, M.L. 1950. *Gray's Manual of Botany*. 8th ed. American Book Company, New York.

Finnigan, J.J. and Brunet, Y. 1995. Turbulent airflow in forests on flat and hilly terrain. Pages 3 – 40 in Coutts, M.P. and Grace, J., eds. *Wind and Trees*. Cambridge University Press, Cambridge.

Fitter, A.H. and Hay, R.K.M. 1981. *Environmental Physiology of Plants*. Academic Press, London.

Flaccus, E. 1959. Revegetation of landslides in the White Mountains of New Hampshire. *Ecology* 40:692 – 703.

Forbes, G.S., Anthes, R.A., and Thomson, D.W. 1987. Synoptic and mesoscale aspects of an Appalachian ice storm associated with cold-air damming. *Monthly Weather Review* 115:564 – 591.

Foster, D.R, Zebryk, T., Schoonmaker, P., and Lezberg, A. 1992. Post-settlement history of human land-use and vegetation dynamics of a *Tsuga canadensis* (hemlock) woodlot in central New England, USA. *Journal of Ecology* 80:773 – 786.

Foster, D.R. 1988. Species and stand response to catastrophic wind in central New England, U.S.A. *Journal of Ecology* 76:135 – 151.

Foster, D.R. and Boose, E.R. 1995. Hurricane disturbance regimes in temperate and tropical forest ecosystems. Pages 305 – 339 in Coutts, M.P. and Grace, J., eds. *Wind and Trees.* Cambridge University Press, Cambridge.

Foster, D.R., Motzkin, G., and Slater, B. 1998. Land use history as a long-term broad-scale disturbance: regional forest dynamics in central New England. *Ecosystems* 1:96 – 119.

Fox, J.F. 1979. Intermediate disturbance hypothesis. *Science* 204:1344 – 1345.

Frelich, L.E. and Lorimer, C.G. 1985. Current and predicted long-term effects of deer browsing in hemlock forests in Michigan, USA. *Biological Conservation* 34:99 – 120.

Fritts, H.C. 1976. *Tree rings and climate.* Academic Press, London.

Fuller, J.L., Foster, D.R., McLachlan, J.S., and Drake, N. 1998. Impact of human activity on regional forest composition and dynamics in central New England. *Ecosystems* 1:76 – 95.

Gall, D.A. and Edmonds, W.J. 1992. *Soil Survey of Wythe County, Virginia.* USDA Soil Conservation Service, in cooperation with Virginia Polytechnic Institute and State University.

Garten, C.T., Huston, M.A., and Thoms, C.A. 1994. Topographic variation of soil nitrogen dynamics at Walker Branch Watershed, Tennessee. *Forest Science* 40:497 – 512.

Gay, D.A. and Davis, R.E. 1993. Freezing rain and sleet climatology of the southeastern USA. *Climate Research* 3:209 – 220.

Gleason, H.A. 1926. The individualistic concept of the plant association. *Bulletin of the Torrey Botanical Club* 53:7 – 26.

Glitzenstein, J.S. and Harcombe, P.A. 1988. Effects of the December 1983 tornado on forest vegetation of the Big Thicket, southeast Texas, U.S.A. *Forest Ecology and Management* 25:269 – 290.

Godman, R.M. and Lancaster, K. 1990. *Tsuga canadensis* (L.) Carr.: eastern hemlock. Pages 604 – 612 in Burns, R.M. and Honkala, R.M., tech. coords. *Silvics of North America.* USDA Handbook 654, Vol. 1. Washington, DC.

Graumlich, L.J. 1993. A 1000-year record of temperature and precipitation in the Sierra Nevada. *Quaternary Research* 39:249 – 255.

Greenberg, C.H. and McNab, W.H. 1998. Forest disturbance in hurricane-related downbursts in the Appalachian Mountains of North Carolina. *Forest Ecology and Management* 104:179 – 191.

Griffith, D.A. and Amrhein, C.G. 1991. *Statistical Analysis for Geographers*. Prentice-Hall, Englewood Cliffs, New Jersey.

Grissino-Mayer, H.D. and Butler, D.R. 1993. Effects of climate on growth of shortleaf pine (*Pinus echinata* Mill.) in northern Georgia: a dendroclimatic study. *Southeastern Geographer* 33:65 – 81.

Haack, R.A. and Byler, J.W. 1993. Insects and pathogens: regulators of forest ecosystems. *Journal of Forestry* 91(9):32 – 37.

Hack, J.T. and Goodlett, J.C. 1960. *Geomorphology and Forest Ecology of a Mountain Region in the Central Appalachians*. U.S. Geological Survey Professional Paper 347.

Hanley, T.A. and Taber, R.D. 1980. Selective plant species inhibition by elk and deer in three conifer communities in western Washington. *Forest Science* 26:97 – 107.

Harrod, J., White, P.S., and Harmon, M.E. 1998. Changes in xeric forests in western Great Smoky Mountains National Park, 1936 – 1995. *Castanea* 63:346 – 360.

Held, M.E. and Winstead, J.E. 1976. Structure and composition of a climax forest system in Boone County, Kentucky. *Transactions of the Kentucky Academy of Science* 37:57 – 67.

Held, M.E., Jones-Held, S., and Winstead, J.E. 1998. Forest community structure and tornado damage in an old-growth system in northern Kentucky. *Castanea* 63:474 – 481.

Hibbs, D.E. 1983. Forty years of forest succession in central New England. *Ecology* 64:1394 – 1401.

Holmes, R.L. 1986. Users manual for program COFECHA. Pages 41 – 49 in Holmes, R.L., Adams, R.K., and Fritts, H.C., eds. *Tree-Ring Chronologies of Western North America: California, Eastern Oregon, and Northern Great Basin*. Chronology Series 6. Laboratory of Tree-Ring Research, University of Arizona, Tucson.

Huffman, G.J. and Norman, G.A., Jr. 1988. The supercooled warm rain process and the specification of freezing precipitation. *Monthly Weather Review* 116:2172 – 2182.

Huntley, J.C. 1990. *Robinia pseudoacacia* L.: black locust. Pages 755 – 761 in Burns, R.M. and Honkala, R.M., tech. coords. *Silvics of North America*. USDA Handbook 654, Vol. 2. Washington, DC.

Huston, M.A. 1979. A general hypothesis of species diversity. *The American Naturalist* 113:81 – 101.

Huston, M.A. 1994. *Biological Diversity: The Coexistence of Species on Changing Landscapes.* Cambridge University Press, Cambridge.

Huston, M.A. and Smith, T.M. 1987. Plant succession: life history and competition. *American Naturalist* 130:168 – 198.

Jacobson, R.B., Miller, A.J., and Smith, J.A. 1989. The role of catastrophic geomorphic events in central Appalachian landscape evolution. *Geomorphology* 2:257 – 284.

Jenkins, M.A. and Pallardy, S.G. 1995. The influence of drought on red oak group species growth and mortality in the Missouri Ozarks. *Canadian Journal of Forest Research* 25:1119 – 1127.

Johnson, P.S. 1990. *Quercus coccinea* Muencch.: scarlet oak. Pages 625 – 630 in Burns, R.M. and Honkala, R.M., tech. coords. *Silvics of North America.* USDA Handbook 654, Vol. 2. Washington, DC.

Johnston, C.A. and Naiman, R.J. 1990. Browse selection by beaver: effects on riparian forest composition. *Canadian Journal of Forest Research* 20:1036 – 1043.

Johnston, R.J. 1980. *Multivariate Statistical Analysis in Geography: A Primer on the General Linear Model.* Longman Scientific and Technical, copublished with John Wiley and Sons, Inc., New York.

Jones, K.F., Muherin, N., and Ryerson, C.C. 1997. *EPRI Freezing Rain Ice Mapping Project: Region 2.* Cold Regions Research and Engineering Laboratory, Hanover, New Hampshire. CR-00020.

Keeter, K.K. and Kline, J.W. 1991. The objective use of observed and forecast thickness values to predict precipitation type in North Carolina. *Weather and Forecasting* 6:456 – 469.

Kelly, D.L., Schaefer, J.T., McNulty, R.P., and Doswell, C.A. III. 1978. An augmented tornado climatology. *Monthly Weather Review* 106:1172 – 1183.

Kochel, R.C. 1987. Holocene debris flows in central Virginia. Pages 139 – 155 in Costa, J.E. and Wieczorek, G.F., eds. *Reviews in Engineering Geology*, vol. 7. Geological Society of America, Boulder, Colorado.

Konrad, C.E. II. 1998. An empirical approach for delineating fine scaled spatial patterns of freezing rain in the Appalachian region of the USA. *Climate Research* 10:217 – 227.

Kutiel, P. and Danin, A. 1987. Annual-species diversity and aboveground phytomass in relation to some soil properties in the sand dunes of the northern Sharon Plains, Israel. *Vegetatio* 70:45 – 49.

Lafon, C.W. 1999. Spatial patterns of ice storm occurrence in the New River Valley. *New River Symposium Proceedings, April 15 – 16, 1999, Boone, North Carolina.* New River Gorge National River, Glen Jean, West Virginia. Pages 68 – 87.

Lafon, C.W., Graybeal, D.Y., and Orvis, K.H. 1999. Patterns of ice accumulation and forest disturbance during two ice storms in southwestern Virginia. *Physical Geography* 20:97 – 115.

Leathers, D.J. 1993. A synoptic climatology of northeastern United States tornadoes. *Physical Geography* 14:171 – 190.

Lemon, P.C. 1961. Forest ecology of ice storms. *Bulletin of the Torrey Botanical Club* 88:21 – 29.

Loehle, C. 1998. Height growth rate tradeoffs determine northern and southern range limits for trees. *Journal of Biogeography* 25:735 – 742.

Lorimer, C.G. 1980. Age structure and disturbance history of a southern Appalachian virgin forest. *Ecology* 61:1169 – 1184.

Lorimer, C.G. 1989. Relative effects of small and large disturbances on temperate hardwood forest structure. *Ecology* 70:565 – 567.

Lorimer, C.G. and Frelich, L.E. 1989. A methodology for estimating canopy disturbance frequency and intensity in dense temperate forests. *Canadian Journal of Forest Research* 19:651 – 663.

Lorimer, C.G. and Frelich, L.E. 1994. Natural disturbance regimes in old-growth northern hardwoods: implications for restoration efforts. *Journal of Forestry* 92:33 – 38.

Lott, J.N. and Sittel, M.C. 1994. *The February 1994 Ice Storm in the Southeastern U.S.* National Climatic Data Center (NCDC), Asheville, NC.

Lott, N., Graumann, A., and Ross, D. 1998. *Eastern U.S. Flooding and Ice Storm.* National Climatic Data Center (NCDC), Asheville, NC. Document from Web site at http://www.ncdc.noaa.gov.

Loucks, O. L. 1970. Evolution of diversity, efficiency, and community stability. *American Zoologist* 10:17 – 25.

Lovelady, C.N., Pulley, P.E., Coulson, R.N., and Flamm, R.O. 1991. Relation of lightning to herbivory by the southern pine bark beetle guild (Coleoptera: Scolytidae). *Environmental Entomology* 20:1279 – 1284.

McCormick, J.F. and Platt, R.B. 1980. Recovery of an Appalachian forest following the chestnut blight or Catherine Keever – you were right! *American Midland Naturalist* 104:264 – 273.

McGee, C.E. 1990. *Nyssa sylvatica* Marsh.: black tupelo. Pages 482 – 489 in Burns, R.M. and Honkala, R.M., tech. coords. *Silvics of North America.* USDA Handbook 654, Vol. 2. Washington, DC.

McKellar, A.D. 1942. Ice damage to slash pine, longleaf pine, and loblolly pine plantations in the Piedmont section of Georgia. *Journal of Forestry* 40:794 – 797.

McMartin, B. 1994. *The Great Forest of the Adirondacks*. North Country Books, Utica, New York.

McQuilkin, R.A. 1990. *Quercus prinus* L.: chestnut oak. Pages 721 – 726 in Burns, R.M. and Honkala, R.M., tech. coords. *Silvics of North America*. USDA Handbook 654, Vol. 2. Washington, DC.

Melancon, S. and Lechowicz, M.J. 1987. Differences in the damage caused by glaze ice on codominant *Acer saccharum* and *Fagus grandifolia*. *Canadian Journal of Botany* 65:1157 – 1159.

Merrens, E.J. and Peart, D.R. 1992. Effects of hurricane damage on individual growth and stand structure in a hardwood forest in New Hampshire, USA. *Journal of Ecology* 80:787 – 795.

Michaels, P.J. 1991. Bringing in the sleeze. *Virginia Climate Advisory, Winter 1991* 14(4):3 – 14.

Miller, J.H. 1990. *Ailanthus altissima* (Mill.) Swingle.: ailanthus. Pages 101 – 104 in Burns, R.M. and Honkala, R.M., tech. coords. *Silvics of North America*. USDA Handbook 654, Vol. 2. Washington, DC.

Mills, H.H. 1984. Effect of hillslope angle and substrate on tree tilt, and denudation of hillslopes by tree fall. *Physical Geography* 5:253 – 261.

Naiman, R.J., Johnston, C.A., and Kelley, J.C. 1988. Alteration of North American streams by beaver. *BioScience* 38:753 – 762.

Nash, T.H., III, Fritts, H.C., and Stokes, M.A. 1975. A technique for examining non-climatic variation in widths of annual tree rings with special reference to air pollution. *Tree-Ring Bulletin* 35:15 – 24.

National Climatic Data Center (NCDC). 1969. *Storm Data*, Vol. 11. U.S. Department of Commerce, National Oceanic and Atmospheric Administration, Asheville, North Carolina.

National Climatic Data Center (NCDC). 1978. *Storm Data*, Vol. 20. U.S. Department of Commerce, National Oceanic and Atmospheric Administration, Asheville, North Carolina.

National Climatic Data Center (NCDC). 1979a. *Climatological Data*, Vol. 84. U.S. Department of Commerce, National Oceanic and Atmospheric Administration, Asheville, North Carolina.

National Climatic Data Center (NCDC). 1979b. *Storm Data*, Vol. 21. U.S. Department of Commerce, National Oceanic and Atmospheric Administration, Asheville, North Carolina.

National Climatic Data Center (NCDC). 1979c. *Surface Airways Hourly TD-3280.* U.S. Department of Commerce, National Oceanic and Atmospheric Administration, Asheville, North Carolina.

National Climatic Data Center (NCDC). 1983. *Storm Data*, Vol. 25. U.S. Department of Commerce, National Oceanic and Atmospheric Administration, Asheville, North Carolina.

National Climatic Data Center (NCDC). 1991. *Surface Airways Hourly TD-3280.* U.S. Department of Commerce, National Oceanic and Atmospheric Administration, Asheville, North Carolina.

National Climatic Data Center (NCDC). 1994a. *Climatological Data*, Vol. 99. U.S. Department of Commerce, National Oceanic and Atmospheric Administration, Asheville, North Carolina.

National Climatic Data Center (NCDC). 1994b. *Hourly Precipitation Data TD-3240.* U.S. Department of Commerce, National Oceanic and Atmospheric Administration, Asheville, North Carolina.

National Climatic Data Center (NCDC). 1994c. *Storm Data and Unusual Weather Phenomena with Late Reports and Corrections*, Vol. 36. U.S. Department of Commerce, National Oceanic and Atmospheric Administration, Asheville, North Carolina.

National Climatic Data Center (NCDC). 1994d. *Surface Airways Hourly TD-3280.* U.S. Department of Commerce, National Oceanic and Atmospheric Administration, Asheville, North Carolina.

National Climatic Data Center (NCDC). 1995. *Cooperative Summary of the Day TD-3200 – Period of Record through 1993.* Vol. 18. U.S. Department of Commerce, National Oceanic and Atmospheric Administration, Asheville, North Carolina.

National Climatic Data Center (NCDC). 1998. *Unedited Local Climatological Data Hourly Observations*, December 1998, Knoxville, TN. Online data from Web site at http://www.ncdc.noaa.gov/.

National Climatic Data Center (NCDC). 1999. Data from NCDC website at http://www.ncdc.noaa.gov/.

National Oceanic and Atmospheric Administration (NOAA). 1979. *Daily Weather Maps: Weekly Series.* U.S. Department of Commerce, Washington, DC.

National Oceanic and Atmospheric Administration (NOAA). 1994. *Daily Weather Maps: Weekly Series.* U.S. Department of Commerce, Washington, DC.

National Oceanic and Atmospheric Administration-Cooperative Institute for Research in Environmental Sciences (NOAA-CIRES) Climate Diagnostics Center. 1998. Images from Web site at http://www.cdc.noaa.gov/.

Neff, D.J. 1957. Ecological effects of beaver habitat abandonment in the Colorado Rockies. *Journal of Wildlife Management* 21:80 – 84.

Nicholas, N.S. and Zedaker, S.M. 1989. Ice damage in spruce-fir forests of the Black Mountains, North Carolina. *Canadian Journal of Forest Research* 19:1487 – 1491.

Nieburger, M., Edinger, J.G., and Bonner, W.D. 1982. *Understanding our Atmospheric Environment.* W.H. Freeman, San Fransisco, California.

Nowacki, G.J. and Abrams, M.D. 1992. Community, edaphic, and historical analysis of mixed oak forests of the Ridge and Valley province in central Pennsylvania. *Canadian Journal of Forest Research* 22:790 – 800.

Oliver, C.D. and Larson, B.C. 1990. *Forest Stand Dynamics.* McGraw-Hill, Inc., New York.

Orlanski, I. 1975. A rational subdivision of scales for atmospheric processes. *Bulletin of the American Meteorological Society* 56:527 – 530.

Orvis, K.H. 1992. Probabilistic Physiographic Approach to Modeling Summer Rainfall in the Sonoran Desert (Arizona). Ph.D. Dissertation, University of California, Berkeley.

Osterkamp, W.R., Hupp, C.R., and Schening, M.R. 1995. Little River revisited – thirty-five years after Hack and Goodlett. *Geomorphology* 13:1 – 20.

Passarelli, R.E., Jr. and Boehme, H. 1983. The orographic modulation of pre-warm-front precipitation in southern New England. *Monthly Weather Review* 111:1062 – 1070.

Pastor, J. and Post, W.M. 1985. *Development of a Linked Forest Productivity-Soil Process Model.* Oak Ridge National Laboratory, Oak Ridge, Tennessee. ORNL/TM-9519.

Peterson, C.J. and Pickett, S.T.A. 1995. Forest reorganization: a case study in an old-growth forest catastrophic blowdown. *Ecology* 76:763 – 774.

Phipps, R.L. 1974. The soil creep-curved tree fallacy. *Journal of Research of the U.S. Geological Survey* 2:371 – 377.

Phipps, R.L. 1982. Comments on interpretation of climatic information from tree rings, eastern North America. *Tree Ring Bulletin* 42:11 – 22.

Pickett, S.T.A. 1980. Non-equilibrium coexistence of plants. *Bulletin of the Torrey Botanical Club* 107:238 – 248.

Pickett, S.T.A. and White, P.S., eds. 1985. *The Ecology of Natural Disturbance and Patch Dynamics.* Academic Press, San Diego.

Poreh, M. and Mechrez, E. 1984. The combined effect of wind and topography on rainfall distribution. *Journal of Hydrology* 72:1 – 23.

Post, W.M. and Pastor, J. 1996. LINKAGES – an individual-based forest ecosystem model. *Climatic Change* 34:253 – 261.

Putz, F.E. and Sharitz, R.R. 1991. Hurricane damage to old-growth forest in Congaree Swamp National Monument, South Carolina, U.S.A. *Canadian Journal of Forest Research* 21:1765 – 1770.

Pyne, S.J., Andrews, P.L., and Laven, R.D. 1996. *Introduction to Wildland Fire*. John Wiley and Sons, Inc.

Quarterman, E., Turner, B.H., and Hemmerly, T.E. 1972. Analysis of virgin mixed mesophytic forests in Savage Gulf, Tennessee. *Bulletin of the Torrey Botanical Club* 99:228 – 232.

Quinn, P.F., Beven, K.J., Lamb, R. 1995. The $\ln(\alpha/\tan\beta)$ index: how to calculate it and how to use it within the TOPMODEL framework. *Hydrological Processes* 9:161 – 182.

Rauber, R.M., Ramamurthy, M.K., and Tokay, A. 1994. Synoptic and mesoscale structure of a severe freezing rain event: the St. Valentine's day ice storm. *Weather and Forecasting* 9:183 – 208.

Reams, G.A. and Van Deusen, P.C. 1996. Detection of a hurricane signal in baldcypress tree-ring chronologies. *Radiocarbon* 14:265 – 271.

Rebertus, A.J., Shifley, S.R., Richards, R.H., and Roovers, L.M. 1997. Ice storm damage to an old-growth oak-hickory forest in Missouri. *American Midland Naturalist* 137:48 – 61.

Rhoades, V. 1918. Ice storms in the southern Appalachians. *Monthly Weather Review* 46:373 – 374.

Richwien, B.A. 1980. The damming effect of the southern Appalachians. *National Weather Digest* 5:2 – 12.

Rogers, R. 1990. *Quercus alba* L.: white oak. Pages 605 – 613 in Burns, R.M. and Honkala, R.M., tech. coords. *Silvics of North America*. USDA Handbook 654, Vol. 2. Washington, DC.

Rolston, H., III. 1989. Biology and philosophy in Yellowstone. *Biology and Philosophy* 4:1 – 18.

Romme, W.H. and Knight, D.H. 1981. Fire frequency and subalpine forest succession along a topographic gradient in Wyoming. *Ecology* 62:319 – 326.

Runkle, J.R. 1982. Patterns of disturbance in some old-growth mesic forests of eastern North America. *Ecology* 63:1533 – 1546.

Runkle, J.R. 1985. Disturbance regimes in temperate forests. Pages 17 – 33 in Pickett, S.T.A. and White, P.S., eds. *The Ecology of Natural Disturbance and Patch Dynamics*. Academic Press, San Diego.

Runkle, J.R. 1990. Gap dynamics in an Ohio *Acer-Fagus* forest and speculations on the geography of disturbance. *Canadian Journal of Forest Research* 20:632 – 641.

Runkle, J.R. 1992. *Guidelines and Sample Protocol for Sampling Forest Gaps*. USDA Forest Service, General Technical Report PNW-GTR-283. U.S. Government Printing Office, Washington, DC.

Russell, E.W.B. 1983. Indian-set fires in the forest of the northeastern United States. *Ecology* 64:78 – 88.

Sakai, A.K. and Sulak, J.H. 1985. Four decades of secondary succession in two lowland permanent plots in northern lower Michigan. *American Midland Naturalist* 113:146 – 157.

Sander, I.L. 1990a. *Quercus rubra* L.: northern red oak. Pages 727 – 733 in Burns, R.M. and Honkala, R.M., tech. coords. *Silvics of North America*. USDA Handbook 654, Vol. 2. Washington, DC.

Sander, I.L. 1990b. *Quercus velutina* Lam.: black oak. Pages 744 – 750 in Burns, R.M. and Honkala, R.M., tech. coords. *Silvics of North America*. USDA Handbook 654, Vol. 2. Washington, DC.

Schenk, H.J. 1996. Modeling the effects of temperature on growth and persistence of tree species: a critical review of tree population models. *Ecological Modeling* 92:1 – 32.

Schowalter, T.D., Coulson, R.N., and Crossley, C.A., Jr. 1981. Role of southern pine beetle and fire in maintenance of structure and function of the southeastern coniferous forest. *Environmental Entomology* 10:821 – 825.

Seischab, F.K., Bernard, J.M., and Eberle, M.D. 1993. Glaze storm damage to western New York forest communities. *Bulletin of the Torrey Botanical Club* 120:64 – 72.

Sharon, D. 1980. The distribution of hydrologically effective rainfall incident on sloping ground. *Journal of Hydrology* 46:165 – 188.

Shrader, J.R. 1994. Schools, business affected by weather. *The Southwest Times, February 11 – 12, 1994* 91(41): 2, 5. Pulaski, Virginia.

Shugart, H.H., Jr. and West, D.C. 1977. Development of an Appalachian deciduous forest succession model and its application to assessment of the impact of the chestnut blight. *Journal of Environmental Management* 5:161 – 179.

Siccama, T.G., Weir, G., and Wallace, K. 1976. Ice damage in a mixed hardwood forest in Connecticut in relation to *Vitis* infestation. *Bulletin of the Torrey Botanical Club* 103:180 – 183.

Smith, H.C. 1990. *Carya tomentosa* (Poir.) Nutt.: mockernut hickory. Pages 226 – 233 in Burns, R.M. and Honkala, R.M., tech. coords. *Silvics of North America*. USDA Handbook 654, Vol. 2. Washington, DC.

Smith, R.B. 1989. Mechanisms of orographic precipitation. *Meteorological Magazine* 118:85 – 88.

Smith, R.L. 1986. *Elements of Ecology*. 2nd ed. Harper and Row Publishers, New York.

Smith, T.M. and Huston, M.A. 1989. A theory of the spatial and temporal dynamics of plant communities. *Vegetatio* 83:49 – 69.

Sousa, W.P. 1979. Disturbance in marine intertidal boulder fields: the nonequilibrium maintenance of species diversity. *Ecology* 60:1225 – 1239.

Southern Appalachian Man and the Biosphere (SAMAB). 1996. *The Southern Appalachian Assessment Terrestrial Technical Report*. Report 5 of 5. USDA Forest Service Southern Region, Atlanta.

Spaulding, P. and Bratton, A.W. 1946. Decay following glaze storm damage in woodlands of central New York. *Journal of Forestry* 44:515 – 519.

Speer, J.H., Swetnam, T.W., Wickman, B.E., and Youngblood, A. In press. Changes in pandora moth outbreak dynamics during the past 622 years. *Ecology*.

Sprugel, D.G. 1991. Disturbance, equilibrium, and environmental variability: what is 'natural' vegetation in a changing environment? *Biological Conservation* 58:1 – 18.

SPSS, Inc. 1999. *SPSS Regression Models 9.0*. SPSS, Inc., Chicago.

Stahle, D.W., Cleaveland, M.K., and Hehr, J.G. 1985. A 450-year drought reconstruction for Arkansas, United States. *Nature* 316:530 – 532.

Stephenson, S.L. 1974. Ecological composition of some former oak-chestnut communities in western Virginia. *Castanea* 39:278 – 286.

Stewart, R.E. and P. King. 1987. Freezing precipitation in winter storms. *Monthly Weather Review* 115:1270 – 1279.

Stokes, M.A. and Smiley, T.L. 1968. *An Introduction to Tree-Ring Dating* University of Chicago Press, Chicago.

Stout, S.L., Marquis, D.A., and Ernst, R.L. 1987. A relative density measure for mixed-species stands. *Journal of Forestry* 85:45 – 47

Swetnam, T.W. and Betancourt, J.L. 1990. Fire-southern oscillation relations in the southwestern United States. *Science* 249:1017 – 1020.

Swetnam, T.W. and Lynch, A.M. 1993. Multicentury, regional-scale patterns of western spruce budworm outbreaks. *Ecological Monographs* 63:399 – 424.

Swetnam, T.W., Thompson, M.A., and Sutherland, E.K. 1985. *Spruce Budworms Handbook: Using Dendrochronology to Measure Radial Growth of Defoliated Trees*. USDA Handbook 639, Washington, DC.

Travis, D.J. and Meentemeyer, V. 1991. Influence of glaze ice storms on growth rates of loblolly pine *Pinus taeda* and shortleaf pine *Pinus echinata* in the Southern Appalachian Piedmont. *Climate Research* 1:199 – 205.

Travis, D.J., Grissino-Mayer, H.D., and Suckling, P.W. 1989. The impact of ice storms on tree ring widths of loblolly pine in northern Georgia. *Proceedings, Sixth Conference on Applied Climatology*, American Meteorological Society, pp J38 – J40.

Turner, M.G., Dale, V.H. and Everham, E.H. III. 1997. Fires, hurricanes, and volcanoes: comparing large disturbances. *BioScience* 47:758 – 768.

U.S. Forest Products Laboratory. 1974. *Wood Handbook: Wood as an Engineering Material.* USDA Agriculture Handbook 72. U.S. Government Printing Office, Washington, DC.

United States Forest Service (USFS). 1999. *Indepdence Day Blowdown.* Document from Superior National Forest Web site at http://www.snf.toofanorth.org.

Walker, L.R. 1991. Tree damage and recovery from Hurricane Hugo in Luquillo Experimental Forest, Puerto Rico. *Biotropica* 23:379 – 385.

Walters, R.S. and Yawney, H.W. 1990. *Acer rubrum* L.: red maple. Pages 60 – 69 in Burns, R.M. and Honkala, R.M., tech. coords. *Silvics of North America.* USDA Handbook 654, Vol. 2. Washington, DC.

Warrillow, M. and Mou, P. 1999. Ice storm damage to forest tree species in the ridge and valley region of southwestern Virginia. *Journal of the Torrey Botanical Society* 126:147 – 158.

Welch, N.T. 1999. Occurrence of fire in southern Appalachian yellow pine forests as indicated by macroscopic charcoal in soil. *Castanea* 64:310 – 317.

Wendel, G.W. and Smith, H.C. 1990. *Pinus strobus* L.: eastern white pine. Pages 476 – 488 in Burns, R.M. and Honkala, R.M., tech. coords. *Silvics of North America.* USDA Handbook 654, Vol. 1. Washington, DC.

White, P.S. 1979. Pattern, process, and natural disturbance in vegetation. *Botanical Review* 45:229 – 299.

Whitney, H.W. and Johnson, W.C. 1984. Ice storms and forest succession in southwestern Virginia. *Bulletin of the Torrey Botanical Club* 111:429 – 437.

Whittaker, R.H. 1956. Vegetation of the Great Smoky Mountains. *Ecological Monographs* 26:1 – 80.

Whittaker, R.H. 1975. *Communities and Ecosystems.* 2nd ed. MacMillan Publishing Company, Inc., New York.

Wilkinson, M. 1993. Tornadoes in the lab. *Knoxville News Sentinel.* Monday, May 3, p B1.

Williams, B.B. 1960. The 1960 ice storm in northern Alabama. *Weatherwise* 13:196 – 199, 203.

Williams, C.E. 1998. History and status of table mountain pine-pitch pine forests of the southern Appalachian Mountains (USA). *Natural Areas Journal* 18:81 – 90.

Williams, C.E. and Johnson, W.C. 1990. Age structure and the maintenance of *Pinus pungens* in pine-oak forests of southwestern Virginia. *American Midland Naturalist* 124:130 – 141.

Williams, C.E. and Johnson, W.C. 1992. Factors affecting recruitment of *Pinus pungens* in the southern Appalachian Mountains. *Canadian Journal of Forest Research* 22:878 – 887.

Appendix

Originally, Speer and I used temperature and precipitation data, rather than Palmer Drought Severity Index (PDSI) to build the climate-response models for the tree-ring analysis (Chapter 5). We obtained monthly temperature averages and precipitation totals from four cooperative weather observation stations near our Gap Mountain and Walker Mountain study sites. Specifically, we used data from the Virginia stations of Burkes Garden, Blacksburg, and Rocky Mount and from the North Carolina station of Mount Airy. We combined the monthly values into seasonal values (Table A.1) and used stepwise regression to relate these variables to ring-width index. Significance level for entry of an independent variable was 0.20, and significance level for a variable to remain in the model was set at 0.30. It was necessary to use these significance levels, rather than the more rigorous levels of 0.05 and 0.10 used in Chapter 5, to obtain regression models for most of the tree-ring series. The resultant climate-response models are reported in Table A.2. Note that we calculated R^2 values, rather than adjusted R^2. The adjusted R^2 values reported in Chapter 5 provide a more accurate assessment of model fit than standard R^2 values. Standard R^2 overestimates the performance of the regression model.

We abandoned these results after finding that ring-width index was related more strongly to PDSI than to simple temperature and precipitation. Indeed, we obtained significant relationships between ring-width index and PDSI for most of the trees when using the 0.05 and 0.10 significance levels (Chapter 5).

Table A.1. Seasonal temperature and precipitation variables included in the original climate response models.

Variable	Variable definition
gs_ppt	Growing-season precipitation – total precipitation for March through August of the year of ring formation
lw_ppt	Late-winter precipitation – total precipitation for January through February of the year of ring formation
ew_ppt	Early-winter precipitation – total precipitation for November through December of the year previous to ring formation
py_ppt	Previous-year precipitation – total precipitation for January through October of the year previous to ring formation
gs_tmp	Growing-season temperature – average monthly temperature for March through August of the year of ring formation
lw_tmp	Late-winter temperature – average monthly temperature for January through February of the year of ring formation
ew_tmp	Early-winter temperature – average monthly temperature for November through December of the year previous to ring formation
py_tmp	Previous-year temperature – average monthly temperature for January through October of the year previous to ring formation

Table A.2. Results of regression analysis using seasonal precipitation and temperature as independent variables. These are defined in Table A.1. The dependent variable is standardized ring width for each tree.

Tree	Regression equation	R^2
	Gap Mountain – chestnut oak	
A	y = – 3.587 + 0.208gs_tmp + 0.0123gs_ppt + 0.0388ew_tmp – 0.012ew_ppt + 0.00336py_ppt	0.437
B	y = – 1.477 + 0.00487ew_ppt + 0.0725py_tmp + 0.0688gs_tmp + 0.00404gs_ppt	0.171
C	y = 0.652 + 0.00487gs_ppt + 0.0369ew_tmp – 0.0064lw_ppt	0.241
D	y = 0.478 + 0.0059gs_ppt + 0.0319ew_tmp	0.328
E	y = – 1.378 + 0.00866gs_ppt + 0.2311w_tmp + 0.0968gs_tmp + 0.035ew_tmp	0.447
F	y = 0.479 + 0.00743gs_ppt + 0.0192lw_tmp	0.170
G	y = – 0.425 + 0.0833gs_tmp	0.062
H	y = – 0.854 + 0.00549gs_ppt + 0.0582py_tmp + 0.0448gs_tmp	0.216
I	y = – 1.526 + 0.145gs_ppt + 0.0941gs_tmp	0.300
J	y = – 0.366 + 0.0541lw_tmp + 0.00467gs_ppt + 0.0804py_tmp – 0.0078lw_ppt	0.355
K	y = 1.709 + 0.00773gs_ppt – 0.092py_tmp	0.413
	Gap Mountain – black oak	
L	y = – 2.187 + 0.0123gs_ppt + 0.00565py_ppt + 0.116gs_tmp	0.290
M	y = 1.654 + 0.00883gs_ppt – 0.09py_tmp – 0.012lw_ppt + 0.0347ew_tmp	0.380
N	y = 0.212 + 0.00939gs_ppt – 0.01lw_ppt + 0.00354py_ppt	0.326
O	y = 0.925 – 0.011lw_ppt + 0.00401gs_ppt	0.143
P	y = 1.150 + 0.0329lw_tmp – 0.011lw_ppt	0.160
Q	y = 0.156 + 0.00707gs_ppt – 0.035lw_tmp + 0.0408ew_tmp + 0.00315py_ppt	0.234
R	y = 0.802 + 0.00704gs_ppt – 0.011lw_ppt	0.146
S	y = – 0.946 + 0.098gs_tmp + 0.00366py_ppt	0.107
T	y = 5.166 – 0.019lw_ppt – 0.135gs_tmp – 0.127py_tmp + 0.0339lw_tmp	0.348
	Walker Mountain – chestnut oak	
A	y = 0.932 + 0.034lw_tmp	0.092
B	y = 1.417 + 0.0042gs_ppt + 0.0158lw_tmp – 0.044gs_tmp	0.157
C	y = 0.521 + 0.00765gs_ppt	0.275
D	y = 0.141 + 0.018lw_tmp + 0.0048gs_ppt + 0.0408py_tmp	0.303
E	y = 0.658 + 0.00677gs_ppt – 0.0076ew_ppt + 0.0166lw_tmp	0.224
F	y = – 2.404 + 0.0122gs_ppt + 0.117py_tmp + 0.0476ew_tmp + 0.0561gs_tmp	0.515
G	y = 0.519 + 0.00543gs_ppt + 0.0076lw_ppt	0.137
H	y = 0.518 + 0.0395lw_tmp + 0.0647py_tmp	0.185
I	y = – 0.823 + 0.0916py_tmp + 0.00721gs_ppt + 0.0339ew_tmp + 0.0183lw_tmp	0.285
J	y = 0.295 + 0.00768gs_ppt + 0.0195lw_tmp + 0.00191py_ppt	0.425
K	y = 0.505 + 0.00515gs_ppt + 0.0339ew_tmp	0.115
	Walker Mountain – black oak	
L	y = 0.562 + 0.00524gs_ppt + 0.0182lw_tmp + 0.00543ew_ppt	0.156
M	y = 0.397 + 0.0035py_ppt + 0.00401gs_ppt	0.087
N	y = 2.771 – 0.103gs_tmp – 0.024ew_tmp	0.135
O	y = 2.055 + 0.0497lw_tmp – 0.071gs_tmp	0.166
P	y = 1.336 – 0.042gs_tmp + 0.00189py_ppt + 0.00281gs_ppt	0.116
Q	y = 1.182 + 0.00748ew_ppt – 0.0034py_ppt + 0.0186lw_tmp	0.203
R	y = 0.502 + 0.00651gs_ppt + 0.0057ew_ppt	0.152
S	y = 0.701 + 0.355lw_tmp + 0.00598gs_ppt – 0.0081lw_ppt	0.157
T	y = 0.396 + 0.00987gs_ppt	0.223

Vita

Charles Lafon was born in Radford, Virginia on September 22, 1970. He was raised in Pulaski County, Virginia, and attended Pulaski County schools. He graduated from Pulaski County High School in June 1988 and entered Emory & Henry College, Emory, Virginia, in August 1988. He received the Bachelor of Arts in Geography, with a minor in Art, in May 1992.

During his undergraduate career, Charles worked on a project funded by the Tennessee Historic Commission and directed by Dr. John Morgan to survey historic buildings in Johnson and Hawkins Counties, Tennessee. He also completed an internship with the Virginia Division of Gas and Oil, Abingdon, Virginia. Following graduation, he worked for one summer as a Camp Counselor at Camp Dickenson in Fries, Virginia.

Charles entered the Master's program in Geography at the University of Tennessee, Knoxville in August 1992 and received the Master of Science degree in August 1995. His M.S. thesis was entitled "Fifty Years of Succession on Abandoned Pastures at the Oak Ridge Reservation, Tennessee: Influences of Pre-Abandonment Land Use on Vegetation Development." During his years in the Master's program, Charles served first as a Graduate Teaching Assistant. During the 1994-95 academic year, he was a Graduate Teaching Associate and taught the two-semester introductory-level sequence in physical geography.

Charles entered the Ph.D. program in Geography at the University of Tennessee, Knoxville in August 1995. He worked during summer and fall 1995 as a Graduate Research Assistant in the University of Tennessee Department of Mathematics on a study of Everglades ecology directed by Dr. Michael Huston and Dr. Louis Gross. During 1996, his assistantship was in the Cartographic Services Laboratory of the Department of Geography, where he helped produce maps and directed undergraduate cartography laboratory sessions. From 1997 to 2000, Charles has been employed as a Graduate Research Assistant in the University of Tennessee Department of Civil and Environmental Engineering, working on an interdisciplinary project

directed by Dr. Michael Huston to characterize and model physical and biotic systems in the southern Appalachians. His Ph.D. dissertation work is a component of this larger project. Following graduation in August 2000, Charles will move to Texas A & M University, where he has accepted a position as Assistant Professor in the Department of Geography.